NÚMERO: 446/2012
UNIVERSIDADE ESTADUAL DE CAMPINAS
INSTITUTO DE GEOCIÊNCIAS

FERNANDO ROSA GUIMARÃES

Análise Espacial Tridimensional e Geoestatística de Dados Multi-Fonte de Superfície e Subsolo Aplicada à Modelagem Prospectiva de Mineralizações Auríferas no Quadrilátero Ferrífero – MG

TESE DOUTORADO APRESENTADA AO INSTITUTO DE GEOCIÊNCIAS DA UNICAMP PARA OBTENÇÃO DO TÍTULO DE DOUTOR EM CIÊNCIAS, NA ÁREA DE GEOLOGIA E RECURSOS NATURAIS.

ORIENTADOR: PROF. DR. CARLOS ROBERTO DE SOUZA FILHO

ESTE EXEMPLAR CORRESPONDE À VERSÃO FINAL DA TESE
DEFENDIDA PELO ALUNO FERNANDO ROSA GUIMARÃES
E ORIENTADO PELO PROF. DR. CARLOS ROBERTO DE SOUZA FILHO

_____

CAMPINAS / SP – 2011

FICHA CATALOGRÁFICA ELABORADA POR
CÁSSIA RAQUEL DA SILVA – CRB8/5752 – BIBLIOTECA "CONRADO PASCHOALE" DO INSTITUTO DE GEOCIÊNCIAS
UNICAMP

G947a

Guimarães, Fernando Rosa, 1972-
Análise espacial tridimensional e geoestatística de dados multi-fonte de superfície e subsolo aplicada à modelagem prospectiva de mineralizações auríferas no quadrilátero ferrífero–MG / Fernando Rosa Guimarães-- Campinas,SP.: [s.n.], 2011.

Orientador: Carlos Roberto de Souza Filho.
Tese (doutorado) - Universidade Estadual de Campinas, Instituto de Geociências.

1.Geociências – Sensoriamento remoto. 2. Mapeamento digital. 3. Sistema de posicionamento global. I. Souza Filho, Carlos Roberto de, 1965- II. Universidade Estadual de Campinas, Instituto de Geociências. III. Título.

Informações para a Biblioteca Digital

Título em inglês: Geophysical and geostatistical analysis of surface and underground muulti-source data applied to prospectivity modelling of gold deposits in Quadrilátero Ferrífero – MG – Brazil.
Palavras-chaves em ingles:
Geosciences - Remote sensing
Digital mapping
Global positioning systems
Área de concentração: Geologia e Recursos Naturais
Titulação: Doutor em Ciências
Banca examinadora:
Carlos Roberto de Souza Filho (Presidente)
Carlos Alberto Mendonça
Emilson Pereira Leite
Jorge Kazuo Yamamoto
Lena Virgínia Soares Monteiro
Data da defesa: 16-12-2011
Programa de Pós-graduação em Geociências

UNICAMP

UNIVERSIDADE ESTADUAL DE CAMPINAS
INSTITUTO DE GEOCIÊNCIAS
PÓS-GRADUAÇÃO EM GEOCIÊNCIAS NA
ÀREA DE GEOLOGIA E RECURSOS NATURAIS

AUTOR: Fernando Rosa Guimarães

"Análise Espacial Tridimensional e Geoestatística de Dados Multi-Fonte de Superfície e Sub-Solo Aplicada à Modelagem Prospectiva de Mineralizações Auríferas do Quadrilátero Ferrífero - MG".

ORIENTADOR: Prof. Dr. Carlos Roberto de Souza Filho

Aprovada em: 16 / 12 / 2011

EXAMINADORES:

Prof. Dr. Carlos Roberto de Souza Filho _____ - Presidente

Prof. Dr. Jorge Kazuo Yamamoto _____

Prof. Dr. Emilson Pereira Leite _____

Profa. Dra. Lena Virginia Soares Monteiro _____

Prof. Dr. Carlos Alberto Mendonça _____

Campinas, 16 de dezembro de 2011

À minha esposa Luciane, minha mãe Marisa e às minhas filhas Beatriz, Alice e Manuela.

AGRADECIMENTOS

À minha esposa Luciane e às minhas filhas Beatriz, Alice e Manuela pelo estímulo incondicional, apoio e compreensão pelas horas de ausência do convívio familiar.

Ao meu orientador professor Carlos Roberto de Souza Filho pela oportunidade, paciência, suporte e prontidão em auxiliar-me em tudo que foi necessário para a execução deste trabalho e pelo exemplo de pesquisador, sempre a procura de novos desafios.

À AngloGold Ashanti que permitiu a realização deste trabalho, dando apoio material e financeiro.

Aos gerentes de exploração da AngloGold Ashanti, Mike Schmulian, Leonardo Henrique de Souza e Paulo de Tarso Ferreira pela oportunidade, suporte e apoio.

Aos geólogos Ulisses Cyrino Penha e Eduardo Zenha Cordeiro pelas sugestões em textos dos Projetos, apoio nos trabalhos de campo e resenhas geológicas.

Aos geólogos Alessandro Henrique Medeiros Silva, Leonardo Henrique de Souza e Paulo de Tarso Ferreira pelas orientações e sugestões nos trabalhos de avaliação de recursos minerais e geoestatística, especialmente na parte de simulação.

Aos geólogos Élio Horikava, Marco Aurélio da Costa, Márcio Sales e Jaime Duchini Jr. pelas valiosas prosas sobre a geologia e ocorrências auríferas no Quadrilátero Ferrífero e em trabalhos de campo.

Aos geofísicos Keith Martin, Jonh Bell e Tony Rojas Vicencio pelas orientações e sugestões nos trabalhos geofísicos.

Ao geógrafo Edivaldo Fiel Lopes pelo incentivo, apoio, suporte e resenhas geo-tecnológicas.

Aos geólogos Luiz Henrique Lisboa, Cláudia Neves e Carlos Paranhos pelo apoio na geologia de subsolo do depósito Lamego.

Ao geólogo Diogo Afonso Costa por me apresentar detalhes de como se diferenciar os tipos de alteração hidrotermal em rochas de testemunho de sondagem da mina de Cuiabá.

Ao meu irmão Hélius pela valorosa e cuidadosa revisão do texto em inglês.

Aos profissionais do galpão de sondagem Carlos Taciano Mendes e Sara pelo apoio nas descrições de testemunho de sondagem e aos demais auxiliares do galpão.

Ao topógrafo Antônio Raimundo dos Reis pelos trabalhos de topografia de campo.

Ao José Geraldo Barbosa e Ricardo Santos Melo pela companhia nos trabalhos de campo.

Ao professor Cleyton Deutsch pelas orientações e pelos valiosos momentos nas aulas de geoestatística.

À Anglo American que através de seus gerentes Sérgio Botelho, Luiz Vannucci, Cláudio Menezes e Charles Valadão permitiram e auxiliaram financeiramente a parte final da jornada deste trabalho.

À Val por fazer minhas matrículas e pela hospitalidade e suporte na Unicamp.

À minha mãe Marisa e irmãos Octávio, Helius e Giselle por participarem permanentemente das etapas da minha vida.

Aos meus amigos Lúcio, Karina, Franco, Camila, André, Juliana e Armostrong pelo apoio sincero e permanente na maior parte dos momentos da minha vida.

Em especial ao meu amigo Gladstok (em memória) pelos momentos que vivemos juntos neste planeta.

Às demais pessoas que contribuíram direta ou indiretamente para a finalização deste Projeto de Doutorado.

UNIVERSIDADE ESTADUAL DE CAMPINAS
INSTITUTO DE GEOCIÊNCIAS

Análise Espacial Tridimensional e Geoestatística de Dados Multi-Fonte de Superfície e Subsolo Aplicada à Modelagem Prospectiva de Mineralizações Auríferas no Quadrilátero Ferrífero–MG

RESUMO

Tese de Doutorado

Fernando Rosa Guimarães

O Quadrilátero Ferrífero é uma das maiores províncias metalíferas do mundo e possui potencial aurífero exploratório considerável visto o grande número de minas que produzem, ou já produziram no passado, milhares de toneladas desse metal. Depósitos auríferos importantes como Mina Grande, Cuiabá e Raposos, considerados gigantes e de classe mundial, além de jazidas de menor porte (Faria, Bicalho, Engenho, D´água, Morro da Glória, etc.), hospedam-se na porção centro-norte do Supergrupo Rio das Velhas (Dorr 1969) e são conhecidas desde o início do século XVIII. Esta tese de Doutorado tem como tema central o desenvolvimento e a aplicação de métodos quantitativos e qualitativos de mapeamento prospectivo tridimensional, que possibilita a seleção e a hierarquização de corpos auríferos potenciais tridimensionais durante programas de exploração mineral, reduzindo riscos e direcionando melhor a continuidade das investigações exploratórias. Além disso, demonstra-se que a aplicação de recursos geoestatísticos auxilia expressivamente o entendimento geológico de depósitos auríferos da província metalogenética do Quadrilátero Ferrífero (QF), pode fornecer evidências de localizações espaciais de domínios auríferos enriquecidos, além de ajudar na quantificação de conteúdo metálico e na classificação de recursos minerais. Esta tese está organizada em um formato de dois desenvolvimentos distintos. O capítulo 1 denominado **"Assinaturas Geoquímicas e Geofísicas de IP, Resistividade e EM de Depósitos Auríferos Mesotermais do Quadrilátero Ferrífero – Estudos de Caso: Depósito Lamego e Adjacências – Brasil"** apresenta resultados de processos de inversão geofísica de levantamentos aéreo e terrestre (IP) que possibilitaram caracterizar as assinaturas dos corpos sulfetados conhecidos do depósito Lamego, além de estimar profundidades e extensões laterais de corpos condutores eletromagnéticos, resistivos e/ou geoelétricos neste depósito. A caracterização diferenciada dos sinais geofísicos de condutividade eletromagnética, efeito IP e resistividade definida no depósito Lamego, onde os controles com os corpos de minério conhecidos foram adequadamente compreendidos, auxiliaram na identificação e na localização de novas extensões de corpos potenciais nos alvos satélites denominados: São José, Biquinha, Bom Caminho e Sobradinho. Adicionalmente, um estudo complementar na região do depósito Morro de Glória foi desenvolvido, e modelos prospectivos fundamentados na integração e análise espacial tridimensional de dados multi-fonte, priorizando o uso de algoritmos avançados de lógica fuzzy e inversão geofísica, que auxiliaram na seleção e hierarquização de corpos auríferos potenciais neste depósito. O capítulo 2 denominado **"Krigagem Ordinária e Simulação Condicional como Suporte na Estimativa, Categorização e Caracterização do Depósito de Ouro do Lamego - Quadrilátero Ferrífero – MG"** apresenta um conjunto de procedimentos geoestatísticos utilizado para obtenção de uma estimativa quantitativa e qualitativa dos teores e volumes dos corpos de minério, que sustentam os números finais do conteúdo metálico do depósito Lamego e a sua categorização em termos de recurso mineral. Dentre os procedimentos utilizados destacam-se: (i) caracterização geológica e da modelagem tridimensional dos corpos de minério; (ii) caracterização do QA/QC utilizado, (iii) estudo exploratório da base de dados e ajuste e análise de variogramas direcionais; (iv) definição de efeito pepita; (v) definição dos parâmetros e aplicação da krigagem ordinária; (vi) validação da krigagem ordinária; (vii) classificação dos recursos baseado nos resultados obtidos na simulação condicional; (viii) análise de como os resultados geoestatísticos, pós validados, podem contribuir no aprimoramento do entendimento do depósito. O conjunto de procedimentos geoestatísticos desenvolvidos neste trabalho serviu não só como um importante experimento para a estimativa de teores e do conteúdo metálico do depósito aurífero Lamego, mas também para auxiliar na categorização dos recursos minerais e aprimorar o entendimento geológico e caracterização dos corpos de minério deste depósito.

STATE UNIVERSITY OF CAMPINAS
INSTITUTE OF GEOSCIENCES

Geophysical and Geostatistical Analysis of Surface and Underground Multi-Source Data Applied To Prospectivity Modelling of Gold Deposits in *Quadrilátero Ferrífero* – MG - Brazil

ABSTRACT
PhD Thesis

Fernando Rosa Guimarães

The *Quadrilátero Ferrífero* (Iron Quadrangle) located in State of Minas Gerais is one of the largest metal bearing regions in the world. The region has considerable gold exploration potential. There are many mines which have produced thousands of tons of gold. Mina Grande, Cuiabá and Raposos are considered world class deposits. Other smaller deposits, including Faria, Bicalho, Engenho, D´água and Morro da Glória, are found in the central-northern area of the Rio das Velhas Supergroup (Dorr 1969). They have been known since the 18th century and are normally associated with a number of geological factors and "coincidences" which have occurred and have manifested in three dimensions. This thesis is organized in two distinct developments. The first Chapter **"Geochemical and Geophysical Signatures of Induced Polarization, Resistivity and Electromagnetic Surveys of Orogenic Gold Deposits in the *Quadrilátero Ferrífero* – Case Studies in Lamego Deposit and Surrounding Targets, Minas Gerais, Brazil,** presents data results of the geophysical inversion from data windows of the survey "Spectrem - Airborne Electromagnetic Survey-2002", along with resistivity and induced polarization (IP) ground surveys. The studies provide a characterization of the signatures of known sulphide bodies from Lamego's deposit and estimates the depth of possible lateral extensions of the electromagnetic, resistive and/or geoelectric conductive bodies in this deposit. This work describes the results of geological, geophysical, and geochemical research conducted in the region between the Lamego and Cuiabá deposits, starting with the methodological characterization, geophysical and geochemical signatures established for the Lamego deposit, aiming at a regional metallogenic analysis and assessment of the potential for locating similar gold deposits. The main objectives of this work is (i) to characterize the behavior of IP signatures, resistivity and air EM of the sulphide host rocks of the gold mineralization of the Lamego deposit, considering the three dimensional geological/geochemical modeling, aligned with the direct inversion process of each of the geophysical properties; (ii) to locate possible lateral extensions and at depth of potential sulphide bodies containing gold mineralization; (iii) to investigate, in depth, the continuity of soil and excavation anomalies through the geophysical sections, which help in locating gold deposits in the north-northwest region of the *Quadrilátero Ferrífero*; (iv) to characterize the methodological criteria for mineral exploration by IP geophysics and three dimensional integration of multi-source information; to appropriately employ the scheduling, configuration, and geophysical inversion methodology used in the Lamego deposit in target satellites to aid the exploration scheduling of surface drilling; to tabulate the main characteristics of geophysical signatures of all surveyed targets and deposits in order to understand the correlation with the different models of researched materials. Additionally, a complementary study applied on Morro da Glória deposit was carry out based on the integration and three dimensional spatial analysis of multi-source data and the use of fuzzy logic algorithms and geophysical inversion. The 3D integration of surface exploration data projected underground, together with geological and geochemical information, combined with geophysical inversion methods applied to electromagnetic data, support this study in the development of a model which has the potential to assist in finding and quantifying new three dimensional auriferous orebodies in Morro da Glória gold deposit, which is located near Belo Horizonte city. The second Chapter **"Ordinary Kriging and Conditional Simulation to Support Quantitative Estimation, Characterization and Classification of the Lamego Gold Deposit – Quadrilátero Ferrífero – Brazil",** presents geostatistical procedures which were used for quantitative estimation of grades and volumes of the orebodies and to support the final figures related to the metal content and classification of the Lamego gold deposit. The ordinary kriging was used in the estimation and Sequential Gaussian Simulation (SGSIM) was used for accessing the uncertainties and guiding the classification of the Deposit. The main procedures used in this work are summarized as follow: (i) geological modeling of the mineralized orebodies; (ii) QA/AC characterization; (iii) exploration data analysis; variogram fitting and analysis; (iv) nugget effect definition; (v) definition of the ordinary kriging parameters; (vi) ordinary kriging validation and (vii) resource classification by SGSIM. Metallogenetical conclusions of Lamego deposit are presented based on geostatistical analysis and include the mean gold distribution of the horizontal volumetric panels indicates that gold grades are lower with increasing depth both in the Carruagem and Arco da Velha orebodies. Conversely, the mean gold distribution of the vertical volumetric panels indicates that gold grades slightly increase following the north direction. This feature can be associated with deformation episodes, which are coincident to the mineralizing hydrothermal fluid accumulation at those sites and/or associated to structural traps in the northern sectors of the aforementioned orebodies.

SUMÁRIO

CHAPTER 1

GEOCHEMICAL AND GEOPHYSICAL SIGNATURES OF INDUCED POLARIZATION, RESISTIVITY AND ELECTROMAGNETIC SURVEYS OF OROGENIC GOLD DEPOSITS IN THE QUADRILÁTERO FERRÍFERO – CASE STUDIES AT THE LAMEGO DEPOSIT AND SURROUNDING TARGETS, MINAS GERAIS, BRAZIL

CHAPTER 2

ORDINARY KRIGING AND CONDITIONAL SIMULATION TO SUPPORTING QUANTITATIVE ESTIMATION AND CLASSIFICATION OF RESOURCES AT THE LAMEGO GOLD DEPOSIT – QUADRILÁTERO FERRÍFERO - BRAZIL

LISTA DE FIGURAS

INTRODUÇÃO

CHAPTER 1

CHAPTER 2

LISTA DE TABELAS

CHAPTER 1

CHAPTER 2

INTRODUÇÃO

Essa tese de Doutorado tem como tema central o desenvolvimento e a aplicação de métodos quantitativos e qualitativos de mapeamento prospectivo tridimensional, visando a seleção e a hierarquização de corpos auríferos potenciais tridimensionais. Tais métodos, adaptados e aplicados no contexto de depósitos auríferos da província metalogenética do Quadrilátero Ferrífero (QF), podem ter um desdobramento prático na redução de riscos e no melhor direcionamento da continuidade das investigações exploratórias. Além disso, demonstra-se que a aplicação de mecanismos geoestatísticos auxilia expressivamente o entendimento geológico de depósitos auríferos do QF; fornece evidências de localizações espaciais de domínios auríferos enriquecidos; além de ajudar na quantificação de conteúdo metálico e na classificação de recursos minerais de depósitos específicos.

A tese está organizada em um formato de dois desenvolvimentos distintos e está sendo apresentada na forma de artigos em inglês para posterior adaptação e submissão a revistas internacionais ou nacionais.

O primeiro capítulo, intitulado **"Assinaturas Geoquímicas e Geofísicas de IP, Resistividade e EM de Depósitos Auríferos Mesotermais do Quadrilátero Ferrífero – Estudos de Caso: Depósito Lamego e Adjacências – Brasil**" compreende a caracterização das intensidades dos sinais geofísicos de condutividade eletromagnética, efeito IP e resistividade dos corpos auríferos do depósito Lamego, associados a diferentes níveis de sulfetação. Os processos de inversão geofísica de dados de levantamentos aéreos e terrestres (IP) aplicados nesse trabalho possibilitaram estimar profundidades e extensões laterais de corpos condutores eletromagnéticos, resistivos e/ou geoelétricos nesse depósito. A caracterização geofísica detalhada, onde os controles com os corpos de minério são conhecidos durante o desenvolvimento das galerias no depósito, auxiliaram na identificação e na localização de novas extensões de corpos potenciais nos alvos satélites denominados: São José, Biquinha, Bom Caminho e Sobradinho. Um exercício complementar na região de Morro de Glória foi desenvolvido e fundamentado na integração e análise espacial tridimensional de dados multi-fonte, priorizando o uso de algoritmos de lógica fuzzy e inversão geofísica, que auxiliaram na localização e hierarquização de corpos auríferos potenciais do depósito Morro da Glória.

No segundo capítulo, intitulado **"Krigagem Ordinária e Simulação Condicional como Suporte na Estimativa, Categorização e Caracterização do Depósito de Ouro do Lamego -**

Quadrilátero Ferrífero – Brasil", são apresentados resultados da avaliação dos recursos minerais do projeto Lamego obtidos através de um conjunto de procedimentos geoestatísticos que suportaram a estimativa dos teores e volumes dos corpos de minério, além da classificação dos recursos minerais em medidos, indicados e inferidos, definidos com base nos resultados da simulação condicional gaussiana. As principais etapas dos desenvolvimentos aplicados nesse capítulo foram: modelagem geológica tridimensional dos corpos de minério, métodos de QA/QC, estudo exploratório da base de dados, incluindo estudos das médias das variáveis, análise dos histogramas de freqüência, estudo bi-variante entre as variáveis ouro e enxofre, ajuste e análise de variogramas direcionais, definição de efeito pepita, definição dos parâmetros para aplicação na krigagem ordinária, validação da krigagem ordinária, classificação dos recursos baseada nos resultados obtidos na simulação condicional e composição de uma análise de como os resultados geoestatísticos podem contribuir no aprimoramento do entendimento do Depósito.

Justificativas

O depósito Lamego é considerado um dos principais depósitos de ouro do Quadrilátero Ferrífero. O conhecimento geológico e geofísico detalhado desse depósito em superfície e sub-superfície é crítico na medida em que pode proporcionar avanços em modelos metalogenéticos e orientar a exploração de depósitos de ouro em terrenos greenstone belt Arqueanos no mundo todo.

Alinhado a essas questões, a importância de se compor uma relação empírica de rochas com diferentes proporções de materiais sulfetados com as respectivas intensidades de sinais geofísicos também motivam este estudo, e podem adicionalmente contribuir em pesquisas exploratórias em regiões geologicamente pouco conhecidas, através dos métodos indiretos de investigação aplicados e desenvolvidos neste trabalho.

Além disso, os controles das incertezas associadas à variabilidade dos teores de ouro, bem como as variações expressivas da geometria e espessura dos corpos de minério, necessitam ser cuidadosamente quantificados, principalmente para serem ponderados em uma etapa de declaração formal de recursos minerais baseados em códigos internacionais de mineração, como por exemplo, o *Australasian Jorc Code*.

Contexto da Pesquisa

O QF representa um terreno granito-*greenstone* coberto por seqüências supracrustais Proterozóicas e está situado na porção sul do Cráton do São Francisco (Figura 1). A sua lito-estratigrafia pode ser dividida em cinco unidades principais (Dorr 1969, Alkmim & Marshak 1998). Estas incluem, da base para o topo, (i) os terrenos granito-gnáissicos de idade arqueana, com intrusões graníticas, pegmatitos e diques máficos; (ii) o Supergrupo Rio das Velhas, que compreende uma seqüência do tipo *greenstone belt* arqueana; (iii) o Supergrupo Minas, uma cobertura plataformal do Paleoproterozóico, contendo rochas metassedimentares clásticas e químicas; (iv) o Grupo Itacolomi e o Supergrupo Espinhaço, ambos de idade mesoproterozóica e compostos de rochas metassedimentares clásticas. A forma quadrangular da região, que gerou o nome QF, é delineada pela distribuição das rochas metassedimentares do Supergrupo Minas.

O Supergrupo Rio das Velhas hospeda as principais mineralizações auríferas do QF, enquanto o Supergrupo Minas contém depósitos de ferro, manganês, calcário e alumínio. A unidade basal do Supergrupo Minas, o Grupo Caraça, também encerra potencial geológico aurífero, pois compreende quartzitos, quartzo xistos e meta-conglomerados do tipo *Witwatersrand.*

O Supergrupo Rio das Velhas foi formalmente subdividido Dorr *et al.* (1957) and Dorr (1969) nos Grupos Nova Lima a Maquiné e corresponde a uma seqüência arqueana do tipo *greenstone belt*. O Grupo Nova Lima corresponde a uma unidade metavulcano-sedimentar basal do Supergrupo Rio das Velhas. Segundo estratigrafia proposta pela CPRM/DNPM (1994), na região de Sabará, Caeté e Nova Lima, que engloba os depósitos do Lamego, Morro da Glória e a mina de Cuiabá, o Grupo Nova Lima compreende (i) uma Unidade Basal, formada essencialmente por rochas meta-ultrabásicas intercaladas a meta-básicas, além de raras meta-ácidas e lentes e camadas esparsas de BIFs; (ii) uma Unidade Intermediária, com metavulcânicas básicas e intermediárias intercaladas a metavulcânicas ácidas, metafufos ácidos, pelitos, BIFs, metacherts e xistos carbonosos; e (iii) uma Unidade Superior, com rochas metavolcaniclásticas ácidas a intermediárias e metaepiclásticas (pelitos e grauvacas) (Figura 2).

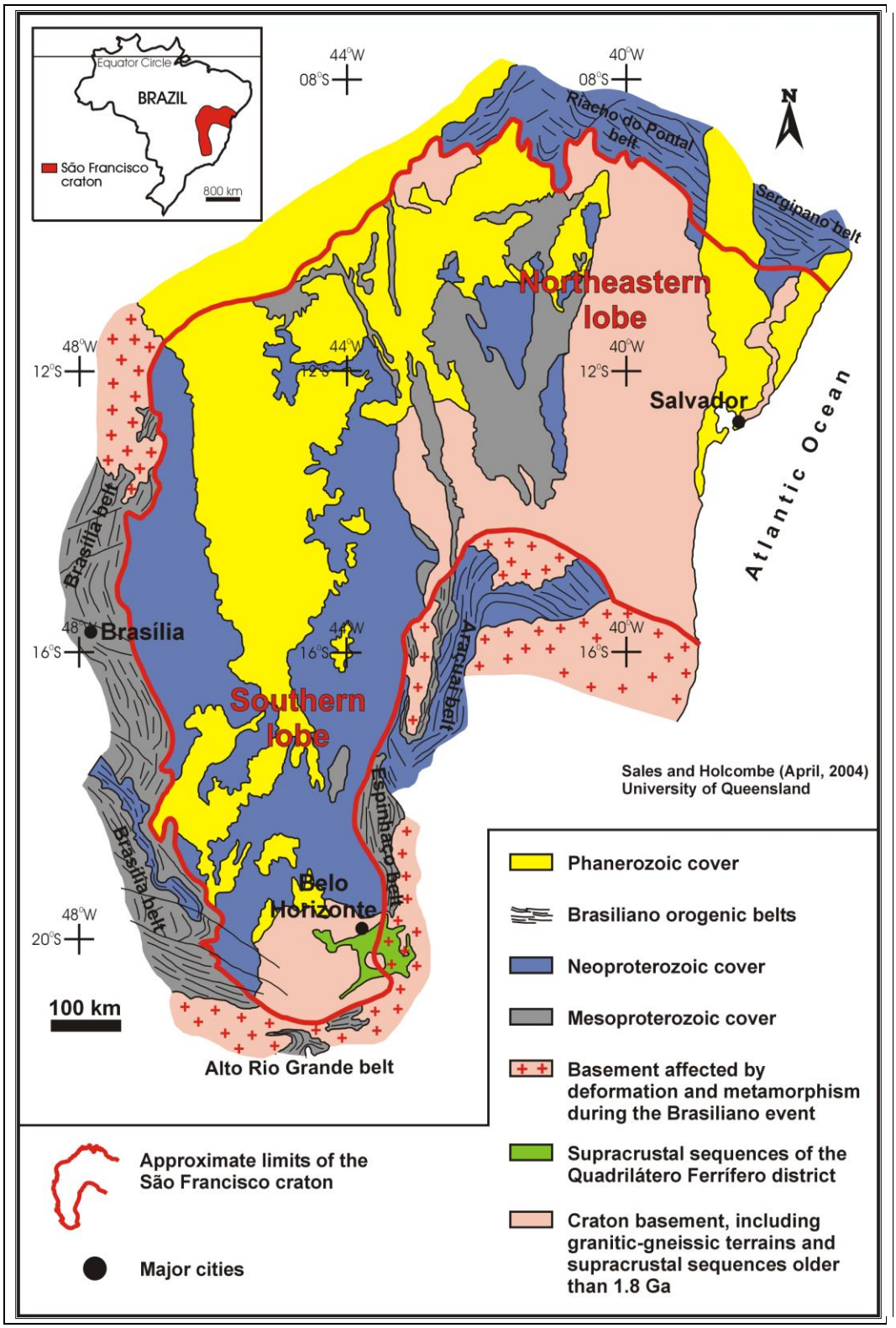

Figura 1: Mapa geológico regional simplificado do Cráton do São Francisco, no qual são destacadas a borda do cinturão orogenético Brasiliano e o distrito do Quadrilátero Ferrífero. Adaptado de Alkmim & Marshak (1998) em Santos Sales & Holcombe (2004).

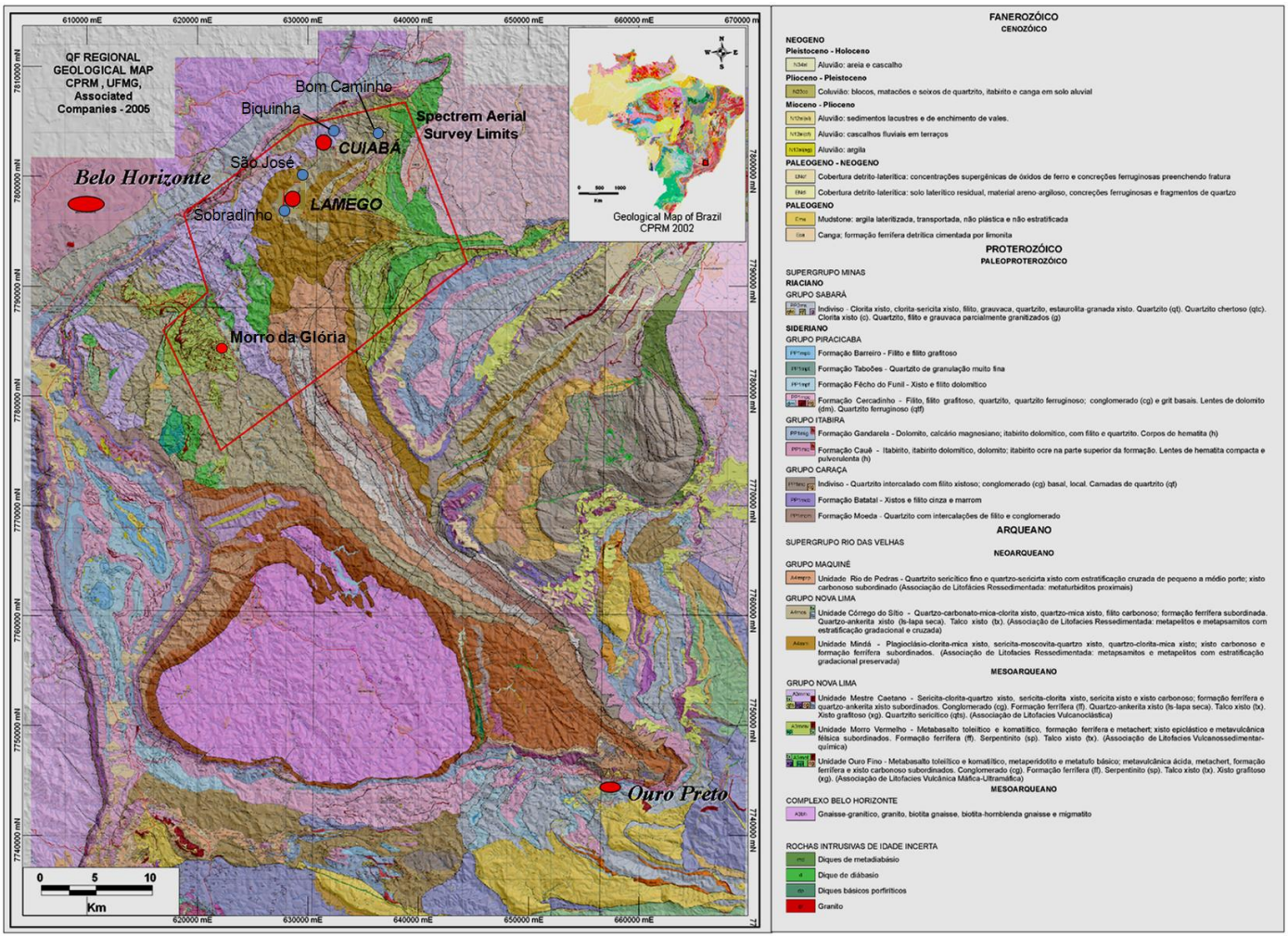

Figura 2: Mapa geológico regional do Quadrilátero Ferrífero (CPRM/UFMG/Companhias Associadas, 2005) combinado com dados do SRTM (Shuttle Radar Topography Mission, 2006).

Estudos geológicos detalhados sobre os depósitos Cuiabá e Lamego são apresentados por Lobatto & Vieira (1998) e Santos Sales (1998). Lobatto & Vieira (1998) discutem os estilos de alteração hidrotermal e a metalogenia da mina de Cuiabá e de outros depósitos auríferos do QF. Ambos os depósitos estão hospedados no Grupo Nova Lima. O Grupo Nova Lima é uma das unidades supracrustais mais estudadas no Brasil devido aos inúmeros depósitos e ocorrências auríferas hospedados em formação ferrífera bandada, destacando-se as minas de Morro Velho, Cuiabá, São Bento e Raposos.

Similarmente a outras províncias auríferas em terrenos granito-*greenstone*, como a do Abitibi (Canadá) e a de Yilgarn (Austrália), o Supergrupo Rio das Velhas e os depósitos de ouro que hospeda tem idade neoarqueana. Já em Barberton (África do Sul), um cràton mais antigo, os

depósitos de ouro são, de modo geral, hospedados em conglomerados arqueanos de bacias tectonicamente estáveis, e não em seqüências de xistos verdes de terrenos *greenstone belts*.

As centenas de ocorrências individuais de ouro no Supergrupo Rio das Velhas tornam esta região uma província aurífera de classe mundial. A maioria dos corpos de minério apresenta dimensões entre 10 e 300m ao longo da direção da foliação regional, 0.5 a 20m de espessura e de 800 a mais de 3000m de extensão (*down-plunge*). Similarmente a outros terrenos arqueanos, o QF possui uma concentração notável de depósitos pequenos e médios (0,1 a 10t Au) (*e.g*., oeste da Austrália, Província Superior, Zimbabwe). A maioria dos depósitos possui reservas auríferas inferiores à 1 tonelada, geralmente por volta de 100kg. Entre os depósitos pequenos estão Córrego do Sítio, Lamego, Faria, Esperança III, Bicalho, Bela Fama, Juca Vieira, Brumal, Boa Vista, Fernandes, Moita, Roça Grande, Bico de Pedra e Pari (Vial *et al.* 2007). Os depósitos de Raposos, São Bento e Passagem de Mariana são exemplos de depósitos de porte intermediário. Morro Velho (455 ton produzidas) e Cuiabá são depósitos de grande porte, comparáveis aos maiores e de mais alto teor conhecidos mundialmente.

Todos estes depósitos são, em maior ou menor grau, estruturalmente controlados, relacionados a zonas de cisalhamento, dobramentos e/ou interseções de elementos estruturais. Sua continuidade, segundo a direção do mergulho, é uma feição recorrente para a maioria dos mesmos.

As mineralizações dos depósitos auríferos do QF foram agrupadas por Vial *et al.* (2007) em seis tipos: (1) Lapa Seca: Morro Velho, Bicalho, Bela Fama; (2) Formação Ferrífera Bandada: Cuiabá, São Bento, Raposos, Faria, Brumal, Roça Grande; (3) Veios de quartzo: Juca Vieira e Fernandes; (4) Sulfetos disseminados com vênulas de quartzo (Moita); (5) Anfibolitos: Pari; e (6) Sulfetos de metais-base disseminados a maciços: Bico de Pedra. O depósito do Lamego se encaixa no grupo 2, apesar de parte expressiva da mineralização ocorrer hospedada em "metachert".

As Geotecnologias vêm sendo aplicadas na academia e indústria mineral em projetos de pesquisa desde a década de 70. Fornece, no século XXI, uma forte contribuição para o auxílio no entendimento geológico de províncias metalogenéticas e depósitos minerais distribuídos por todo o mundo. Isso foi possível em função da evolução dos mecanismos computacionais, avanços progressivos de memória e capacidade de processamento dos computadores, aliado ao progresso de algoritmos de diversas naturezas e *software* de processamento de dados espaciais e avaliação de recursos minerais.

Processos de inversão geofísica têm sido aplicados em diversos depósitos minerais nos últimos anos com o objetivo de (i) estimar a profundidade de corpos condutores eletromagnéticos, magnéticos ou com propriedades físicas distintas; (ii) definir melhor os limites de abrangência lateral e longitudinal de domínios mineralizados; e (iii) auxiliar em pesquisas exploratórias, principalmente de metais base, ouro e ferro. Li & Oldenburg (2003) discutiram historicamente a evolução do processo de inversão através de métodos de barreiras logarítmicas usando gradientes conjugados. Phillips *et al.* (2001) aplicaram processos de inversão geofísica ao depósito de sulfeto massivo vulcanogênio a cobre-zinco de San Nicolas no México. Esses autores mostraram que os resultados da inversão de dados de magnetometria terrestre, polarização induzida (IP) e gravimetria são capazes de caracterizar, com sucesso, a geometria dos principais corpos mineralizados. Silva *et al.* (2001) demonstram a importância de se utilizar modelos de referência definindo-se limites confinantes ao processo de inversão. Esses limites podem se referir, por exemplo, a domínios litológicos tridimensionais conhecidos que possuem características físicas compatíveis com o método geofísico aplicado. Esses limites auxiliam na filtragem da não unicidade das soluções fornecidas no processo de inversão. Dentith (2003) publicou um conjunto de assinaturas geofísicas de depósitos minerais australianos, o que representou um marco na geofísica da Austrália no começo da última década. Dos 21 casos históricos apresentados, 9 usaram inversão geofísica e produziram resultados significativos. Oldenburg & Pratt (2007) contribuíram com uma completa análise da aplicação do processo de inversão geofísica, caracterizando, na teoria e na prática, detalhes de procedimentos de inversão na exploração mineral. Segundo os autores, a última década foi marcada por grandes avanços no processo de inversão de vários tipos de dados geofísicos. Os avanços foram promovidos principalmente pelo desenvolvimento de otimizações matemáticas, visualização e poder computacional. Para o problema da inversão na exploração mineral, Oldenburg & Pratt (2007) separam três grandes categorias: Tipo I: inversão de corpos discretos, Tipo II: inversão pura da propriedade e Tipo III: inversão litológica.

Já a análise *fuzzy* neste trabalho tem o objetivo de selecionar, qualitativamente, através de operadores fuzzy aplicados aos dados multi-fonte, áreas e sólidos tridimensionais em superfície e subsolo, para hierarquizar domínios auríferos já conhecidos e localizar novos potenciais para investigação. A teoria da lógica fuzzy (Bonham-Carter, 1994) comporta uma escala contínua de pertinência aos conjuntos de dados estudados, variando de 1.0 (pertinência total) até 0.0 (não-pertinência total). Desta maneira, medições individuais de uma variável podem ser classificadas

de acordo com o grau de pertinência ao conjunto "Anomalia" (Bonham-Carter, 1994). Valores muito altos serão certamente anômalos, possuindo uma pertinência fuzzy (fuzzy membership) “um”, enquanto valores muito baixos ou abaixo do *background* terão pertinência fuzzy “zero”. Entre estes dois extremos existe toda uma faixa de possíveis valores de pertinência. A combinação entre os mapas de evidências foi estabelecida através de operadores fuzzy descritos em An et al. (1991) e Bonham-Carter (1994). Exemplos da utilização da lógica *fuzzy* em pesquisa mineral são fartamente encontrados na literatura (e.g., An *et al*. 1991; Bonham-Carter *et al*. 1988; Bonham-Carter 1994; Bonham-Carter 1997; Braghin 1998; Chinn & Ascough 1997, Nóbrega 2001, Nykänen 2008).

No primeiro capítulo é apresentada uma tabela sumarizada com um conjunto de resultados quantitativos referentes às intensidades dos sinais de geofísica aérea e terrestre dos principais corpos sulfetados do depósito Lamego e dos alvos satélites. Através desta tabela foi possível estabelecer características específicas que associam as informações de concentrações de teores de sulfetos em cada corpo de minério estudado, com as respectivas intensidades dos sinais de condutividade eletromagnética, efeito IP e resistividade DC. Com essa caracterização, as metodologias de investigação desenvolvidas neste trabalho podem auxiliar em pesquisas exploratórias em áreas que ainda o conhecimento geológico é embrionário ou em áreas onde o conjunto de informações exploratórias é escasso.

Os resultados obtidos na região do depósito Morro da Glória ponderados pela metodologia das múltiplas seções horizontais, submetidas aos operadores de lógica *fuzzy,* apresentaram uma correlação geométrica tridimensional bastante significativa com o produto do processo de inversão geofísica de dados EM, embora em níveis de escala ou resoluções diferenciados. Ambos os modelos apresentaram também uma “coincidência” expressiva quando comparados aos corpos mineralizados conhecidos e já lavrados no depósito Morro da Glória.

O conjunto de procedimentos geoestatísticos desenvolvidos no capítulo 2 serviu não só como um importante experimento para a estimativa de teores e do conteúdo metálico do depósito aurífero Lamego, mas também para auxiliar na categorização dos recursos minerais e aprimorar o entendimento geológico e caracterização dos corpos de minério deste depósito. A krigagem ordinária, efetuada separadamente para cada um dos corpos do depósito Lamego, objetivou a geração de modelos de blocos que preenchem os sólidos confeccionados na modelagem geológica tridimensional com teores de ouro estimados, fornecendo assim um mecanismo consistente para a avaliação geoestatística do depósito. Em conseqüência, durante processos de validação da

krigagem ordinária, importantes características do depósito Lamego foram realçadas, permitindo um enriquecimento substancial do conhecimento geológico e de potencial aurífero dos principais corpos mineralizados.

CHAPTER 1

GEOCHEMICAL AND GEOPHYSICAL SIGNATURES OF INDUCED POLARIZATION, RESISTIVITY AND ELECTROMAGNETIC SURVEYS OF OROGENIC GOLD DEPOSITS IN THE *QUADRILÁTERO FERRÍFERO* – CASE STUDIES AT THE LAMEGO DEPOSIT AND SURROUNDING TARGETS, MINAS GERAIS, BRAZIL

SUMMARY

The Lamego gold deposit is located in the northeastern sector of the *Quadrilátero Ferrífero,* along the same structural trend of Cuiaba gold mine. The mineralization is hosted by NeoArchean rocks at the base of the Rio das Velhas Supergroup (greenstone belt) and is of orogenic type. The stratigraphic succession of the deposit is composed of rocks metamorphosed at green schist facies. This succession includes, from base to top: metamafic rocks, banded iron formation (BIF), gray quartz veins (as stratabound, boudinaged and irregular masses), carbonaceous schist, pelitic schist, and volcanoclastic schist. The deposit is comprised in an anticline with some 4.8km perimeter, axis oriented towards NE and flanks dipping 20° to 30° ESE. The mineralization is divided into the Carruagem, Arco da Velha, Queimada, and Cabeça de Pedra orebodies, which are hosted by hydrothermally altered BIFs and gray quartz veins. Gold occurs in pyrite and in free form. The gold mineralization is structurally controlled and related to hydrothermal alteration. The alteration includes areas of chloritization, carbonatization and sericitization, predominantly observed in metamafic rocks. Sulphidation (mainly pyrite) is recorded in BIFs and, subordinately, in gray quartz veins and carbonaceous schist.

The Lamego deposit and surrounding areas were surveyed in 2002 by an Airborne Electromagnetic System (Spectrem). Later, in 2007, the same area was covered by resistivity and induced polarization (IP) ground surveys.

This chapter presents the results of the geophysical inversion of data from these two surveys, combined with geological and geochemical data. The study provides a characterization of the geophysical signatures of known sulphide bodies at the Lamego deposit and an estimation of the depth and possible lateral extensions of orebodies, considering their electromagnetic, resistive and/or geoelectric conductive responses. These signatures were used to investigate a larger area around Lamego, making it possible to expand the pool of potential sites for gold in the form of smaller satellite targets.

Geophysical inversion in mineral exploration is divided into three categories: Type I - inversion of discrete bodies; Type II - pure or direct inversion of the property; and Type III - lithological inversion. Type II inversion was used in this research as three dimensional geological models were not employed as a reference for adjusting the direct inversion product. The sections of resistivity and chargeability (voltage decay) were generated from algorithms that use the finite element method in 2D, although topography was also incorporated in the data modeling. The product of the inversion of both surveys suggests individualized correlations with known orebodies of the Lamego deposit, and indicates some potential anomalies that are geologically consistent.

1 - INTRODUCTION

The *Quadrilátero Ferrífero* (QF), located in State of Minas Gerais, is one of the largest metal-bearing regions in the world. It hosts a large number of mines that have produced thousands of tons of gold since the 18th century. Major gold-bearing deposits such as Mina Grande, Cuiabá and Raposos are considered gigantic (>250t Au) and world class (>100t Au) (Groves *et al.* 2005). Other smaller deposits (Lamego, Faria, Bicalho, Engenho, D´água and Morro da Glória), are found in the central-northern area of the Rio das Velhas Supergroup (Dorr II 1969).

The orogenic Lamego gold deposits, owned by AngloGold Ashanti Brasil Mineração Ltda., are located in the N-NW portion of the Archean-Paleoproterozoic metallogenic province of the *Quadrilátero Ferrífero* (QF). This province is a historical gold, iron, manganese, and bauxite producing region, among other mineral assets, with a combined gold production of over 800 tonnes of metal. The Lamego deposit, which is currently at the pre-feasibility stage, is located 7.5 km southeast of the city of Sabará and 13 km southeast of Cuiabá gold mine (Figure 1).

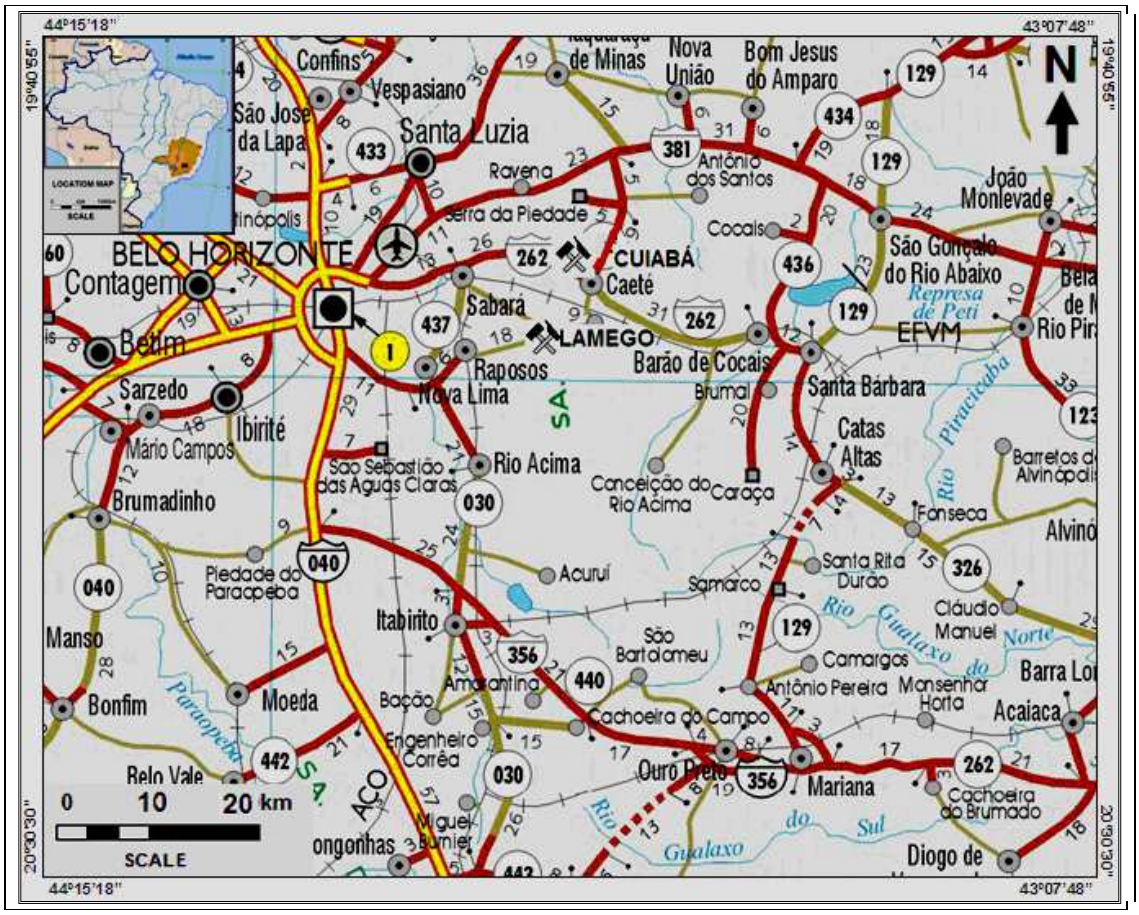

Figure 1: Location map and access to the Lamego deposit in the Minas Gerais State.

Geological studies of Lamego deposit are presented by Santos Sales (1998) and Guimarães et al. (2008). Lobatto & Vieira (1998) discuss the styles of hydrothermal alteration and metallogeny of the Cuiabá mine and other gold deposits in the *Quadrilátero Ferrífero*. These deposits are hosted by Nova Lima Group rocks - a basal metavolcanic-sedimentary unit of the Archean Rio das Velhas Supergroup, which comprises a greenstone belt sequence. The Nova Lima Group is a vastly studied supracrustal unit in Brazil due to the numerous gold-bearing deposits and occurrences hosted in banded iron formations, especially in the Morro Velho, Cuiabá, São Bento and Raposos mines.

This work aims to portray the geological, geochemical and geophysical signatures of the Lamego gold deposit by means of inversion methods. The knowledge acquired from Lamego is also used to enhance regional mineral prospectivity modeling of similar deposits and assessment of possibly new mineral resources. Satellite targets denominated São José, Biquinha, Sobradinho, Bom Caminho and Morro da Glória were also approached by ancillary data integration and further investigation by IP geophysical sections and drilling campaigns.

The investigation is strongly based on results yielded by geophysical data inversion acquired during two geophysical surveys: the Airborne Electromagnetic System (SPECTREM), flown in 2002, and resistivity and induced polarization (IP) ground surveys conducted in 2007.

Additionally, this study provides a characterization of the geophysical signatures of known sulphide bodies at the Lamego deposit and an estimation of the depth and possible lateral extensions of orebodies, considering their electromagnetic, resistive and/or geoelectric conductive responses. These signatures were used to investigate a larger area around Lamego, making it possible to expand the pool of potential sites for gold in the form of smaller satellite targets.

Geophysical inversion has been implemented using the database of various mineral deposits in recent years with multiple objectives, including: (i) estimation of the depth of electromagnetic, magnetic conducting bodies or those with different physical properties, (ii) better definition of lateral and longitudinal borders of the mineralized areas; (iii) assistance of mineral exploration projects, with focus on base metals, gold and iron. Li & Oldenburg (2003) discuss the historical evolution of the inversion process through the Logarithmic Barrier Method, using conjugated gradients. Phillips et al. (2001) applied geophysical inversion processes to the massive volcanogenic sulphide copper-zinc deposit in San Nicolas, Mexico. These authors showed that the results of the inversion of the land magnetometry data, induced polarization (IP) and gravimetry successively characterized the geometry of the main mineralized bodies.

Additionally, a complementary study in Morro da Glória gold deposit was developed to compare the geophysical inversion results against a 3D fuzzy logic analysis considering modeled gold orebodies, soil and stream sediments campaigns and information related to the geometry of old excavations. This study assisted in the consolidation of prospective detailed models of Morro da Glória auriferous mineralization based on the integration and 3D analysis of multi-source data considering fuzzy logic and geophysical inversion algorithms, providing new potential lateral extension in this deposit.

Specific objectives of this study are summarized below:

1 – To detail the local geology of the Lamego and Morro da Glória gold deposits, besides four satellite targets, through geological mapping and integration of old available data.

2 – To characterize the signal intensity of induced polarization (IP), resistivity and airborne electromagnetic (EM) signatures of the sulfide-bearing host rocks of the Lamego gold deposit, considering three dimensional geologic and geochemistry modeling of the orebodies, associated with products yielded by the direct inversion of the aforementioned geophysical properties;

3 – To locate possible lateral extensions and depth of potential sulfide bodies containing gold mineralization associated with the Lamego deposit;

4 – To investigate, in depth, the continuity of soil anomalies and excavations of the satellite targets through geophysical sections, which may help in the position of drilling and locating potential gold deposits in the north-northwest region of the *Quadrilátero Ferrífero* (Rio das Velhas Supergroup);

5 –To establish a methodological criteria for mineral exploration by IP geophysics and three-dimensional integration of multi-source data;

6 –To employ the geophysical inversion methodology used in the Lamego deposit in satellite targets;

7 –To tabulate the main characteristics of geophysical signatures of all surveyed orebodies of Lamego deposit and satellite targets in order to associate with different proportions of sulfides and lithologies.

8 – To develop the mineral resource evaluation of Lamego gold deposit based on both ordinary kriging and conditional simulation methods to supporting quantitative estimation, characterization and mineral resource classification.

9 – To consider metallogentic issues of the studied areas based on the results of the ordinary kriging analysis and association with geophysical results.

2 – REGIONAL GEOLOGY

The *Quadrilátero Ferrífero* (QF) is located in the southern portion of São Francisco Craton (Figure 2) and comprises Archean granite-greenstone terranes overlain by Proterozoic supracrustal sequences. Its stratigraphy can be divided into five main units (Dorr II 1969, Alkmim & Marshak 1998), and includes, from base to top, Archean granite-gneiss terranes with granite intrusions, pegmatites and mafic dykes; the Archean Rio das Velhas Supergroup, which is a classic greenstone-belt sequence; the Paleoproterozoic Minas Supergroup, which is a platformal cover containing clastic and chemical metasedimentary rocks; and the mesoproterozoic Itacolomi Group and Espinhaço Supergroup, composed of clastic metasedimentary rocks. The QF region is named after its quadrangular shape, which is distinguished by the metasedimentary rock distribution of the Minas Supergroup.

The Rio das Velhas Supergroup was formally subdivided by Dorr et al. (1957) and Dorr (1969) into the older Nova Lima Group and the younger Maquiné Group.

According to the stratigraphy proposed by Zucchetti *et al.* (1996), in the Sabará-Caeté region – where the Lamego deposits and the Cuiabá mine are located – the Nova Lima Supergroup comprises a Basal Unit formed essentially by intermixed meta-ultrabasic and metabasic rocks, as well as rare meta-acidic rocks, lenses, and sparse layers of banded iron formations (BIFs); an Intermediate Unit, consisting of basic and intermediate metavolcanic rocks intermixed with acidic metavolcanic rocks, acidic meta-tuffs, pelites, BIFs, gray quartz veins, and carbonaceous schists; and an Upper Unit, comprising acidic to intermediate metavolcaniclastic and meta-epiclastic rocks (pelites and graywackes) (Figure 3).

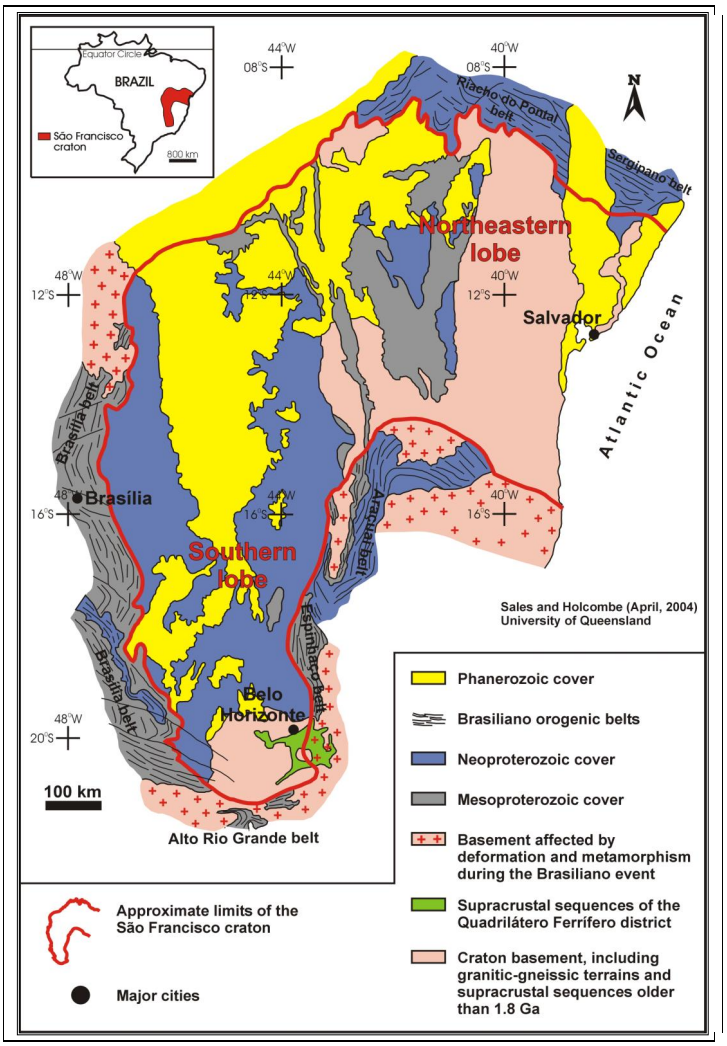

Figure 2: Simplified regional map of the São Francisco Craton showing the bordering Brasiliano orogenic belts and the Quadrilátero Ferrífero. Adapted from Alkmim & Marshak (1998) and Santos Sales & Holcombe (2004).

The Rio das Velhas Supergroup hosts the major gold mineralizations of the QF, whereas the Minas Supergroup contains iron, manganese, limestone and aluminum deposits.

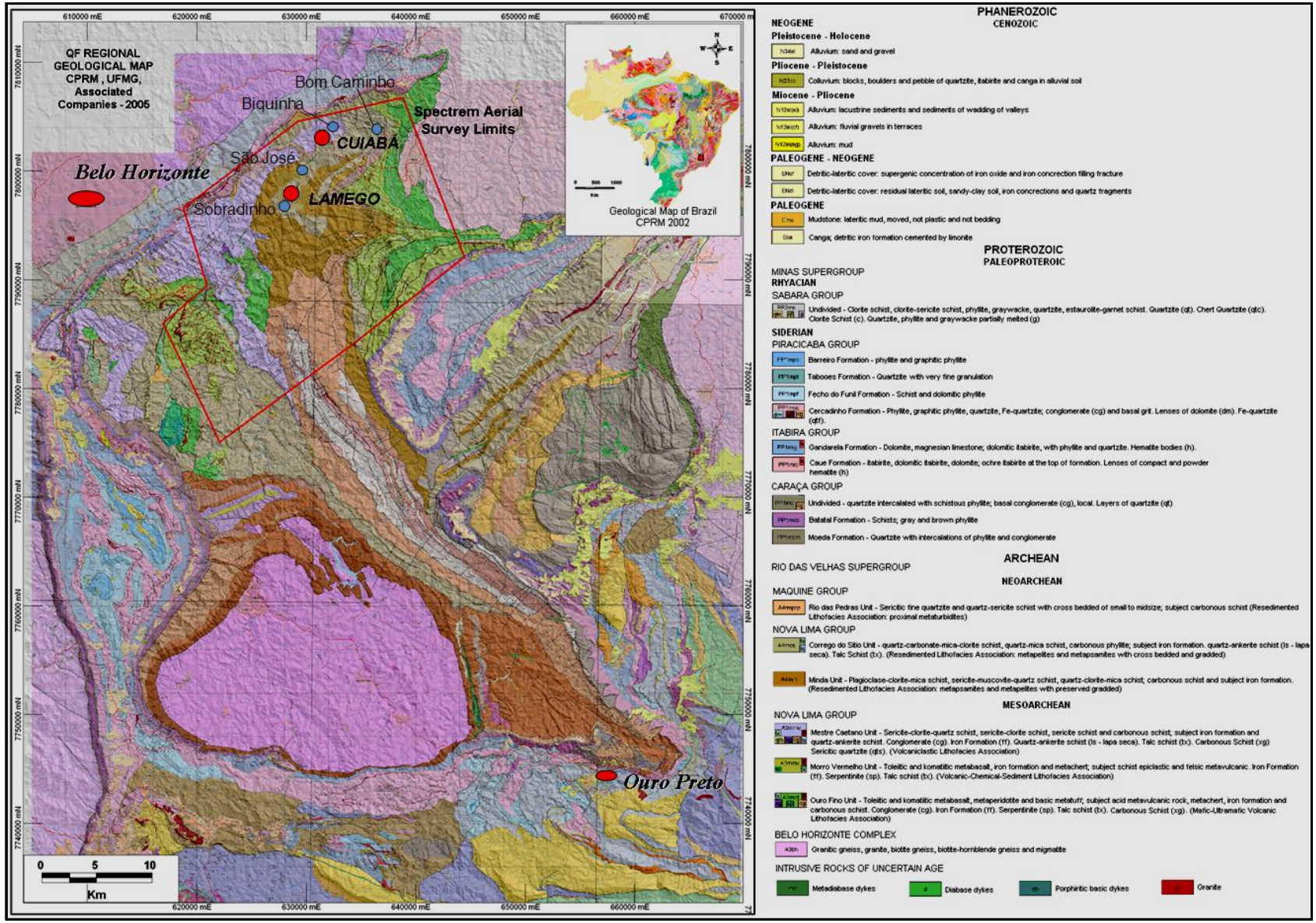

Figure 3: Regional geological map of the *Quadrilátero Ferrífero* (CPRM 2005), merged to Shuttle Radar Topography Mission (SRTM 2006) data in the background.

Tectonic Evolution

Based on a review of geochronological and geological data, Lobato *et al.* (2001) proposed the following succession of tectonic events for the QF:

1. Main period of crustal growth prior to 2.9 Ga, followed by several short, episodic tectonic events from 2860 to 2600 Ma. The first occurred at 2860 Ma and involved migmatization of old TTG terranes;

2. Evolution of the Rio das Velhas greenstone belt, associated with tectono-metamorphic and magmatic events from 2780 to 2700 Ma;

3. Cratonization and sedimentation on stable platform followed by intrusion of granites at 2600 Ma. Platform sedimentation of carbonates at 2400 Ma, indicating a long period of tectonic stability;

4. Transamazonian Orogeny involving consumption of oceanic crust and generation of mantle-related tonalites and trondjemites from 2162 to 2124 Ma, followed by intrusion of syn- to late-collisional granites of crustal derivation, and foreland-basin-type sedimentation. The collapse of the orogen led to the development of structures of the dome-and-keel type, which is the prevailing structure in the QF (Alkmim & Marshak 1998). U-Pb ages of titanites between 2060 and 2030 Ma define the period of this final phase of crustal distension;

5. Post-Transamazonian events had a minor impact on the tectonic evolution of the QF.

Global Metallogenetic Aspects

Similarly to other gold provinces in granite-greenstone terranes, such as the Abitibi in Canada and the Yilgarn in Australia, the Rio das Velhas Supergroup is of Neoarchean age. In the older Barberton greenstone belt (South Africa), the gold deposits are, in general, hosted by Archean conglomerates in tectonically stable basins, rather than by greenstone sequences.

Hundreds of individual gold occurrences in the Rio das Velhas Supergroup make this region a world class gold province. Most of the orebodies are 10m to 300m in length along the strike, 0.5m to 20m wide, and extend 800m to >3000m down plunge. Similarly to other Archean

terranes (e.g., Western Australia, and the Upper Province in Zimbabwe), the QF shows a remarkable concentration of small- and medium-size deposits (0.1 to 10t Au). For most of such deposits, reserves are of less than 1 ton, usually around 100kg. Among the small-size deposits are Córrego do Sítio, Lamego, Faria, Esperança III, Bicalho, Bela Fama, Juca Vieira, Brumal, Boa Vista, Fernandes, Moita, Roça Grande, Bico de Pedra, and Pari (Vial *et al.* 2007), whereas Raposos, São Bento and Passagem de Mariana are examples of medium-size deposits, and Morro Velho (455 tons produced) and Cuiabá are world-class deposits (Figure 4).

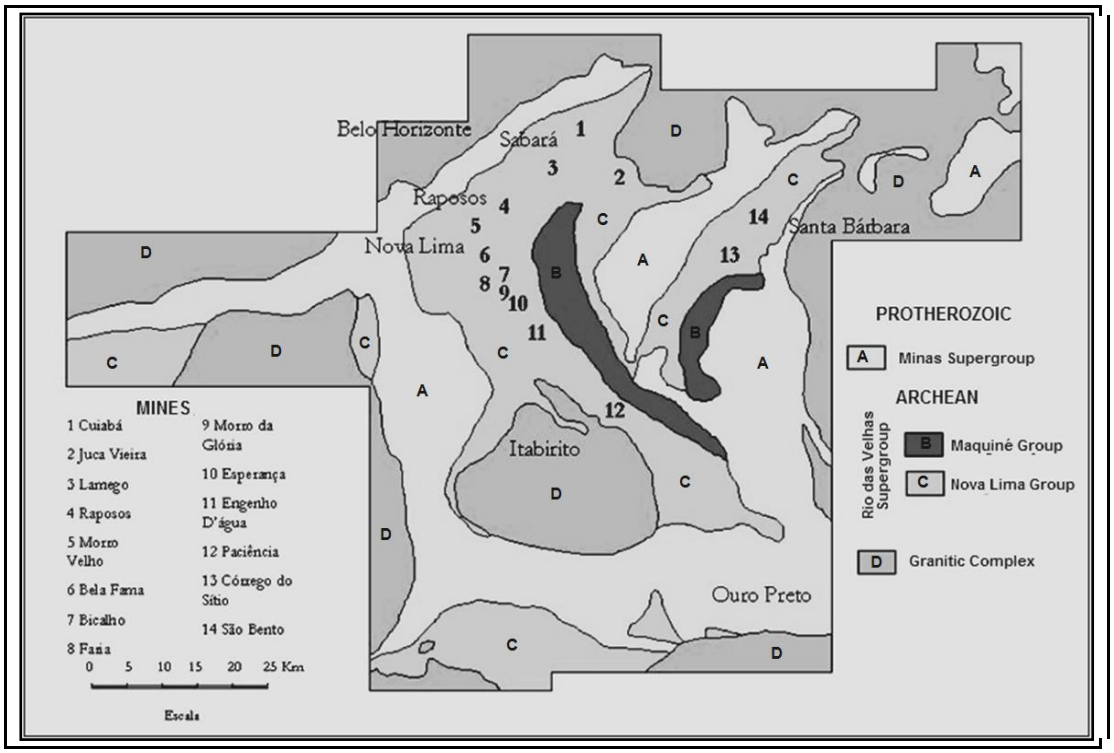

Figure 4 – Simplified geological map of the *Quadrilátero Ferrífero* showing the location of the main gold deposits. The Lamego deposit is indicated by number 3.

All these deposits are structurally controlled and related to shear zones, folds, and/or intersections of structural elements. Extensive down-plunge continuity is a consistent feature of most of the deposits.

Vial *et al.* (2007) grouped the gold deposits of the QF into six types: (1) *Lapa Seca*: Morro Velho, Bicalho, and Bela Fama; (2) Banded iron formation: Cuiabá, São Bento, Raposos, Faria, Brumal, and Roça Grande; (3) Quartz veins: Juca Vieira and Fernandes; (4) Disseminated sulfides with quartz veinlets: Luzia da Mota; (5) Amphibolites: Pari; and (6) Disseminated to

compact base-metal sulfides: Bico de Pedra. The Lamego deposit fits into type 2, although a substantial portion of the mineralization occurs within gray quartz veins in stratabound layers.

The hypothesis that the BIF lithotype from Lamego and Cuiabá deposits represents a single stratigraphic horizon, located at the contact between middle and upper units of the Nova Lima Group, has important prospective implications. Current knowledge indicates that both structures that encompass the Lamego and Cuiabá deposits represent surface expressions (structural windows) of refolded antiforms in the Sabará-Caeté region (Santos Salles 1998). The possible existence of 'blind' folded structures (and therefore, hidden orebodies, with no surface expression) on a kilometric scale, accessible only by diamond drilling, supported AngloGold Ashanti's decision, in the late 1990s, to invest in geochemical surveys by stream sediment and soil pattern sampling, as well as geophysical (electro-magnetic, magnetic, induced polarization (IP)), surveys. These enhanced exploration campaigns have given rise to new targets near Lamego, coined Biquinha, Bom Caminho, São José, Sobradinho, and Morro da Glória.

3 – GEOLOGY OF LAMEGO GOLD DEPOSIT

The stratigraphic sequence found at the Lamego deposit (Figure 5), from base to top, consists of mafic to intermediate metavolcanic rocks (hydrothermally altered or not); banded iron formation - BIF (hydrothermally altered or not) and gray quartz veins; carbonaceous to graphitic schists, metapelites and felsic metavolcanoclastic rocks. Quartz veins and mafic dykes intersect and intrude these rocks locally.

The Lamego deposit is characterized by orebodies associated with banded iron formation (BIF) and gray quartz veins, in proportions that vary substantially from one orebody to another. The mineralized horizons are stratigraphically located above the metamafic rocks and below the carbonaceous schists, pelitic schists and metavolcanoclastic rocks.

3.1 –Structural Geology

The Lamego deposit is comprised by an overturned isoclinal antiform with its axis trending southeast (Figure 5). The antiform has a perimeter of approximately 4,800m and a

maximum width of 450m. Its limbs are oriented along an average strike of N35ºE with an average dip of 25ºSE.

Four orebodies are comprised in this overall structure (Figuras 5 e 6): Arco da Velha in the normal limb of the antiform; its counterpart, Queimada in the inverted limb; Cabeça de Pedra (hinge zone); and Carruagem in the northeastern end, where the limbs of the antiform are practically merged at shallower levels.

Drill holes have confirmed the continuity of the structure to a depth of at least 550m. Deeper drilling at Cabeça de Pedra and Arco da Velha orebodies indicated a flattening of the down-plunge (e.g., 16º at Arco da Velha orebody).

Faults with a general NW trend truncate a portion of Arco da Velha and Cabeça de Pedra orebodies, whereas NS faults locally disrupt part of the mineralized structure at the Carruagem orebody.

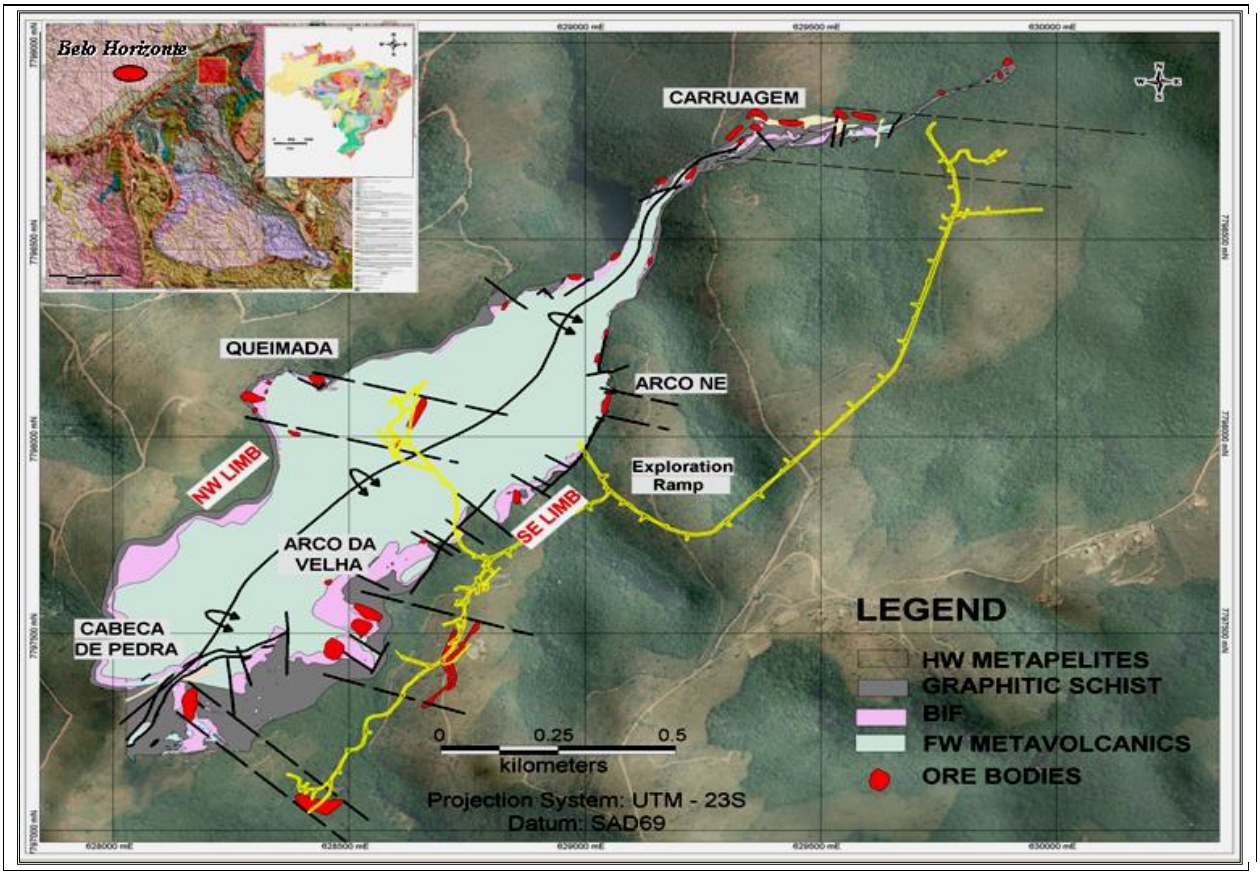

Figure 5 - Simplified geological map of the Lamego deposit. HW = hanging wall. FW = footwall.

The tectonic evolution proposed by Vieira (1991) and Toledo (1997) to explain the Lamego macrostructure consists of a D1 folding phase, followed by a D2 shearing phase. D1 folds correspond to non-cylindrical, normal to inclined antiforms. Anticline axis subparallel to the mineral stretching lineation are associated to D2 shearing. The stretching lineation, therefore, coincides with the fold axis. Foliation S1 is subparallel to the bedding; S2 is the axial plane of the macrostructure, parallel to the western, inverted flank (Queimada). Both foliations developed consonantly with shear zones, which function as channelways for ascending hydrothermal fluids.

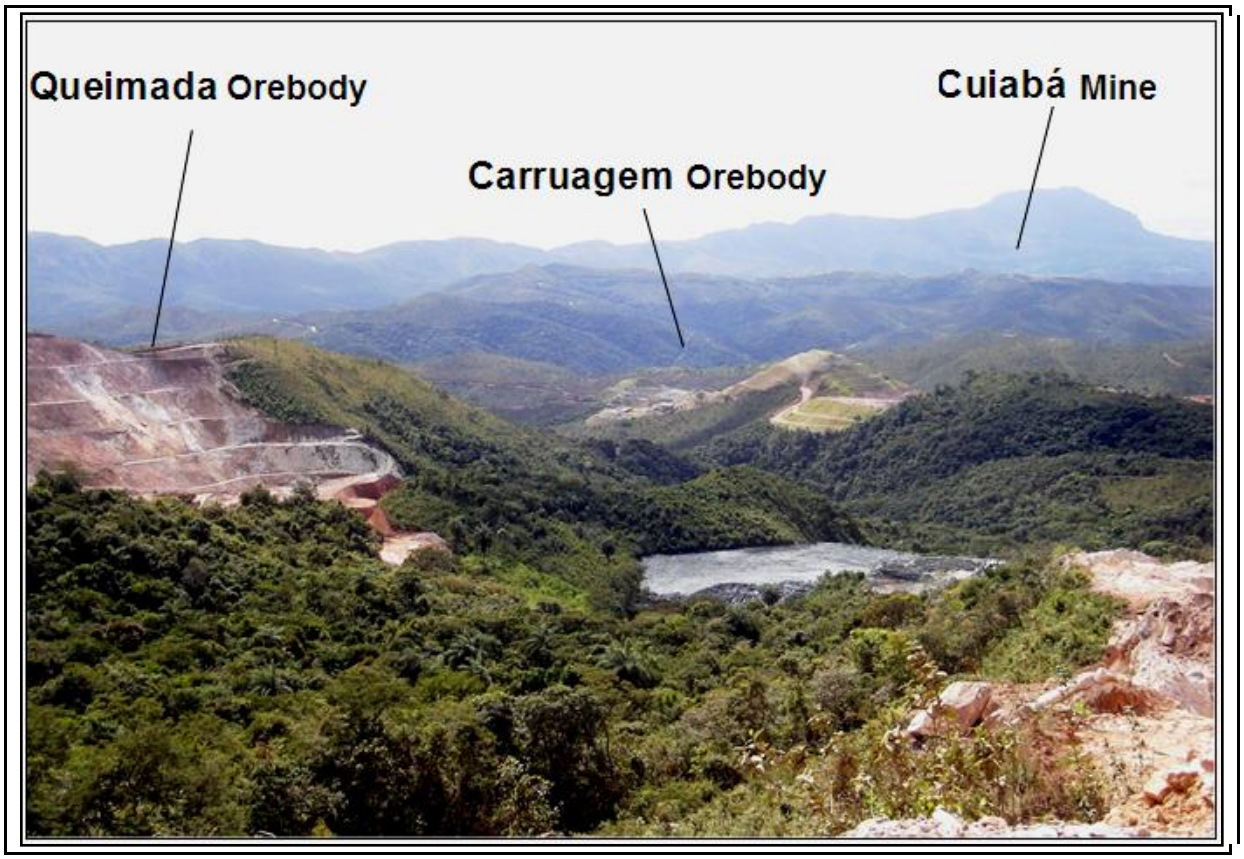

Figure 6 - Wide-angle view of Carruagem and Queimada orebodies (oxidized portion). The large gray patch in the center-right portion of the picture is the waste pile yielded from underground mining operations at the Lamego mine.

Approximately 134,000 meters of exploratory drilling were undertaken for the Lamego Project to date in order to properly reveal the structure of the deposit. The amount of drilling provides a notion of the geometric complexity of the mineralized zones as described on Chapter 2.

3.2 – Description of Lithologies

After conducting an extensive petrographic studies of drilling core samples from several gold mines hosted by greenstone sequences in the QF, Vieira & Oliveira (1988) named the rocks currently used in core descriptions, both at the mine and outcrops, as follows:

(i) Carbonate-quartz-sericite schist with gray carbonaceous matter (metapelite), locally coined as "**X1**". It occurs at the top of the stratigraphic column, either directly above the carbonaceous schist (**XG**) or intermixed with felsic metavolcanoclastic rocks (**XS**). It occasionally shows gradational, centimetric to decimetric bedding, with quartz-carbonatic bands that change to sericitic-carbonaceous bands. It often contains veinlets of quartz (Figure 7A).

(ii) Carbonate-plagioclase-chlorite-sericite-quartz schist (felsic metavolcanoclastic rock) or '**XS**'. This metavolcanoclastic rock is characterized by fragmented, roundish phenocrysts of bipyramidal quartz, indicating the occurrence of reworking in a marine environment. Gradational bedding is common.

(iii) Quartz-carbonate-sericite carbonaceous black schist or '**XG**'. This rock has a very fine grain size, and when associated with micro-folded quartzose veinlets, shows an anastomosed foliation. Slicken sides and fault striation is frequent, as well as pressure shadow zones around pyrite porphyroblasts (Figure 7B).

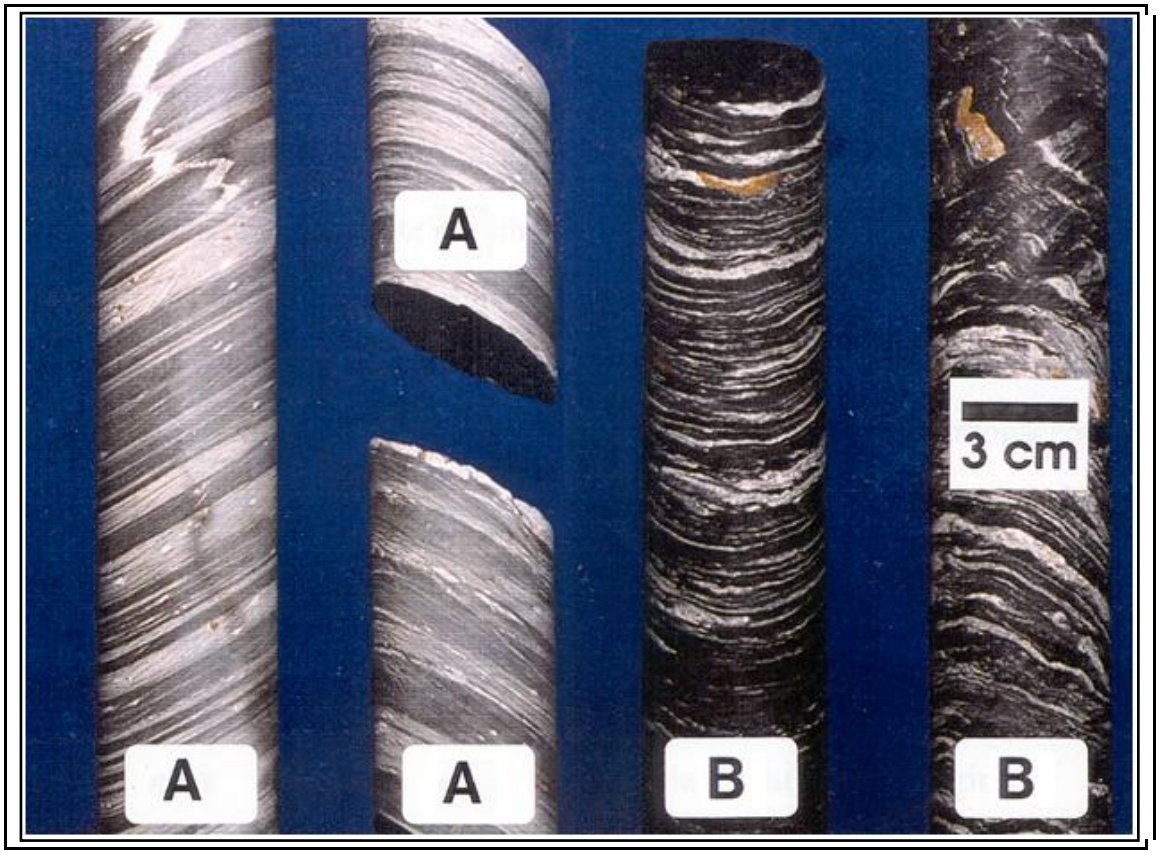

Figure 7 – Drilling cores: (A) Carbonate-quartz-sericite schist; and (B) Quartz-carbonate-sericite carbonaceous black schist.

(iv) Banded iron formation (**BIF**). It is composed of beige quartz-carbonatic bands alternating with white to light gray quartzose bands. The bands are generally centimetric, at times millimetric. Carbonaceous films may occur. Quartz-rich levels crop up across the BIF. Sulfidization layers are commonly in all orebodies (Figure 8).

(v) Gray quartz veins "**GQZ**", also interpreted originally as a metachert. These veins appear in shades of gray to dark gray and are usually compact. They typically display a particular texture that resembles jaguar hide. Locally they can be carbonate-rich and/or carbonaceous-rich; in the latter, an incipient foliation is observed. Recrystallization and association with quartz veins are frequent (Figure 9).

(vi) Sericite-chlorite-quartz-carbonate schist, or '**X2CL**', plus gray schist (carbonatization zone above mafic or intermediate rocks). This rock is marked by intercalations of beige sericite-rich and green chlorite-rich layers, usually showing a discrete foliation. The transition to X2 is

gradational. Both X2 and X2CL can contain carbonatic microporphyroblasts and quartz-carbonatic veinlets.

Figure 8 – Banded iron formation (brown portion) with hydrothermal alteration associated, crossed by quartz veins. Cabeça de Pedra orebody.

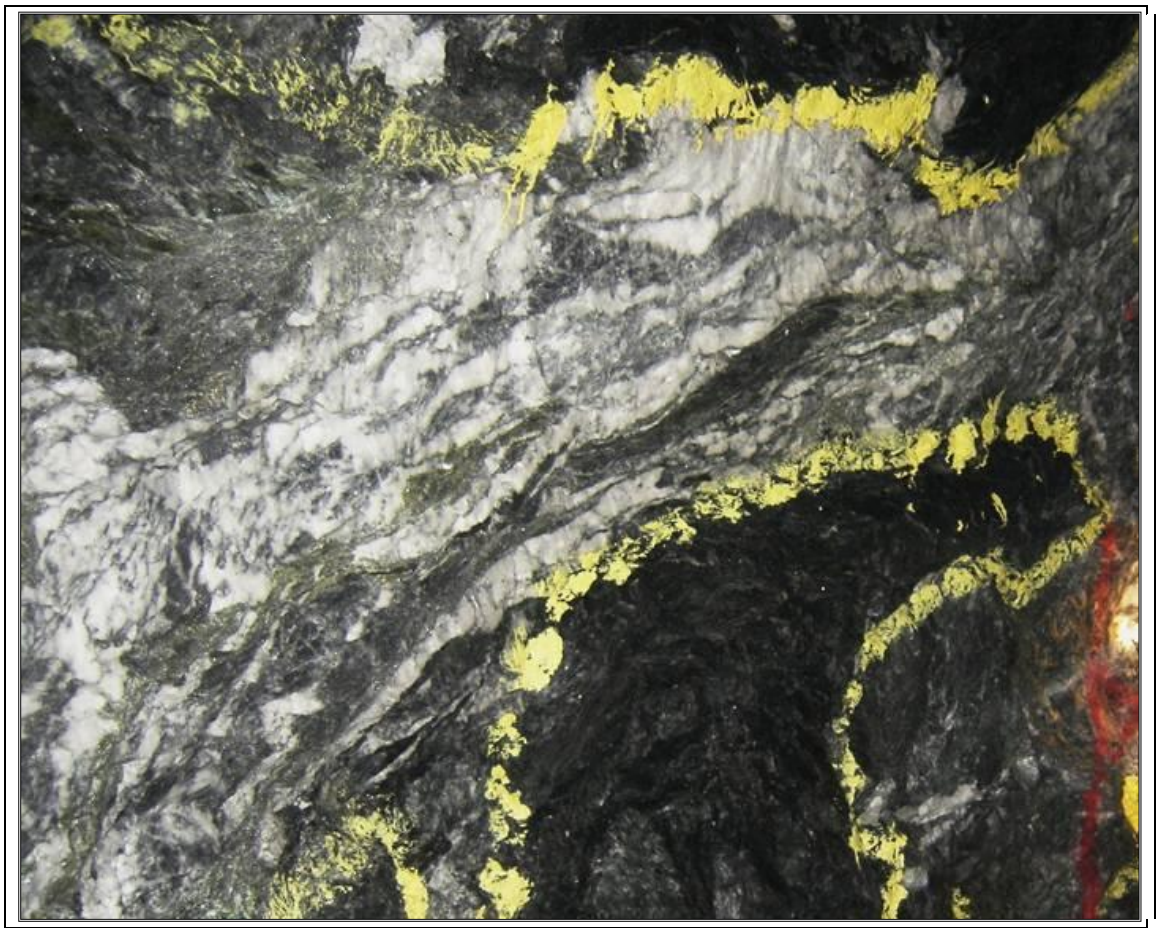

Figure 9 – Quartz vein in contact with carbonaceous schists in high strain zones. Yellow lines mark ore limits. Carruagem oreboby.

(vii) Quartz-carbonate-sericite schist, or '**X2**'. This rock appears in shades of beige and materializes the sericitization zone developed over the metavolcanic rocks. Foliation is incipient where carbonate prevails over sericite.

(viii) Quartz-carbonate-plagioclase-chlorite schist, or '**MANX**'. This rock is dark-green and correspond to chloritized metabasalt/andesite (Figure 10). It is marked by medium to pronounced foliation and by the presence of post-kinematic calcite porphyroblasts.

(ix) Metabasalt/meta-andesite, or '**MAN**'. This rock is composed of plagioclase, chlorite, quartz and actinolite. Albitized basalts occur stratigraphically below the BIF layer, in the center of the antiform, which makes them similar to andesites. These basalts are compact, occasionally display variolitic texture, and are replaced by clinozoisite in an actinolite/tremolite and chlorite matrix.

(x) Metadiabase, or '**MD**'. This is a dark green rock, with compact texture and composed of quartz, plagioclase, actinolite, chlorite and clinozoisite. It occurs in the form of dykes, and its coarse texture makes it distinguishable from MAN.

(xi) Carbonate-quartz-plagioclase-chlorite schist, or '**MDX**' (chloritized metadiabase). It occurs in the form of dykes, and is characterized by pronounced foliation.

Figure 10 – Contact of metabasaltic rock (top right corner) preserved of hydrothermal alteration, with metabasalt submitted at chloritization process.

3.3 - Hydrothermalism

The Lamego gold mineralization is associated to an orogenic type, with chloritization, carbonatation and sericitization hydrothermal zones dominantly found in metamafic volcanic rocks, and sulfidization zones in BIF and gray quartz veins.

The mineral assemblage observed in the regional metamorphism indicates weak metamorphism, with temperatures ranging from 350 to 430°C (Vieira 1991). The regional metamorphism contains carbonate as an accessory mineral, and plenty of epidote and actinolite, which indicates small proportions of aqueous fluid. The hydrothermalism is characterized by high CO2 concentration (plenty of carbonate) and larger proportion of water (absence of epidote and

actinolite, and presence of chlorite, which contains a larger proportion of OH in its structure). K, S, Au, As, B, and Ba, among other elements, have also been introduced together with H_2O and CO_2 during the hydrothermalism (Vieira 1991).

The magmatic textures, including pillows and variolites in metabasalts, are largely obliterated inside the hydrothermal zones. The hydrothermalized rocks are mylonites with boudinated, sigmoidal, or folded quartz veins. Microscopically, they are characterized by an anastomosed mylonitic foliation, S-C structures, and rotated, recrystallized poikiloblasts with pressure shadows. The minerals have been elongated and stretched along the main lineation. Quartz, carbonate and albite show dynamic comminution and recrystallization, notably a growth of both quartz and carbonate grains (Vieira 1991). Hydrothermalized schists show ductile deformation features, whereas in BIFs the deformation is ductile-brittle to ductile. Moreover, BIFs also show tension gashes, micro-faults with rotated blocks, and breccias.

The following hydrothermal zoning at Lamego deposit and its surroundings was developed above the mafic rocks (Figure 11), associated with D1 deformation phase responsible for the antiform macro structure:

(i) Chloritization zone (MANX): Marked by strong mineral hydration, with transformation of amphibole into chlorite, which is the dominant mineral in the zone. Dynamic recrystallization of the plagioclase and discrete carbonatization (replacement of plagioclase by calcite) are also typical features of this zone;

(ii) Carbonatization zone (X2CL): The carbonate, which is the dominant mineral, becomes richer in iron, ankerite or ferroan dolomite, being a product of plagioclase transformation. Discrete sericitization, turmalinization and sulfidization also occur within this zone;

(iii) Sericitization zone (X2): Sericite, the ubiquitous mineral in this zone, occurs in association with chlorite. Discrete albitization and turmalinization and discrete to pronounced sulfidization and silicification are observed here.

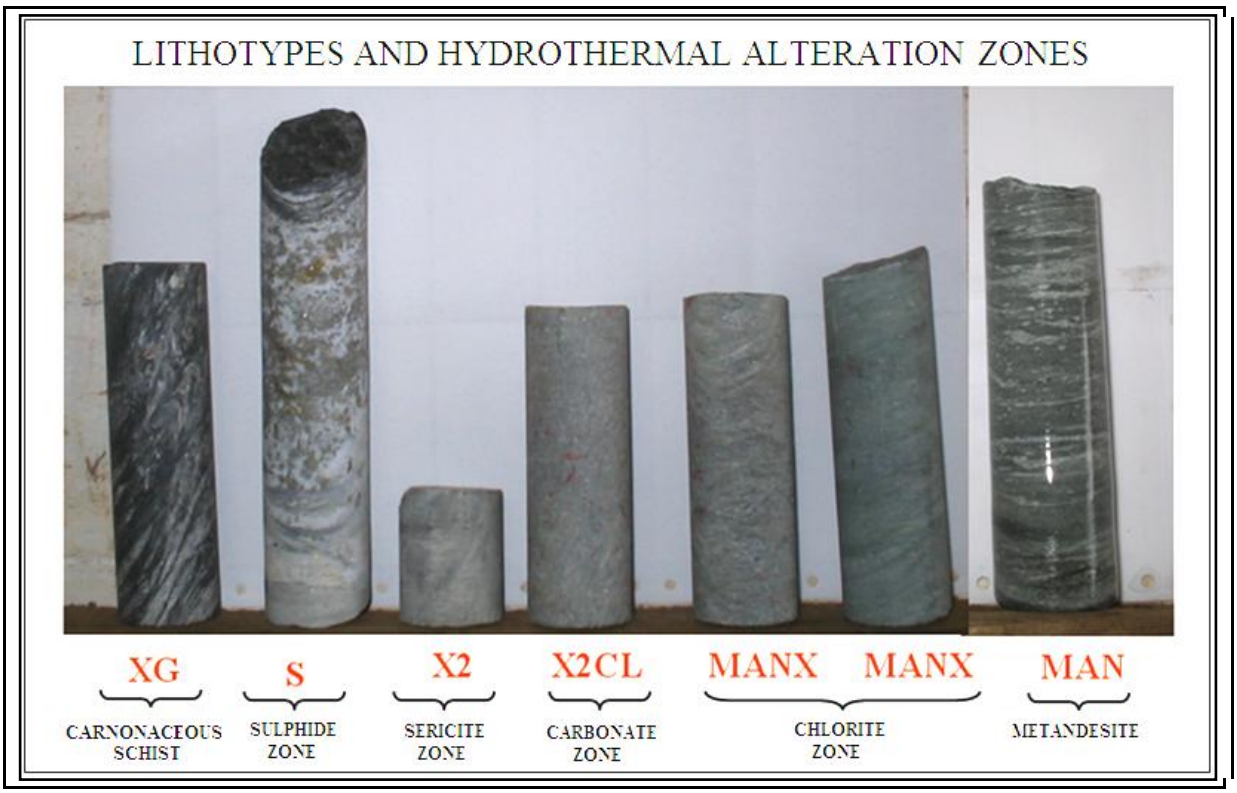

Figure 11 – Main hydrothermal alteration rocks of the Lamego Deposit.

3.4 - Mineralization

The orebodies comprise both BIFs and gray quartz veins and are characterized by sulfidization either in bands, disseminated or as fracture fillings. The plunge of the ore shoots coincides with the mineral stretching lineation.

The sulfidized bodies hosted by BIF at Lamego correspond to type 2 as defined by Vial (2007) and are composed of pyrite, and subordinately pyrrhotite and arsenopirite. The sulfides fill fractures together with quartz, and replace carbonate-rich bands in the BIF either symmetrically or asymmetrically to the fracture.

In contrast to the Cuiaba deposit, the gray quartz veins at Lamego form a stratabound horizon that is usually in contact with the BIF layer. These masses of gray quartz can show an irregular shape, boudinated or not, discordant to the bedding, which provides further evidence of its hydrothermal, structurally-controlled origin. The greater resistance of the quartz veins to deformation is responsible for its differential shearing, which creates conditions for the accumulation of sulfides and native (free) microscopic gold in fractures. Secondarily, gold is found included in pyrite grains. These gray quartz veins show the “jaguar hide” texture - a feature

attributed to the high content of fluid inclusions. In some places there are decimetric to metric portions of BIF 'floating' in the quartz vein, suggesting that the original BIF has been consumed by the silica-rich hydrothermal fluid.

The mineralization controls appear to have a very strong structural component, being associated with shear zones, folds, or host-rock replacements along bedding, fractures, foliations or shear zones. The orebodies were substantially deformed, and occasionally the hosting carbonaceous schists and nearby quartz veins can contain gold. The gold distribution is very irregular, with the orebodies showing great variation in thickness and grade, both along strike and plunge directions. The delineation of these orebodies (mining areas) is performed chiefly by chemical determination.

The gold at Lamego forms an alloy with silver, with a gold-to-silver ratio of 7:1 (Ribeiro-Rodrigues 1998), either as xenomorphic grains or as fillets, along fractures in sulfide grains. Gold associated with pyrrhotite is the coarsest particle (i.e., 50µm to 120µm in size), usually occurring along the margins of the grains. Gold associated with pyrite is 10µm to 50µm in size, and occurs essentially as inclusions. Gold associated with arsenopyrite (as inclusions) and gangue (inclusions or at the interface of the grains) is typically less than 10µm in size (Vieira 1991).

3.5 - Orebodies

Carruagem Oreboby

The Carruagem orebody is located at the junction zone of the two flanks in the NE portion of the major structure. At the first level, it is a boudinaged orebody with two large disruptions of the structure, which are followed by eastward displacement. The structures trend 34^{o}NE along the strike, and the plunge is approximately 95^{o}/22^{o} (Figure 12).

The mineralization is not directly associated with sulfidation, given that native (free) gold is frequently found in samples extracted from sampling channels and boreholes. Stratabound gray quartz veins are the dominant host to the gold. No key reef horizon has been identified for the mineralization, which occurs in a disseminate manner and therefore renders difficulties for the conduction of a representative channel-sampling campaign.

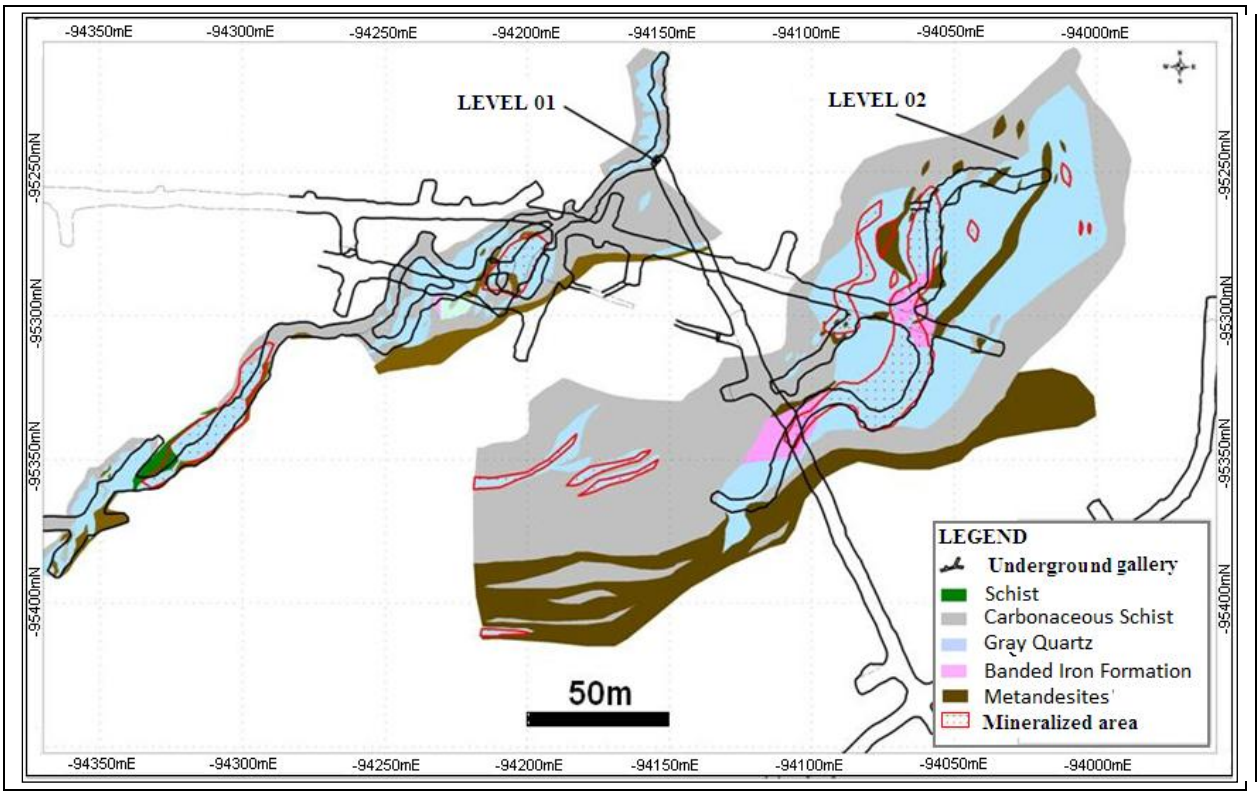

Figure 12 – Geological map of the Carruagem orebody and the mineralized area – Levels 1 and 2.

Disruptions are also observed in level 2, including major displacements of more than 30m. Level 2 comprises portions of BIF within gray quartz masses and vice versa (Figure 13). Differently than observed at level 1, the two mineralized limbs at level 2 are not evident. This is because the metandesite positioned between the limbs is highly altered (X2 and X2Cl) and disrupted, making the interpretation difficult.

High sulfidization portions are usually found in the Carraugem orebody, mainly associated with gray quartz masses (Figure 14).

Figure 13 – Islands of BIF preserved with high sulfidation within a gray quartz mass - Carruagem orebody.

Figure 14 – Drillcore sample with aggregates of pyrites within gray quartz mass.

Cabeça de Pedra Orebody

The Cabeça de Pedra orebody is located in the hinge region of the large Lamego structure. The area that shows economic feasibility contains 70% of BIFs and 30% of gray quartz veins. The presence of faulting makes stratigraphy difficult to follow in certain places (Figure 15). Usually, XG and metapelites (X1) occur in the hanging wall contact, and meta-andesites in the footwall. The average plunge measured for this orebody is 125º/25º.

The development in this orebody is concentrated in the excavations of the ramp to reach level 2.

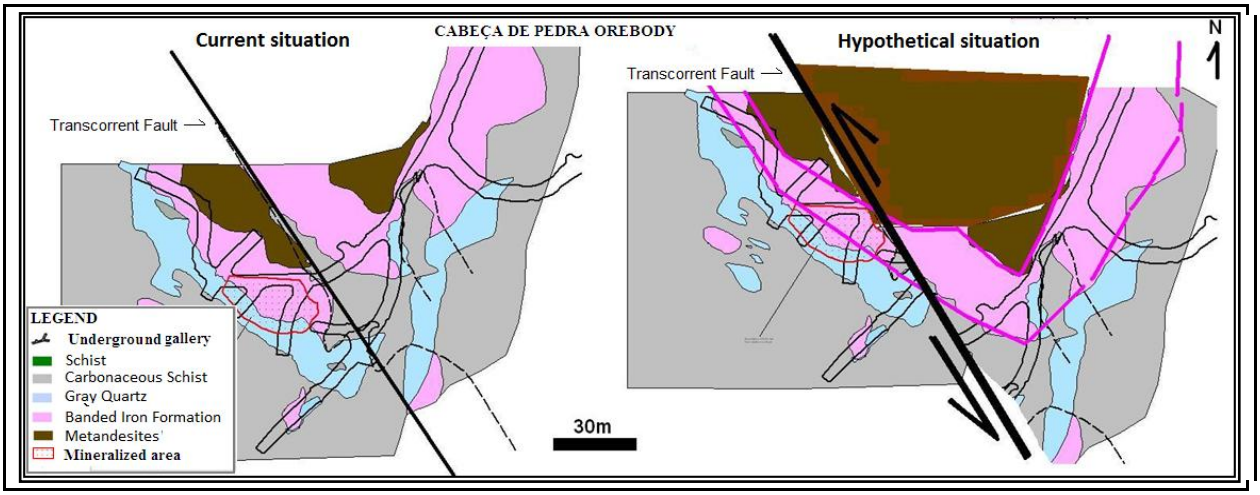

Figure 15 – Geological map of the Cabeça de Pedra orebody and mineralized area – Level 01

Arco da Velha Orebody

The Arco da Velha orebody is located in the normal, eastern flank of the large fold. It extends approximately 250m (level 01) along the strike. In the northeastern portion of the orebody, the mineralization is concentrated in the gray quartz veins, whereas in the southeastern portion it is concentrated in the BIF. XG and X1 occur in the hanging wall contact, whereas the hydrothermal alteration zone marked by the metandesite (MANX) occurs in the footwall (Figure 16).

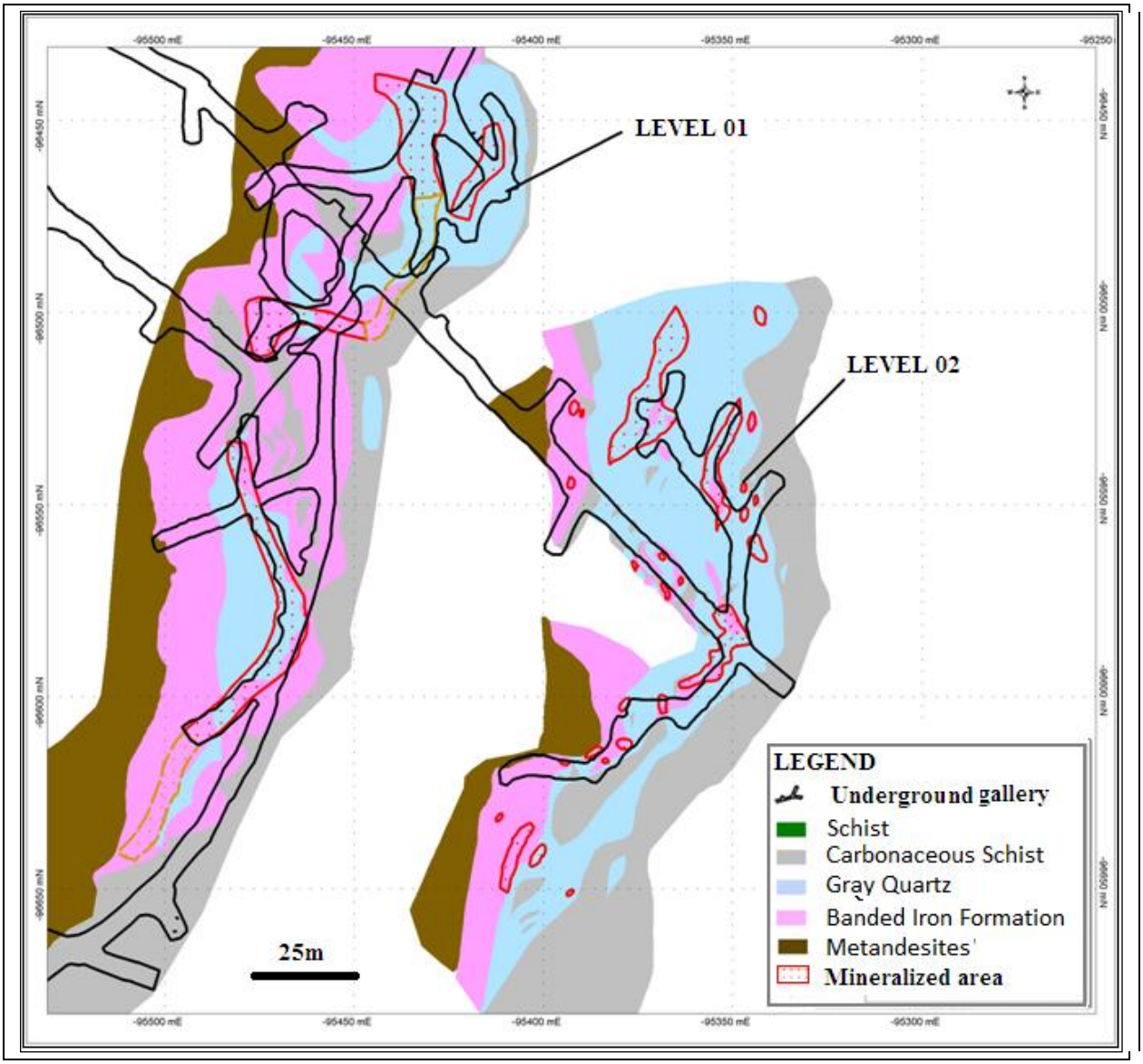

Figure 16 – Geological map of the Arco da Velha orebody – Levels 1 and 2. Mineralized domains are highlighted in red.

The BIF and gray quartz masses structure are very thick, but the mineralization does not occur in the entire structure. This situation poses some difficulties to the development and mining along the orebody, since there are no geologic guides such as lithological contacts to be followed. There is no preferred horizon for the enrichment – the mineralization occurs near to the footwall contact, in the hanging wall contact and in the center of the structure.

Usually, the mineralized portions are also rich in pyrite, although the occurrence of high percentages of pyrite with low gold grades, or no gold at all, is common. In order to minimize

errors and optimize the development, horizontal drilling campaigns are conducted at the level of the development, thus making it possible to predict the behavior of the mineralization along the strike.

At level 01, only two barren spots interrupting the mineralized structure were mapped. At level 02, however, the number of barren gaps between mineralized portions is significantly larger, with parallel structures occurring at close distance from each other, which makes them more difficult to mine because of rock stability problems.

The structures usually strike NE-SW with an average plunge of 105º/25º.

Queimada Orebody

This orebody is located in the inverted or western flank of the large fold. At level 1, only 90m of the mineralized zone (considering a total of 250m along the strike) showed economic feasibility. BIFs are dominant, with mineralized gray quartz veins occurring mainly in the footwall contacts of the structure. In contrast to what is observed in the normal flank (Arco da Velha orebody), the hydrothermal alteration zone (metandesites, X2 and X2Cl) occurs in the hanging wall contact, whereas the metapelites and XG are detected in the footwall (Figure 17). The average plunge of this orebody is 102º/29º.

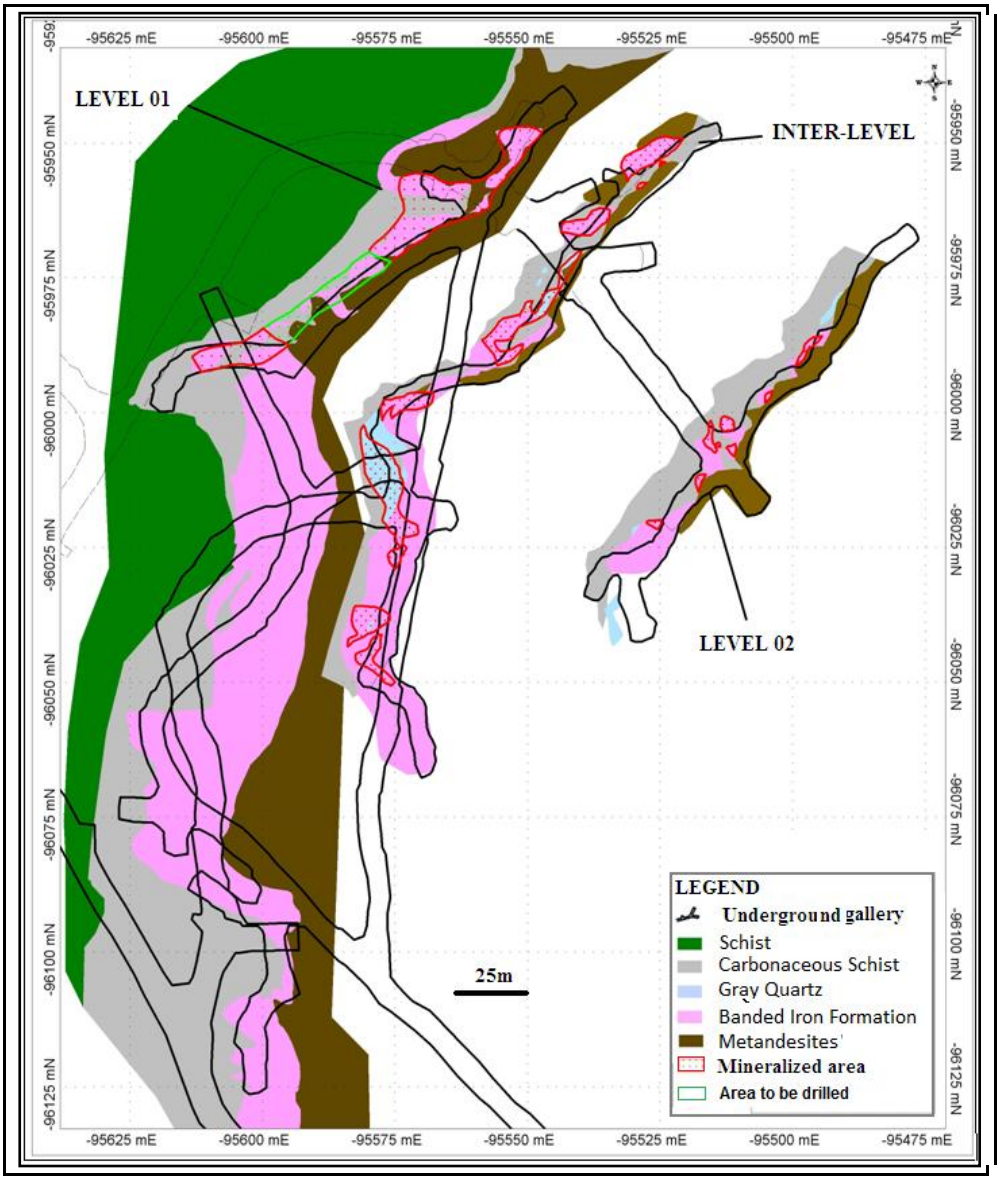

Figure 17 – Geological map of the Queimada orebody: levels 1 and 2 and intermediate level.

In addition to level 1, two other levels are exposed, namely: the intermediate level (12m below level 1) and level 2 (50m below level 1).

The NE portion of the structure is characterized by thin BIF layers, which makes it possible to observe the FW (XG e X1) and the HW (MAN) contacts. There are interruptions in the structure at the contact of XG with MAN. In this portion, the intermediate level, which is composed of extremely sulfidized BIFs (mainly pyrite and arsenopyrite), shows high gold grades.

The SW sector is characterized by a thicker BIF and therefore the underground development does not always expose the HW and FW contacts. Although the structure here is

more continuous, gold grades are lower. Level 2 showed a negative result for the mining activity because the mineralized portions were very small and with grades lower than expected.

4 – METHODOLOGICAL BACKGROUND

In this chapter, the employed methods are presented as follows: (i) firstly, details are given about the airborne geophysical survey and pre-processing and processing procedures applied to the data; (ii) secondly, background work on geophysical inversion processes and the application of inversion algorithms to the EM data are presented; (iii) thirdly, the applied ground IP technology, including program, methods, arrangement and interpolation, beyond inversion of the resistivity and chargeability themes, are described; (iv) fourthly, multi-thematic fuzzy-Boolean models are explained as to assist in integration of multi-source data. This last method was applied only for the Morro da Glória deposit.

The final results obtained on the basis of each applied methodology are presented in the following sections, combined with the geological and geochemical results individually for each deposit and satellite target.

4.1 – Airborne Geophysics – SPECTREM

In 1982, the Anglo American Corporation (AAC) hired the A-Cubed firm from Toronto, Canada, to built a new wideband, digital, towed bird AEM system called PROSPECT 1 (Annan, 1986). In 1988, the development of the system was taken over by AAC. After extensive modifications, the prototype system became operational in 1989, when it was coined SPECTREM. In 1990, a new research and development program started and all the electronic hardware and software were replaced in the system. At the completion of the program in 1993, noise levels were reduced by a factor of 5 compared to the original prototype system. Since 1993, further upgrades have been made to increase the reliability of the system and further reduced its noise levels (Klinkert *et al.,* 1997).

The SPECTREM system has a time domain STEP response that was chosen because of its wide bandwidth and better geological noise rejection in the search for highly conductive massive sulphide bodies. At 90Hz base frequency, SPECTREM's bandwidths cover delay times with

window centers from 22 to 4156 microseconds versus the 220 to 3300 microseconds off time window centers of the PULSE system. The SPECTREM delay times result in a better shallow sounding capability (Klinkert *et al.,* 1997).

Processing of airborne data – SPECTREM

In this study, in addition to processing the geochemical and geological information used in three-dimensional modeling of the gold-bearing mineralization in the Lamego, digital data were also used from an aerial geophysical survey by AngloGold Ashanti Brasil Mineração Ltda called "Spectrem Airborne Electromagnetic Survey-2002". Electromagnetic (EM) data only was used here, particularly for identifying regions with advanced sulphitization processes and, consequently, with gold-bearing potential.

Some of the most important pre-processing of the EM data is conducted directly on the aircraft during the data acquisition. The data are subjected to a de-convolution to remove unwanted signals and converted to square waves. The next step in processing is to separate the signals into 8 channels or windows. As the SPECTREM system initiates measurements to connect the transmitter, it is necessary to separate the primary field (transmitted) from the secondary field (induced). The last channel measures only the primary field. So, it can be subtracted from the other channels to separate the secondary electromagnetic field, finally resulting in 7 channels from which geological information can be extracted (Spectrem Aerial Survey 2002).

The spikes in the lines were removed using Naudy-type three-point filters. Decorrugation filters were applied to reduce the “fishbone” effects created by geometric anisotropy inherent to the aerial electromagnetic system. Micro-leveling processes were applied in all 7 EM channels to reduce small residual errors, which were not effectively subtracted in the drift corrections made directly on the aircraft.

Anomalies in the magnetic and electromagnetic data caused by anthropogenic influences, (e.g., power transmission lines at various magnitudes, near electrical transformers, and aerial ropeways used to transport gold ore to the processing stations), were removed or smoothed out. Figure 18 briefly illustrates the main characteristics of the airborne geophysical survey.

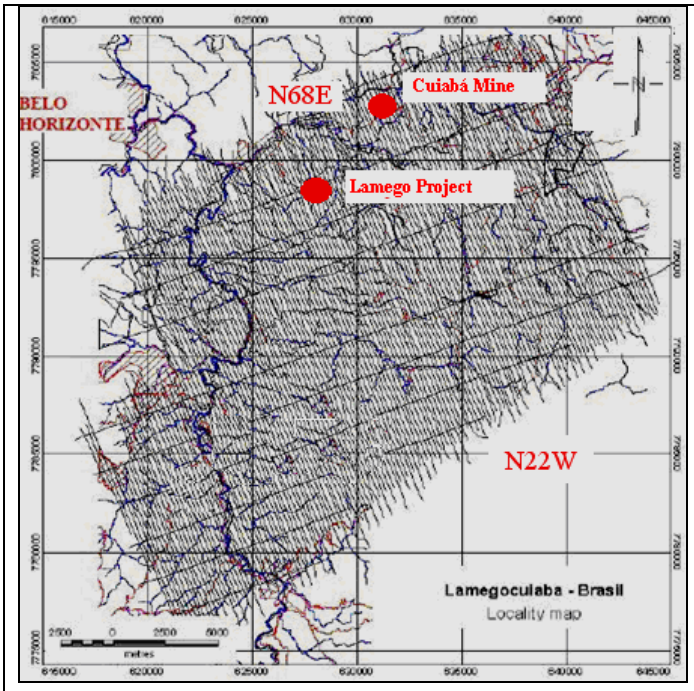

SUMMARY OF SPECIFIC DETAISL OF THE AERIAL SURVEY	
Aircraft type	DC3 – TP67
Nominal aircraft speed	60 m/s ~ 216 km/h
Nominal aircraft altitude	90m
Nominal flight-line direction	158 = N22W
Nominal flight-line spacing	200m
Nominal tie-line Direction	248 = N68W
Nominal tie-line spacing	2000m
EM Base Frequency	90 Hz
Acceptable Kilometers flown	2504 Km
Projection\Datum	UTM zone 23S - WGS 84

Figure 18 – Details of the airborne geophysical survey. Spectrem Airborne Electromagnetic Survey-2002 by AngloGold Ashanti Brasil Mineração Ltda.

4.2 – Geophysical Inversion - Background

Geophysical inversion processes have been applied to various mineral deposits over the last several years with the objective of (i) estimating the depth of the magnetic or conductive bodies, or bodies with distinct physical properties; (ii) better defining the lateral and longitudinal range limits of mineralized areas; and, (iii) assisting in exploration, mainly with base metals, gold and iron.

Li & Oldenburg (2003) discuss the historical development of the inversion process through their Logarithmic Barrier method using conjugated gradients. Phillips *et al.* (2001) applied geophysical inversion processes to a volcanogenic massive sulphide deposit of copper-zinc in San Nicolas, Mexico. These authors showed that by inverting terrestrial magnetometry, induced polarization (IP) and gravimetric data, they were able to successfully characterize the geometry of the main mineralized bodies.

Silva et al. (2001) demonstrated the importance of using reference models defining the constraints limits in the inversion processes. These limits can be, for example, known three dimensional lithological areas which have physical characteristics that are compatible with the

geophysical method applied. These limits assist in filtering out non-uniqueness from the solutions provided by the inversion process.

Dentith (2003) published a set of geophysical signatures of Australian mineral deposits, which represented a milestone in Australian geophysics at the beginning of the decade. Of the 21 case histories presented, nine used geophysical inversion and produced significant results.

Oldenburg & Pratt (2007) contributed to a complete analysis of the application of the geophysical inversion process, characterizing in theory and in practice, details for inversion procedures in mineral exploration. According to the authors, the last decade was marked with major advances in the process of the inversion of various types of geophysical data. Advances have been promoted mainly by the development optimization mathematics, visualization and computational power.

In addressing of the inversion problem applied to mineral exploration, Oldenburg & Pratt (2007) created three large categories: Type I: Discrete Body Inversion; Type II: Pure Property Inversion; and, Type III: Lithologic Inversion.

Type I: Discrete Body Inversion

The inversion problem is formulated to find a relatively small number of homogeneous bodies which may not completely fill a 3D volume. The physical property, size or form of the body can also be evaluated. The bodies can be simple volumetric plates, ellipsoids or complex geological forms that can be parametrically described.

Simple parameterization or multiple bodies are used to model discrete changes in the properties of underground rocks. Each surface includes a volume of rock which has uniform physical properties. Examples of forms that can be adequately modeled are illustrated in Figure 19.

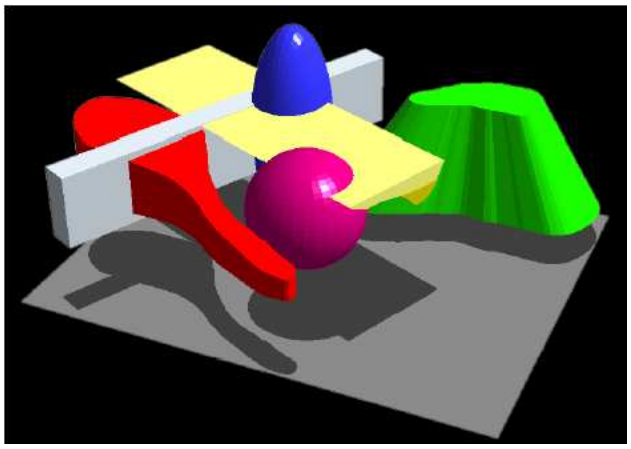

Figure 19: Example of discrete surfaces enclosing volumes of uniform physical properties. Shapes include an extruded map polygon, an extruded polygonal section, an ellipse, a sphere, a frustum, and a tabular body. Discrete bodies can be combined to construct complex geologic models (Oldenburg & Pratt, 2007).

In Figure 19, the sphere, the ellipse and the tabular body all have simple analytical expressions and can be easily parameterized. The solids with polygonal sections can be manipulated in a map view or section.

The advantages which result from the use of the parameterization method include: (i) speed of the inversion process; (ii) focus on target anomalies; (iii) pre-prepared parameterizations for some known forms; (iv) Easy representation of geological limits; (v) covers the properties of most volumetric solids; (vi) estimation of the depth of the top of the anomaly; (vii) estimation of the three dimensional position of geological bodies; (viii) possibility of more refined details of the geological limits.

Research that uses the Type I inversion process has been focused on locating body extensions with simple forms, with the aim of emulating the problems of complex geological models, which assists in more detailed investigations of mineral deposits.(Pratt, Foss e Roberts, 2006).

Type II: Pure Property Inversion

The objective of this inversion is to find a function which characterizes the distribution of the physical property. As a generic example, one can obtain an appropriate model "m" by minimizing the objective function:

$$\phi_m(m) = \alpha_s \int_\Omega w_s \left(m - m_{ref}\right)^2 dv + \alpha_x \int_\Omega w_x \left[\frac{d\left(m - m_{ref}\right)}{dx}\right]^2 dv +$$
$$\alpha_y \int_\Omega w_y \left[\frac{d\left(m - m_{ref}\right)}{dy}\right]^2 dv + \alpha_z \int_\Omega w_z \left[\frac{d\left(m - m_{ref}\right)}{dz}\right]^2 dv \quad \textbf{(1)}$$

In equation (1) from de Oldenburg & Pratt (2007), the m_{ref} is a reference or initial model of the inversion process. The coefficients α control the relative importance of smoothing in various directions, comparing to the approximation of the background, and *w(s)* are functions of weight. All these parameters must be specified for the inversion process and the complexity is a function of what is known about the model. For example, in a greenfield area, the reference model can be a uniform volume, while in an area where there is a known deposit (brownfield), the reference model can have a more complex structure with various sizes and shapes. The functions of weight can also be used to help honor the prior information in various positions in the model.

Additional information about Type II inversions can be found in Oldenburg & Pratt (2007).

Type III: Lithological Inversion

In this case, the inversion problem is formulated in a geological area and the relationship between the rock units and physical properties must be well understood. Each cell in the model has one particular type of rock related to it. The cells are completely filled with volumes. One cell can have a small rectangular unit (as used in the problem applicable to Type II), a discrete large body (as in the Type I example), or a combination of the two. The difference is that the parameters can be associated with the location of the boundaries and/or the rock type.

The classifications above are mainly to be understood as a structure, and secondly as a way to categorize different inversion algorithms. Many existing algorithms can be executed in

more than one category. For example, the VPmg algorithm (Fullagar 2004) can change the location of an interface or can find a smooth distribution of the properties of a defined geological unit. Therefore, it has elements that can be characterized as both Type I and Type II and depending on its implementation, can be considered as a Type III inversion. Similarly, the existence of a reference model allow the inversion of UBC-GIF operating in Type II or Type III mode. ModelVision (Pratt *et al.* 2007) can also be thought of as a hybrid model which incorporates methodological aspects of Type I and Type III together. Other formulations, such as the geostatistical inversion of GeoModeller (Guillen *et al*. 2004) and the stylized inversions of QuickMag (Pratt *et al.* 2001) are more directly categorized as Type III inversions.

The important thing is that all types share a similar objective of trying to extract a coherent geological interpretation from geophysical data. The adopted procedure, more than anything, depends on the limits of the area, the scale of the geological information, precision, relative cost, processing time and interactivity. Processing time is not proportionate to the number of parameters and can vary from seconds to days (Oldenburg & Pratt, 2007).

Geophysical inversion is normally applied along parallel line sections of the survey to estimate the depth of the conductive mass in the respective section. However, the inversion can also be done in three dimensions, where the spacing between the sections is close enough, in a situation where three dimensional interpolations are permissible. The product of this process is defined by a model of matrix blocks, which makes an integrated visualization with other three dimensional information possible. This facilitates the process of understanding the geology of the study area and as a consequence, contributing to better one's economic resources.

4.3 – Ground Geophysics Survey - Induced Polarization and Resistivity

Basic Concepts

Induced polarization (IP) was used in the past mainly in the exploration of base metals and, to a lesser extent, the search for groundwater. Although the Schlumberger brothers, pioneers in exploration geophysics, have recognized the phenomenon of induced polarization for at least 60 years ago, its popularity as an exploratory tool came to light only in the mid 1950s (Telford *et al.*, 1990).

An illustration of induced polarization can be obtained by a pattern of four electrodes in a scattering of DC resistivity, by an abrupt cessation of the current. The voltage crosses the potential electrodes and generally is not remitted to zero instantaneously, but is reduced relatively slowly after a large initial decrease in the original fixed value. If the current is turned on again, the potential, after a sudden initial increase, builds up over a time interval similar to the original amplitude (Telford *et al.*, 1990). Figure 20 shows the sources of the induced polarization effects in comparison of the decay curves and RC circuit.

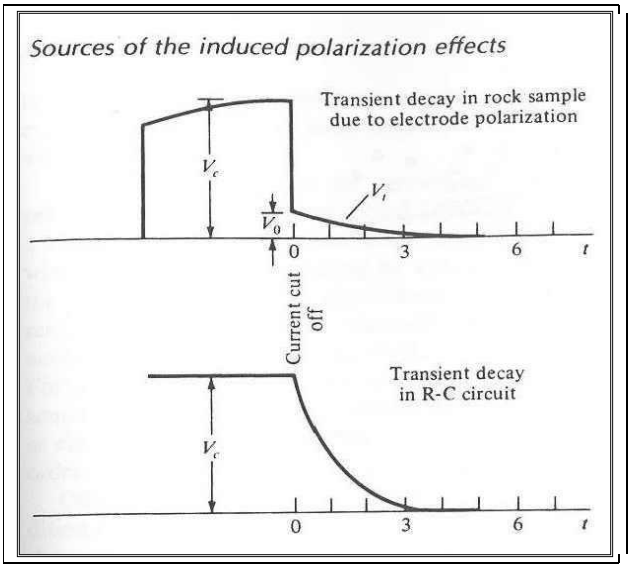

Figure 20 – Comparison of the decay curves and RC circuit (Telford *et al.*, 1990).

In one type of IP detector, the decay voltage is measured as a function of time in various ways. This method is known as IP in the time domain. Because the accumulation time is also finite, it does not interfere with the apparent resistivity (complex impedance) and should vary with the frequency, decreasing as the latter increases. Thus, the measure of ρ_a from two or more frequencies, usually below 10 Hz, is another detection method. The latter is known as the IP in the frequency domain. Figure 21 shows different measurements of the IP effect in the time domain: (a) Comparison between *V(t)* and *Vc*; (b) *V(t)* integral in a time interval (Telford *et al*. 1990).

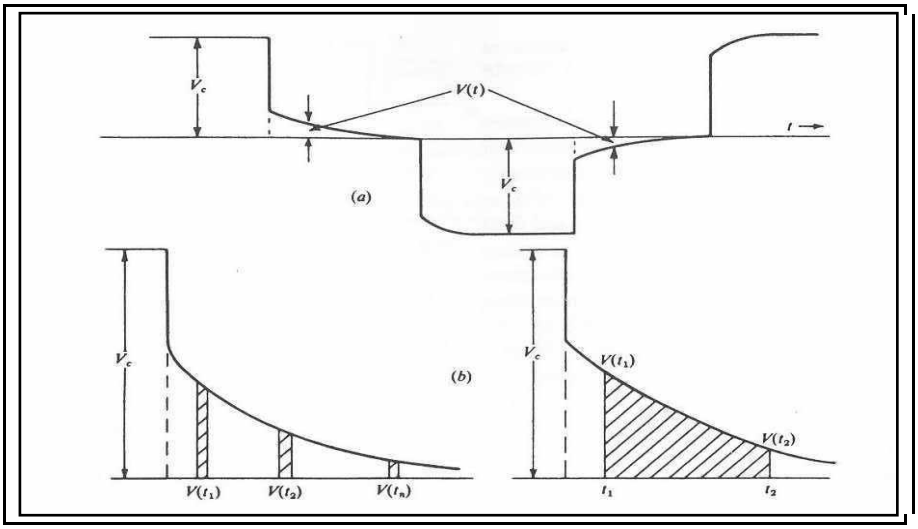

Figure 21 - Different measurements of the IP effect in the time domain. (a) Comparison between V (t) and Vc; (b) V (t) integral in a time interval (Telford *et al*. 1990).

The chargeability effect can be established by:

$$M = 1/V_c \int_{t_1}^{t_2} V(t)\, dt \qquad [1]$$

and is most commonly used to measure the IP effect in the time domain. When *V(t)* and *Vc* have the same unit, chargeability is measured in milliseconds.

Although types and levels of mineralization do not yet have fixed IP value response, tables prepared by Telford *et al*. (1990) were made through the empirical evaluation of field results. Table 1 lists chargeability values of a set of minerals in a concentration of up to 1% of the total sample. The duration of the current of the square-wave was 3s and decay was integrated over 1s. These figures seem to be somewhat high as compared to regular field measurements, since no currents are used with very long time cycles or such a long integration of the full-time decay curve.

Table 1 – Chargeability of some minerals, Telford *et al*. (1990).

Mineral	Chargeability (ms)
Pyrite	13.4
Chalcocite	13.2
Copper	12.3
Graphite	11.2
Chalcopyrite	9.4
Bornite	6.3
Galena	3.7
Magnetite	2.2
Malachite	0.2
Hematite	0.0

Table 2 shows responses of various types of rocks, mineralized or not. In this situation, the charge time was long (~1min) and the decay curve was integrated throughout its duration (except for the initial transient and final noise).

Table 2 – Chargeability of some rocks, Telford *et al.* (1990).

Material	Chargeability (ms)
20% sulfides	2,000 – 3,000
8 – 20% sulfides	1,000 – 2,000
2 – 8% sulfides	500 – 1,000
Volcanic tuffs	300 – 800
Sandstone, siltstone	100 – 500
Dense volcanic rocks	100 – 500
Shale	50 – 100
Granite, grandodiorite	10 – 50
Limestone, dolomite	10 – 20

One of the first applications of 2D inversion in mineral exploration was in the Century zinc deposit, in Australia (Mutton 1997). There the mineralization occurs preferentially associated with a carbonaceous schist unit with fine grains of sphalerite and galena and, secondarily, pyrite. A pseudo-section of apparent resistivity is shown in Figure 22. Before using the inversion process, the standard method for interpreting these data was to make inferences using pseudo-section compilations. Each sample, however, represents an overall average of the conductivity and the volume of sensitivity is dependent on the positions of current and receiver

electrodes. Only under rare circumstances did the image or presentation of the data approximate the geology.

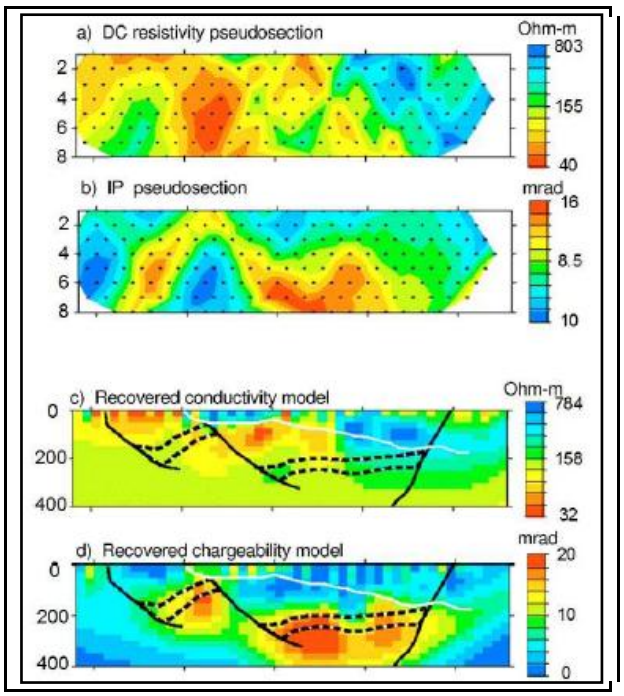

Figure 22 - Pseudo-sections of resistivity and IP are shown in (a) and (b), respectively. Inverted sections of conductivity and chargeability are shown in (c) and (d), respectively (Mutton 1997, quoted in Oldenburg & Pratt 2007).

5 – GEOPHYSICAL RESULTS AT LAMEGO DEPOSIT AND SÃO JOSÉ TARGET

The results presented in this section comprises an integration of geophysical, geological and geochemical information from the Lamego deposit and São José target. Results for others targets (Biquinha, Sobradinho, Bom Caminho and Morro da Glória) are also presented individually in the subsequent sections.

5.1 – Electromagnetic Results of Lamego Deposit

The electromagnetic results obtained by the Spectrem survey in the region of the Lamego deposit highlight a major anomaly in the Tauz Channel in a peripheral area with dimensions that approximate the dimensions of the mega-structure of the deposit. This anomaly has, at the surface, displacement in the direction of the dip of the main ore bodies. As the Tauz Channel has investigation characteristics at depths greater than 150m, the anomaly allowed the visualization of

the continuity in depth of the electromagnetic conductive bodies, which, in this case, are represented by bodies with prominent sulphidation along with an envelope of carbonaceous schist, which together accentuate the intensity of the anomaly (Figures 23A and 23B).

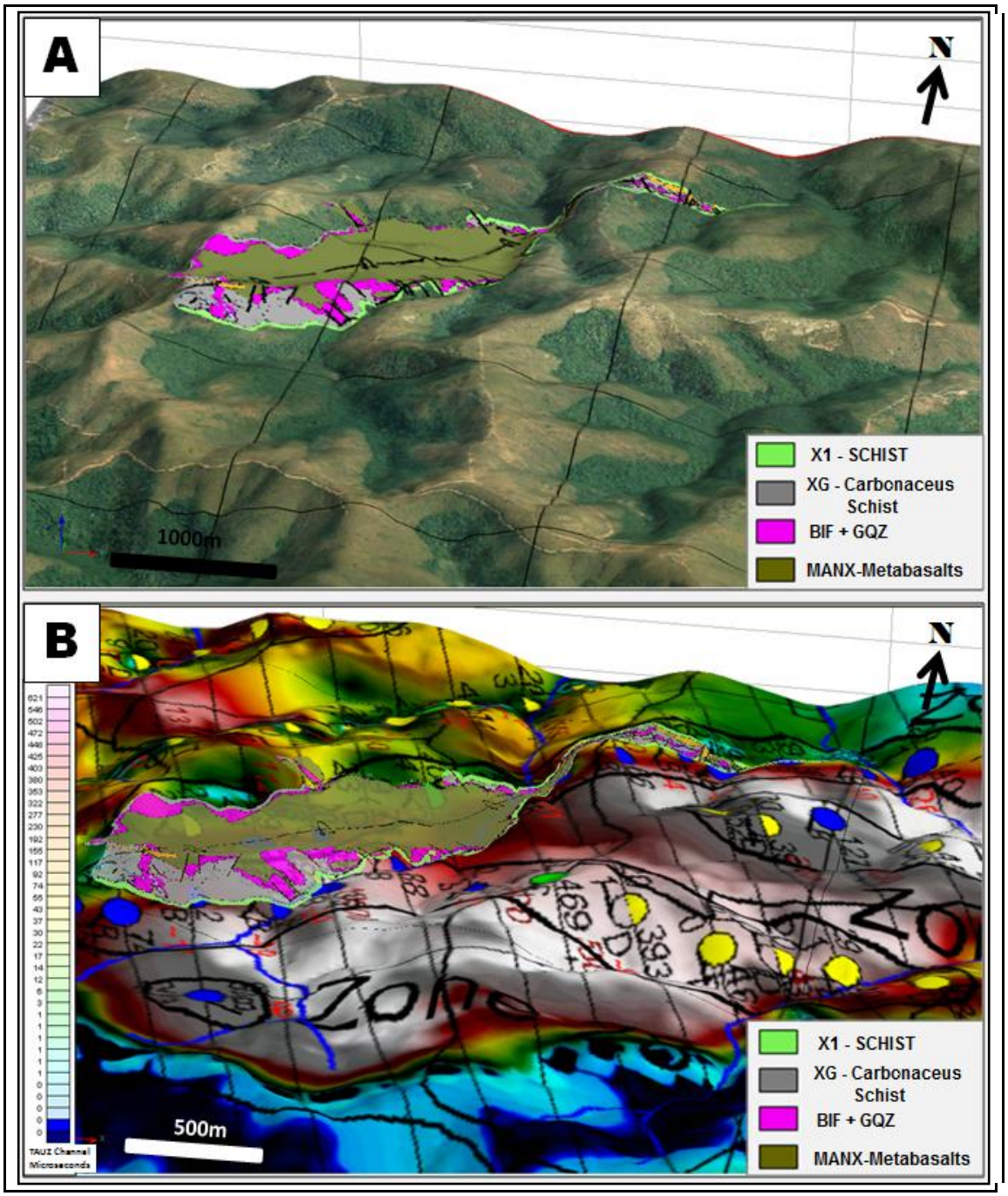

Figure 23 – (A) Digital elevation model integrated with the geological surface map. (B) EM anomalies (Tauz Channel) integrated with geological surface map (translucence).

5.2 – Geophysical Inversion of Electromagnetic Data

The geophysical inversion of the electromagnetic data in this study was performed only for the Tauz Channel because it is one of the channels responsible for investigations into the deeper levels and showed better correlations to the projections of the known sulphide orebodies (Figure 24).

The inversion performed on the electromagnetic conductivity data was processed for the entire survey and did not consider the information on the volumes of three-dimensionally modeled solids. Therefore, this approach differs from the Type I inversion (inversion of discrete bodies) from Pratt & Oldenburg (2007), since no form or known combination of geometric shapes was considered as a reference model during the inversion process.

This study used a three dimensional block diagram as a reference model. The upper face of the model matches the surface topography and was properly shifted down to a depth of 150m. Parameterization exercises, varying the functions of weights and the variables that control the smoothing in various directions, were performed throughout the entire survey in order to obtain a direct inverted model. In this case, the electromagnetic conductors correlated vertically with the main gold-bearing deposits in regions such as Cuiabá, Lamego and other smaller deposits such as Morro da Glória.

Figure 24 shows the result of the inversion of the electromagnetic Tauz Channel, together with the three-dimensional geological models generated from the results of drill core samples. The geological modeling was limited to samples with gold grades above 2.5g/t and a real thickness of more than 1.6m. On the product of the inversion process showed on Figure 24, the selected blocks corresponds to electromagnetic conductivity higher than 250 mS/m.

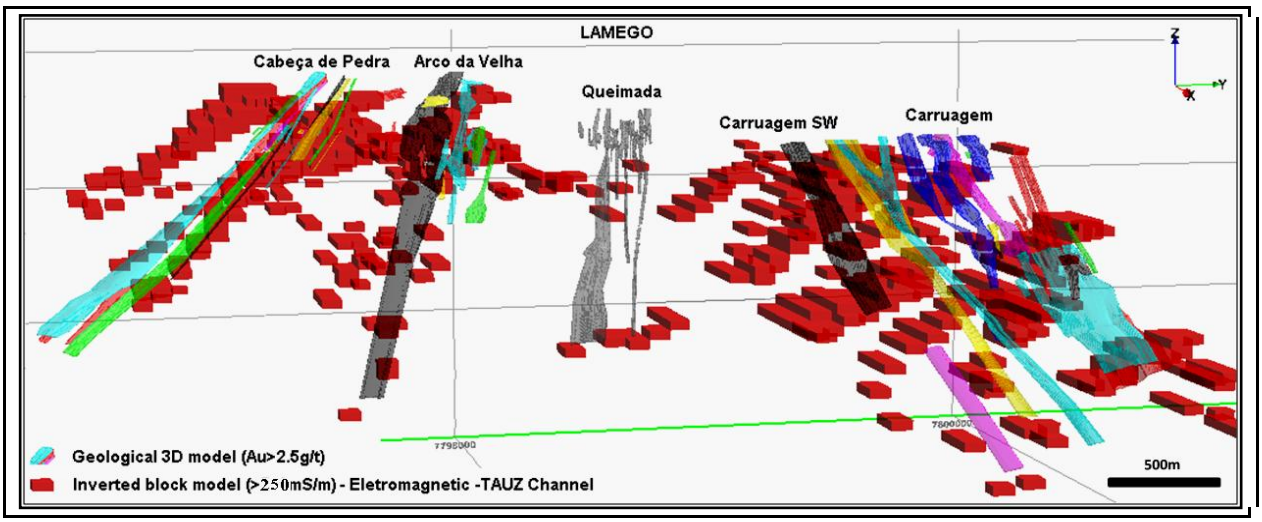

Figure 24 – 3D geological models with inverted electromagnetic raster block model (Tauz Channel).

The result of direct three-dimensional inversion in the Lamego region presented some significant responses from the exploratory viewpoint and the inversion process itself:

(i) at shallow depths (up to 150m), the correlation between the known sulphide bodies and the inverted EM model is not well adjusted at higher structural levels when compared to deeper levels; this can be recognized in nearly all the bodies; (ii) at deeper levels, electromagnetic anomalies have continuities relatively parallel to the direction of the plunges and dips, largely in the sulphid-richer bodies: Carruagem and Cabeça de Pedra; (iii) an anomaly in the SW region of the Cabeça de Pedra body was recognized, demonstrating a potential for future investigations, and (iv) the presence of additional anomalies in the SW continuity of the Carruagem body also shows considerable exploration potential in this region.

5.3 – IP Survey of the Lamego Deposit and the São José Target and Drilling Results

The four parallel IP sections carried out longitudinally to the Lamego deposit and its possible continuation to the northeast (São José target) were spaced 200m apart. Thus, the estimated depth of the anomalies, or of the modeled bodies, was approximately 100m, 200m, and 300m for the IP1, 2, and 3, respectively (Figure 25) representing individual investigation depths. The purpose of this configuration was (i) to evaluate the characteristics of the IP signatures and resistivity of the known modeled bodies, (ii) to find other potential bodies not reached by

previous shallow drillings, and (iii) to recognize possible lateral extensions of sulphide horizons not previously modeled or drilled.

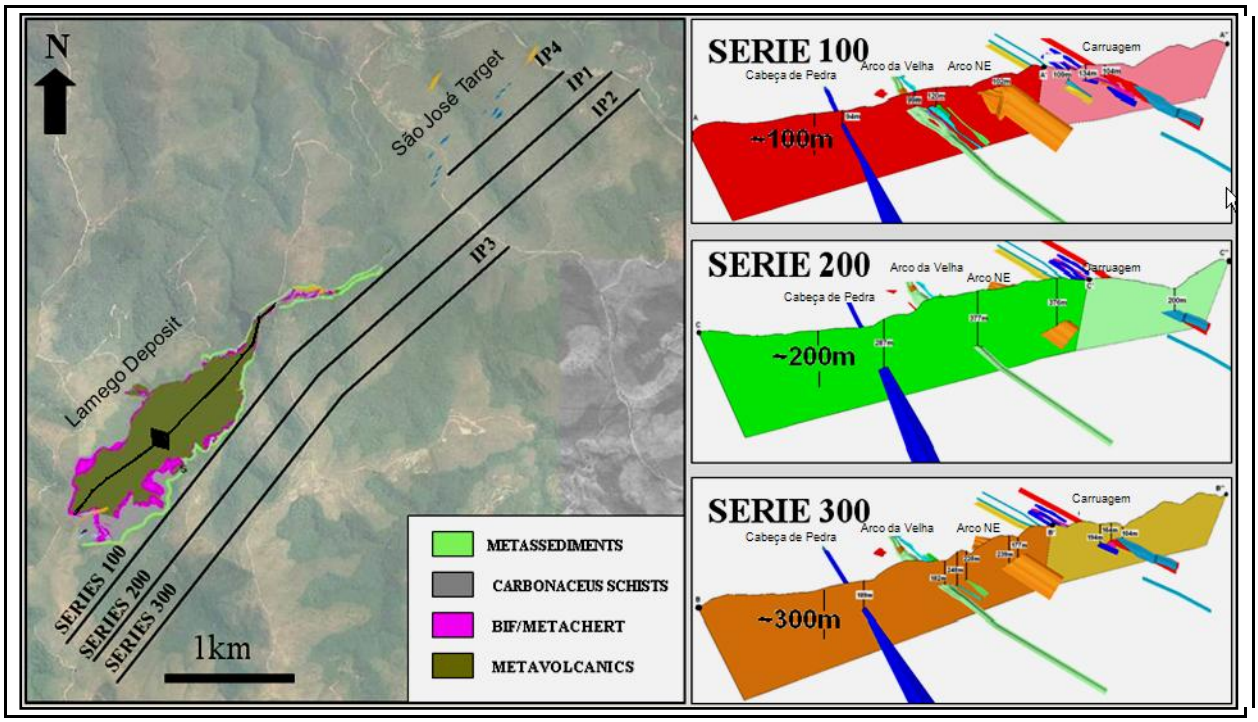

Figure 25 – Left: simplified geologic map of the Lamego deposit and location of IP sections surveyed southeast of the deposit and southeast of the São José target. An Ikonos true color composite imagery in the background. Right, vertical sections with projections of the mineralized bodies of the Lamego deposit. In each associated depth (Serie 100 refers to 100m depth, Serie 200 refers to 200m depth and Serie 300, 300m depth).

Four IP lines were studied. Lines 1, 2, and 3 were surveyed with a = 100m, and line 4 with a = 50m ("a" is the spacing between the receivers). Six depth levels were recorded for all lines with 2-seconds integration time (Figure 26). In the resistivity and induced polarization study, a dipole-dipole configuration was used, making it necessary to inject a current I (amperes) to the underground by means of a dipole current, recording a drop in the *V* potential (in milliVolts) in another dipole far from the first one (potential dipole).

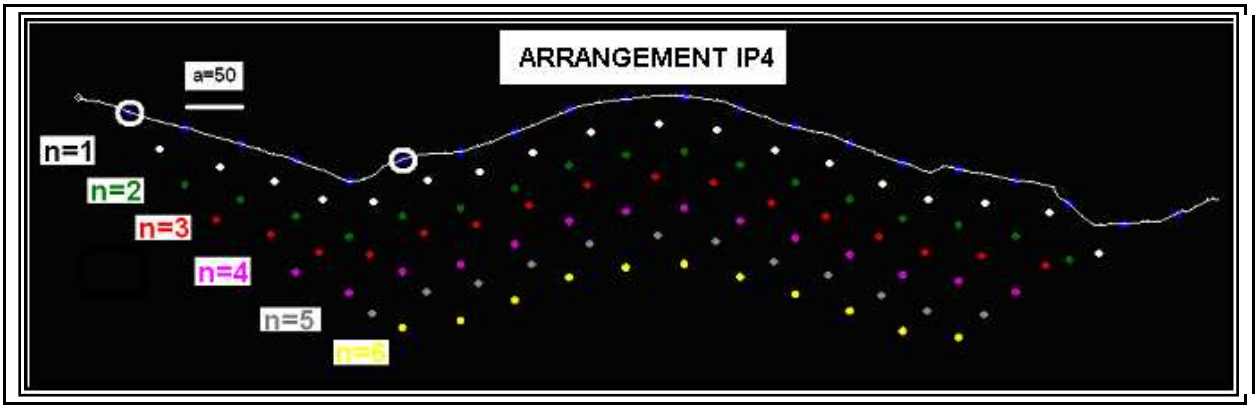

Figure 26 - Schematic arrangement of the IP4 section - São José Target, oriented SW-NE ("a" is the spacing between the receivers and "n" are the samples with the positioning of the depth of the readings of the signal).

The resistivity of the medium is proportional to the ratio between the voltage and current (V/I). This procedure makes it possible to take simultaneous measurements with up to six values of potential drop for each current dipole.

In the time domain, the IP effect (chargeability [mV/V]) manifests itself as a transient voltage when the excitation current is abruptly cut off. This temporal decay curve is sampled at a series of moments to determine the chargeability (IP effect), which corresponds to the area below the transient curve.

The inversion models of resistivity and chargeability (voltage decay) were obtained by using the ResCalc and IP_Avg variables, respectively. The models were obtained without any preference for dip, that is to say, no horizontal or vertical preference was given to the polarized bodies (Type II inversion from Oldenburg & Pratt, 2007).

The pseudo-sections of resistivity and chargeability were interpreted with the RESIX IP2DI software, especially using the *Zong Smooth Model Algorithm*, best known by ZONGE 2D (cf. http://www.interpex.com/). The applied algorithm is based on the finite element method in two dimensions, which incorporates the topography to the modeling of the Resistivity and IP data.

Starting with the grids of the inverted models of resistivity and IP, sections and vertical half-derivative (0.5dv) maps were calculated. These end products highlight the changes in both the resistivity and IP and also enable the anomalies to be properly established.

After completing all processing steps, the three-dimensional geometric sections must be corrected so that the data are formatted in a single space platform.

In the region of the Lamego deposit, a sub-horizontal surface layer was detected with a thickness between 80 and 100m and values far below 12mV/V. Under this surface layer, devoid of IP effects, anomalous values greater than 15mV/V were recorded, significantly correlated with the sulfide ore bodies (Figure 27).

Figure 28 shows the results of the inversion of the resistivity property at IP1, together with surface geological and geochemical information (São José Target), in addition to three-dimensional geological models of the Lamego deposit ore bodies. It is noted that the Carruagem orebodies, in which there is a predominance of highly resistive quartz veins, shows a good correlation to deeper resistivity anomalies and a lateral continuity. The Arco da Velha and Queimada bodies are the only ones that form a mirroring between the two sides, that is to say, a sub-vertical drill hole positioned to reach the Arco da Velha body should intercept, in depth, the mineralized horizon of the inverted side (Queimada orebody) of the mega-structure. The duplication of the resistivity effect occurs in this position, in which the fault moves to depths greater than 300m. The Arco da Velha orebody was also marked by the resistivity model, which recognized the gray quartz vein *stratabound* packages at up to a thickness of 30m. In the Cabeça de Pedra orebody, which also contains decametric stratabound packages of gray quartz veins, the resistivity effect was mitigated due to the thick envelope of carbonaceous schist in its hanging wall.

IP anomalies (chargeability) from the IP1 section (Figure 29) show an excellent correlation with the ore bodies modeled in Carruagem, which, although not presenting a significant correlation between gold levels and sulfide content, could still locally contain reasonable amounts of pyrite, either in gray quartz vein or BIF. Also evident is the continuity of the IP anomaly to the northeast of the main structure, interpreted as being marked by bundles of intensely sulfide carbonaceous schists, although virtually gold free. On the other hand, in the resistivity section (Figure 28), the anomaly is interrupted to the northeast, demonstrating the termination of this northern ore body.

The chargeability anomaly from the IP1 section satisfactorily marks the sulfide domains. This was observed almost continuously from the southernmost edge of the Cabeça de Pedra

orebody to the northeastern edge of the Arco da Velha orebody. This anomaly is also supported by geochemical measurements of sulphur content obtained from borehole samples. However, the gold-bearing mineralization is shown to be discontinuous between the two bodies.

The chargeability anomalies from the subsequent IP sections (IP2 and IP3) produced for the Carruagem orebody display a continuity that is consistent with the direction and known dip of that body. The same was not verified for the Arco da Velha and Cabeça de Pedra orebodies (Figure 30). This lack of correlation is mainly due to the lack of coincidence between these orebodies and large gold-bearing sulfide masses, as discussed by Guimaraes *et al*. (2008).

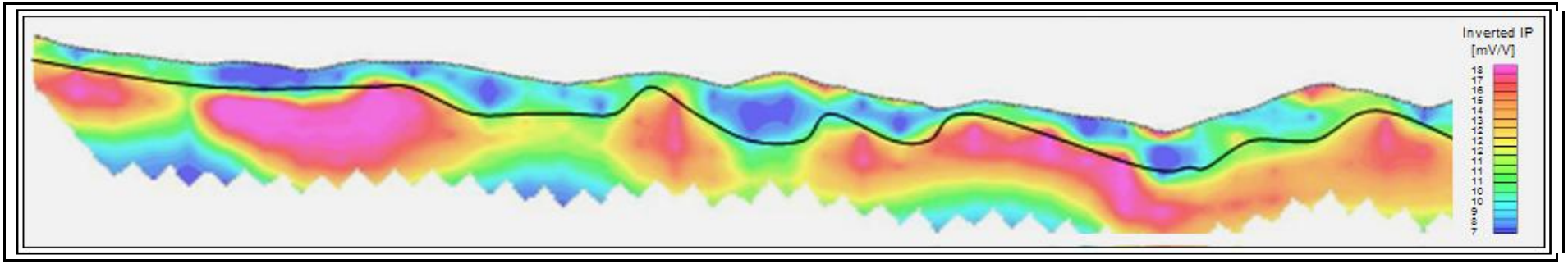

Figure 27 – Inverted SW-NE section - IP1 - Chargeability with low values layer between 80 to 100m deep range.

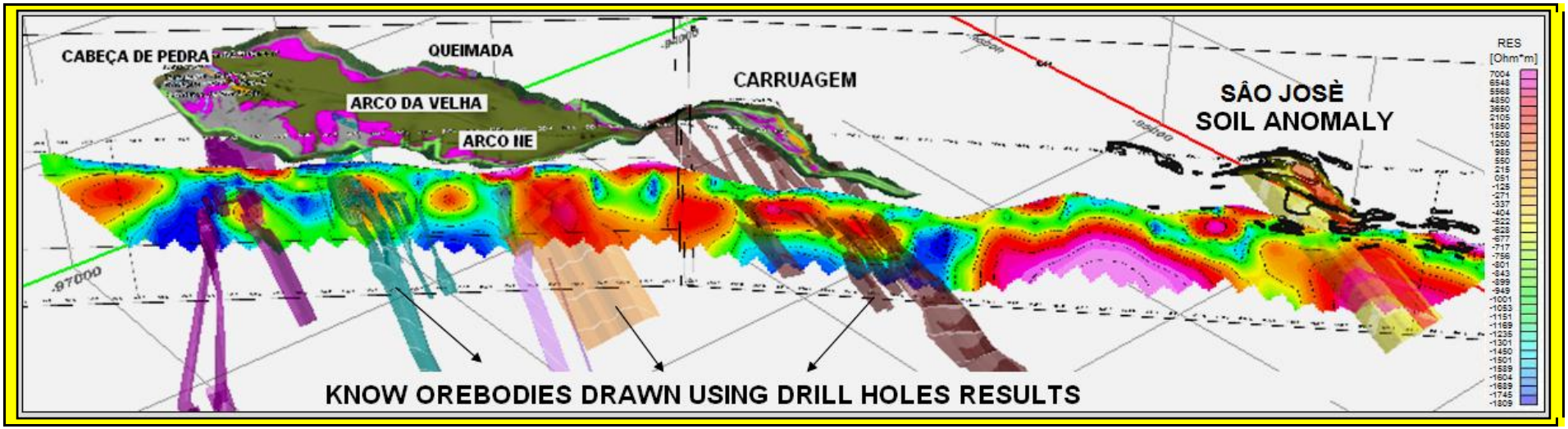

Figure 28 - SW-NE-IP1 section – Resistivity values, with surface geological and geochemical information and three-dimensional geological models of Lamego deposit with gold orebodies. The São José Target is at the right portion of figure represented by soil anomalies projected on underground. Note the location of this section in Figure 9.

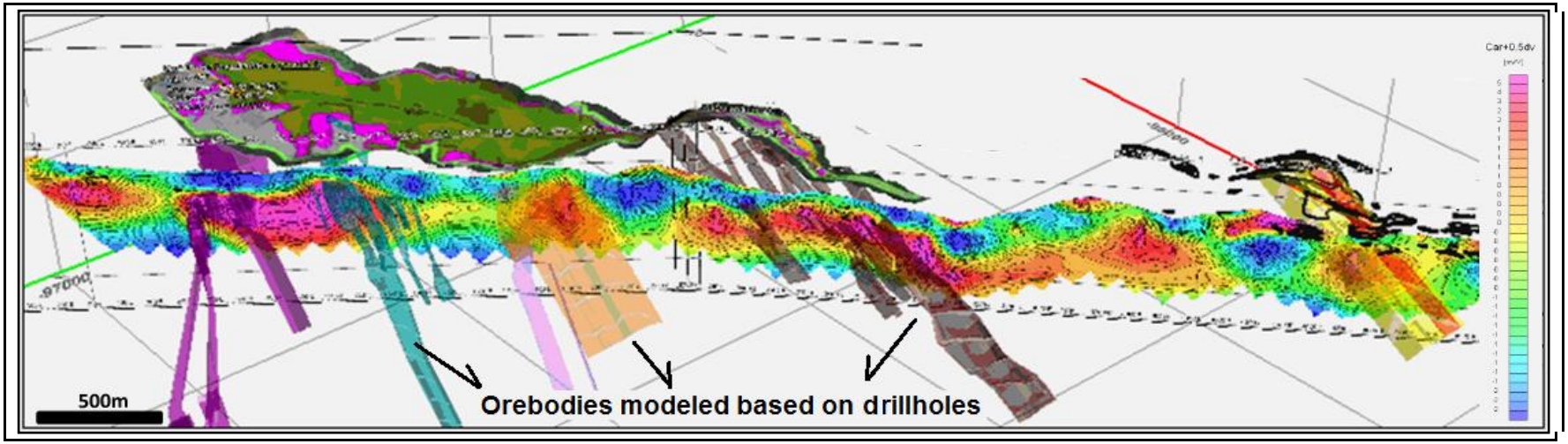

Figure 29 - IP Anomalies (Chargeability - 0.5 derivatives) from the IP1 section with information from the gold orebodies of the Lamego deposit. Note good correlation between modeled orebodies and IP anomalies.

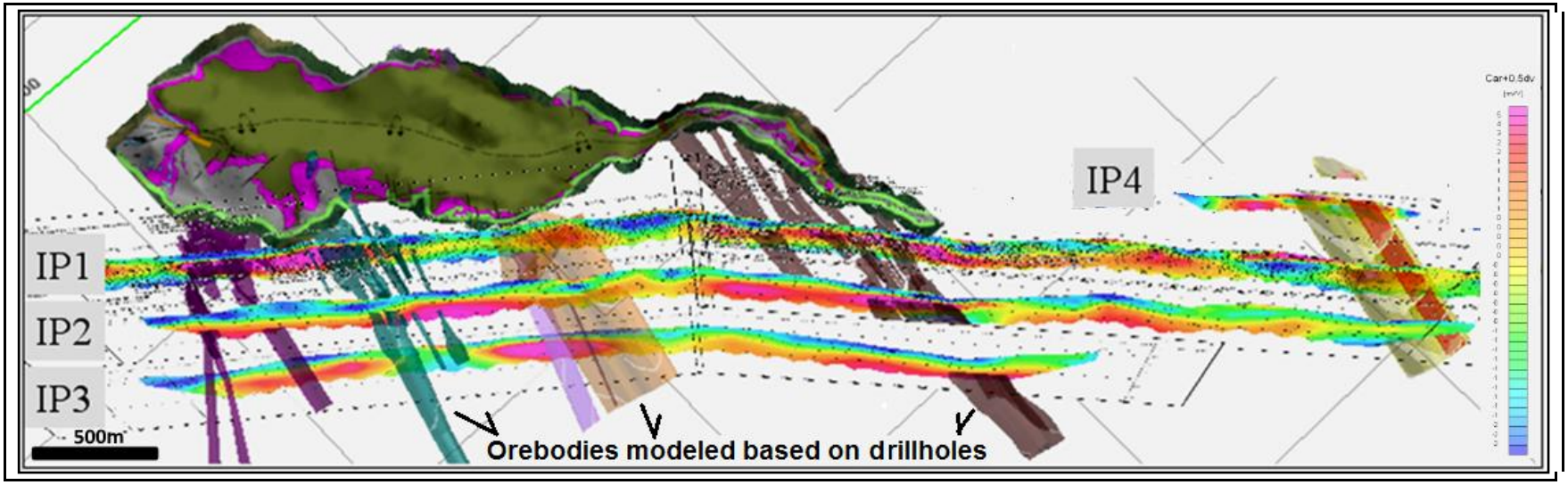

Figure 30 - IP sections integrated with geological information, orebodies modeled based on drillholes information, and soil anomalies of the São José target projected on underground.

Figure 31A shows the results of exploratory drilling and resistivity anomalies considering the IP1 section, which is located at the southwestern sector of the Carruagem orebody. A recent survey (red drill holes) intercepted a secondary anomaly with positive results for sulfide and gold. Figure 31B shows a good match between richer ore zones and resistivity anomalies at the São José target.

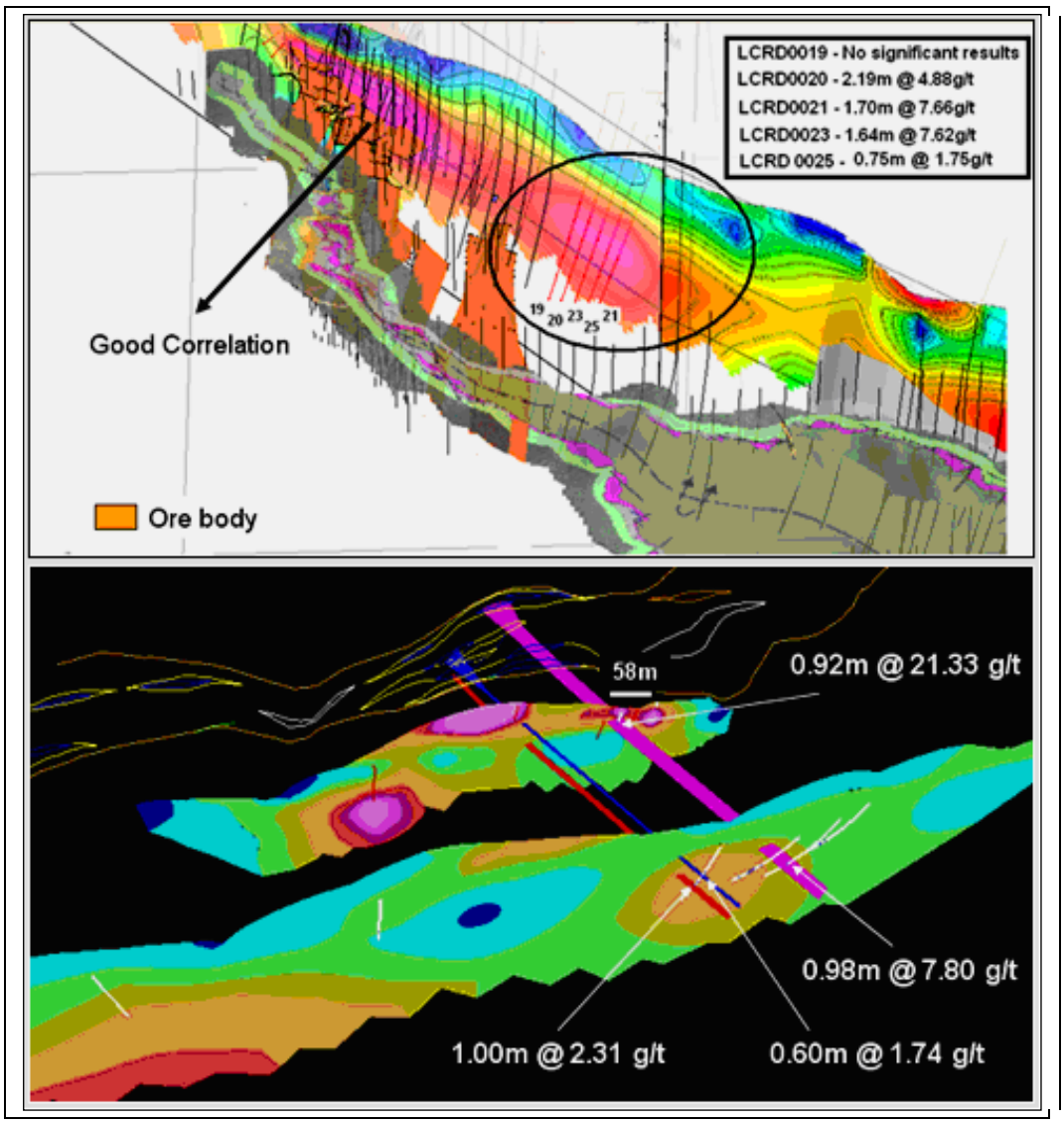

Figure 31 – Geophysical sections with drillings (in red and circled) carried out to test resistivity anomalies in the Carruagem orebody (upper figure) and in the São José target (lower figure).

All the information used here in gold prospectivity was visualized and integrated in a 3D GIS platform (Figure 32). The anomalous EM blocks (90th percentile) indicate that Cabeça de Pedra and Arco da Velha orebodies show continuity in depth (down plunge) along a slightly different direction from the actual plunge measured underground. In fact, these anomalies outline,

with significant quality, the shallower levels of sulphidization in these two mineralized areas. Extensive sulphide-rich packages of carbonaceous schist that envelop the Cabeça de Pedra orebody may also be responsible for these different directions of the actual mineralized plunge.

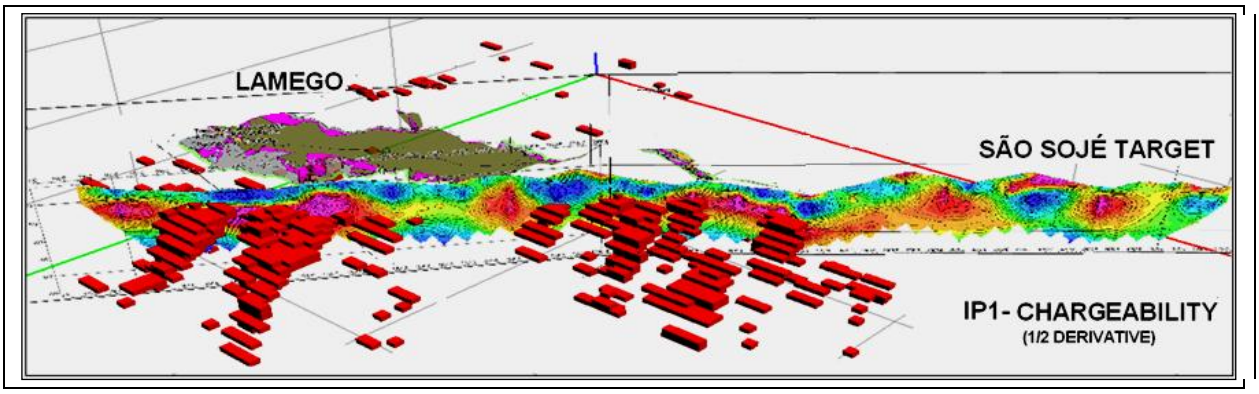

Figure 32 – Three-dimensional integration of the 3D voxel model (Inverted EM – percentile 90 - red blocks) with IP section (1/2 derivative) in the Lamego deposit and São José Target.

6 – SATELLITE TARGES

Based on results obtained on Lamego deposit, similar studies were developed for more four satellite areas: Biquinha, Sobradinho and Bom Caminho targets corresponding to the same stratigraphic level of Lamego deposit; and Morro da Glória positioned western of *Quadrilátero Ferrífero*.

6.1 – BIQUINHA TARGET

The Biquinha target is located 900 m northeast of the open pit of the Cuiabá mine (Figure 3). It includes a series of old excavations oriented in S80°E and N20°E directions (Figure 33). Outcrops are scarce and seven boreholes were interpreted to reveal geologic aspects of the area.

Rocks that commonly bear gold mineralization as observed in Lamego (gray quartz vein and BIF) or Cuiabá (BIF) were not intercepted in the drill holes, thus hindering the establishment of a stratigraphy for the target. The predominant intercepted rock is a light gray, fine-to-medium grained, metavolcaniclastic rock, with incipient to moderate foliation. There are, to a lesser extent, metric intercalations of dark, gray metapelitic rocks and, more rarely, black carbonaceous

schist with intervals rich in fine to medium grained pyrite crystals. Quartz veins are abundant, either milky white or gray in color, with a decimetric to metric thickness.

IP Results from the Biquinha Target

The IP sections in the Biquinha target are spaced of 100 m, thus allowing for more detailed information. Figure 33 shows a grid of soil samples with gold anomalies, old excavations and the 3 IP lines considered in this work.

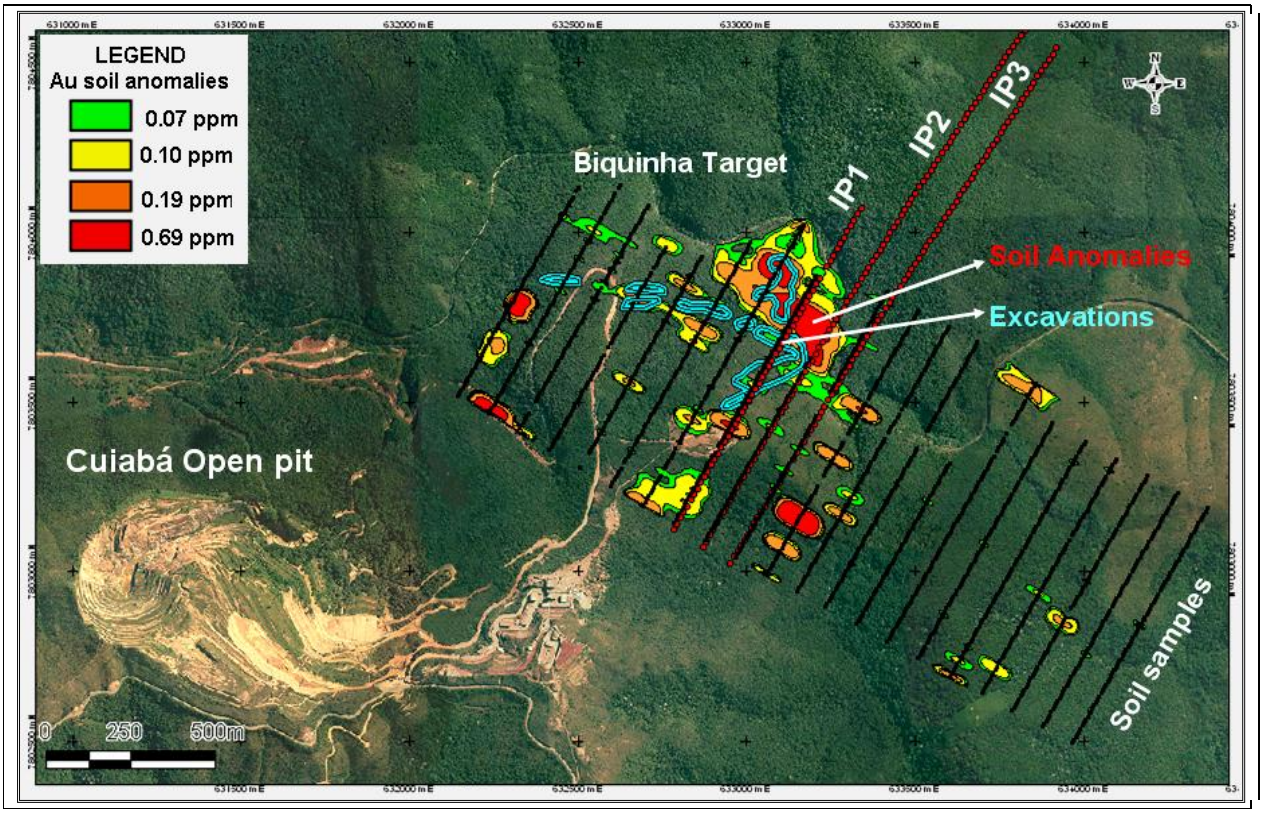

Figure 33 – Biquinha target, which is located in the vicinity of the Cuiabá mine. Gold anomalies in soils samples (higher anomalies in red), old excavations (in ciano) and position of IP sections.

The chargeability anomalies mapped with the IP sections show a good spatial correlation with the main soil anomalies. New potential prospects were also revealed. The SW chargeability anomaly (IP1 – Figure 34) is represented at surface by materials of anthropogenic origin, such as water pipes and masonry buildings. However, the anomalies registered in the subsequent sections (IP2 and IP3) suggest a straight association with the orebody and its continuity down plunge.

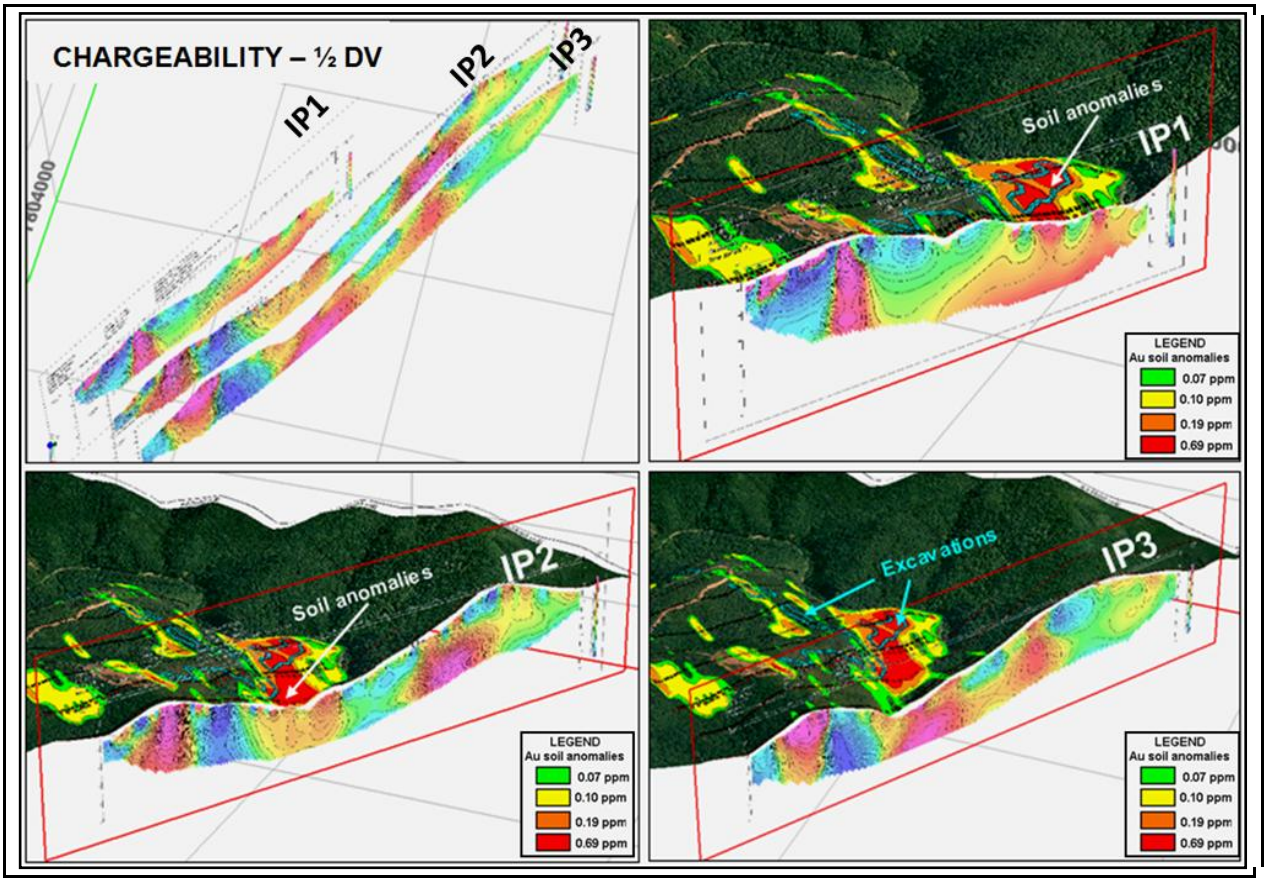

Figure 34 – Biquinha target: three-dimensional integration of the IP sections with soil geochemical data and surface excavations.

Borehole samples of the Biquinha target were analyzed for gold but no geochemical anomalies were discovered to date. Nevertheless, prominent sulphidization, dominated by pyrite, may reach up to 5% of the sample, showing coherence with the mapped IP anomalies.

6.2 – SOBRADINHO TARGET

The Sobradinho target is located 7 km northwest of Raposos and it is near the Lamego open pit mine (Figure 3). The area comprises rocks of the Nova Lima Group, including mafic and intermediate metavolcanic rocks interlayered with metapelitic beds; metric levels of carbonaceous schist, and a horizon of BIF (Figure 35). The configuration of this lithological set is not sufficiently understood, although available field data and drillings have established that the rock package is folded.

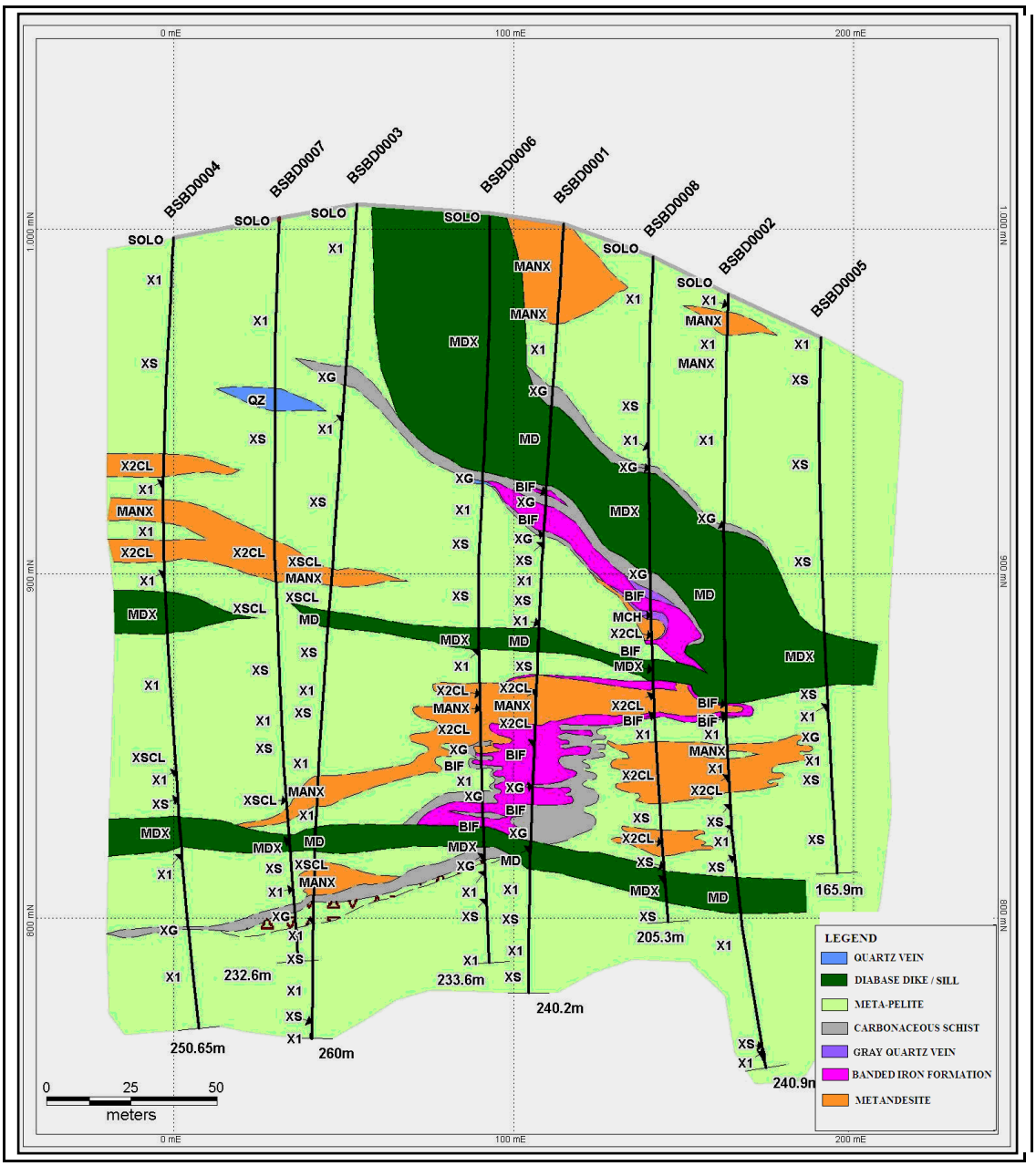

Figure 35 – Vertical N30E geological section of the Sobradinho target, interpreted using exploration drill holes.

Macroscopically, the metapelitic rocks display millimetric banding conferred by alternating bands of quartz-carbonate with micaceous beds and quartz-carbonate aggregates. Occasionally, euhedral and subeuhedral pyrite crystals occur in a disseminated or aggregate form. Centimetric to decimetric quartz venulations are common and may appear either concordant or

cross-cut the foliation. The metapelitic rocks are constituted by quartz, carbonate, sericite, chlorite, graphite and silica, and display a granolepidoblastic texture.

In addition, carbonaceous schist (Figure 36A) contains thin films of sericite, quartz, and carbonate. It has a thicknesses ranging from 0.5m to 3.0m and usually occurs associated with layers of BIF.

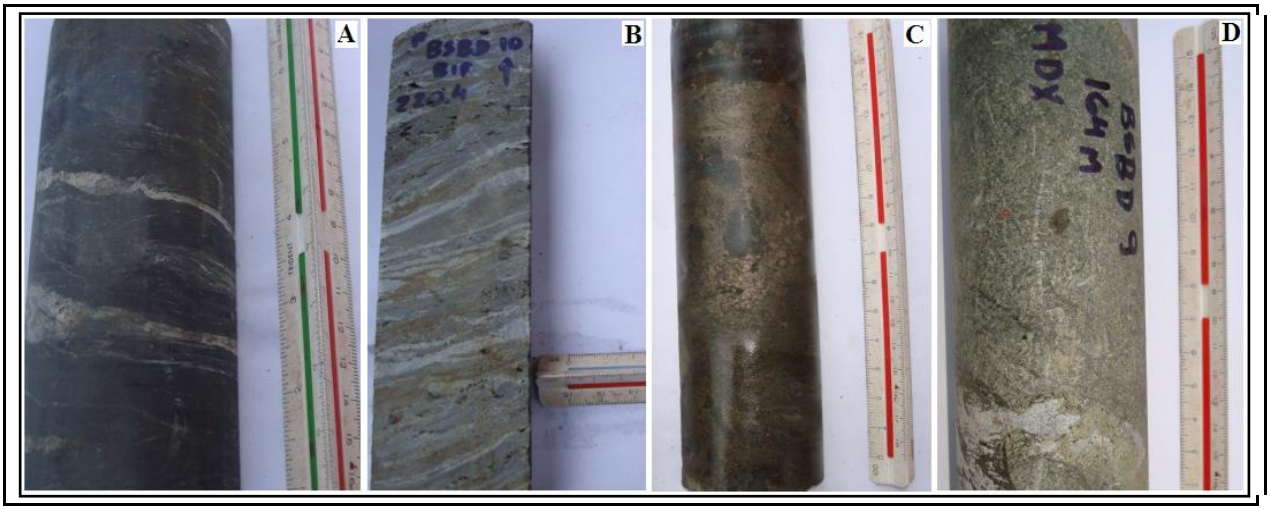

Figure 36 - Lithotypes of the Sobradinho target. A-carbonaceous schist; B-Banded Iron Formation composed of quartz, carbonate and sulfide layers; C- Massive sulfide (aggregates of pyrrhotite); D-metabasic intrusive rock.

Macroscopically, the BIF has its banding defined by milli-decimetric bands, with a coloration of light gray to cream (iron carbonate bands), dark gray (carbonate-carbonaceous bands), white (quartz bands), and yellow (sulfide bands). The BIF (Figure 36B) consists of quartz, carbonates, and sulfides. Subordinately, it contains iron oxides, chlorite, carbonaceous films, sericite, and chloritoid. The quartz and carbonate are fine-grained and the texture is laminated and granoblastic. The sulfide zones are predominantly composed of pyrite, but aggregates of pyrrhotite crystals occur frequently in areas near the hinge (Figure 36C). The sporadic presence of chlorite in the BIF is interpreted as a result of contact metamorphism of diabase dikes and sills usually observed at drilling intersections (Figure 36D). The intense folding that affects the whole package is most noticeable in the BIF layer, which is about 350 m long, with thicknesses ranging from 0.5m to 8.5m.

Structurally, there is the presence of a persistent regional N20E-N50E foliation, dipping 30º-55º to SE. Locally, *boudin* structures within the BIF are observed (Figure 37). Intersection lineations, mineral lineations, and quartz rods dip between 20° and 40° to E along an azimuth of

approximately 85° (Figure 38). The average attitude of mineral lineations in the area is N85E/35°ENE.

Figure 37 – Old excavation in the friable and oxidized banded iron formation. Sobradinho Target.

Figure 38 – Mineral lineation in the banded iron formation. Sobradinho Target.

Gold-bearing Mineralization in the Sobradinho Target

Gold grades from borehole samples extracted from the Sobradinho target were not available for this research. Only a few low grades of gold are known to date in oxidized BIF samples obtained at shallow exploration trenches.

Core samples with high concentrations of sulfides (pyrrhotite + pyrite) mainly in BIF were used to create a 3D geological model. The model was generated on the basis of 8 drill holes located along a N30E section, and the surface geological map prepared using the geologic information yielded in the trenches. Intervals with 7% or more of sulfides are observed on some boreholes. Figure 39 shows an Ikonos true color composite imagery draped over a digital elevation model and their 3D integration with a geological section, drill holes and a wireframe (isosurface) of sulfidized BIF.

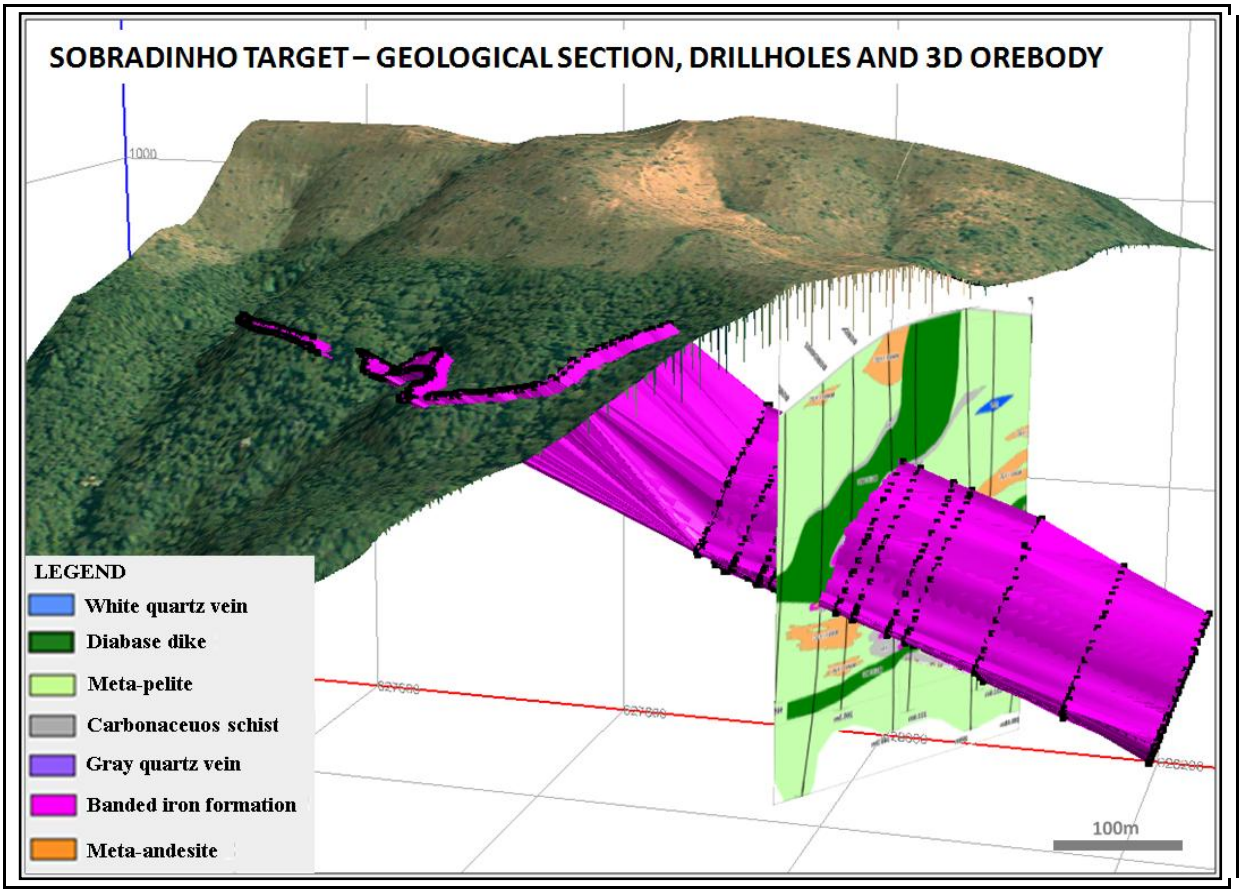

Figure 39 – 3D integration of DEM plus Ikonos image, geological section, drill holes and wireframe of BIF with 3D limits. Sobradinho target

EM and IP Results from the Sobradinho Target

EM data in the Sobradinho target show a well-defined electromagnetic conductive anomaly, although with a moderate intensity of the signal (<100mS/m). Figure 40 shows a 3D integration of surface EM data (Tauz Channel), inverted EM showed as a raster block model (above the 90th percentile) and the geological section of the Sobradinho target.

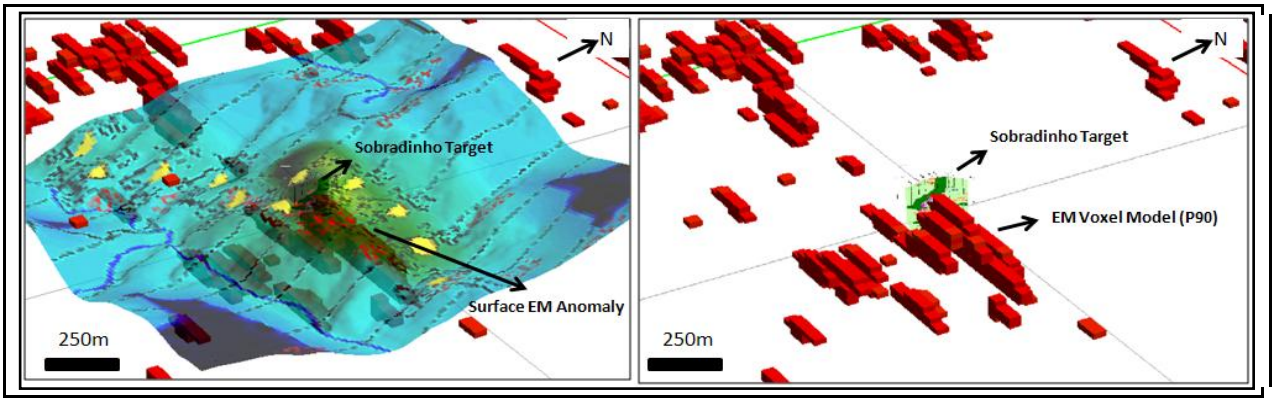

Figure 40 – 3D visualization of surface EM data, inverted EM displayed as a raster block model and a geological section of the Sobradinho target.

The modeled BIF layers enriched in sulfides presented a positive IP effect in the ground geophysical survey. The results of chargeability presented on IP sections demonstrate that the depths of IP anomalies correspond to the intersection of the geological model in each of the three sections. In addition, IP effect values are more intense here when compared to the other satellite targets. This feature is due to the high ratios of pirrhotite/pyrite that occur in this deposit. Figure 41 shows the integration of a 3D Ikonos imagery with three IP sections (chargeability) and a wireframe of the modeled BIF layer.

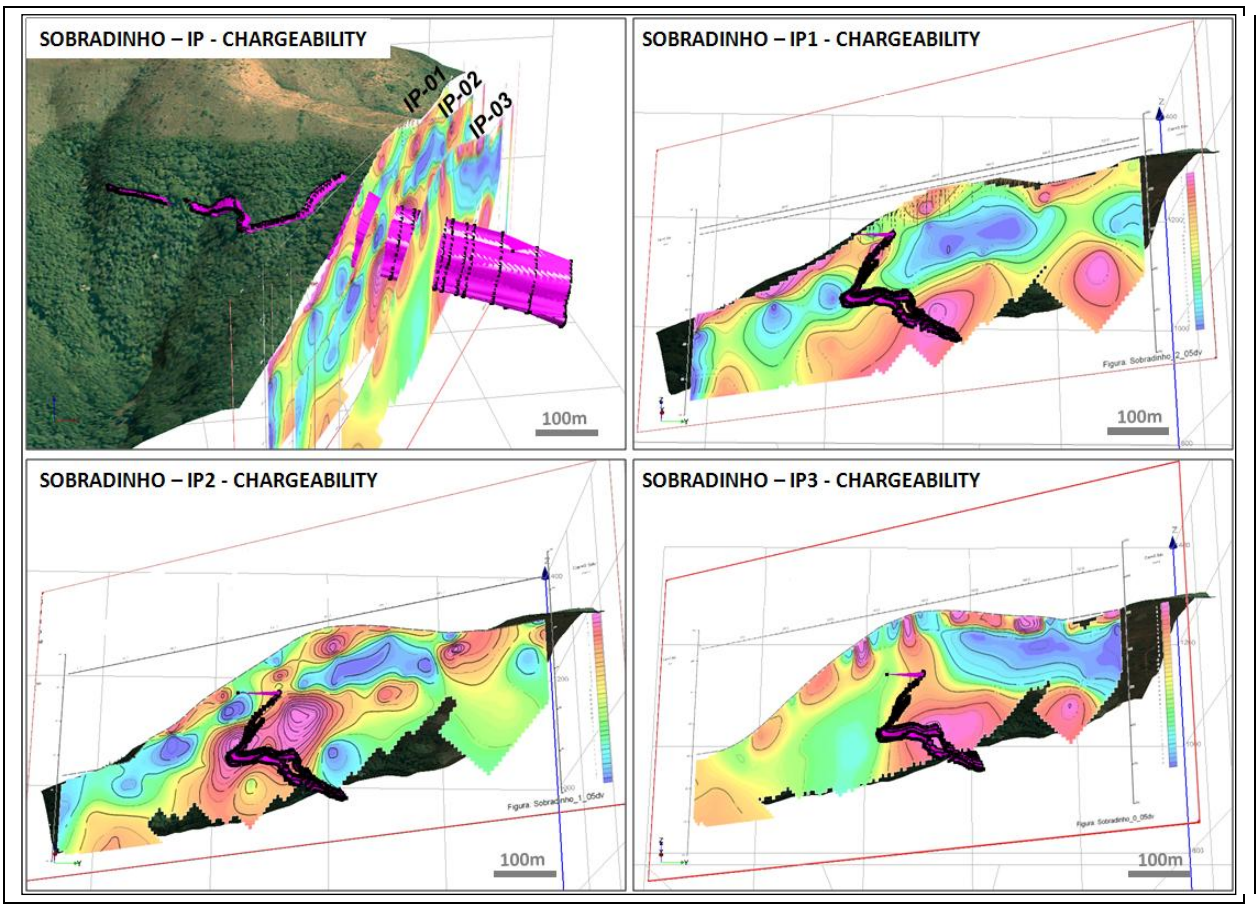

Figure 41 - 3D integration of the three IP sections with BIF wireframe.

Figure 42 shows the resistivity results on IP-01 and IP-02 sections. Note that low resistivity values indicate that quartz masses are absent in mineralized areas indicated by drill holes and in the geological section. In this case, the absence of resistive rocks corroborates with negative anomalies. Two other anomalies that appear on the lower left corner of Figure 41 possibly represent quartz-rich layers.

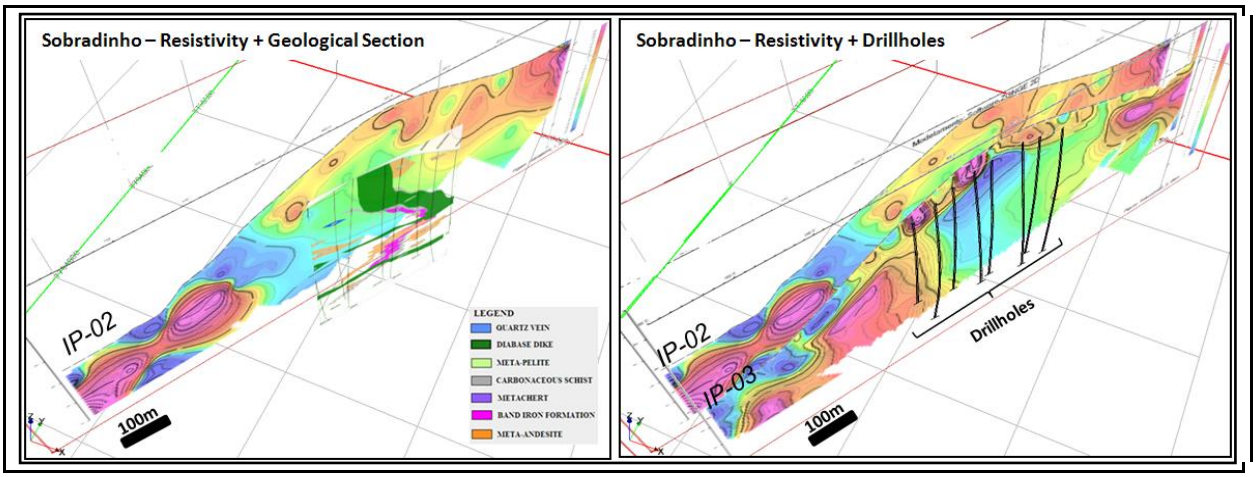

Figure 42 - 3D integration of IP-02 and IP-03 resistivity sections with a representative geological section. Black lines/curves are drill holes.

6.3 – BOM CAMINHO TARGET

The Bom Caminho target is located on the southwestern limb of Serra da Piedade, approximately 3 km west of the Caeté city.

Two large open pit excavations and four smaller ones are observed in the area, with sizes ranging from 100 m to 300 m in diameter (Figure 43). The pits are arranged in a general N30E direction and so are the rocks layers, which dip to the SE. Shear zones trend to N20E and are significant structural features. The mineral lineation on shear planes has an attitude of 120/35º.

As shown in Figure 43, the western portion of the area is composed of an upper unit constituted of metapelites (X1), locally carbonaceous, with intercalations of acidic metavolcanic and subordinate intermediate rocks (man), as well as thin horizons of BIF. The central domain is composed of intercalations of basic and intermediate metavolcanic rocks with layers of BIFs. In the eastern domain predominates the basal unit with mafic metavolcanic rocks with intercalations of ultrabasic metavolcanics and subordinately acid metavolcanics, locally with levels of metachert (MCH). In the contact region with gneisses rocks, chlorite-rich phylonites are common.

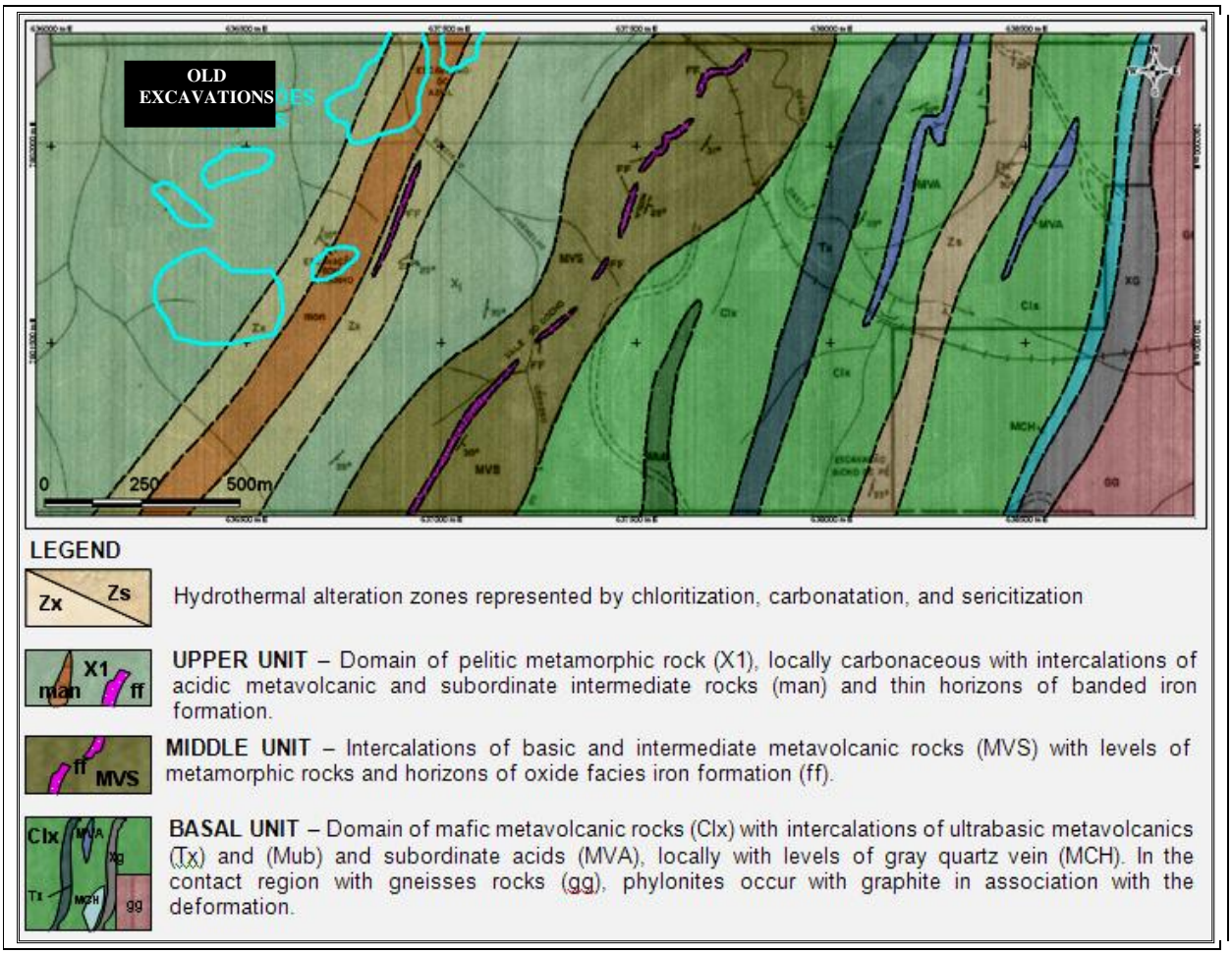

Figure 43 - Schematic geological map of the region of the Bom Caminho target. The units referred to belong to the Nova Lima Group. Source: Duchini Jr (1992).

Overall, the dominant rock is a volcaniclastic greenish-gray schist, medium to coarsely-grained. In drill cores, these rocks are foliated, with abundant sub-millimeter to millimeter dark, gray quartz crystals. Petrographic analysis revealed them to be volcanic quartz crystals (Vieira, DNPM Annual Report 1979). Locally, it is possible to distinguish, in the same rocks layers of medium/fine sand fractions, silt and clay, which are useful in determining the top and base stratigraphic relationships.

The metapelitic rocks are regularly foliated and locally dark gray when enriched in carbonaceous films. The metavolcaniclastic rocks, quartz-sericite-chlorite-carbonate-plagioclase schist, with frequent intersections in metric drilling intervals are affected by hydrothermalism related to carbonatation, chloritization, sericitization and, more rarely, sulphidization (mainly pyrite). The crystals of pyrite, as a rule, are widespread; locally forming fillets aligned parallel to the S2 foliation and in amounts generally less than 2%.

Layers were intercepted in old exploratory drill holes with up to 7m of carbonaceous schist with incipient sulphidization, interlayered with metavolcaniclastics.

In the basal unit of the Nova Lima Group, outcrops of undifferentiated mafic schist, talc schist (Figure 44), serpentine, carbonaceous schist and the described metavolcaniclastics rocks predominate, with this set overlaying the Caeté granite-gneiss in the extreme eastern of the area.

Figure 44 – Decimetric level of weathered talc schist intercalated with metavolcaniclastic schist. Bom Caminho target.

Decimetric lenses of banded iron formation and sulphide quartz-carbonate veins occur in a dispersed manner in the area, both associated with the median unit of the Nova Lima Group (Figure 45).

Figure 45 – Banded iron formation intercalated with weathered metamorphic schist. Bom Caminho target.

Gold-bearing Mineralization of the Bom Caminho Target

The regularity of the foliation observed in the drilling cores, and the small number of quartz veins in the sections drilled in the past, showed the incipient existence of tectonism, which does not favor the development of hydrothermal fluids. However, the existence of reactive rocks such as BIFs, although localized, and the occurrence of rocks capable of causing the "ponding" of hydrothermal fluids (e.g., carbonaceous schist) could facilitate reactions that can alter the fluid, including sulphidization.

Two IP geophysical sections were performed and assisted in establishing the possible plunge of the gold mineralization. In the past, regional plunge directions were tested in this target, which were different from the directions given by the IP survey results.

EM and IP Geophysics of the Bom Caminho Target

EM anomalies in the vicinity of the excavations motivated the need to program IP sections. Two N30E-trending sections were scheduled and submitted to the IP survey in order to establish the resistive potential and chargeability of possible extensions in depth of the materials mined in the past and located inside the old excavations. The results from these sections reveal an

IP anomaly positioned in the projection of larger excavations, with a plunge close to 120/35 and sub-parallel to the foliation (Figure 46).

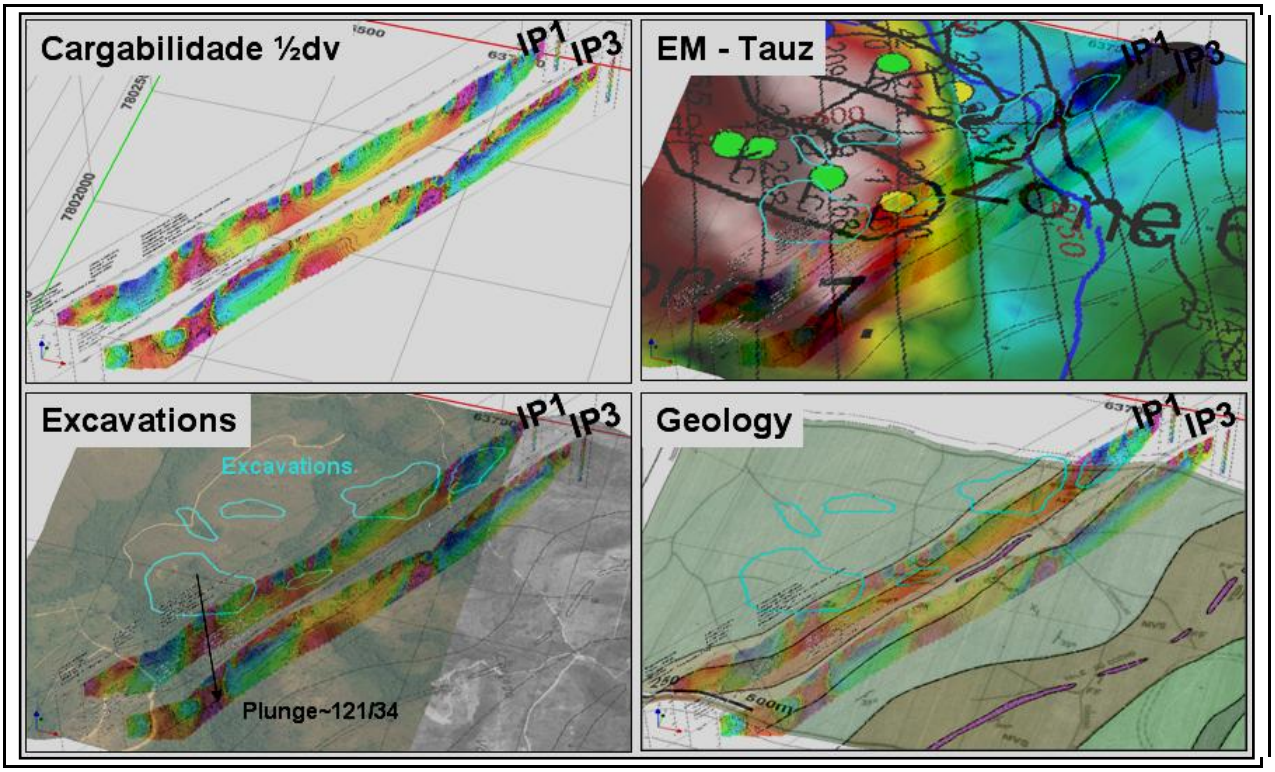

Figure 46 – Three-dimensional integration of the IP sections with surface data. Bom Caminho target.

Programmed drill holes were positioned on chargeability anomalies and a group of another IP section on East portion will help to understand better the mineralization of this area.

7 – GEOPHYSICAL SIGNATURES OF THE STUDY AREAS

Table 3 summarizes a group of geophysical signal intensities and sulfide grade data of each study area above described. With these data it is possible to compare and understand with more clarity the characteristics of the mineralization in each area.

Table 3 – Geophysical signatures of the studied areas.

DEPOSIT	OREBODY	SPECTREM EM (TAUZ CHANNEL)	IP EFFECT (CHARGEABILITY)	OBSERVED RESISTIVITY	PYRRHOTITE	PYRITE
		mS/m	mV/V	Ohm*m	%	%
LAMEGO	CABEÇA DE PEDRA	387	23.2 (1)	605 (1)	<0.5	9.1
	ARCO DA VELHA	203	17.7 (1)	3094 (1)	<0.5	7.2
	CARRUAGEM	207	26.3 (2)	3620 (1)	<0.5	5.3
TARGETS	SÃO JOSÉ	68	17.4 (1)	9622 (1)	-	3.1
	BIQUINHA	92	18.0 (1)	2135 (1)	-	0.5
	SOBRADINHO	97	33.0 (1)	254 (1)	2.0	5.7
	BOM CAMINHO	135	9.0 (2)	3813 (2)	-	0.2

(1) IP-01; (2) IP-02

Some explanations and comments about the Table 3 are described below:

- The grade of sulfide for each orebody of the Lamego deposit was obtained through the estimated block model in the same vertical plan of the IP section survey. On the other hand, the sulfide values of satellite targets were calculated direct from the composited samples of the drill holes.
- In general, the proportion of sulfide grades, intensity of chargeability and electromagnetic results of Lamego´s orebodies and the satellite targets have a positive correlation. For high grades of sulfide the values of IP effect and EM results have high intensities.
- In general, the intensity of EM signal of Lamego deposit is greater than another satellite targets. This can be explained by the thick envelope of carbonaceous schist that occurs there, while in satellite targets it occurs with minor proportions. Moreover, the carbonaceous schist beyond to be electromagnetic conductor have frequently high grades of sulfides also.
- The EM values of Cabeça de Pedra orebody is higher than the others bodies. This can be explained because this orebody is positioned on the hinge of the big anti-form structure and consequently the package of the carbonaceous schist becomes thicker and the two limbs closer to the other, increasing the intensity of the EM signal.
- The low values of resistivity in Cabeça de Pedra could be associated to the high proportions of carbonaceous schist too, although the gray quartz packages are also relatively expressive.
- The high values of resistivity in São José target cannot be right. This area was interpreted as the result of insufficient energy to cross the uneven surface. This problem may also be related to different rock types found at Lamego and the São José Target; in other words, to their different rocky backgrounds. In addition, there are no EM anomalies in this area.

- The greater value of chargeability (33mV/V) is presented in Sobradinho target. In this Deposit the values of pirrhotite are greater than the others and possibly this mineral is more sensible to IP effect.
- The low values of resistivity in Sobradinho target are coherent because the amount of siliceous material there is scarce, only small layers of gray quartz can be found close to the BIF.

8 – MORRO DA GLÓRIA DEPOSIT

The Morro da Glória gold deposit, located southeast of Belo Horizonte (Figure 3), is considered as complementary study of this research and used as reference for the development of an exercise that focus on application of the multi-thematic fuzzy-Boolean models and inversion algorithms to assist in integration of multi-source data, as presented in Guimarães *et al.* (2006).

8.1 – Morro da Glória Geological Settings

The plunge of the main ore body at this deposit is structurally controlled by N75E - trending fold axis, dipping 35^{o}NE. The masses of gold-bearing sulphides are hosted by metric to decametric layers of banded iron formation (BIF) and metachert parallel to the hinges of mesoscopic folds. The BIFs are interdigitated with carbon-rich schists, chlorite-quartz-mica schists and metandesites, which define distinct concentric zones of hydrothermal alterations near the sulphide/mineralized bands.

The known lithologies in the Morro da Glória region are stratigraphically positioned in the basal unit of the Nova Lima Group, which in turn forms the lower portion of the Rio das Velhas Supergroup in the QF.

The dominant geomorphological feature in the Morro da Glória region is the Serra dos Três Irmãos, which is a reference for the structural analysis of the ore and has ridges that run in an E-W direction. This area consists of Banded Iron Formation - BIFs (with an estimated thickness between 50 and 60 metres), sericite-quartz schist, chloritic schist, and chloritic-quartz-carbonated-sericitic schist, occasionally interdigitated with plagioclase-quartz-chlorite schist.

The BIF is the main host of the gold mineralization in the Morro da Glória region. Locally, gold is also found associated with silica-rich levels (metachert). The characteristic compositional banding of Morro da Gloria BIFs consists of alternating millimetric and centimetric levels enriched with carbonate (ankerite), intercalated silica levels, ferrous-

magnesium and, subordinately, films of sericite. Processes resulting in the substitution of carbonate with sulphides (dominantly pyrite with lesser amounts of pyrrhotite and arsenopyrite) are characteristic of the advanced stage of hydrothermal alteration in these rocks.

Metandesites form a stratigraphic unit below the BIFs. These rocks locally display volcanic variolitic textures and frequently contain distinct halos of hydrothermal alteration. Vieira & Oliveira (1988) define three concentric zones of hydrothermal alteration within gold deposits hosted by greenstone sequences in the QF: a chlorite-rich outer zone, a carbonate-rich intermediate zone and a sericite-rich inner zone, closer to the ore.

Stratigraphically, the Morro da Glória region is set on a base of meta-ultramafic rocks, komatiites, meta-andesites and basaltic komatiites, with their respective alteration products, followed by a banded iron formation and metachert, carbonaceous schists, covered by carbonaceous metapelitics, gradually moving to metapelitics and felsic metatuffs.

The mineralized bodies occur mainly in massive sulphides (Figure 47A) associated with the hinges of the mesoscopic folds essentially in contact with the BIF (Figure 47B) with carbonaceous schists and subordinately in silificated zones with metachert sulphide.

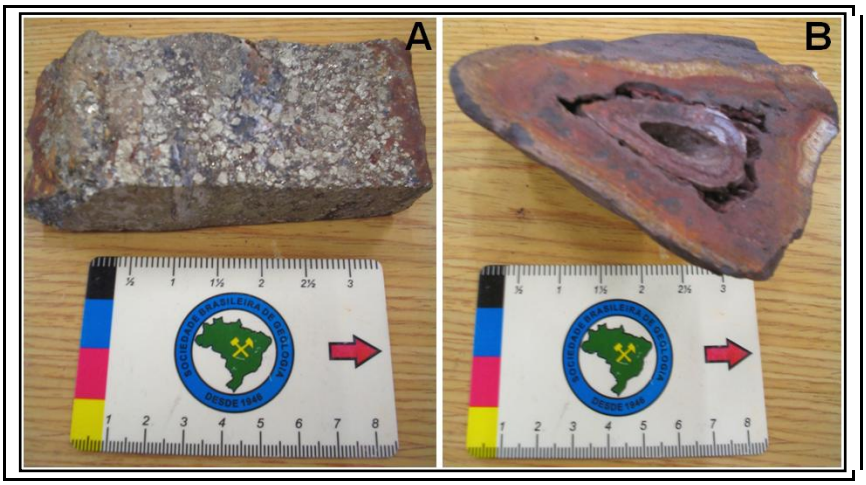

Figure 47: A – Massive Sulphide with aggregates of subeuhedral pyrite crystal; B) banded iron formation with folded features.

The meso-structures that are characteristic of the region are defined by the combination of sinformal folds, a host of bodies denominated as Mina Rica (southern part of Serra Três Irmãos) with an axial plane between N65^{o}E and N80^{o}E, associated with an anti-form which is located at its hinge, the Santo Antônio and Vum-Vum bodies with an EW axial plane, both defined by the

folding of the primary layer S_0 in the BIFs (Figure 48A). This conjunction was created in the D1 phase which corresponds with a tectonic compression with a SSE vergence.

Figures 48B and 48C, respectively, show the simplified 3D configurations of the different lithologies and main ore bodies spatially projected in the Morro da Glória region. The directions and angles of the average plunges of the ore bodies in the Morro da Glória region vary between N70E and N85E, dipping between 30 and 40 degrees.

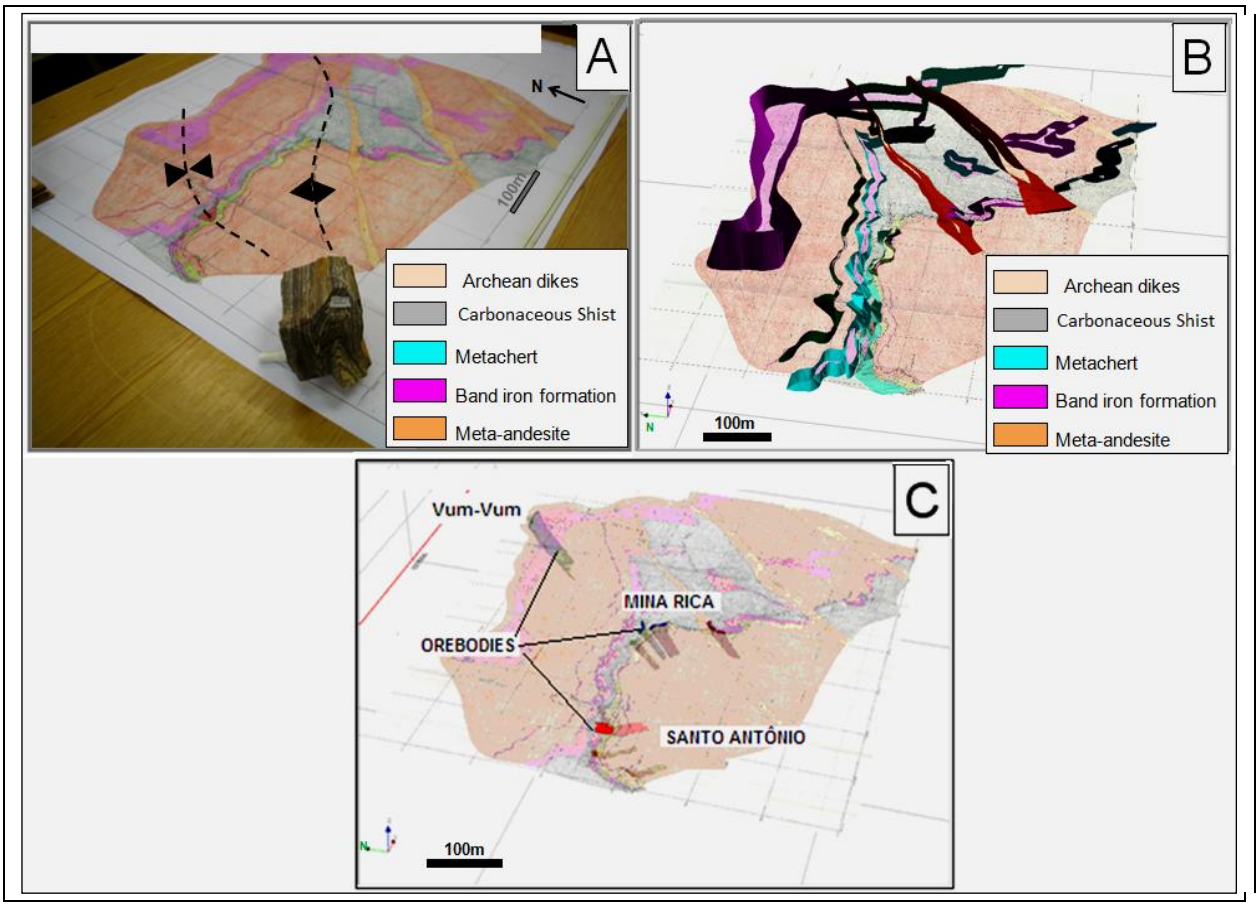

Figure 48 – A – Underground geological map of level 4 (level 770m); B – three dimensional configuration of main lithologies; C – main ore bodies projected in depth.

8.2 - Dataset

The data set used in this research is summarized in Figure 49. Figure 49A is a digital terrain model (DTM) with a geological map of the surface and the location of the 61 diamond drill holes. Figure 49B is a three dimensional geological model created using the borehole information together with surface and subsurface maps for levels 3 and 4.

The geochemical analyses of the soil in this region were performed during the 90's. Samples were collected at 40 meters intervals along lines spaced approximately 100m apart (Figure 49C). Sediments in the region were sampled and analyzed in 2007. The analytical chemical results from stream sediments samples were represented by anomalous basin limits (Figure 49D).

Figure 49E illustrates a set of old excavations plotted on old maps and checked in the field. A group of gold-bearing ore bodies were modeled from the boreholes and chip channels collected on underground galleries between level 2 and level 4 (Figure 49F). The old excavation limits were also used to generate solid/wireframes and connected using the combined information in areas where there was no geochemical information regarding gold and sulphur at shallow depths and at the surface.

Figures 49G and 49H illustrate the results of the Spectrem airborne-geophysical survey performed in 2002. Figure 49G shows the analytical signal of the total magnetic field and Figure 49H is the Tauz channel product from the electromagnetic survey.

The main characteristics of the aero-geophysical survey performed by AngloGold Ashanti Brasil Mineração Ltda (AGAM), called *Spectrem Airborne Electromagnetic Survey – 2002*", are described in Figure 18. The flight lines are spaced 200m apart at N22^{o}W, which is almost perpendicular to the direction of the ore body plunges in this region.

8.3 - Methods

The procedures used in the preparation and three dimensional analysis of the data, upon which this study is based, can be summarized in the following steps: (1) field investigation; (2) three dimensional modeling of the mineralized gold-bearing bodies, ferriferous formations and metachert (quartz horizons), including exploration and channel data; (3) processing information from old excavations and geochemical analytical results for soils and stream sediments; (4) preprocessing and processing aerial geophysical information (Spectrem Aerial Survey, 2002), including electromagnetic data inversion and developing the three dimensional block matrix; (5) projection of surface information underground; (6) generation of horizontal sections, developing the two dimensional limits of the intersections of each theme analyzed; (7) evaluation of anomalies using the multi-thematic fuzzy-Boolean model and the development of a preliminary three dimensional model; (8) comparative analysis of the preliminary fuzzy-Boolean model with the known ore bodies; (9) readjustment of the three dimensions based on the positions of the

known ore bodies; (10) comparative analysis between anomalous spots defined in the fuzzy-Boolean model, known ore bodies and the results of the aerial electromagnetic data inversion process; (11) analysis of new modeled anomalous targets and programming of additional exploration to investigate potential anomalies.

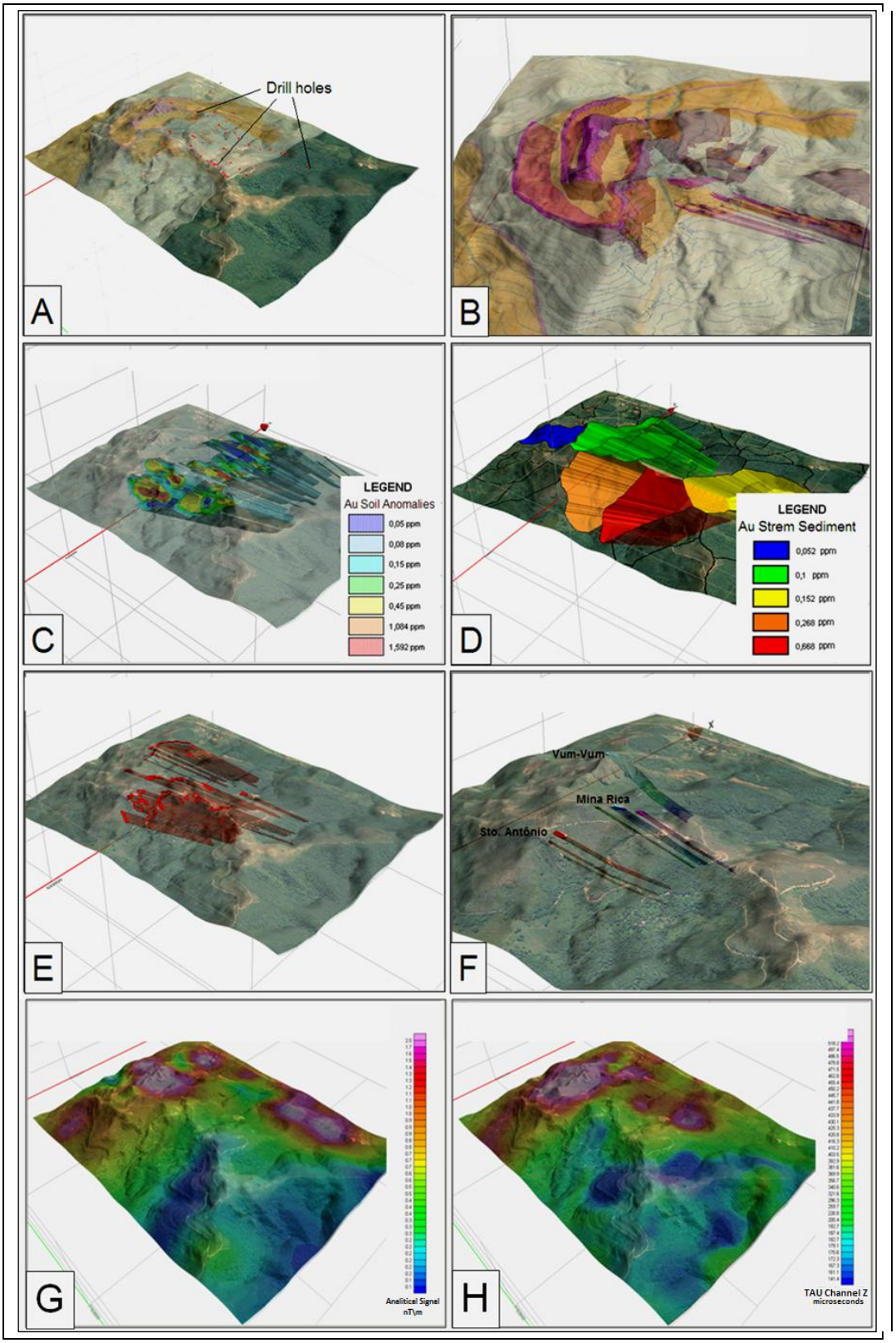

Figure 49 - Schematic configuration of Morro da Gloria data (A) surface geological map; (B) 3D geological model; (C) Au soil anomalies projected in depth; (D) catchment basins built from stream sediment gold values; (E) ancient excavations; (F) main known ore bodies; (G) analytical signal of total magnetic field; (H) Tauz channel of electromagnetic survey.

Field Investigation

The main magnetic and electromagnetic anomalies, as well as geochemical anomalies and the limits of old excavations were verified in the field. There are known banded iron formations which are strongly compacted, dark grey in color and contain euhedral crystals of magnetite located mainly on the crest of the Serra dos Três Irmãos, where the magnetic anomaly is more pronounced. Additionally, areas where there are soil anomalies, the banded iron formation is more heavily weathered and is light grey in color with crystals of pyrite and limonite. The presence of magnetite decreases significantly in these areas. In the area of old excavations, only schistose rocks are apparent because practically all the sulphide material, possibly mineralized, was extracted in the past. However, residual BIFs with incipient sulphidation were seen in the walls of some of the gullies.

Three Dimensional Geological Modeling

Two 3D geological models were generated for the Morro da Glória deposit using 3D modeling software (Datamine). The first model corresponds to the limits of the mineralized gold-bearing ore bodies which were generated from the analytical results from the boreholes and underground galleries channels of levels 3 and 4. Only results greater than 2g/t in composite samples were considered in this model. The second corresponds to the banded iron formation packages independently modeled. However, metachert and venulous quartz packages as well as diabase dykes were also individually modeled in three dimensions. This model was also based on surface geological contact limits, old geological maps of levels 3 and 4, as well as lithological information from the boreholes and channels.

Processing the Geochemical Information of Soils and Sediments

The chemical analysis results of the soil were interpolated using the minimum curvature method and the anomalous areas were categorized as illustrated in Figure 4C. Results falling within the limits of 0.15g/t to 1.6g/t were considered anomalous in this region. In this study, the chemical analysis results of the sediment samples were represented by semi-automatically defined anomalous basin limits, starting with a base three dimensional topographic scale hybrid of 1:25,000 and 1:2000 (Figure 4D). Sediment analysis results falling within the limits of 0.1g/t to 0.7g/t were considered anomalous in this region.

Airborne Geophysical Results at Morro da Glória

The Morro da Glória region is characterized by resistive host rock with electromagnetic conductive horizons associated essentially with carbonaceous schists, BIF with some magnetite and, subordinately, schistose rocks or metachert with possible enrichment of sulphides which often contain auriferous mineralizations. The magnetic anomalies were already characterized mainly by iron formations with magnetite, as shown in Figure 49G.

In this region the layer of weathering rock is not very thick or conductive; this makes the interpretation of the data relatively straight forward, with the exception of where the layers plunge relatively smoothly. Where the plunges are less than 25 degrees, it becomes difficult to determine the exact direction of the dip from the aerial electromagnetic data. However, the plunge of the sulphide and mineralized bodies in the area reach as much as 35 degrees in some places, facilitating the interpretation process.

The result of the aerial investigation by Spectrem survey, represented by the TAUZ channel (i.e. one of the channels used for the investigation at deeper levels), shows anomalies with the presence of electromagnetic conductive rocks in areas corresponding to the projection of the main deep ore bodies, followed by the preferred plunge directions, mainly in the Santo Antônia and Mina Rica bodies (Figure 50).

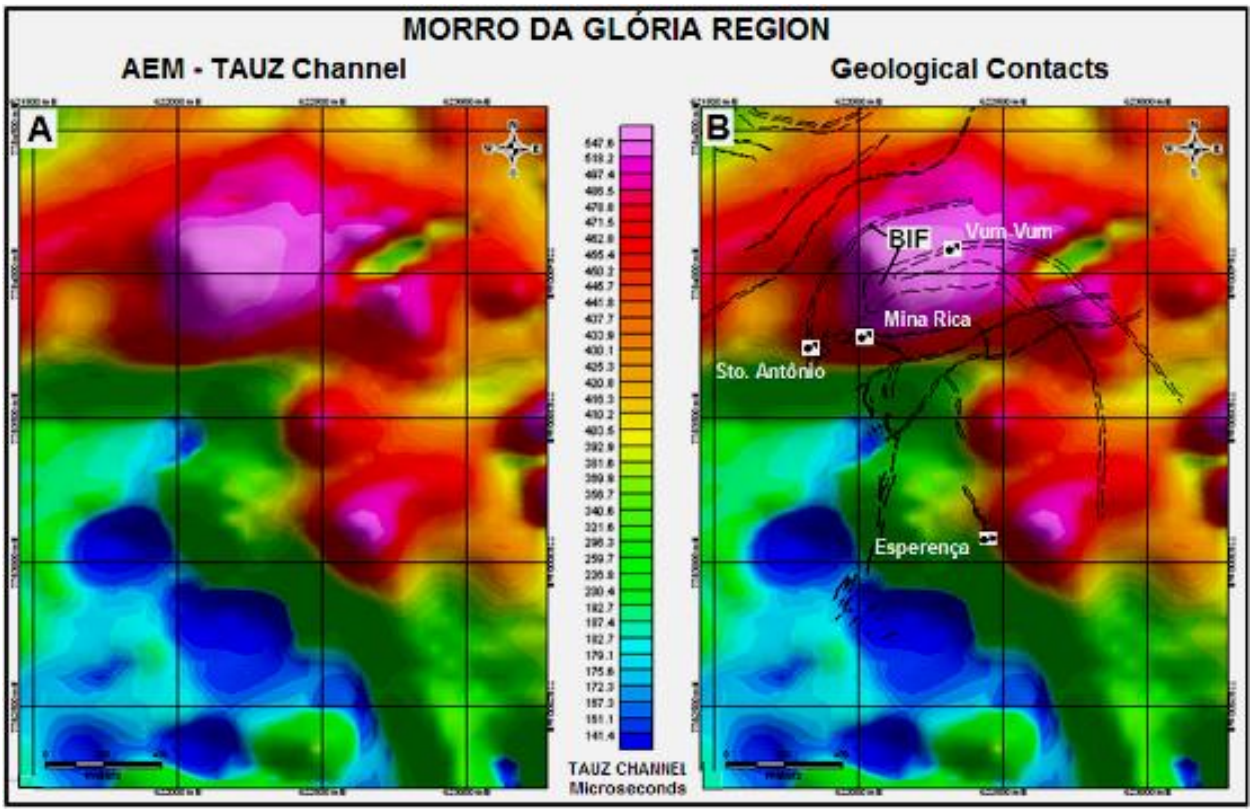

Figure 50: (A) Product derived from airborne electromagnetic data - TAUZ Channel. (B) TAUZ Channel plus geological contacts. The main known ore bodies (Mina Rica, Santo Antônio, Vum-Vum and Esperança) are shown with their respective average plunge directions.

In order to correlate the three dimensional underground information with the aerial electromagnetic data, the inversion process was performed.

Geophysical Inversion of EM Data – Morro da Glória

The geophysical inversion process in this study was applied only to the Tauz channel which is one of the channels used in the investigation of deeper levels and that produces the best correlations in terms of the projection of known sulphide bodies (Figure 51).

The inversion was performed on the electromagnetic conductivity data. It was processed for the entire survey and did not effectively considered information regarding three dimensional cartographic solid volumes. Therefore, this approach differs from the Oldenburg & Pratt (2007) Type I inversion, since no known form or combinations of geometric shape were used during the inversion process.

This study used a three dimensional block diagram as a reference model whose the upper face of the model corresponded with the surface topography and was properly shift down to a depth of 150m. Parameterization exercises varying the functions of weight and the variables that

control the smoothing in various directions were performed throughout the entire survey in order to obtain a direct inverted model, in which the electromagnetic conductors correlated vertically with the main gold-bearing deposits in regions such as Cuiabá, Lamego and other smaller deposits such as Morro da Glória. The result obtained for the inversion process in this study of the Morro da Glória region is shown in Figure 51.

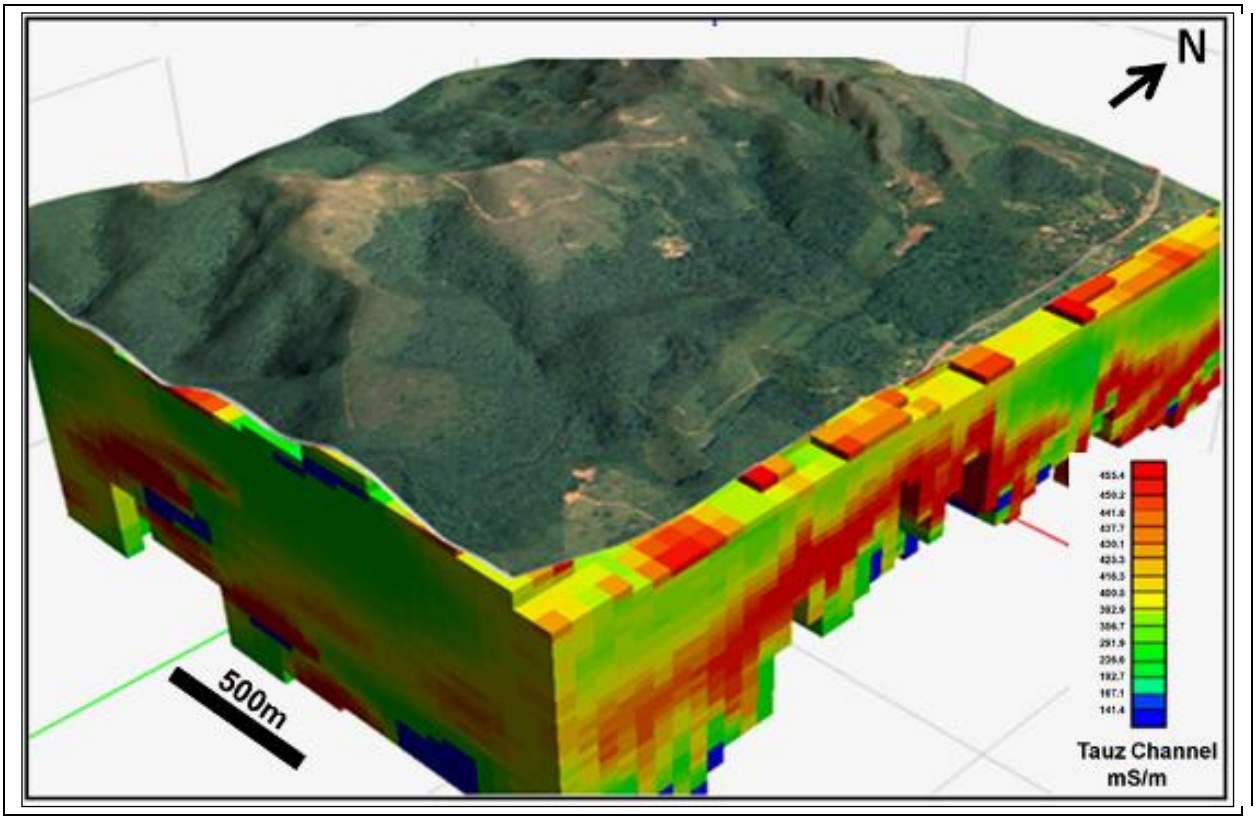

Figure 51: Raster blocks of electromagnetic Tauz channel of Morro da Glória region.

Although Oldenburg & Pratt (2007) considered that three dimensional geological models could be incorporated and used in conjunction with a pure inversion, the authors also postulated that the main characteristic of a Type II inversion is a direct property inversion - the process used in this study.

The information used in the three dimensional models of ore bodies or complex solids resulting from the geological interpretation of sulphide BIFs can be used in future studies as solids or reference models that are Type III inversions. In this case, the solids can be filled and used as reference models to adjust and better refine direct inversion or pure physical property inversions.

Projection of Depth and Horizontal Slices of the Analyzed Subjects;

After completing the pre-processing, processing and the integration of the themes into the previously discussed GIS platform, the projection on depth of the information is applied, generating horizontal slices which allows for the creation of two dimensional limits of the intersection of each analyzed subject (Figure 49).

The plunge of the ore bodies in this orogenetic deposit are structurally controlled mainly by fold axes in N75E/35^{o}NE direction. Therefore, the geochemical information of the sediment, soil and magnetic anomalies was projected according to the average direction and plunge ore body, while the limits of the old excavations follow the directions and plunges of each know ore bodies varying between N70E and N85^{o}E with plunges between 30 and 40 degrees to the NE.

Multi-Thematic Fuzzy-Boolean Model

The fuzzy analysis in this study has the objective of qualitatively select three dimensional volumes and solids on the surface and underground through fuzzy logic applied to the processed themes in order to heirarchize the known auriferous areas and locate new potentials for investigation.

The fuzzy logic theory (Bonham-Carter, 1994), holds a continuous scale of pertinence to the set of studied data varying from 1.0 (total pertinence) down to 0.0 (non-pertinence). Thus, individual measurements of a variable can be classified according to the degree of relevance to the "Anomaly" (Bonham-Carter, 1994). Very high values are likely anomalies, having a fuzzy pertinence (fuzzy membership) of "one". Between these two extremes, there is a whole range of possible values of pertinence. The combination between the evidence maps was established through fuzzy operators (An *et al.* 1991; Bonham-Carter 1994). The operator "Fuzzy AND" corresponds to the Boolean "AND", and when applied in a continuous distribution (such as contained in the range from 0 to 1), it returns the lowest value from amongst the evidence. The operator "Fuzzy OR" (equivalent to the Boolean "OR"), returns the greatest value from amongst the evidence when applied to a continuous distribution. The Fuzzy Algebraic Product **(P)** consists of the product between the evidences and has a minimizing character in the sense that the final product is the result of the combination of various evidence maps through the multiplication of values in the 0 to 1 range. Consequently, lower values are derived from those contained in the input maps Since the Fuzzy Algebraic Sum **(S)** simply consists of the sum of various evidence maps and has a characteristic inversion of the Algebraic Fuzzy Product, in which the fuzzy

membership values add up resulting in a product in which the values of the final map are greater than those on the evidence maps. Figure 52A gives examples of results supplied by these operators, starting with illustrative input data.

In the spatial analysis defined by mineral favorability maps, the Fuzzy operators "AND" or "OR" are not routinely used and do not, in fact, represent a superposition of the effects of each of the input maps. The satisfactory combination of the evidence maps is done through the "Fuzzy Product" and "Fuzzy Sum" operators. However, the most effective way to counteract the minimizing effect of the "Fuzzy Product" and the maximizing effect of the "Fuzzy Sum" is obtained through the Fuzzy Gama operator **(G)** (Bonham-Carter 1994) (see Figure 52A).

The Fuzzy Gamma operator is defined in terms of the Fuzzy Product and Fuzzy Sum in the form (Bonham-Carter 1994):

$$G = (S)^{\gamma} * (P)^{(1-\gamma)} .$$

Where the γ (gamma), situated in the range between 0 to 1 and defines the additive or subtractive contribution of Fuzzy Sum and Fuzzy Product operators. Using γ=1, the Fuzzy Gamma operator corresponds to the Fuzzy Algebraic Sum (essentially in an additive character), therefore, when γ=0, the Fuzzy Gama operator will correspond to the Fuzzy Algebraic Product and have a subtractive character (Figure 52B). Choosing the value for γ is the responsibility of the analyst and depends on the type of response one wishes to find.

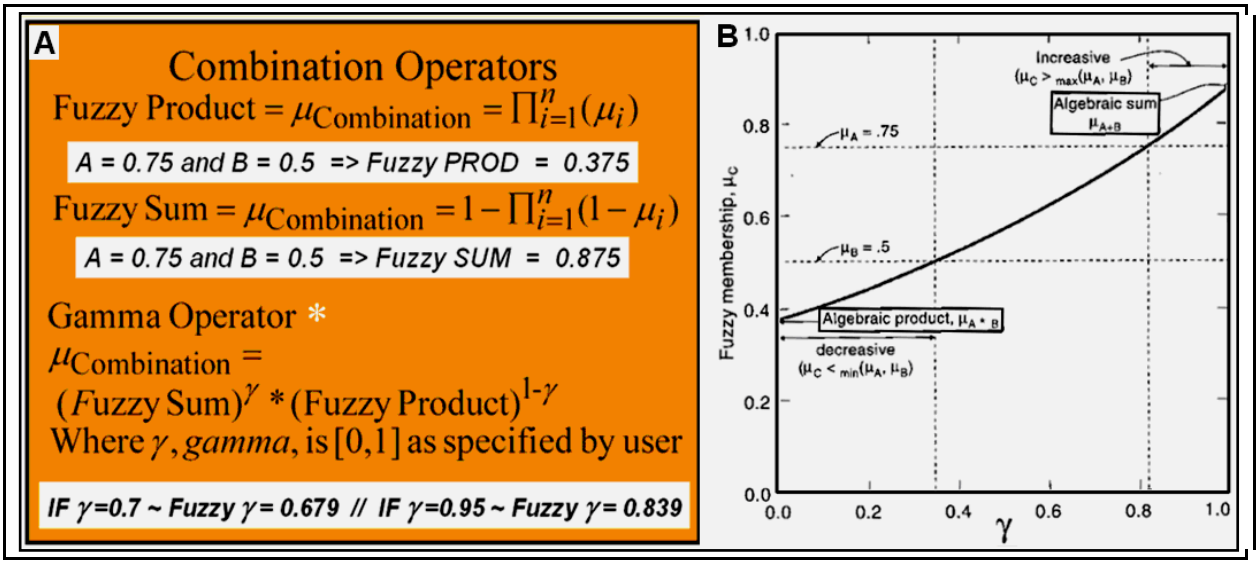

Figure 52 – A – Summary of fuzzy operators; B – comparative curve of fuzzy operators and variation as a function of different input gamma values (modified Bonham-Carter 1994).

Examples of the use of fuzzy logic in mineral research are abundant in literature (An *et al*. 1991; Bonham-Carter *et al*. 1988; Bonham-Carter 1994; Bonham-Carter 1997; Braghin 1998; Chinn & Ascough 1997; Nóbrega 2001, Nykänen 2008), etc.

In this study, the evidences were combined through the operator Fuzzy Gama. The value used for γ was 0.9 (stronger additive contribution). The classification of the evidence map in the fuzzy memberships was defined in terms of a subjective evaluation by the specialist, and in this case the categorical information was: lithological information, soil and sediment geochemical data, old excavation limits and aerial magnetometry geophysical results (Figure 49).

The final map of surface favorability was generated from the application of the operator Gamma=0.9 from the fuzzy analysis, starting with a table of weights which were previously categorized by the sensitivity of the geological knowledge (Table 4).

Table 4: Scheme of weights used in the fuzzy gamma method.

Geology	
Au Value	Class
BIF+MCH	0.75

Excavation	
Type	Class
EXC	0.90

MAG - AS	
nT	Class
>23700	0.75

Catchment	
Au Value	Class
0.05 ppm	0.70
0.10 ppm	0.75
0.15 ppm	0.78
0.27 ppm	0.79
0.67 ppm	0.80

Soil	
Au Value	Class
0.15 ppm	0.81
0.25 ppm	0.82
0.45 ppm	0.83
1.08 ppm	0.84
1.59 ppm	0.85

Weights scheme - reclassification

The geochemical model with the three dimensional ore body limits was produced with the interpretation of the exploration data and channels from the underground galleries serving as a calibration reference for the predictive fuzzy Boolean model.

The most know gold-bearing deposits in the Quadrilátero Ferrífero, independent of their size, have records of old surface studies, with a strong remobilization of material, and promoting the creation of gullies and ravines which are very prominent today. These geomorphological features are well marked at the Cuiabá, Mina Velha and Raposos mines and have also developed in the Morro da Gloria region. For this reason, in the measurement of weights, the excavation limits is the category with the greatest value (Table 4).

Although all the excavations have the same weight in this study, they could also be sub-divided and attributed varying weights for different parametric dimensions (Figure 49E). The ore bodies modeled using the boreholes and channels from underground galleries at levels 2 to 4 were

not used as a subject in the fuzzy analysis, but were considered in the quality control of the fuzzy product.

Before projecting each theme in depth following the average direction and plunge of the ore bodies, it is necessary to project the vectors of each one which was mapped previously in a two dimensional plane in a digital terrain model. This procedure is necessary so that each piece of information has its real expression effectively reproduced in the three dimensional surface, thereby maximizing the cartographic accuracy and giving a true representation of the superficial terrestrial data.

8.4 - Comparative Results of Applied Methods at Morro da Glória Deposit

The results of this study correspond to mineral favorability maps generated from the application of fuzzy operators to the discrete themes, as well as the product of the inversion process applied in aerial geophysical electromagnetic conductivity data. The results also correspond well to a comparative analysis between the products produced in this study and to known ore bodies.

Figure 53 shows the surface mineral favorability map with the fuzzy membership scale established as a function of the weights used in Table 4. The anomalous areas calculated on the surface reveal a potential region in the form of an oval, which had not been observed in previous studies. On the surface, this form resembles the main feature of the Cuiabá mine which is a world class deposit in the QF. Although the region of the Vum-Vum target is composed of a thick layer of BIF and presents geomorphological expression, the main anomaly region is in the area of the Santo Antônio and Mina Rica ore bodies. The latter has a lower geomorphologic expression and hosts sulphide horizons in thinner BIF layers with small horizons of metachert. This configuration suggests that this maybe be considered as a deposit with expressive potential, at least in terms of exploration.

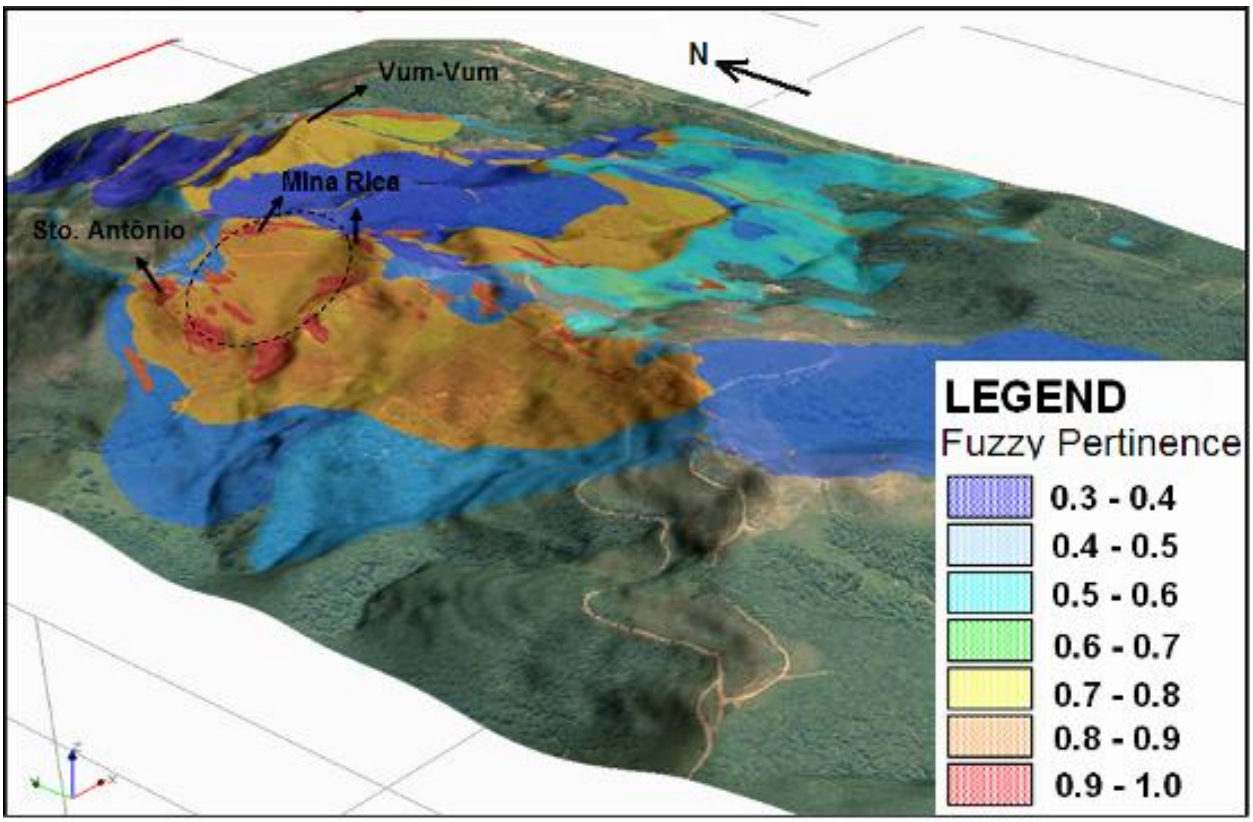

Figure 53 – Surface final fuzzy map of Morro da Glória region.

The limits of the old excavations were also projected to depth following average direction and plunges of each of the known ore bodies (since the majority of these excavations involved a mineralized gold-bearing body). The soil and sediment geochemical information and magnetic anomalies were also projected according to the average plunge of the known mineralized bodies (N75E/35^{o}N). The 3D lithological model was generated from the exploration information, the geological map of 770m level and a geological surface map. The horizontal mineral favorability maps were then calculated at 75m intervals (Figure 54).

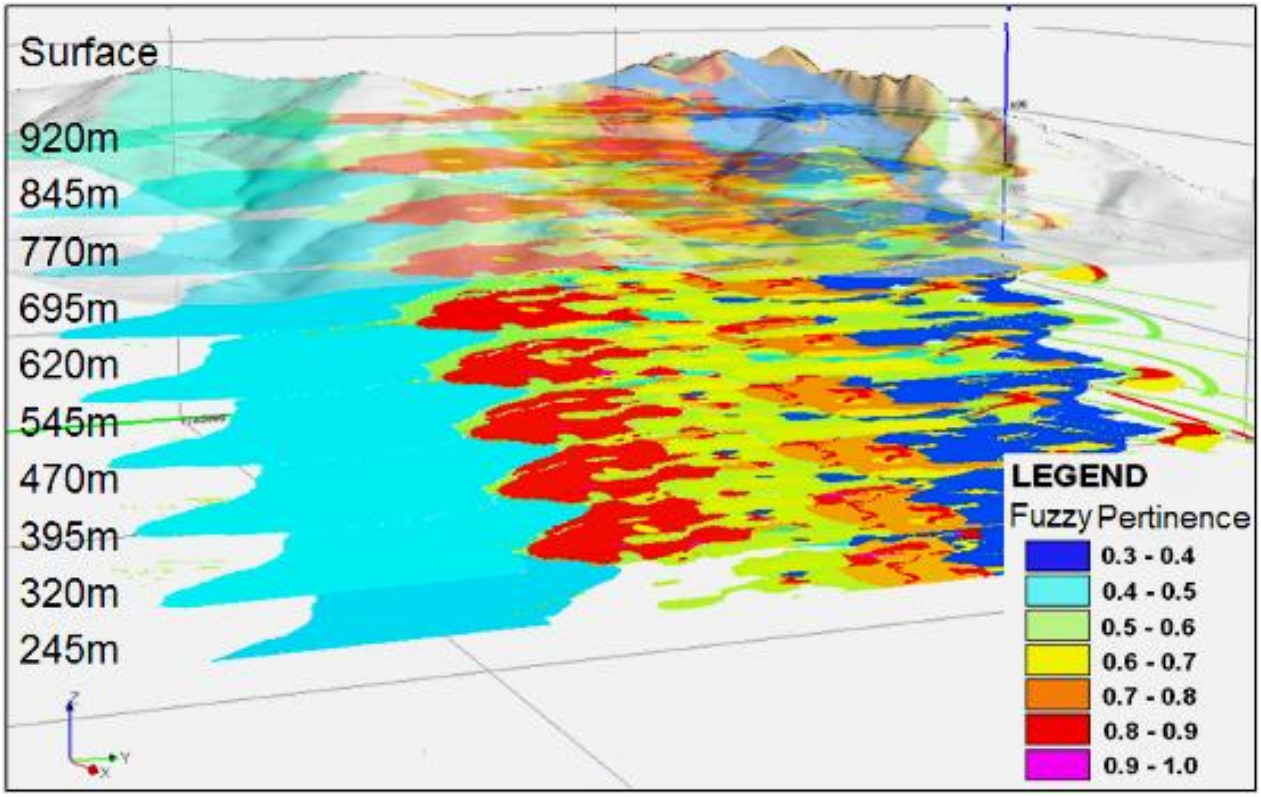

Figure 54: Underground multiple fuzzy gamma results (for each 75m).

Comparing the results of the three dimensional sections that were modeled through the application of the proposed methods with the known mineral bodies down to level 4, and projecting these bodies to depth, an excellent correlation was obtained. New anomalous volumes with considerable exploration potential were also modeled and recorded as having follow-up investigation potential (Figure 55).

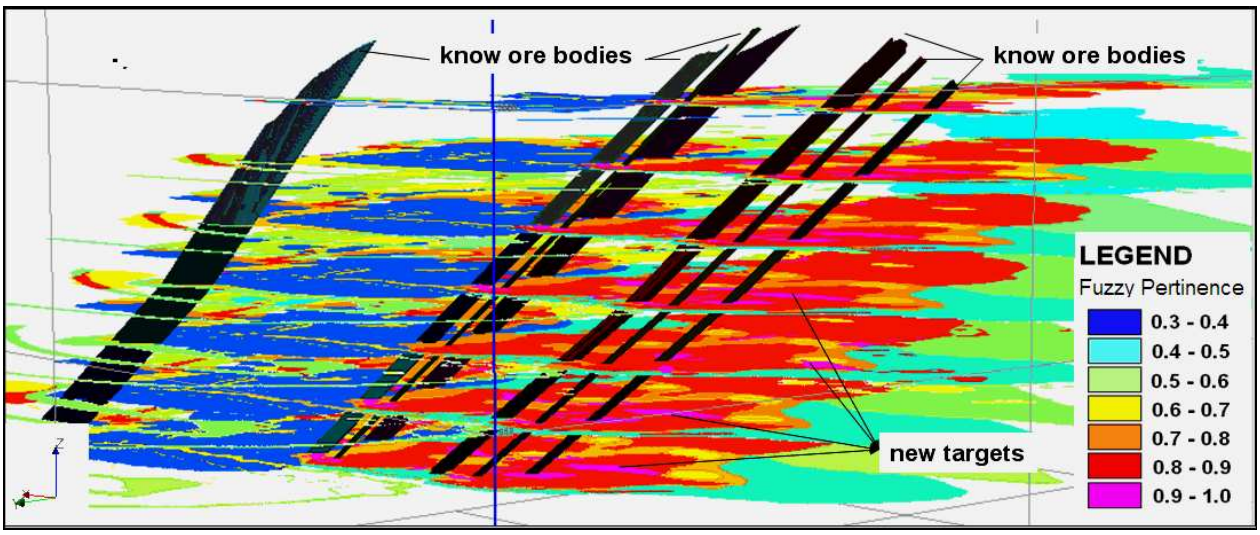

Figure 55: Multiple fuzzy gamma maps *vs.* modeled orebodies based on chemical results from drillholes.

Special mention must be made in relation to the projection of information to very significant depths. It is not advisable to project the results to depths beyond the levels of available information. Thus, the greater the distance between the levels of existing information and the last modeled section, the lower the accuracy of the modeling process. The projection of information to a certain depth also depends on the behavioral characteristics and geological and structural complexity of each deposit. It is the responsibility of the analyst to define the maximum depth of the model. The gold bearing deposits of the QF have distinct characteristics and are quite diverse with regard to continuity and variability in depth, therefore care must be taken when establishing the final depth of the model.

On the other hand, the results of the direct inversion on the electromagnetic conductivity data (Tauz channel) in the Morro da Glória (Figure 56) revealed three suggestive indications in the understanding and characterization of the geological deposit:

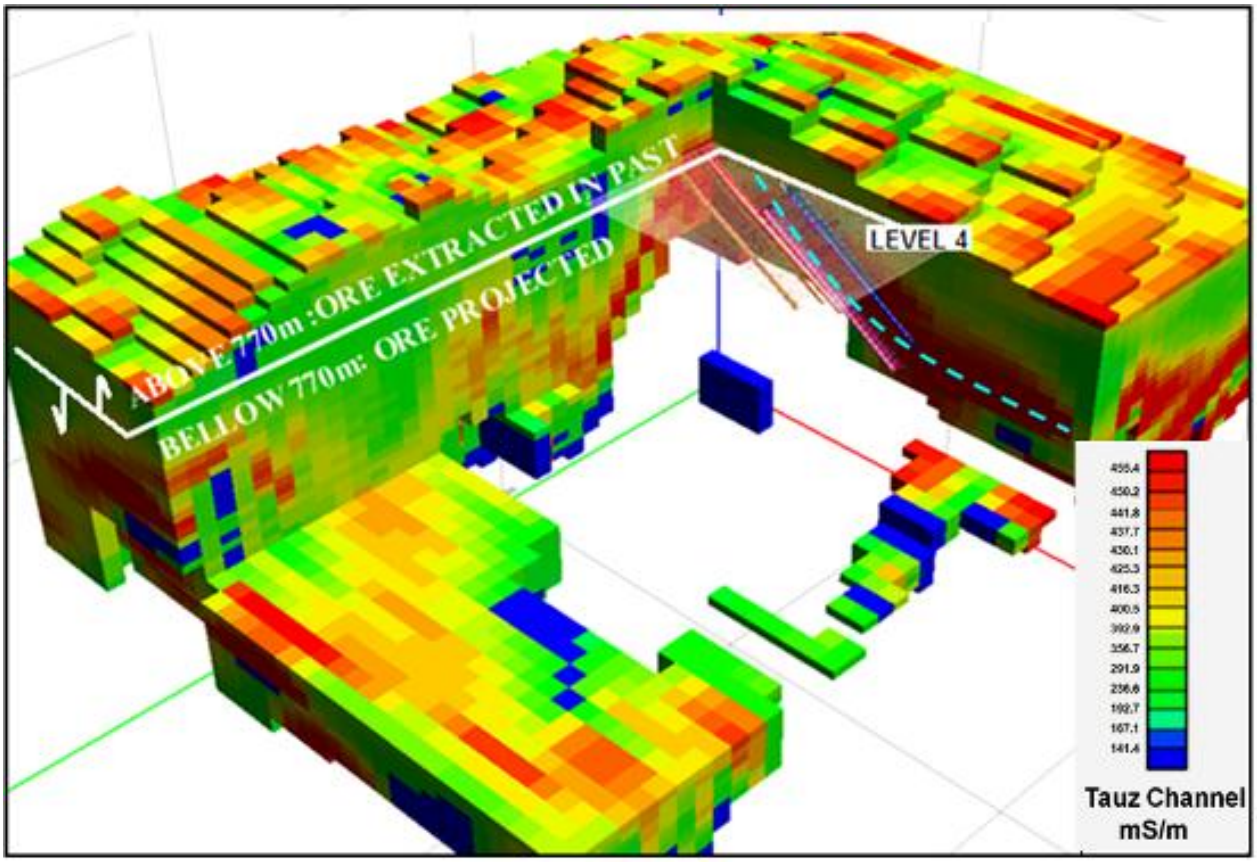

Figure 56: AEM raster matrix model clipped to the furthest underground development. The diagram shows the high correlation between the beginning of the AEM 3D anomaly and level 4 (770m) of the mine (actual level under development). Dotted blue line shows the anomaly inflection at depth.

(i) The estimated depth defined by the beginning of the electromagnetic conductive anomaly coincides very well with the level of underground development where the mine was stopped (770m). This indicates that above this level, the sulphide mass, which characterized an anomaly at a higher level, was already extracted. Therefore, the method had the capacity to define very well the depth of the start of the conductive sulphide material, which is still present in this location (Figure 56);

(ii) Almost all of the large gold-bearing deposits in the QF show, at depths below 500m (depending also of the size of the deposit), a softening/flat of the plunge angle of the ore body – a phenomena related to the regional deformation. In this case, below the 400m level, the conductive anomaly also showed smoothing, indicating the probable continuity of the mineralized body at depth according to the illustration on Figure 56, indicated by the dotted blue line;

(iii) The presence of additional anomalies, which are outside the coverage limits of the fuzzy analysis, indicated new potential targets (Figure 58).

The results obtained from the inversion process of the electromagnetic conductivity information, could be incorporated as a new theme in further fuzzy analyses which was performed using only geochemical, geological and magnetic data. However, there are restrictions to this type of joint analysis. Amongst the disadvantages of using the product of the geophysical inversion in the fuzzy analysis are: (i) the inadequate resolution of the blocks in the inverted model (50m). The ore bodies are restricted and this resolution is not sufficient for greater detail; (ii) at shallow depths, the electromagnetic conductivity intensity values are low for this type of inversion which causes negative interference on the product of fuzzy operations at levels close to the surface.

Nevertheless, it was possible to compare and analyze the results together, since they are grouped together into the same computational platform. A three dimensional cubic cut from the inverted model is shown in Figure 57 together with the fuzzy section from 395m. It can be seen that the product of the inversion volumetrically coincides well with the gamma product from he fuzzy logic near this depth. The smoothing of the EM anomaly at depth shown in the inverted model in Figures 56 and 57, exemplarily confirms real smoothing of the ore body plunge, as previously interpreted. Therefore, one should be cautious when making interpretations based on product derived from indirect data alone.

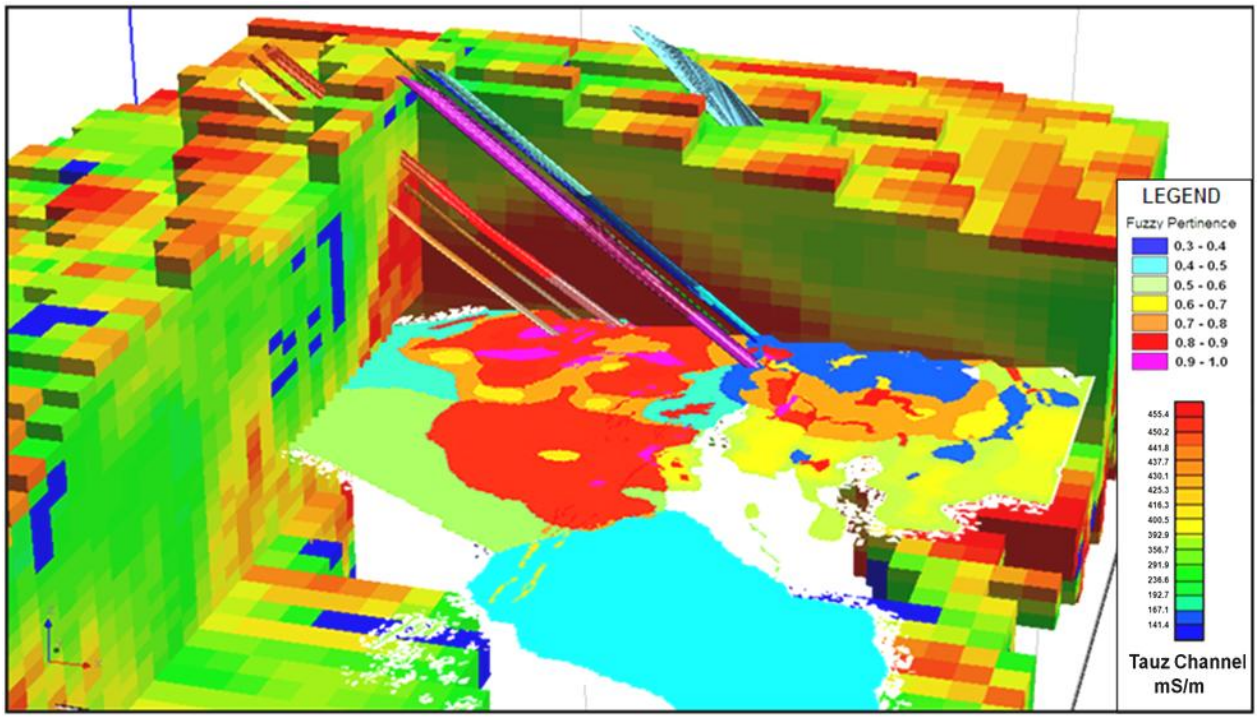

Figure 57: AEM voxel model integrated with a horizontal slice (level 395) yielded from the fuzzy gamma product.

Figures 58A and 58B show a section with the results from the fuzzy analysis at a depth of 595m with two different thresholds of the inverted geophysical model: 80^{th} and 90^{th} percentiles respectively.

The anomalies in the inverted models are represented by transparent parallelepipeds in black. These figures show that for this level, an excellent correlation exists between the anomalous areas in red and the fuzzy analysis in magenta. Furthermore, blocks with electromagnetic intensities above the 80^{th} percentile (Figure 58A), also reveal a continuity in the electromagnetic conductive anomaly, although lower in the both north and south, which extends the prospective potential of the deposit.

Figure 58B also indicates the existence of a prominent correlation between the two models. However, this correlation is not as expressive in the shallower sections. In this case, the volumes of the three dimensional solids at shallower depths were not used in the inversion process in this study.

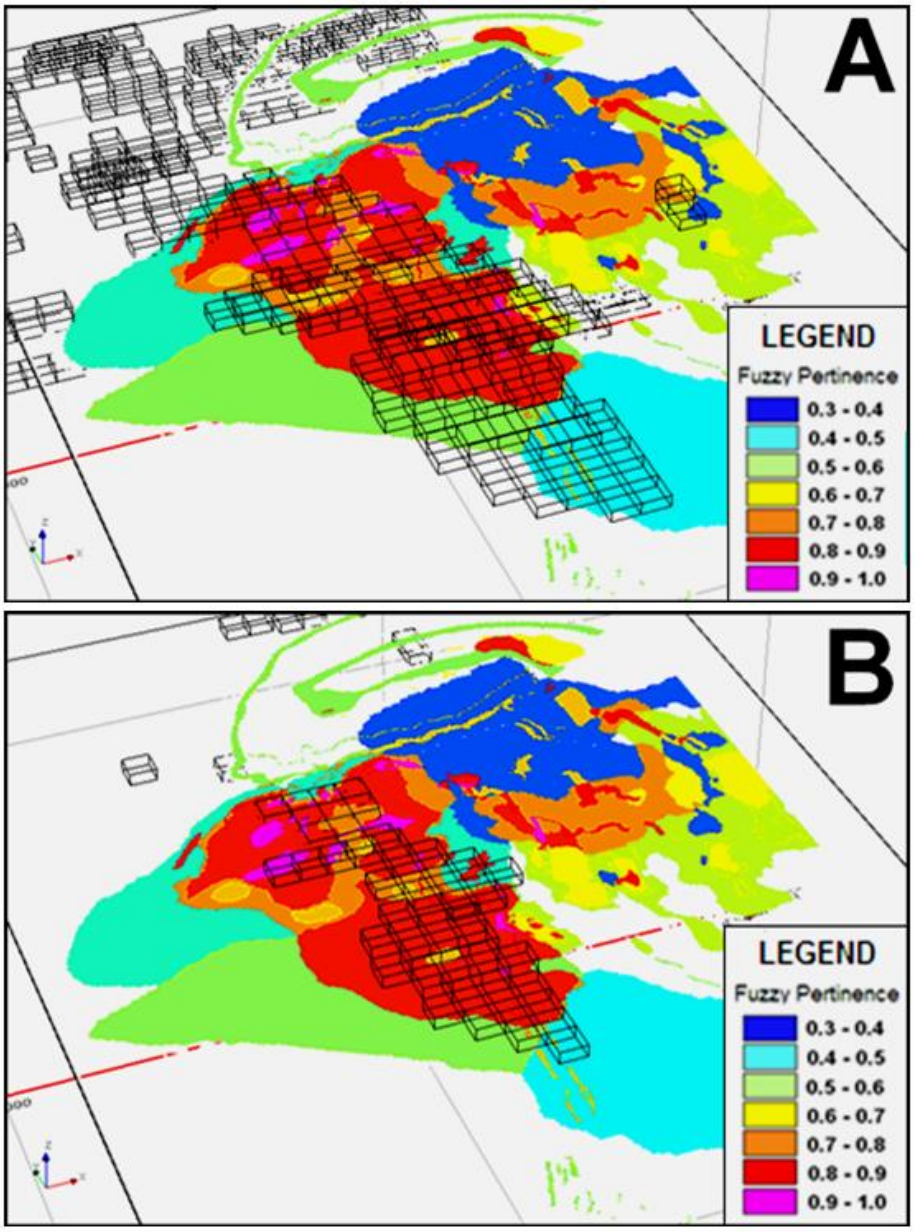

Figure 58: AEM inverted model with different thresholds. (A) percentile 80. (B) Percentile 90. The model is shown combined with a slice (level 595) extracted from the fuzzy gamma product.

9 – CONCLUSIONS

The main conclusions from this study are as follows:

With regard to chargeability and resistivity, the IP1 geophysical survey sections generated results highly correlated to known orebodies of the Lamego deposit. The conductive anomalies resulting from inversion of the EM data also corroborated with the IP data and location of existing orebodies.

The IP2 and IP3 sections show no consistent continuities for the orebodies along the plunge. Nonetheless, they revealed acceptable estimated depths of the geophysical anomalies in the Carruagem orebody.

A significant anomaly in the Arco NE body confirmed the presence of high volume of sulfide in this orebody, despite having insignificant gold content.

The IP sections contributed to showing the southern continuity of the Carruagem body, which was subsequently confirmed by the positive results of the surface exploration drilling.

A large anomaly located in the northeastern extension of the Carruagem body was modeled and tested. The results obtained by drilling did not confirm this anomaly, which was interpreted as the result of insufficient energy to cross the uneven surface. This problem may also be related to different rock types found at Lamego and the São José Target; in other words, to their different rocky backgrounds. In addition, there are no EM anomalies in this area.

At the São José target, the integration of data from geological mapping, soil geochemistry, IP and excavations has so far resulted in exploratory success for drill holes.

The IP anomalies in the Biquinha, Sobradinho and Bom Caminho targets exhibited a good correlation with geological and geochemical surface information projected following the dip direction on underground.

The summarized table with the main characteristics of sulfide proportions of the Lamego orebodies and satellite targets, together with a group of geophysical intensities from different surveys, was capable to characterize some orebodies rich in sulfides and consequently with possibilities of having good gold grades.

The techniques and methods combined in this research, coupled with the information displayed in Table 3, can be useful in future mineral exploration for areas with limited surface geological information. This would be particularly relevant in green field projects and in areas where thick weathering layers are predominant.

The results obtained from the method of subjecting multiple horizontal sections to fuzzy logic operators presents significant geometrical correlation with the product of the geophysical inversion process of the electromagnetic conductivity data in Morro da Glória deposit, albeit at different resolutions or scales.

CHAPTER 2

ORDINARY KRIGING AND CONDITIONAL SIMULATION TO SUPPORTQUANTITATIVE ESTIMATION AND RESOURCE CLASSIFICATION AT THE LAMEGO GOLD DEPOSIT – QUADRILÁTERO FERRÍFERO - BRAZIL

SUMMARY

The Lamego gold deposit is located in the northwestern sector of the Quadrilátero Ferrífero (State of Minas Gerais, Brazil), along the Cuiabá gold mine trend. Its economic and technical pre-feasibility study was approved in September/2009. This deposit is hosted by Neoarchean rocks of the Nova Lima Group, Rio das Velhas Supergroup. It is situated in an antiform structure, comprising a perimeter of 4.8 km, with a NE-trending axis and limbs dipping 25º to ESE. The mineralization comprises the Carruagem, Cabeça de Pedra, Arco da Velha and Queimada orebodies, which are hosted mainly by hydrothermally altered banded iron formations (BIFs) and quartz veins. Gold occurs as free specks or associated to pyrite grains. The mineralized horizons are located above the meta-mafic rocks and below carbonaceous, meta-pelitic and meta-volcanoclastic schists. The mineralization is interpreted as of mesothermal type, with concentric hydrothermal zones. From the unalterated, inner to proximal ore zones, domains rich in chlorite, carbonate and sericite are observed predominantly in the meta-mafic rocks, whereas sulfidization occurs mainly in BIF and associated to quartz veins. Presently, the geological resources at Lamego are around 1.3MOz and mineable resources are approximately 370KOz.

This work aims to evaluate both ordinary kriging and conditional simulation methods to support quantitative estimation, characterization and classification of the Lamego deposit. Some 900 drill holes and 1500 underground channels support the geostatistical analysis. The purpose of ordinary kriging is to estimate gold grade values in the blocks for which there are no samples, involving those between two developed mine levels, or those between surface and/or underground core-drilling sectors. Conditional simulations are used for accessing the uncertainties interrelated to the classification of the deposit, as well as for generating probabilistic estimates of the parameters that shall honor the variability of the sampled populations. Spatial distribution resulting from the calculated values makes it possible to access the uncertainty. For calculations of the uncertainty in panels relating to quarterly or annual periods, the Sequential Gaussian Simulation was the method employed, which generates a distribution of 100 possibilities or realizations of grades and thicknesses for each estimated SMU (Selective Mining Unit).

Conclusions on metallogenic aspects of the Lamego deposit were yielded on the basis of geostatistical analysis. The mean gold distribution of the horizontal volumetric panels indicates that gold grades are lower with increasing depth both in the Carruagem and Arco da Velha orebodies. Conversely, the mean gold distribution of the vertical volumetric panels indicates that gold grades slightly increase following the north direction. This feature can be associated to deformation episodes (that are coincident to the mineralizing hydrothermal fluid accumulation at those sites) and/or to structural traps in the northern sectors of the aforementioned orebodies. The bivariate study of Au and S (scatter plots) was probably the most significant to define the guide reefs of the Lamego deposit. The correlation coefficients vary for different orebodies. In the Carruagem orebody this factor is much lower (0.22) than the others. Therefore, geostatistics highlighted a population with high gold and low sulfur grades, which is of key importance. At these sites gold is frequently associated to micro-fractured, gray quartz veins and occurs as free gold. This makes difficult the visual control of such orebodies during underground development since the classic targeting method is guided by observable high concentration of sulfides at the outcrops.

1 – HISTORICAL DATA

The Lamego gold deposit, owned by AngloGold Ashanti Brasil Mineração Ltda, is sited in the northwestern part of the *Quadrilátero Ferrífero* (Iron Quadrangle) metallogenetic province - a historic producer of gold, iron, manganese and limestone, as well as other mineral commodities. It has been studied since 1981. From 1985 to 1990, a surface exploratory program was carried out along 5.7 km of iron formation, when the existence of 27 different mineralized zones hosted in gray quartz veins and banded iron formation were revealed. These mineralized zones were later designated as Arco da Velha, Queimada and Cabeça de Pedra orebodies.

For the purpose of making a detailed evaluation of the sulfate potential of these orebodies, a ramp was developed, from level 932m to level 1, at an elevation of 880m, where the aforementioned orebodies were exposed. The obtained results from this campaign were not sufficient to support the feasibility of the project. The activities stopped and the drifts were flooded in 1997.

A new drilling campaign began in 2001, targeting the recently discovered Carruagem orebody. The results of this campaign were positive and supported a new approach to the Project, associated with the Cuiabá mine expansion. Dewatering of the drifts started in 2002 and a new descending ramp was excavated for the purpose of intercepting the Carruagem target at the 744m elevation. A conceptual study was issued in December 2004, motivating the approval of a pre-feasibility study.

The oxidized portion of the deposit is currently being mined by MSOL-Jaguar Mining Inc.

The geological resources of the Lamego deposit (reference date July 2008) approximates 4,100,000 tonnes with *in situ* average gold grade of 4.3g/t. This amounts to approximately 42.4 tons of gold, with 8% of the total metal content being classified as measured, 29% as indicated, and 63% as inferred. Mineable resources at Carruagem, Cabeça de Pedra and Arco da Velha orebodies (reference date July 2008) sum up to 2,164 ktonnes with a gold grade of 5.01 g/t.

The objective of this work is to apply a group of geostatistical methods, particularly ordinary kriging and conditional simulation, to estimate the metallic content of the Lamego deposit; to assist the classification of the ore in terms of measured, indicated and inferred resources, depending on the confidence level of the estimate; and to advance the present geologic and metallogenetic knowledge of the deposit.

Processing steps that precede the ordinary kriging includes geologic modeling, spatial data exploration, generation of adjusted sample composites, probability distribution function analysis, investigation of scatterplots between different variables, capping definition, variogram fitting and definition of a set of input parameters for kriging.

Conditional simulations are used here to assess the uncertainties comprised in the evaluation of the deposit, as well as for generating probabilistic estimates of the parameters that shall confirm the variability of the samples. The results of the conditional simulation are employed to assist the classification of the resources.

2 - MINERAL RESOURCES

Lamego's mineral resources are represented by individual block models in the five major orebodies of the deposit. The block models were generated by ordinary kriging estimation considering 3D geologic models for each orebody. The geologic models were developed based on multiple sections positioned orthogonal to the plunge of the mineralized horizons, allowing the use of all available geochemical results. These include Au-grades from samples extracted from channels at the development fronts and from drilling cores. The sets of attributes for the block models are described in table 1.

Table 1 – Attributes used in the block models for the Lamego deposit orebodies.

Attribute	Description
ZONE	Designates the mineralization zones. It is divided into oxidized and sulfidized. The blocks situated below the oxidation surface have the attribute ZONE=2, whereas the blocks located above the oxidation surface are stamped with ZONE=1
LITO1	LITO1=1 → BIF; LITO1=2 → GQZ; LITO1=3 → QZF; LITO1=4 → XG…
DENSITY	Density in g/cm^3
TONNES	Tonnage of the individual block (in metric tons), used for assessing the geological resources.
AU	Ore grades in g/t
AS	Arsenium grades in ppm
S	Sulfur grades in %
CAT	Classification of mineral resources CAT=1 → Measured CAT=2 → Indicated CAT=3 → Inferred

The geostatistical procedures employed here are presented in the following sections. They were used for quantitative estimation of grades and volumes of the orebodies and to support the

final figures related to the metal content of the Lamego deposit. The purpose of ordinary kriging is to estimate gold grade values in the blocks for which there are no samples, involving those between two developed mine levels, or those between surface and/or underground core-drilling sectors. It is based on a set of channel and core samples selected from the wireframes of the geological models, and also studies of the 3D trends of the grades along the plunge, strike, and thickness.

2.1 - Database

Practically all the orebodies consist of a group of small enriched horizons. They were individualized in discontinuous wireframes. The entire Carruagem orebody extends approximately 290m along the strike, with significant discontinuities. The total length of the underground galleries developed at Carruagem is 926m, including levels 1 and 2. To date, there are *(i)* 301 drill holes in this orebody, including long holes drilled from the surface, old short holes, and holes drilled during underground development; *(ii)* 426 channels, *(iii)* more than 12,700 samples with Au grade, and a substantial number of samples with S and As grades. Subsequently to the selection of samples from within the geologic model, a sub-set of 1,872 samples was individualized and subjected to geostatistical evaluation. The same procedure of separation of the anomalous samples located within the interpreted solids was used for each of the other orebodies, which were then subjected to evaluation studies. For the interpretation, a minimum of 1.6m of thickness and at least 2.5g/t of Au composited grade were used. Table 2 summarizes the volume of information available to date for each orebody of the Lamego deposit.

Table 2 – Summary of the exploration data available to the Lamego deposit.

LAMEGO - SUMMARY OF THE DATA						
ORE BODY	**Drill holes**	**Channels**	**Total samples (Au)**	**Selected samples (Au)**	**Selected samples (S)**	**Development (m)**
Carruagem	301	426	12706	1872	948	926
Cabeça de Pedra	138	239	9238	709	519	357
Arco da Velha	320	446	12928	2214	702	916
Queimada	170	400	5204	863	593	1255*
Total	**929**	**1511**	**40076**	**5658**	**2762**	**3454**

Project data related to channels and drill holes were centralized in an Oracle database and managed by the Fusion/Century system. The centralization of this information allows rapid, easy, safe and reliable data insertion, editing and migration. The database contains information such as lithological and structural descriptions, geochemical analyses, densities, as well as additional information characterizing the drill holes in detail.

In order to ensure the validity and reliability of the estimation process, a strict quality control is required, which enables the identification of possible irregularities in the grade and geometry of the modeled orebodies.

Figure 1 shows schematic views with drill holes, channels and wireframes of each orebody.

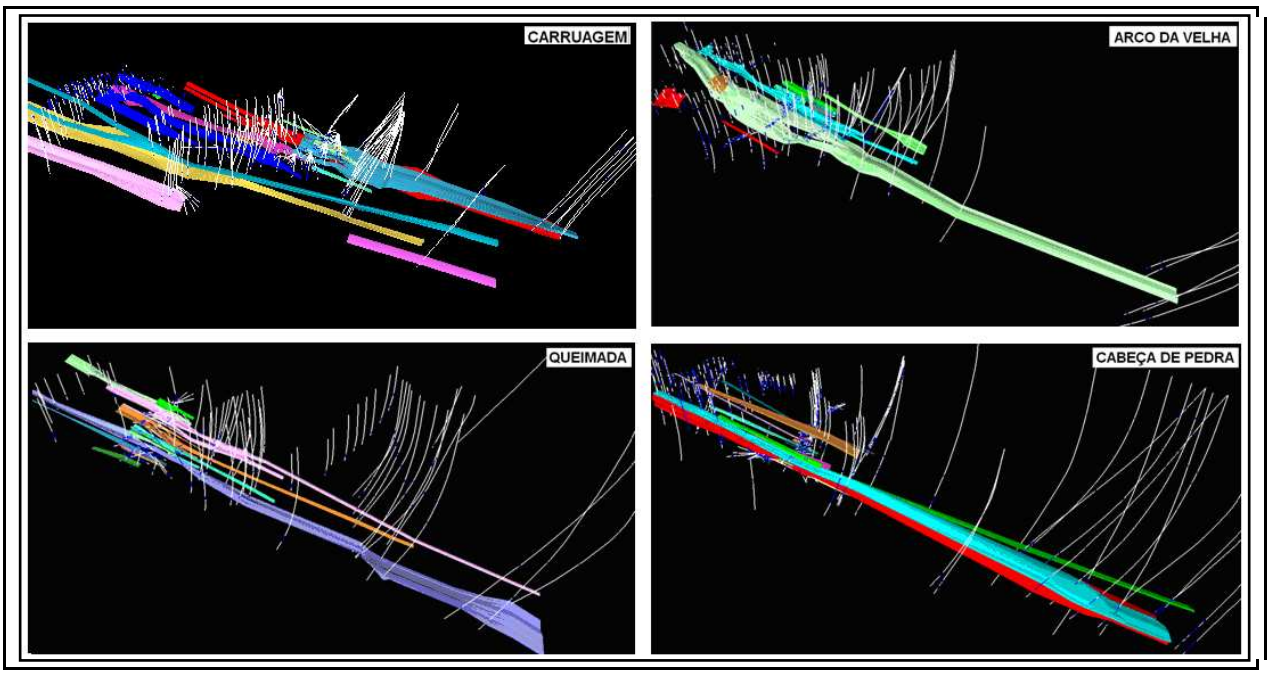

Figure 1 – Schematic views with drill holes, channels and wireframes of each orebody. Different and random colours represent individual ore shoots.

2.2 - QA/QC

Lamego project's Quality Assurance (QA) and Quality Control (QC) meet the requirements of international standards. The samples are analyzed at the chemical laboratory of Queiroz Plant, and a duplicate is made at an external laboratory (SGS). A table summarizing the number of Lamego Project's samples used for QA/QC was prepared for the pre-feasibility study (Table 3).

During the process of sample preparation and grouping into batches to be sent to the laboratory, standard samples and blank samples are inserted. For every ten rock samples, a standard, high-grade sample is included together with a blank sample, or a standard low-grade sample. This serves to evaluate the laboratory and identify with more reliability the origin of occasional problems.

The blank samples included in the batches serve to evaluate whether there was any contamination during both the handling and the preparation of the material, any inversion or

swapping of samples, as well as to evaluate the quality of the reagents, especially litharge (PbO), which can be contaminated with gold.

The standards used were provided by RockLAB, which holds an international certificate. They were analyzed to measure the accuracy or inaccuracy of laboratories by comparing the results from standards samples with different pre-established values between 1.8 g/t and 5.9 g/t. The laboratory's performance considering this procedure is summarized in Table 3. The distribution charts comprising the contents of standard and blank samples, with the respective standard deviation limits, are presented in Figures 2 to 6.

Table 3 – QA/QC summary of the blanks and RockLAB standards - Lamego Project.

ROCKLAB STANDARDS - QA/QC - LAMEGO PROJECT

Standard	Element	Value (g/t)	Sdv	Total stds	Out of 1 stdv	Out of 2stdv	Out of 3 stdv	% out of 1stdv	% out of 2stdv	% out of 3stdv
B	Au ppm	0.025		456	2	0	10	0.44	0.00	2.19
SI25	Au ppm	1.801	0.044	130	9	2	3	6.92	1.54	2.31
SJ10	Au ppm	2.643	0.060	183	83	1	9	45.36	0.55	4.92
SK11	Au ppm	4.823	0.110	17	4	2	3	23.53	11.76	17.65
SL20	Au ppm	5.911	0.176	101	15	6	3	14.85	5.94	2.97
SL34	Au ppm	5.893	0.140	27	2	0	0	7.41	0.00	0.00
TOTAL				**914**	**115**	**11**	**28**	**16.42**	**3.30**	**5.01**

Contamination problems that usual occur include: *(i)* positive results in blank samples and/or; *(ii)* results from standard samples outside the standard deviation margins. When contamination is suspected, after an attempt to identify its origin, a new set of analysis comprising 20 samples, adjacent to the problematic sample, is performed.

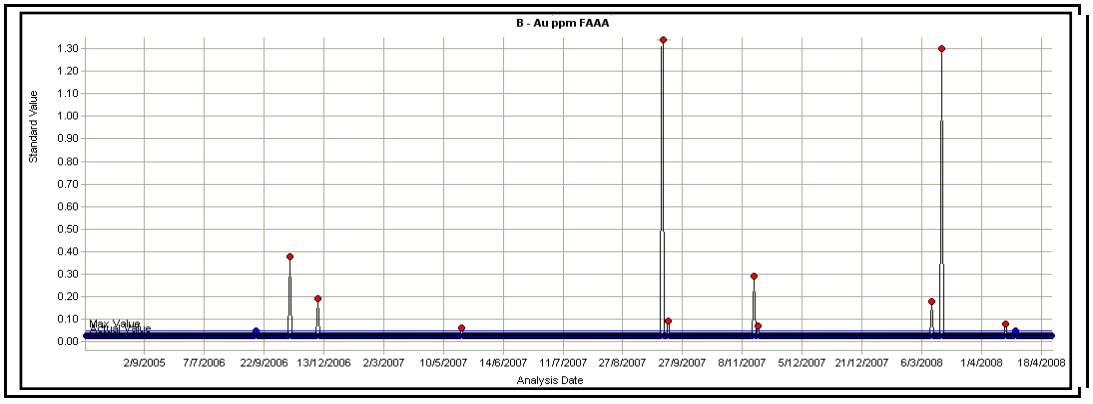

Figure 2 – Result of blank samples – QAQC

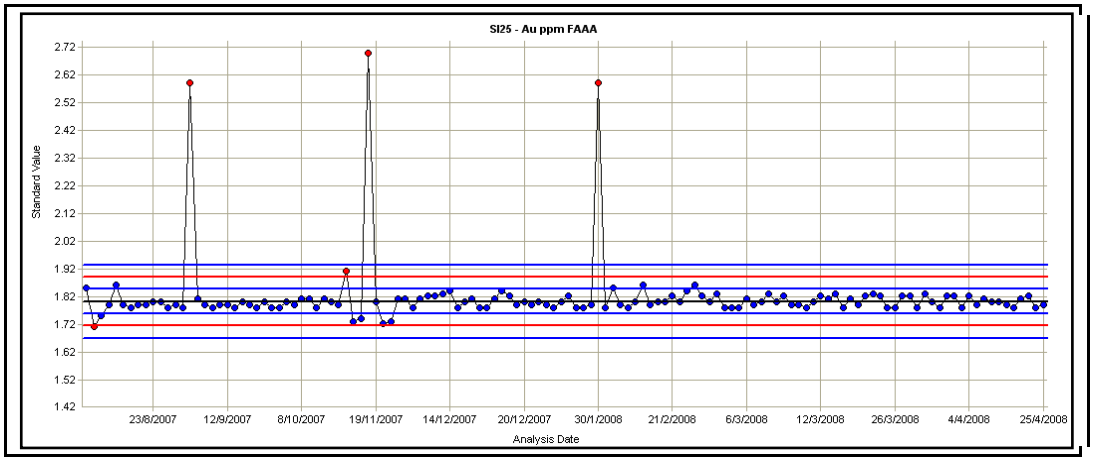

Figure 3 – Result of SI25 standard - 1.801g/t - QAQC

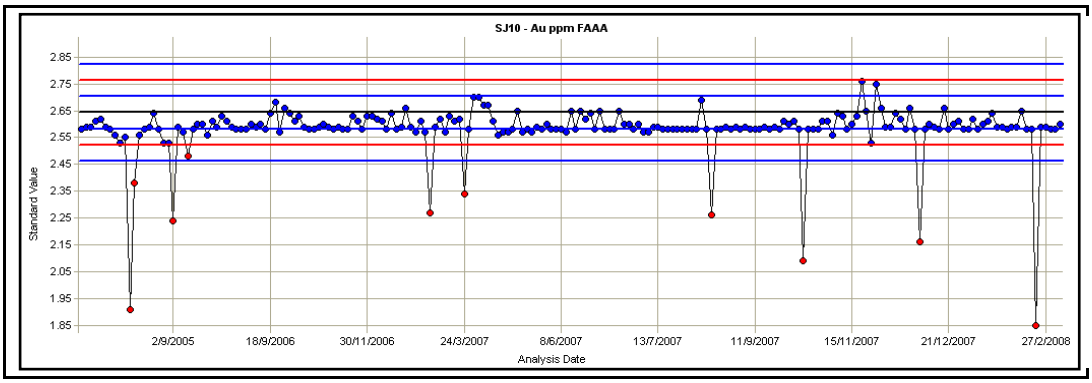

Figure 4 – Result of SJ10 standard - 2.643g/t – QAQC

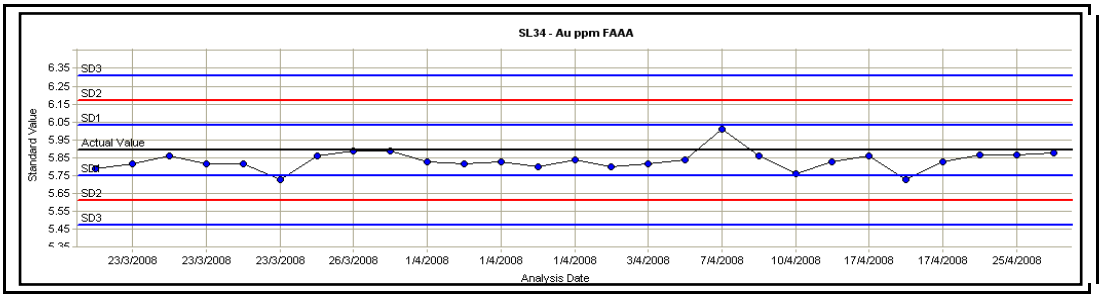

Figure 5 – Result of SL34 standard – 5.893g/t – QAQC

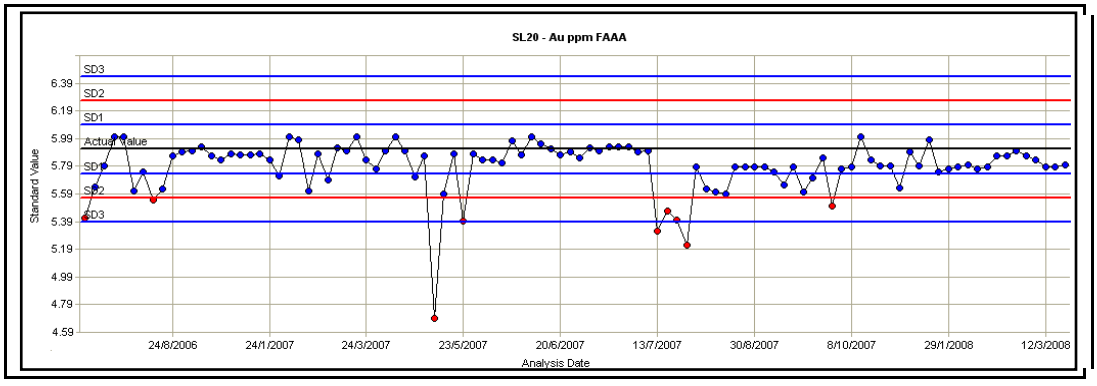

Figure 6 – Result of SL20 standard – 5.911g/t – QAQC

Approximately 850 core samples and 522 channel samples from all orebodies were selected and sent to an external laboratory (ALS Chemex) for cross-check analysis. A large portion of the core samples were taken within the limits of the modelled orebodies. They were sampled at random, without distinction of content, date, or any other criteria. Figure 7 shows scatter plots comprising the comparison of the results. It can be seen that the correlation index yielded from the comparison is within an acceptable limit (>85%).

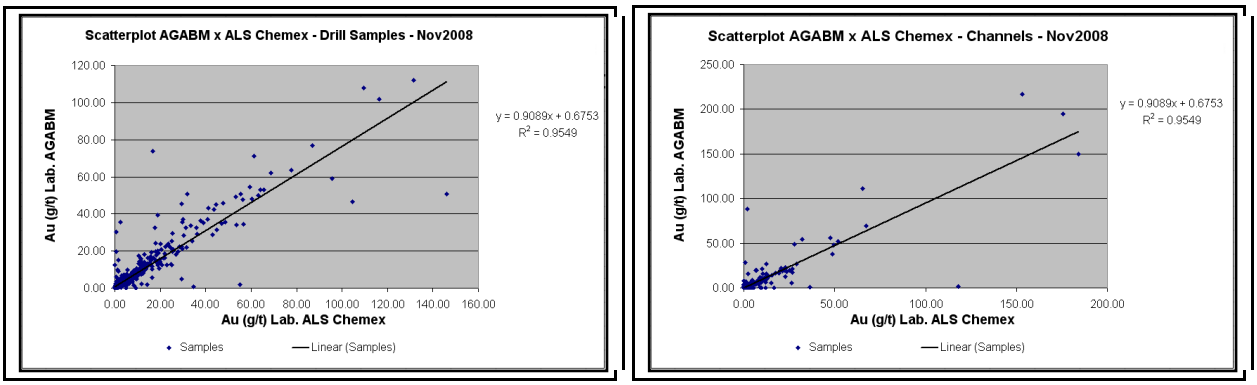

Figure 7 – Original *vs* re-analyzed data of the Lamego Project.

2.3 - Density Calculation

A large portion of the core samples at Lamego has a density measurement calculated by the immersion method. The average density for the orebodies varies as a result of different average percentages of sulfide for each orebody. Their average densities are summarized in Table 4.

Table 4 – Average densities of Lamego orebodies.

AVERAGE DENSITY OF LAMEGO ORE BODIES				
	Carruagem	Arco da Velha	Cabeça de Pedra	Queimada
Density (g/cm3)	2.87	2.91	2.92	2.95

2.4 - Geological Modelling

The appropriate geological modeling of the geometry of orebodies is perhaps the most important step in the evaluation of a mineral deposit. During 3D geologic modelling, it is essential to respect geologic and structural concepts, as well as to consider the mining methods that shall be used in ore extraction, so as to outclass the chemical results for the variable being analyzed (in this case, gold). For the modeling of Lamego orebodies, an actual minimum thickness of 1.6m to 2.0m and grades of more than 2.5g/t in composite samples were used.

Therefore, high-grade samples located in rocks such as carbonaceous schists and metandesites – that is, outside the lithologic horizons regarded as rock to be mined (BIF and GQZ in Lamego's case) – were excluded from the interpreted 3D solids.

Structural discontinuities, such as faults, folds and fractures observed both underground and at surface outcrops were charted and considered during geological modeling, as well as foliation attitudes observed in drilling cores. This helped the interpretation in places with complex geometric connection of mineralized horizons, in sectors both orthogonal to and along the plunge.

The stratigraphic sequence was respected, so as not to mistakenly link a stratigraphic horizon of the inverted limb to a mineralized horizon belonging to the normal limb, especially when these limbs are very close to each other (e.g., tracts of the Carruagem orebody).

Figure 8 summarizes the workflow of the main procedures here employed. These include the acquisition process, geological interpretation and modelling, evaluation and categorization of resources at the Lamego deposit.

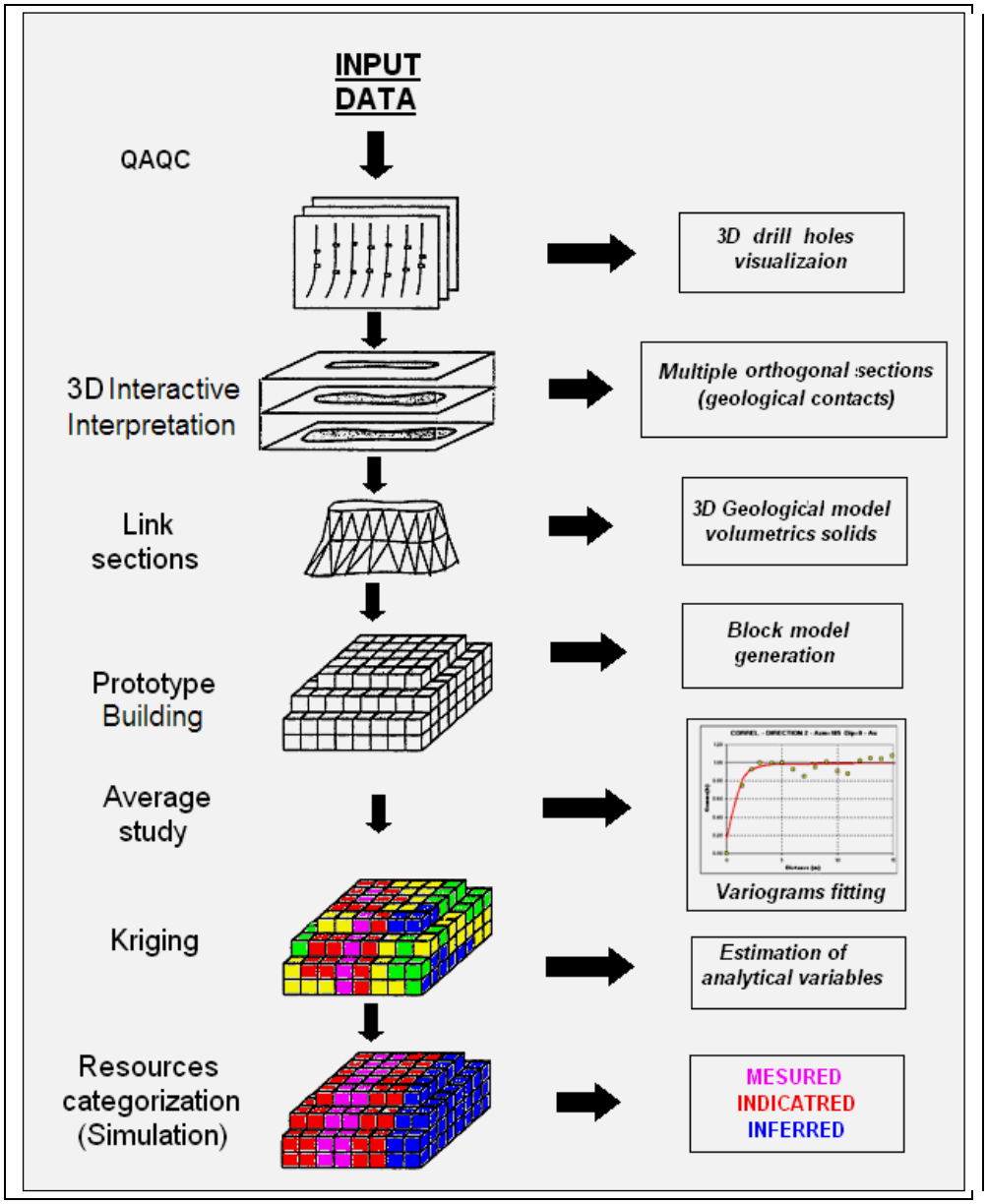

Figure 8 – Methodological workflow.

2.5 – GEOSTATISTICAL ESTIMATION

The best estimator of a set of regionalized variables is not a simple, geometrically weighted mean of the sampled values, but rather a combination of the collected samples. Using this approach, not only their relative position are considered, but also the spatial links underlying the phenomenon, as well as values external to the zone that is to be estimated (Valente & Girodo, 1977).

The problem in finding the best possible linear estimator based on all available samples was solved by Matheron (1962, 1963). Matheron`s *kri*~~*g*~~*ging estimator* is described in detail in section 2.5.3**.**

2.5.1 - Lamego: Data Exploration

Study of averages

Herein, the objective is to assess and control the values of the mean gold grades both before and after the composition of samples in regular lengths, and after the study of the capping, which are some of the steps that precede the estimation by ordinary kriging.

The composition of samples in defined intervals contributes to the consistency of the database and smoothes the shape of the frequency histogram. For the composition of samples from both the Carruagem orebody and the other orebodies, a length close to the mean of the lengths of the channels was adopted, and the different lithological types were respected. Figure 9 shows two frequency histograms of sample lengths prior to and after the composition. A composition length of 0.7m was adopted, and a maximum length of 1.05m and a minimum of 0.4m were respected. For the Carruagem orebody, after the composite, the PDF (Probability Distribution Function) approximated a Gaussian distribution and the number of samples increased from 1872 to 1900, as expected.

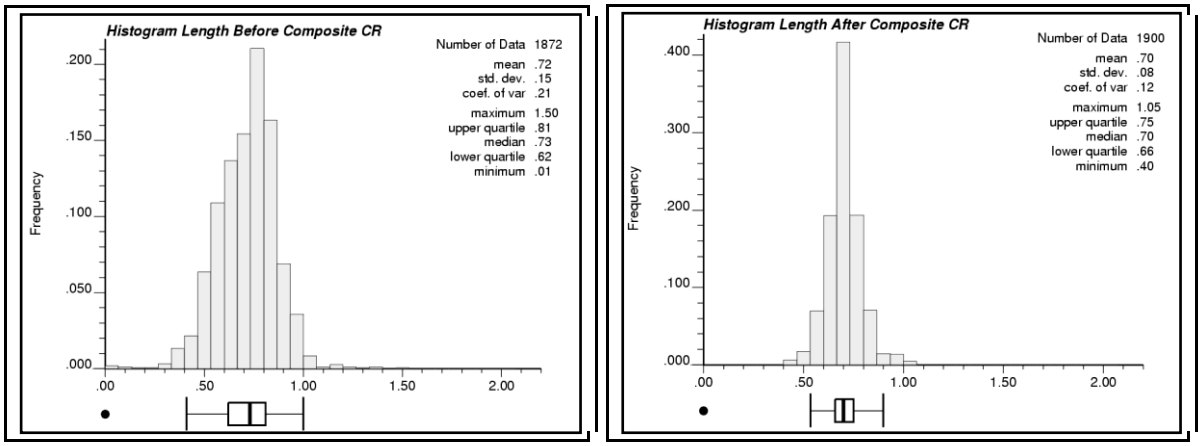

Figure 9 – Length sample histograms before and after composite of the Carruagem orebody. The number of sample increased from 1872 to 1900 (increase of 1.5%) after the composition.

The behavior of the mean values of gold and sulfur grades also changed after the composition process. Figure 10 shows the behavior of the means and the frequency histograms for gold at Lamego orebodies, both prior to and after composite and capping. A slight decrease in mean grades is noted in all orebodies. In the Carruagem orebody, however, the decrease in the

mean grade after capping was more significant. This is due to the existence of a large number of samples with values greater than 55g/t, and to the strong nugget effect caused by the occurrence of native gold in the rocks that form this orebody. After composite, the Au sample mean grows up from 9.08g/t to 9.35 g/t, but the difference is close to 3.0%. The PDF after composite becomes much more symmetric.

The main reason to study the means, prior to and after each one of the processes involved in the evaluation, is to identify possible, significant changes in values that may indicate some problem in a particular procedure, and consequently, may mislead the estimation of the deposit.

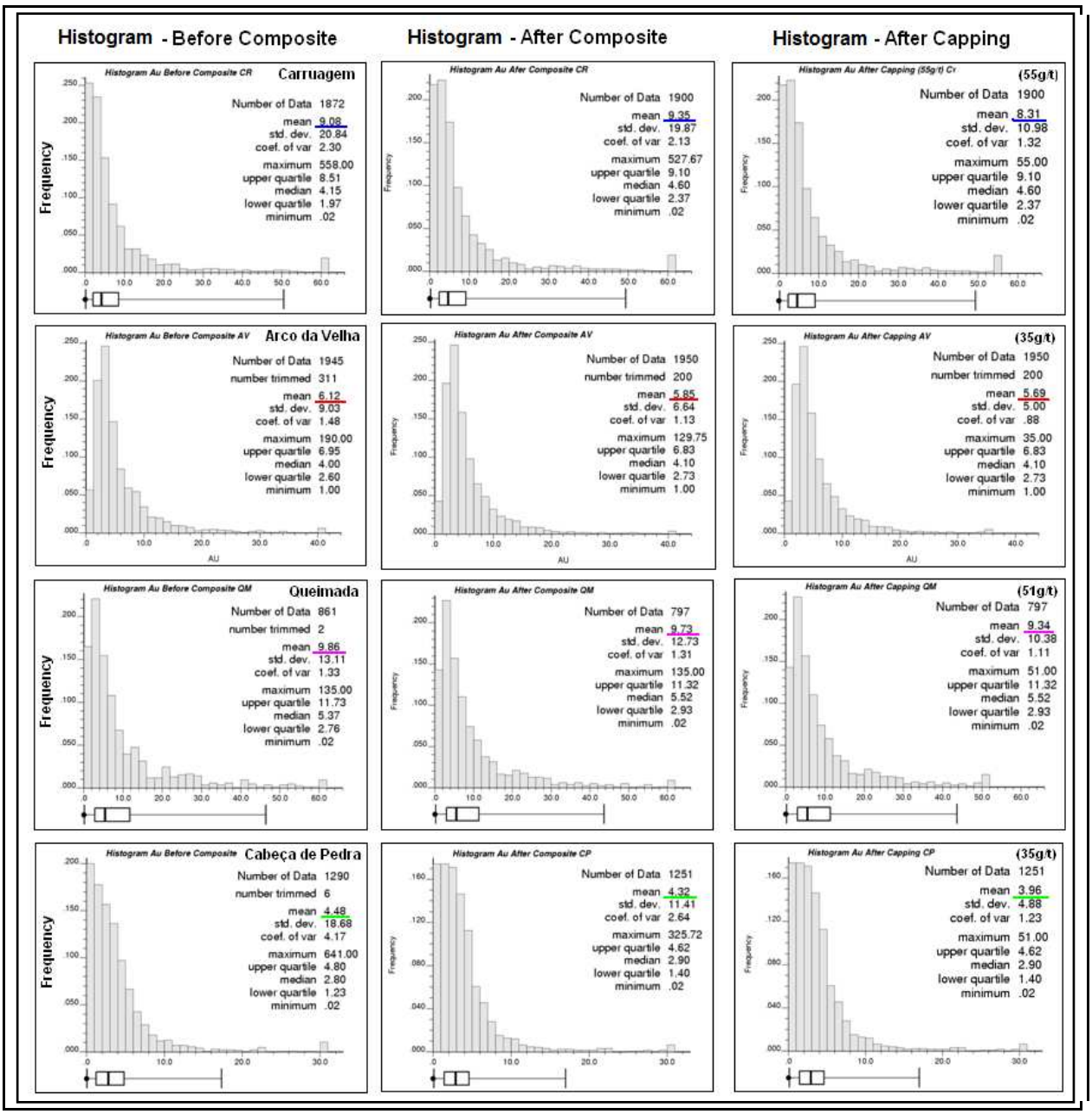

Figure 10 – Behavior of the means and the frequency histograms for gold at Lamego orebodies, both prior to and after each procedure employed to the evaluation of the deposit.

Bi-variate Method

For the bi-variate study, scatterplots of all orebodies were generated to determine the comparative behavior of gold and sulfur grades, since gold occurs associated essentially with pyrite. The correlation factor varies from one orebody to another. The Carruagem orebody has a very low factor (0.22), which means that the scattering of the samples indicates a highly random behavior. This may be explained as being due to the strong nugget effect, which was also confirmed in the variograms produced for this orebody. Carruagem has a particular high grade of

native (free) gold, mainly in the gray quartz veins, posing difficulties for the visual control during underground development, which is guided by high sulfur concentrations and, in this case, can be complex.

Figure 11 shows Au vs S scatterplots for the Lamego orebodies. The orebody with the highest correlation index is Queimada. This shows close Au and S mean values and a correlation index greater than 50%, corroborating the macroscopic aspects of the ore that eventually can reach more than 30% of sulfide.

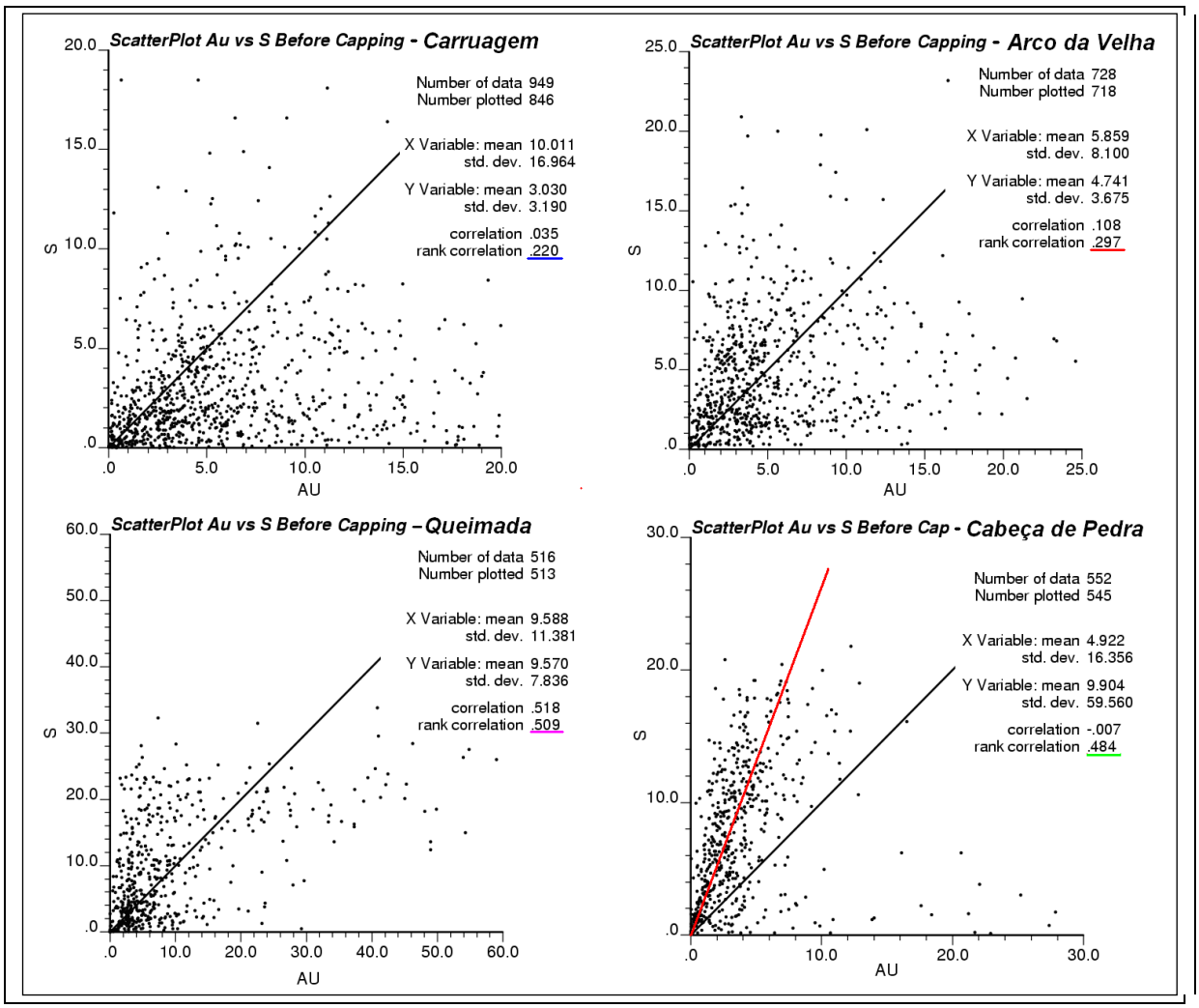

Figure 11 – Au *vs* S scatters plots.

The Cabeça de Pedra orebody also displays a correlation index close to 50%. However, gold grades here are lower. The Au mean value is about half the mean value of S grades.

Capping Definition

Cumulative-probability logarithmic and arithmetic plots help defining cut-off grades for the highest values of the population, which may be associated with the nugget effect or merely with local gold-enrichment phenomena. The reduction from the highest grade values to the upper cut-off limit provided by the probability plots helps obtaining a more continuous population and creating a more reliable system for estimation and simulation, in addition to eliminating possible overestimation during the evaluation of the mineral deposit.

The cumulative-probability arithmetic plots show the beginning of the discontinuity at lower values of gold grades, as compared to the logarithmic plots (Figure 12). Although in the arithmetic plots it is possible to reduce the grade curves to continuously increasing values that are closer to the values defined by the capping, the limits at the very beginning of the discontinuity were used, which reflects a more conservative approach. Figure 12 shows the probability plots for the Lamego orebodies. For the Carruagem orebody, the capping in the probability arithmetic plot shows the beginning of the discontinuity at 55g/t. The logarithmic plots show a discontinuity close to the 105g/t grade, which is considered too high, also taking into account the sensitivity of the geology of this deposit orebodies. For the Arco da Velha and Cabeça de Pedra orebodies, the capping difference between the different plots was not so substantial (from 40g/t to 35 g/t in AV, and from 35 g/t to 23 g/t in CP), as compared to those for the Carruagem and Queimada, where the values were almost halved.

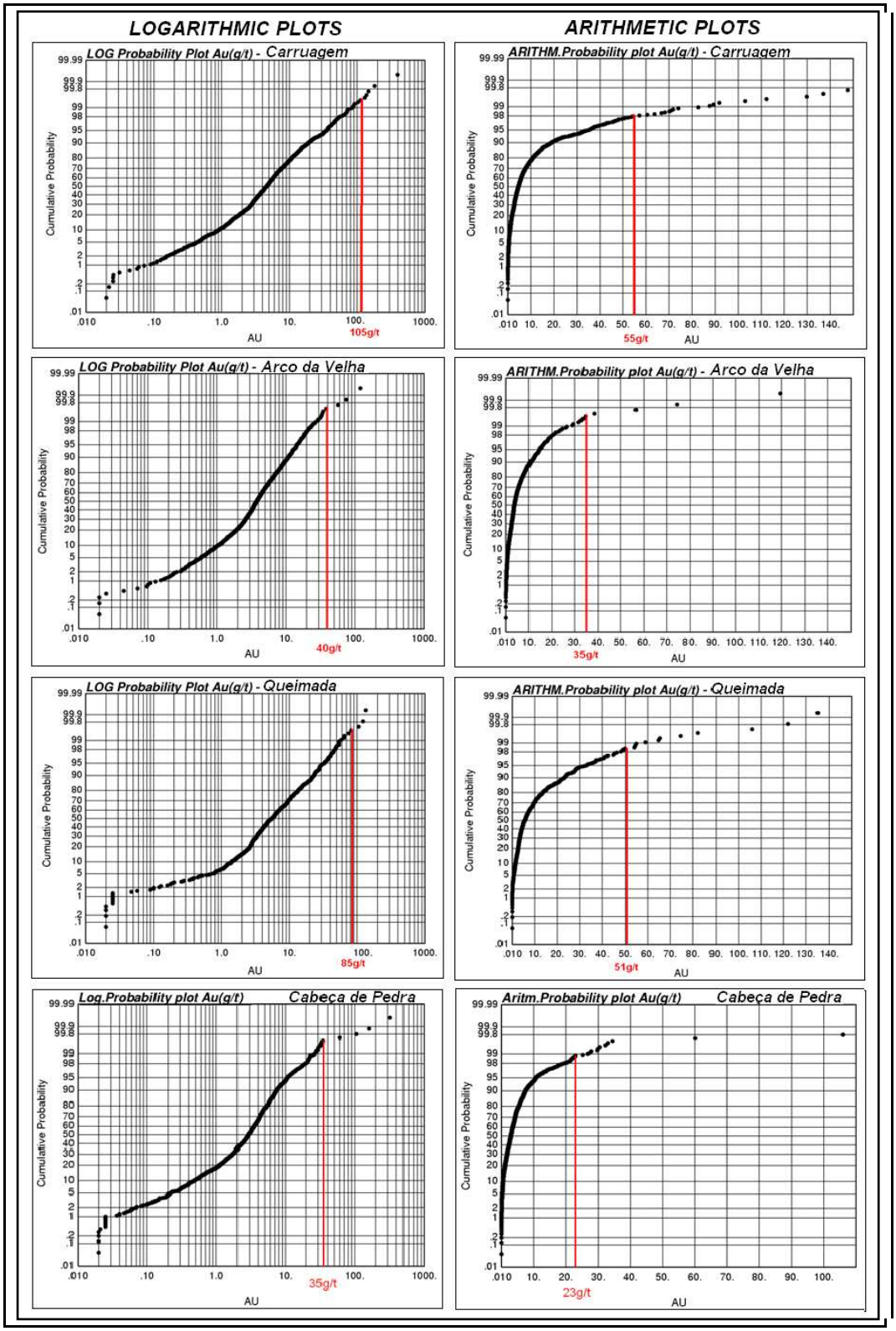

Figure 12 – Capping definition for Au values using logarithmic and arithmetic probability plots. The arithmetic plots show lower values of capping than logarithmic plots, with differences much more expressive in the Carruagem and Queimada orebodies. For estimation, the arithmetic plots were employed, which are more conservative.

2.5.2 - Variography – Variogram Fitting and Analysis

In a geometric field, consider two points, **x** and **x+h**, where **h** is a vector. The variogram **2γ(h)** is the mathematical expectancy of the square of the increments of the regionalized variable in the direction defined by vector h. In other words, the variogram **2γ(h)** is the average square of the differences between all the existing pairs of points in the geometric field, spaced apart by the distance **h** (Valente & Girodo, 1977). It can be represented by the equation (Deutsch & Journel, 1998):

$$2\gamma(\mathbf{h}) = E\{[Z(\mathbf{u}) - Z(\mathbf{u}+\mathbf{h})]^2\}.$$

Traditionally, variograms, rather than the covariance, have been used in spatial variability modelling, although kriging systems are more easily solved with covariance matrices (Deutsch & Journel, 1998).

Nugget effect definition – Omni-directional variography

In the variography carried out for Lamego orebodies, initially the variability was obtained for short distances, since they provide an important parameter for the fitting of the variograms and for defining gold-grade variability. The nugget effect is obtained considering either the smallest scale of the deposit or the variability for each sample interval, and calculating the variograms based on the composite data, in view of the length of the composite samples and the capping of each orebody. Figure 13 shows the Omni-directional variograms for Lamego orebodies.

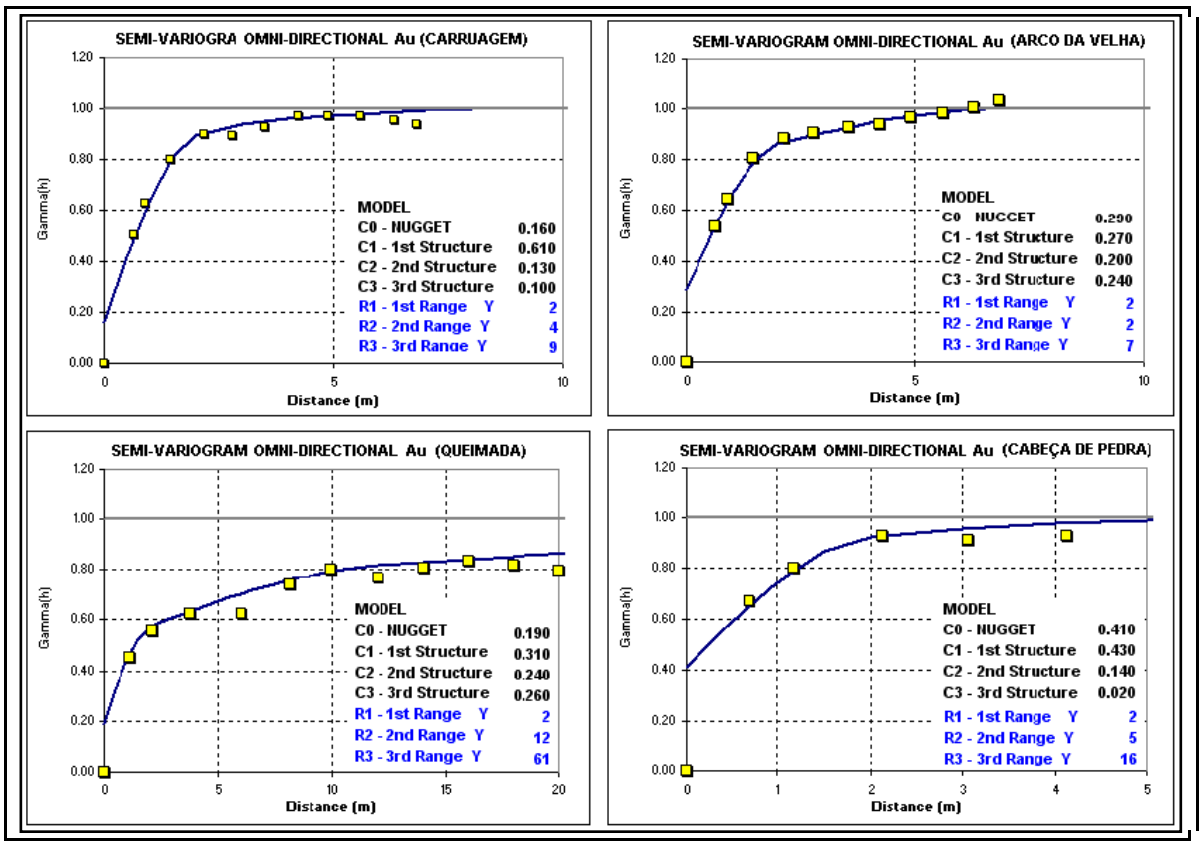

Figure 13 – Gold - Omni-directional variograms and definition of nugget effect.

Directional Variography

The directional variograms were calculated to determine the spatial variability of gold grade. They were based on the directions and dips of the geologic models that pre-indicated the anisotropy of the mineralized bodies. No spatial tools were used in defining the preferred directions of such possible anisotropies. That is, with the opening of the most part of the two levels, which are vertically spaced 50m apart, a substantial confidence level was obtained for the directions and dips of the orebody plunges.

Figure 14 summarizes the directional variograms for Lamego orebodies that represents the main direction of the mineralization. It is noted that along directions sub-parallel to the strike (Direction 2) or to the development of the orebodies, the variograms are more continuous than along plunge directions, where the amount of information is relatively reduced. All the variograms were standardized for a sill equals to one.

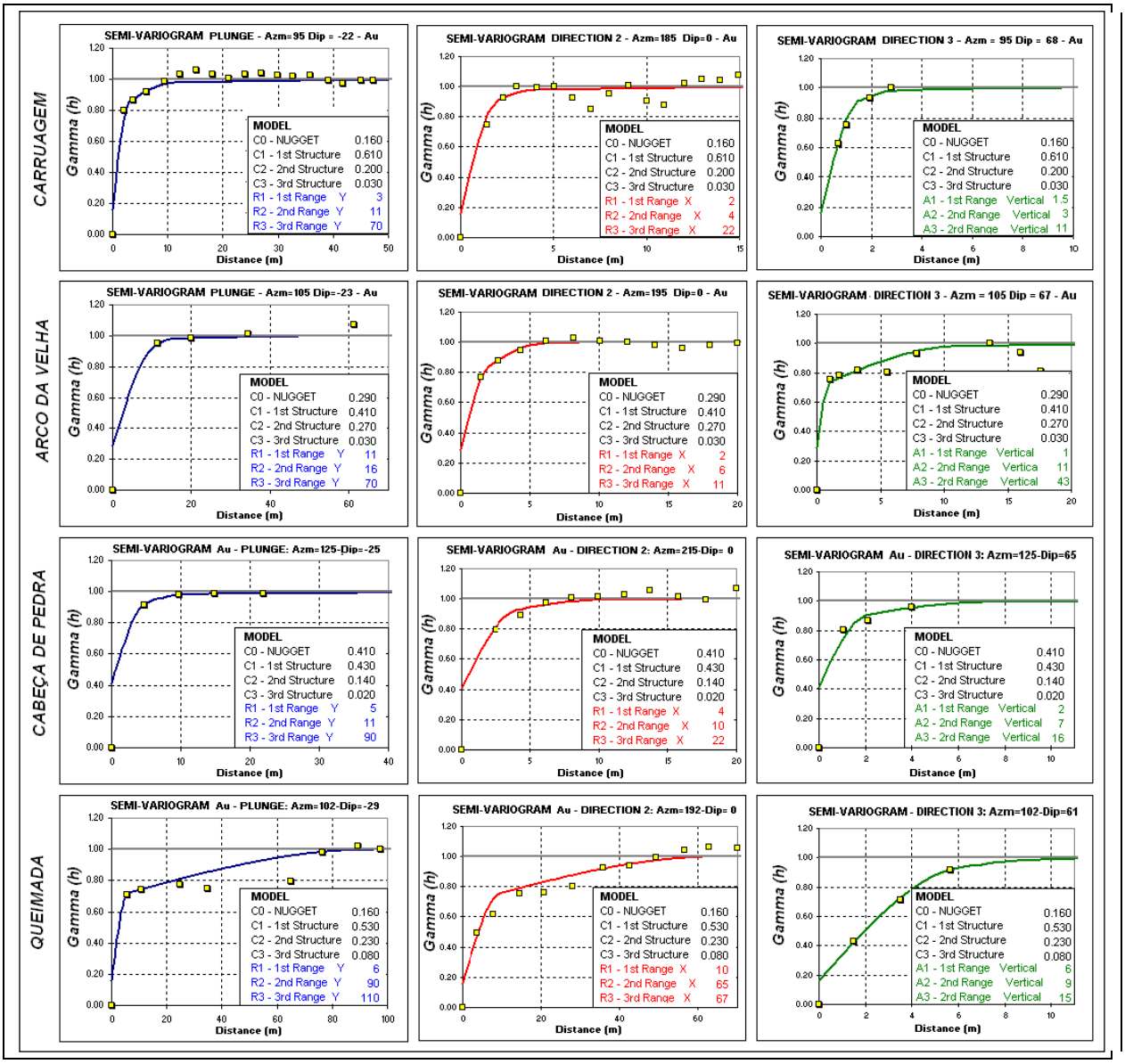

Figure 14 – Directional variograms for Lamego orebodies.

2.5.3 - Estimation by Ordinary Kriging

Concepts

Kriging is "*a collection of generalized linear regression techniques for minimizing an estimated variance defined from a prior covariance model*" (Olea, 1991 *in* Deutsch, 1998). All versions of kriging are elaborated on the basis of a linear regression algorithm and a corresponding estimator, so that:

$$[\mathbf{Z}^*_{SK}(\mathbf{u})-\mathbf{m}(\mathbf{u})] = \sum_{\alpha=1}^{n} \lambda_\alpha(\mathbf{u})\,[\mathbf{Z}(\mathbf{u}_\alpha) - \mathbf{m}(\mathbf{u}_\alpha)],$$

where Z(u) is the RV (Random Variable) model at location **u; $\mathbf{u}_\alpha$´s** are the **n** data locations; $m(\mathbf{u}) = E\{Z(\mathbf{u})\}$ is the location-dependent expected value of RV $Z(\mathbf{u})$; and $Z^*_{SK}(\mathbf{u})$ is the linear regression estimator, also called *Simple Kriging* (*SK*) e*stimator*.

Considering a non-sampled value $z(\mathbf{u_0})$ to be estimated from surrounding data with known values $z(\mathbf{u})$, α=1,...,n, then the RF (Random Function) model $Z(\mathbf{u})$ is stationary, with mean value *m* and covariance $C(\mathbf{h})$. In this simple version, also known as *Simple Kriging* (SK), the algorithms consider the linear estimator as

$$\mathbf{Z}^*_{SK}(\mathbf{u_0}) = \sum_{\alpha=1}^{n} \lambda_\alpha(\mathbf{u})\mathbf{Z}(\mathbf{u}_\alpha) + \Big[1- \sum_{\alpha=1}^{n} \lambda_\alpha(\mathbf{u})\Big]\mathbf{m}.$$

The weights $\lambda_\alpha(\mathbf{u})$ are determined for minimizing the error variance, and are also called estimation variance. This minimization results in a series of normal equations:

$$\sum_{\alpha=1}^{n} \lambda_\beta(\mathbf{u})\mathbf{C}(\mathbf{u}_\beta - \mathbf{u}_\alpha) = \mathbf{C}(\mathbf{u} - \mathbf{u}_\alpha), \text{ for } \alpha = 1,..., n.$$

The corresponding minimized estimation variance, or kriging variance, is

$$\sigma^2_{SK}(\mathbf{u}) = C(\mathbf{0}) - \sum_{\alpha=1}^{n} \lambda_\alpha(\mathbf{u})\mathbf{C}(\mathbf{u} - \mathbf{u}_\alpha) \geq \mathbf{0}.$$

Simple Kriging is usually preceeded by Ordinary Kriging (OK), where the sum of the weights $\Sigma^n_{\alpha=1}\,\lambda_\alpha(\mathbf{u})$ is constrained to sum up to 1. This establishes an estimator $Z^*_{OK}(\mathbf{u})$ that does not require prior knowledge of the stationary mean *m*, and therefore it can be said that $E[Z^*_{OK}(\mathbf{u})]=E[Z(\mathbf{u})]$ and results in the following Ordinary Kriging estimator:

$$\mathbf{Z}^*_{OK}(\mathbf{u_0}) = \sum_{\alpha=1}^{n} \lambda_\alpha^{(OK)}(\mathbf{u})\,\mathbf{Z}(\mathbf{u}_\alpha)$$

Therefore, the ordinary kriging estimator is a type of simple kriging estimator where the constant value of the mean is replaced by the dependent estimator $m^*(\mathbf{u})$:

$$\mathbf{Z}^*_{OK}(\mathbf{u}) = \sum_{\alpha=1}^{n} \lambda_\alpha^{(SK)}(\mathbf{u})\mathbf{Z}(\mathbf{u}_\alpha) + \Big[1- \sum_{\alpha=1}^{n} \lambda_\alpha^{(SK)}(\mathbf{u})\Big]\mathbf{m}^*(\mathbf{u})$$

where $\lambda_\alpha^{(OK)}$ are the ordinary kriging weights and $\lambda_\alpha^{(SK)}$ are the simple kriging weights.

Ordinary kriging is regarded as a non-stationary algorithm that uses data from moving neighborhoods, corresponding to a non-stationary RF model with varying means and stationary covariance. This ability to re-scale Z(u) locally in the RF model for different values of the mean $m^*(\mathbf{u})$ explains the extreme robustness of the ordinary kriging algorithm. Ordinary kriging has been a consistent anchor in Geoestatistics (Deutsch & Journel, 1998).

Ordinary Kriging for Lamego Orebodies

The ordinary kriging was carried out separately for each of the Lamego orebodies. It was based on drill holes and channels together, both considering the same support of sampling in terms of length and weight. The purpose was to generate block models to fill the solids constructed by 3D geological modelling, with estimated gold grades. The strategy was to provide a consistent mechanism for geostatistical evaluation, making it possible to obtain the approximate total metal content of the deposit.

Prior to using the ordinary kriging algorithms, a set of procedures was followed, including:

(i) generation of a reference ellipse, to obtain a 3D visualization between the geometry of the orebodies and that of the ellipse, with the dimensions and directions of the x, y and z axis coherent with the main 3D elongations of the geological model (Figure 15);

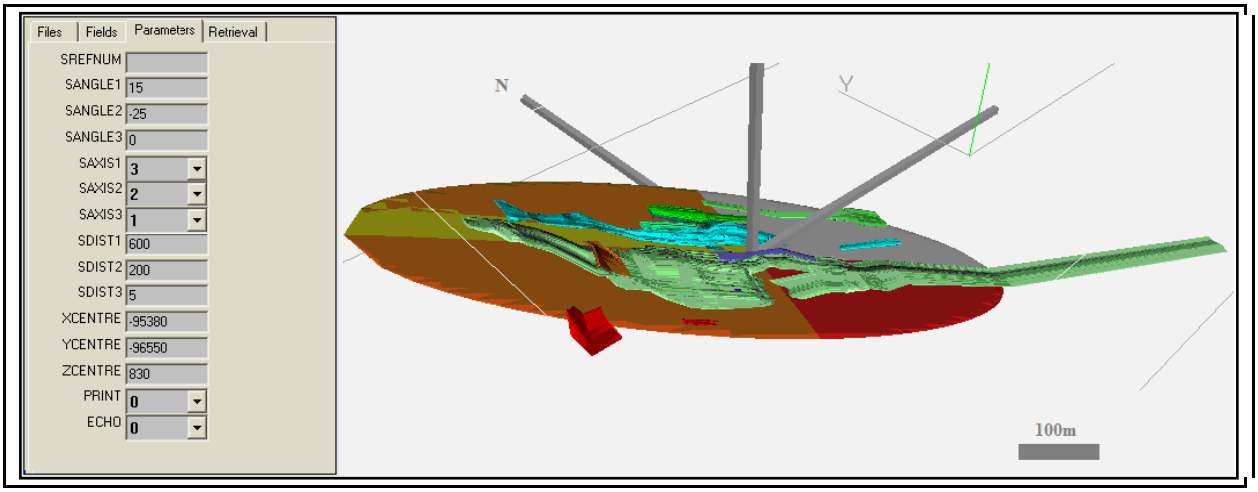

Figure 15 – Example of reference ellipse with different angles and sizes in the xyz axes - Arco da Velha orebody (random colors).

(ii) creation of empty block models *(prototypes)* that host no information and are sufficiently large to contain all the wireframes of each orebody (Figure 16);

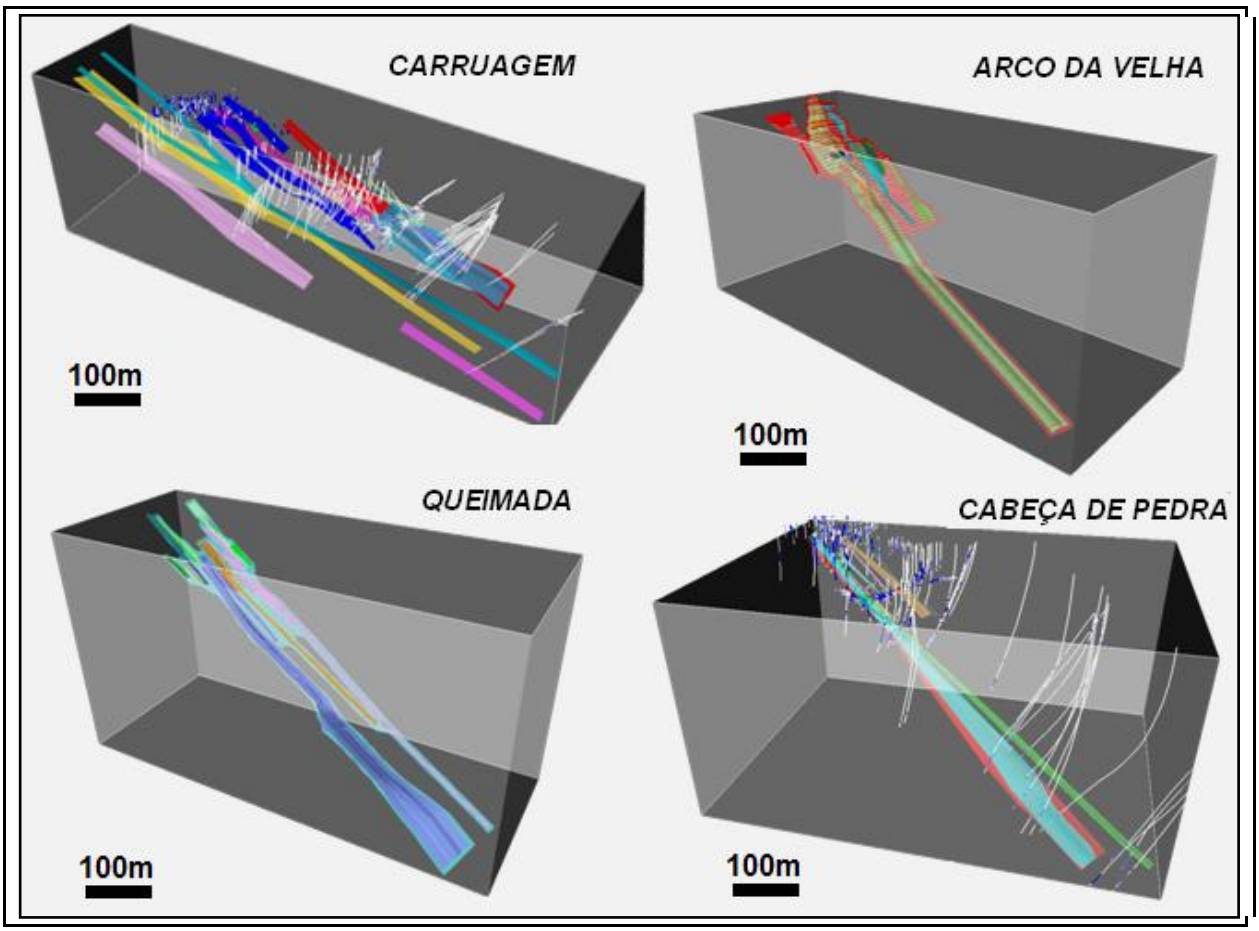

Figure 16 – Prototype models (grey blocks).

(iii) Preliminary definition of block sizes by analyzing the smoothness of the diagram involving "block size *versus* kriging variance". The curve is generated by creating blocks of different sizes and with the same center coordinate, plus calculating the kriging variance for each of the blocks. The variance values begin to stabilize close to 0.12, which corresponds to a block size or SMU (Selective Mining Unit) of 10m (Figure 17). The blocks with different sizes were calculated based on the same group of samples.

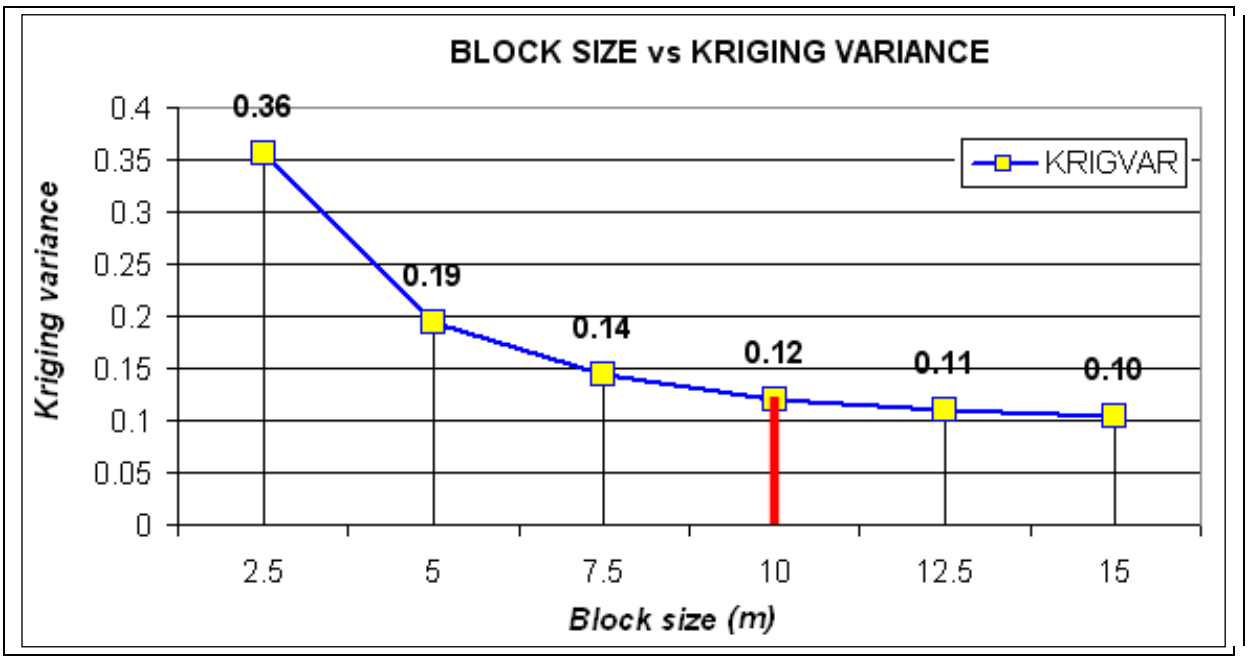

Figure 17 – Block size definition - kriging variance *vs* block size.

(iv) separation of samples and blocks that are above and below the oxidation surface. Blocks located below this surface correspond to sulfidized ore, whereas those located above correspond to oxidized ore. The oxidation surface was generated by 3D interpolation of points that corresponds to changes in the degree of weathering. In the drilling cores this points mark the limits between fresh rocks and rocks that show some degree of alteration;

(v) definition of variables, estimation parameters, input/output files, capping values for each of the orebodies, estimation method, parameters of the modeled variograms, dimensions and directions of the ellipses, including search volumes, etc.

The search volumetric ellipsoids are used to assist in the interpolation of grades. These volumes are defined based on the parameters obtained in the variographic modelling, by associating them with the maximum distances to the ellipsoid axes. The results are also affected by: (i) maximum and minimum number of samples considered for estimating each block; (ii) subdivision of search volumes into regular sectors, providing a better definition on the anisotropy control; and (iii) minimum requirements within sectors for the estimation. Figure 18 shows an example of the Datamine parameter file used in the ordinary kriging of the Carruagem orebody, with the respective parameters used in the search volume. The search strategy employed, summarized herein, includes the following rules: (i) division of the ellipsoid into 8 sectors (octants); (ii) use of a minimum of 2 sectors or octants for each estimated block; (iii) use of a minimum of 5 samples for each estimated block; (iv) use of a maximum of 24 samples per block

(to avoid significant grade smoothing); (v) use of samples within each of the wireframes related to the small mineralized horizons of the orebodies only.

The search ellipsoids were scaled up in multiple phases. The scale of the search volume was gradually increased by multiples of the original input values – that is, multiples of the maximum distance for each of the directions considered for the range of the variograms. Blocks that were not estimated during the first pass were only estimated after increasing factors of 2x and 3x in successive passes, until all blocks were estimated with an increase of 5x the maximum distance of the ranges. With this approach, more than 80% of the blocks were estimated, considering a maximum search volume equals to 3x the distance of the range along the plunge, and constantly respecting the geological correlation of Au within all mineralized lenses. Figure 34 presents the results of the variographic study for the Carruagem orebody, including parameters such as anisotropy angles, structures and variogram models in three directions used in the ordinary kriging of this orebody.

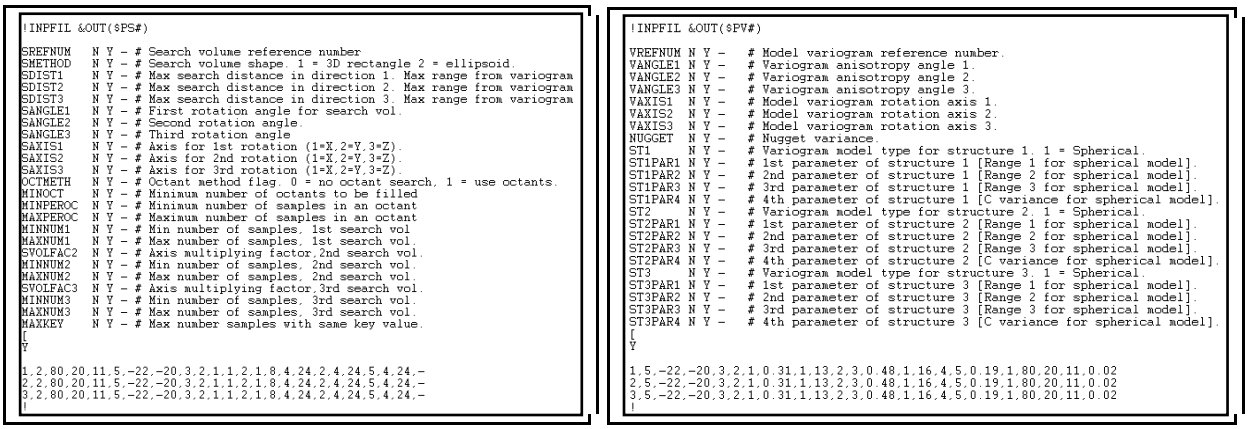

```
!INPFIL &OUT($PS#)

SREFNUM   N Y - # Search volume reference number
SMETHOD   N Y - # Search volume shape. 1 = 3D rectangle 2 = ellipsoid.
SDIST1    N Y - # Max search distance in direction 1. Max range from variogram
SDIST2    N Y - # Max search distance in direction 2. Max range from variogram
SDIST3    N Y - # Max search distance in direction 3. Max range from variogram
SANGLE1   N Y - # First rotation angle for search vol.
SANGLE2   N Y - # Second rotation angle.
SANGLE3   N Y - # Third rotation angle
SAXIS1    N Y - # Axis for 1st rotation (1=X,2=Y,3=Z).
SAXIS2    N Y - # Axis for 2nd rotation (1=X,2=Y,3=Z).
SAXIS3    N Y - # Axis for 3rd rotation (1=X,2=Y,3=Z).
OCTMETH   N Y - # Octant method flag. 0 = no octant search, 1 = use octants.
MINOCT    N Y - # Minimum number of octants to be filled
MINPEROC  N Y - # Minimum number of samples in an octant
MAXPEROC  N Y - # Maximum number of samples in an octant
MINNUM1   N Y - # Min number of samples, 1st search vol
MAXNUM1   N Y - # Max number of samples, 1st search vol.
SVOLFAC2  N Y - # Axis multiplying factor,2nd search vol.
MINNUM2   N Y - # Min number of samples, 2nd search vol.
MAXNUM2   N Y - # Max number of samples, 2nd search vol.
SVOLFAC3  N Y - # Axis multiplying factor,3rd search vol.
MINNUM3   N Y - # Min number of samples, 3rd search vol.
MAXNUM3   N Y - # Max number of samples, 3rd search vol.
MAXKEY    N Y - # Max number samples with same key value.
[
Y

1,2,80,20,11,5,-22,-20,3,2,1,1,2,1,8,4,24,2,4,24,5,4,24,-
2,2,80,20,11,5,-22,-20,3,2,1,1,2,1,8,4,24,2,4,24,5,4,24,-
3,2,80,20,11,5,-22,-20,3,2,1,1,2,1,8,4,24,2,4,24,5,4,24,-
!
```

```
!INPFIL &OUT($PV#)

VREFNUM N Y -   # Model variogram reference number.
VANGLE1 N Y -   # Variogram anisotropy angle 1.
VANGLE2 N Y -   # Variogram anisotropy angle 2.
VANGLE3 N Y -   # Variogram anisotropy angle 3.
VAXIS1  N Y -   # Model variogram rotation axis 1.
VAXIS2  N Y -   # Model variogram rotation axis 2.
VAXIS3  N Y -   # Model variogram rotation axis 3.
NUGGET  N Y -   # Nugget variance.
ST1     N Y -   # Variogram model type for structure 1. 1 = Spherical.
ST1PAR1 N Y -   # 1st parameter of structure 1 [Range 1 for spherical model].
ST1PAR2 N Y -   # 2nd parameter of structure 1 [Range 2 for spherical model].
ST1PAR3 N Y -   # 3rd parameter of structure 1 [Range 3 for spherical model].
ST1PAR4 N Y -   # 4th parameter of structure 1 [C variance for spherical model].
ST2     N Y -   # Variogram model type for structure 2. 1 = Spherical.
ST2PAR1 N Y -   # 1st parameter of structure 2 [Range 1 for spherical model].
ST2PAR2 N Y -   # 2nd parameter of structure 2 [Range 2 for spherical model].
ST2PAR3 N Y -   # 3rd parameter of structure 2 [Range 3 for spherical model].
ST2PAR4 N Y -   # 4th parameter of structure 2 [C variance for spherical model].
ST3     N Y -   # Variogram model type for structure 3. 1 = Spherical.
ST3PAR1 N Y -   # 1st parameter of structure 3 [Range 1 for spherical model].
ST3PAR2 N Y -   # 2nd parameter of structure 3 [Range 2 for spherical model].
ST3PAR3 N Y -   # 3rd parameter of structure 3 [Range 3 for spherical model].
ST3PAR4 N Y -   # 4th parameter of structure 3 [C variance for spherical model].
[
Y

1,5,-22,-20,3,2,1,0.31,1,13,2,3,0.48,1.16,4,5,0.19,1,80,20,11,0.02
2,5,-22,-20,3,2,1,0.31,1,13,2,3,0.48,1.16,4,5,0.19,1,80,20,11,0.02
3,5,-22,-20,3,2,1,0.31,1,13,2,3,0.48,1.16,4,5,0.19,1,80,20,11,0.02
!
```

Figure 18 – Parameters for the search volume (left) and variogram model (right) - Carruagem orebody.

Before definitely assigning the results of the ordinary kriging, a set of validations of the block models is required, as well as a review of the conditional expectation.

Ordinary Kriging Validation

The main procedures for kriging validation are summarized as follows:

1. Visual examination, using only the result of the first search of the ellipse (Figure 19A) . The values of the estimated blocks are compared to those of the composite samples;

2. Visual comparative check considering the second and third searches (Figure 19B and C);
3. Identification of those blocks that remain non-estimated after all the searches and, if necessary, manual fitting of these blocks by means of filling in appropriate values (knowledge driven);
4. Merge of the block models estimated in the volumetric searches with the manually-stamped block models;
5. Final visual check of the block models combined with the composite samples;
6. Stationary analysis, by comparing average Au grades in horizontal volumetric slices (obtained separately from the database) with the composite samples and the estimated block models (i.e., analysis of support change);
7. Final analysis of the swath plots and, if necessary, adjustment of the incoherent results obtained throughout the process.

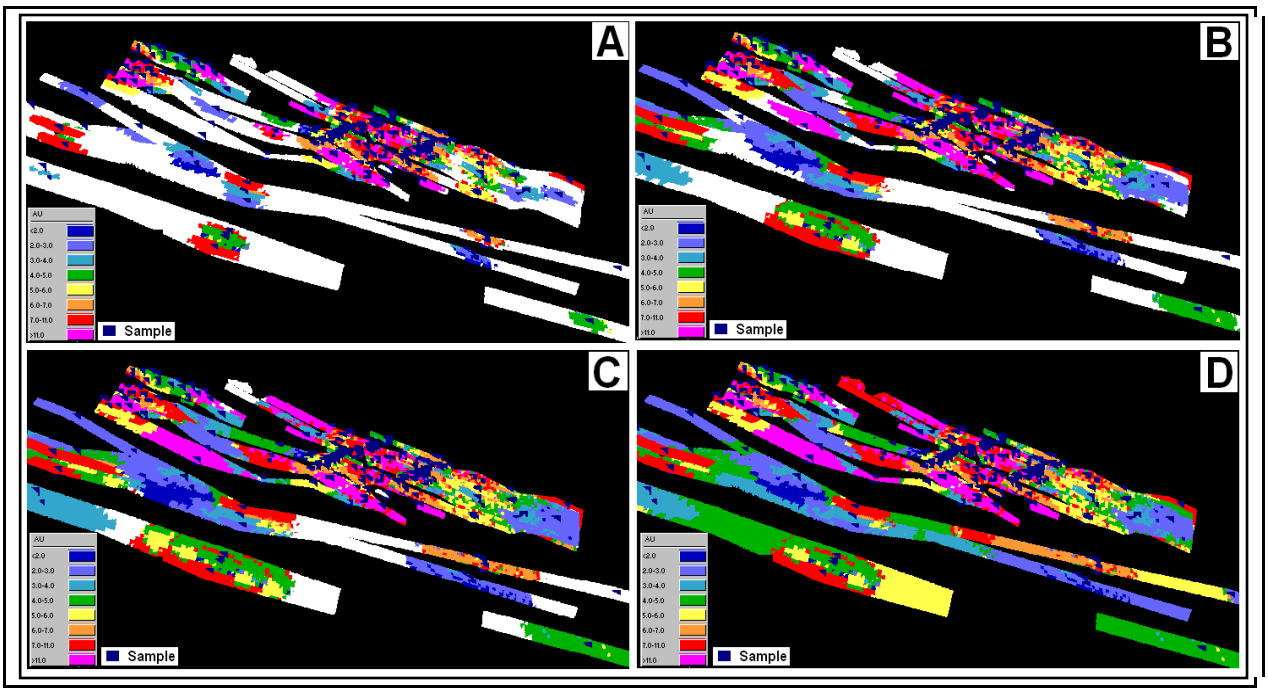

Figure 19 – Validation of kriging results for each search volume of the Carruagem orebody: **A** - primary check, using the first search ellipse (80m, 20m, 11m); **B** – second visual check with 2nd search ellipse (160m, 40m, 22m); **C** – third visual check with 3rd search ellipse (240m, 60m, 11m); **D** –check with nrd search ellipse.

The ordinary kriging validation steps described above were repeated for all other orebodies of the Lamego deposit.

Stationary Analysis

The ordinary kriging validation is based on comparing the mean values obtained in the estimated block models with the mean values of the declustered samples divided into volumetric slices spaced horizontally 50m apart (Figure 20A) and vertically 25m apart (Figure 20B). The volumetric means of the estimated blocks were weighted according to their tonnage, whereas the volumetric means of the samples were weighted according to the declustered weights.

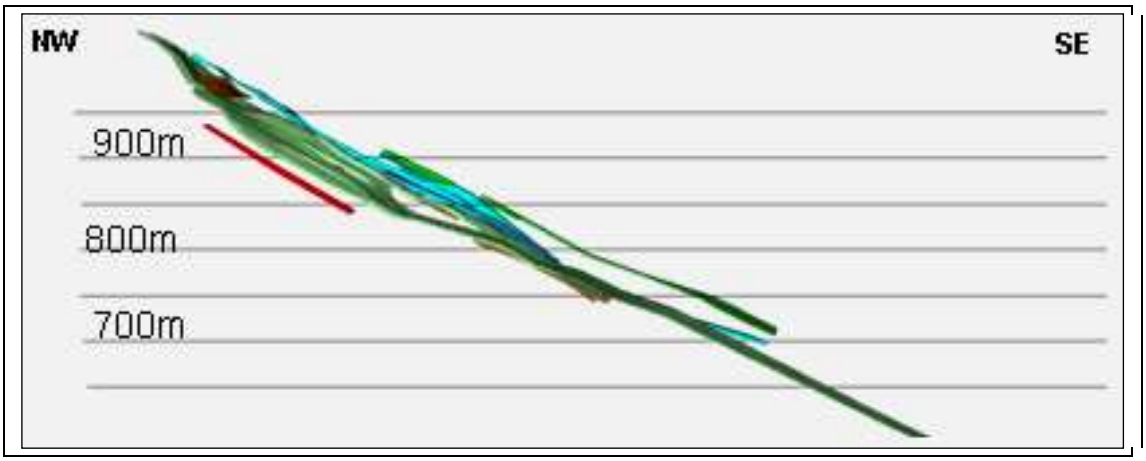

Figure 20A – Example of horizontal volume slices (50m) of the Arco da Velha orebody (random colors).

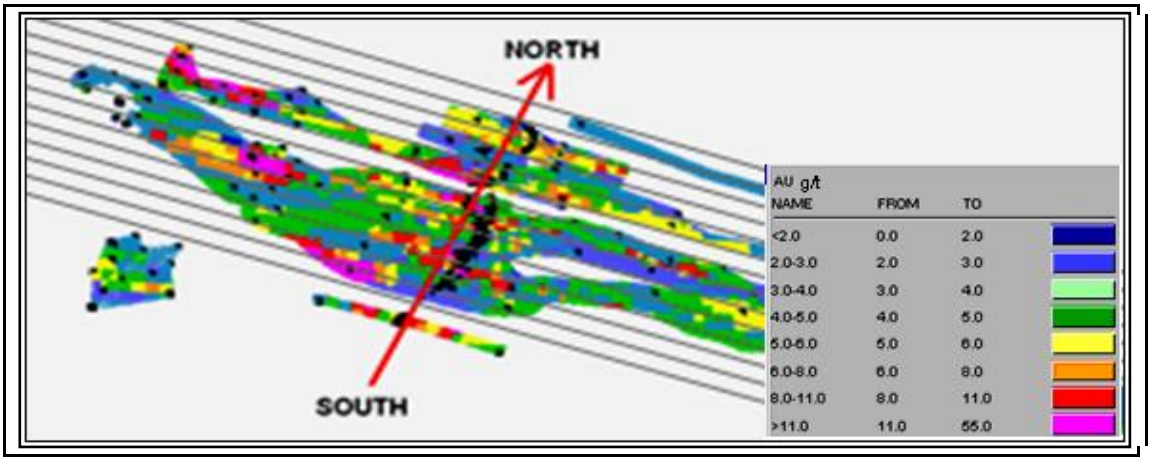

Figure 20B – Example of vertical volume slices (25m) of the Arco da Velha orebody.

In general, the curves of the horizontal volumetric slices of estimated blocks are close to the points of declustered samples (Figure 21). Slightly lower mean values occur especially where there is a larger number of samples (along levels 1 and 2 in all orebodies). At levels with a smaller number of samples, the differences between block and sample means are greater, and the results of the blocks tend to approximate the overall mean of each orebody. At the Carruagem and

Arco da Velha orebodies, a slight decrease in gold-grade at depth is observed. This phenomenon, however, may be associated with the lack of information about these places. The proximity of the two curves indicates that the parameters of the search ellipsoids as well as the variographic and ordinary-kriging parameters were properly obtained.

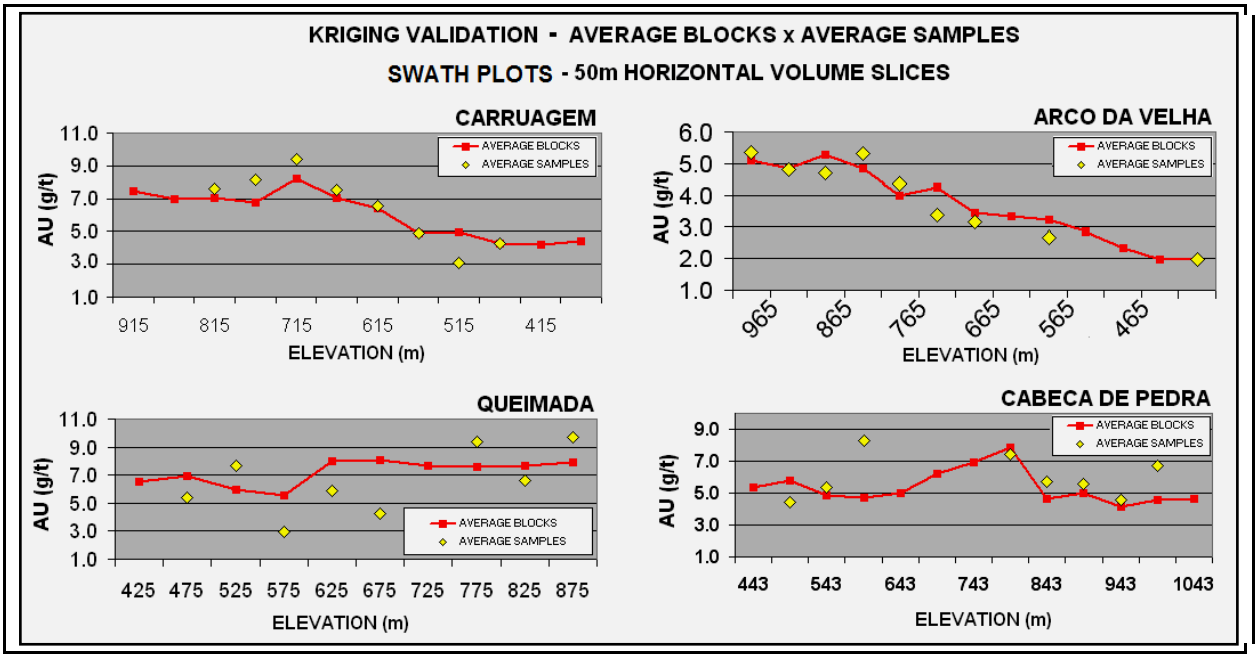

Figure 21 – Kriging validation. Graphical relationship between mean estimated blocks and declustered mean sample of the horizontal volume slices. Slices are displaced at 50m apart in depth.

In the vertical volume slices generated every 25 meters from South to North (Figure 22) showed a slight regionalized gold-grade increase in the northern portions of almost all orebodies. This phenomenon is more significant in the Carruagem and Arco da Velha orebodies. It may be associated with local geologic discontinuities or to the direction of the regional deformation, which would be responsible for the concentration of richer zones at these sectors. The curves of the vertical volumetric slices remained close to each other, confirming the proper configuration of the ordinary kriging parameters for the deposit.

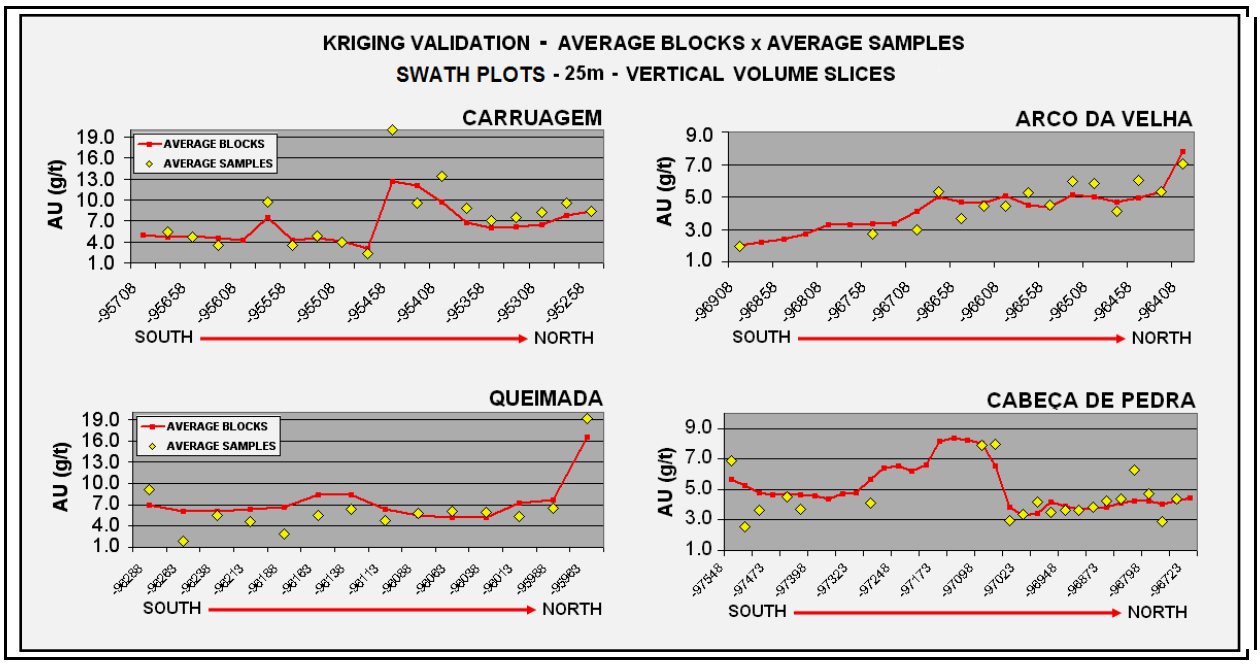

Figure 22 – Kriging validation. Graphical relationship between mean estimated blocks and declustered average sample of the vertical volume slices. Slices are 25m apart from south to north.

After completion of the ordinary kriging validation, external wireframes of all orebodies were generated, and a kriging estimation of this external envelope was made. For this estimation, only samples not belonging to the geological model were included – that is, samples external to the model in a radius of about 5m. The conception of a block model in the neighborhood with low grades allows these values to be taken into account in further calculations of the grade dilution. Figure 23 shows a sector of level 2 in the Carruagem orebody. External blocks are shown in blue and were estimated separately. The mean for these blocks is close to 0.47g/t. This procedure also makes it possible the selection of where the dilution shall be performed, either in the *hanging wall* or in the *footwall,* depending which grade of the envelope is higher.

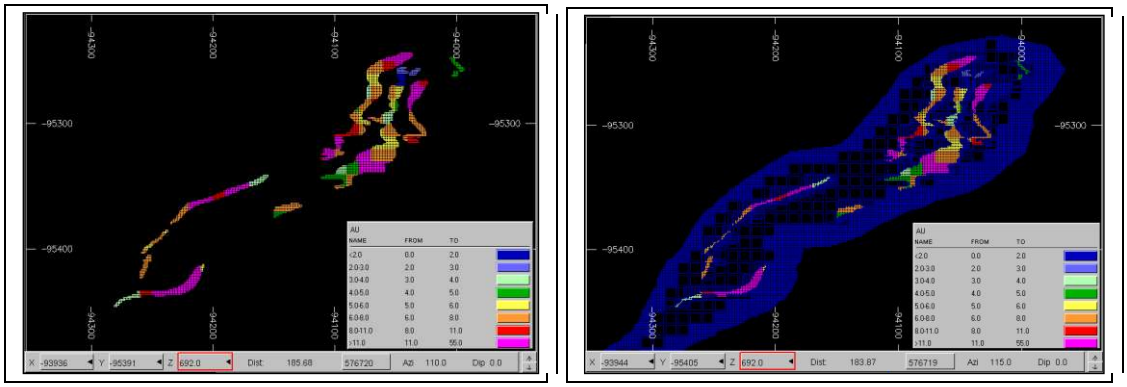

Figure 23 – Carruagem orebody at level 2 – horizontal slices with and without outside dilution area.

The ordinary kriging results for all the orebodies are shown in Figure 24.

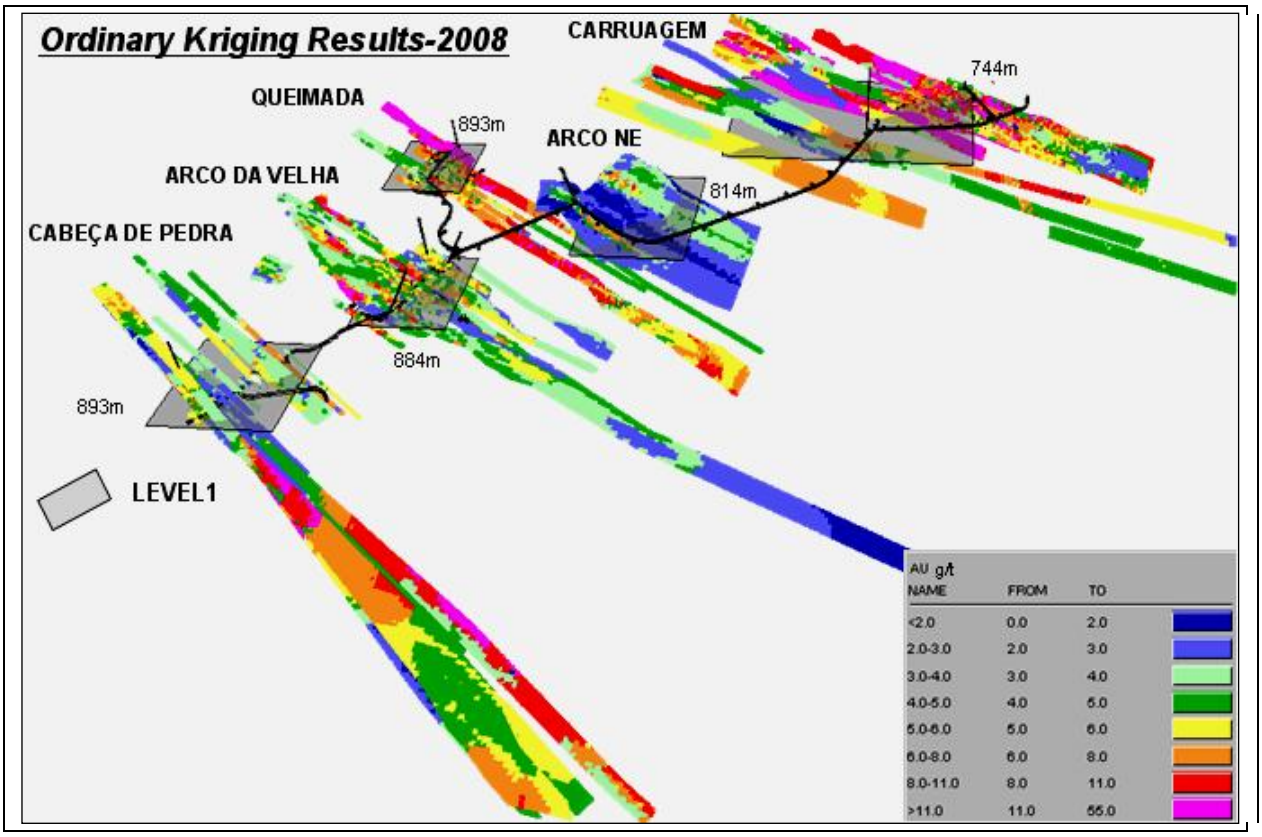

Figure 24 – Concluding block models of all orebodies.

Figure 25 shows the volume of estimated geological resources at Lamego over the last 5 years. It can be noted that although the total of resources shows differences not greater than 20%, the change in the classification of the resources was quite substantial, primarily with regard to measured resources.

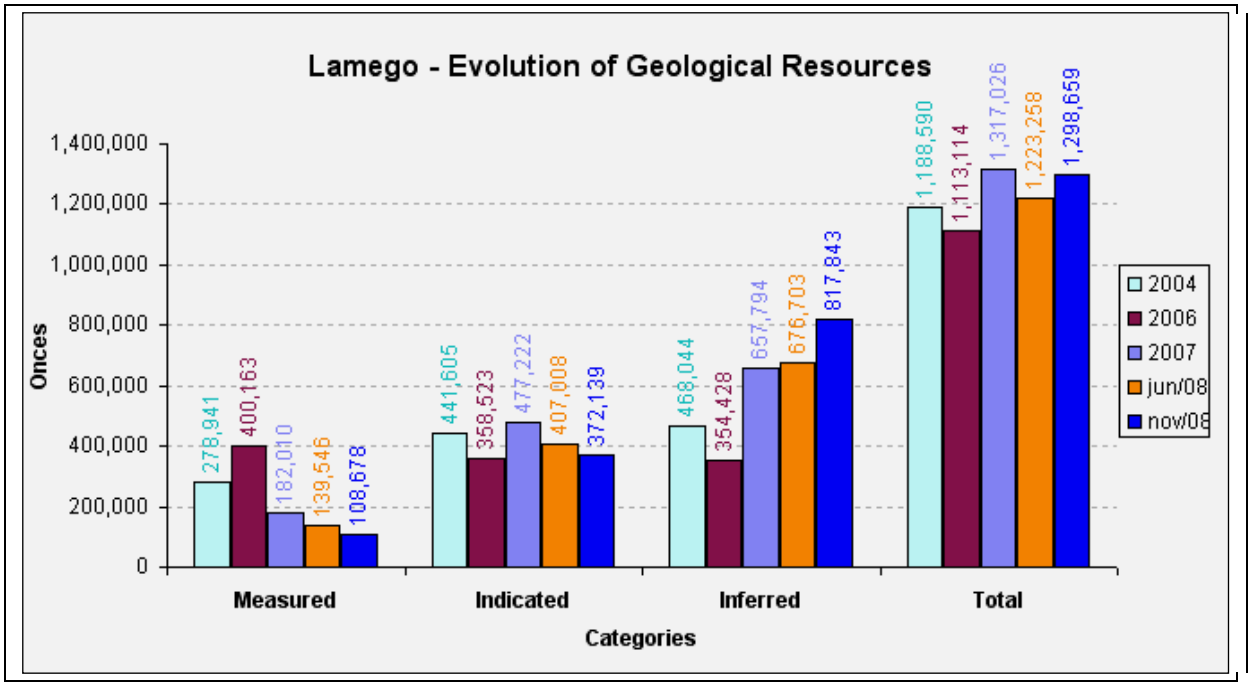

Figure 25 – Evolution of Lamego geological resources since 2004.

2.6 - Grade-Tonnage Curve

The grade-tonnage curve of the Lamego deposit, shown in Figure 26, was constructed considering all orebodies.

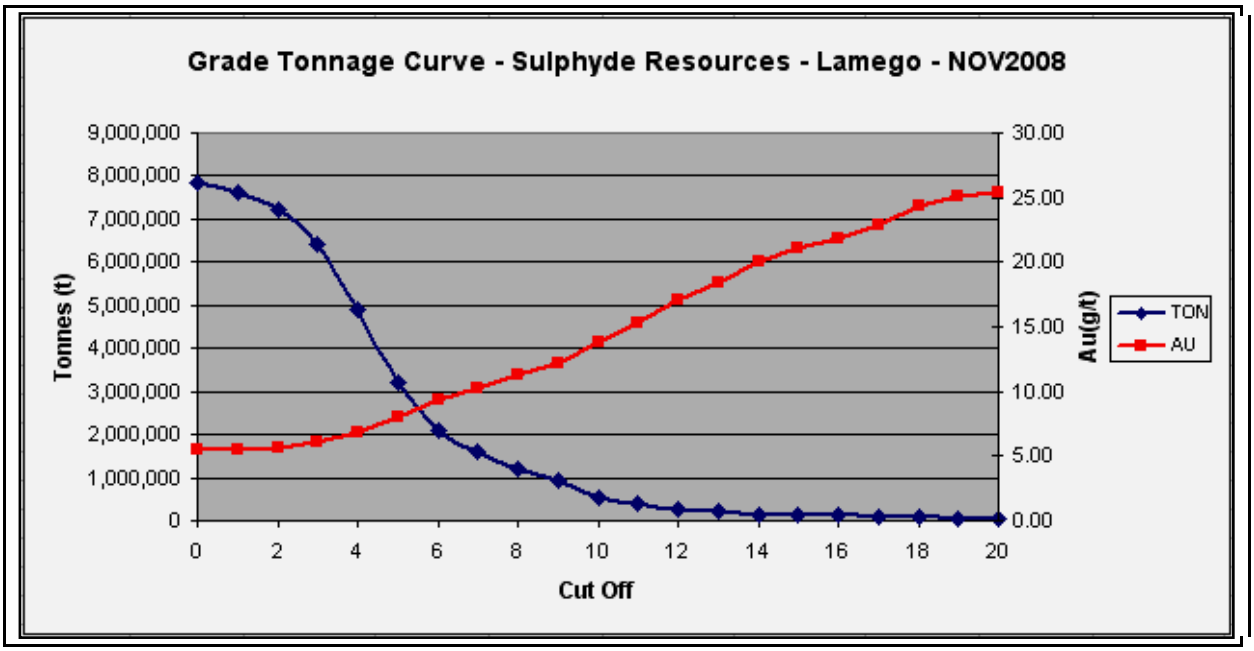

Figure 26 – Grade-tonnage curve of the Lamego deposit.

2.7 - Mineral Resources Classification

The Sequential Gaussian Simulation (sgsim.exe algorithm) was used in this work to assist the classification of the mineral resources of the Lamego deposit and to define the uncertainty associated to such classification.

Simulation Concepts

The simple kriging system (SK) can be understood as the condition to identify the covariance of $Z^*_{SK}(\mathbf{u})$ with any of the *n* data $Z(\mathbf{u}_\alpha)$ to the covariance model. In this sense, SK is the first step towards simulation, which is the process of reproducing a covariance model. But SK is rather incomplete in that the covariance between any two SK estimators $Z^*_{SK}(\mathbf{u})$ and $Z^*_{SK}(\mathbf{u}')$ at two different locations $\mathbf{u} \neq \mathbf{u}'$ is incapable to identify the model value $C(\mathbf{u}-\mathbf{u}')$. Sequential simulation is able to add the value $Z^*_{SK}(\mathbf{u})$, corrected for its smoothing, into the dataset used at subsequent nodes $\mathbf{u}'$ (Journel, 1993; *apud* Deutsch, 1998).

Conditional simulation was initially developed to correct for the smoothing effect shown on maps produced by the kriging algorithm. Indeed, kriging estimates are weighted moving averages of the original data values; thus they have less spatial variability than the data. Moreover, depending on the data configuration, the degree of smoothing varies in space, entailing possibly artefact structures. Typical conditional simulation algorithms trade the estimation variance minimization for the reproduction of a variogram/covariance seen as a model of spatial variability. A smoothed map, as provided by kriging, is appropriate for showing global trends. On the other hand, conditionally simulated maps are more appropriate for studies that are sensitive to patterns of local variability such as flow simulations (Hewett, 1986; Journel & Alabert, 1990; *apud* Deutsch, 1998). A suite of conditionally simulated maps also provides a measure (model) of uncertainty about the attribute(s) spatial distribution.

A set of L realizations from any specific simulation algorithm (in this case, the Sequential Gaussian Simulation algorithm) can be used to determine probabilities of occurrence of specific functions of these realizations only if the L realizations are "equiprobable" - that is if any of the L realizations has the same probability to be drawn as any other among L. Such equiprobability is achieved if each realization can be identified to a single random number (the realization seed number) uniformly distributed in [0,1] – in other words, if each realization can be reproduced exactly by re-running the simulations algorithm using its seed number. Naturally, equiprobability refers to a specific simulation model including its RF model (if any), all parameter values, the

implementation algorithm and a computer code. In case another simulation model or another implementation of the same RF model is used, it generates a different set of realizations, leading to different probability assessments (Journel, 1994, 1996; *apud* Deutsch, 1998).

Sequential Gaussian Simulation (SGSIM)

The most straightforward algorithm for generating realizations of a multivariate Gaussian filed is provided by the sequential principle. Each variable is simulated sequentially according to its normal Cumulative Distribution Function (CDF), which is fully characterized through a SK system. The conditioning data consists of all original data and all previously simulated values found within a neighborhood of the location being simulated.

According to the H. Zhu & Journel, 1993; *in* Deutsch, 1998, the conditional simulation of a *continuous* variable $z(\mathbf{u})$ modelled by a Gaussian-related stationary RF $Z(\mathbf{u})$ is implemented as follows:

1. Determine the univariate CDF $Fz(z)$ representative of the entire study area and not only the z sample data available. Declustering may be needed if the z data are preferentially located;
2. Using the CDF Fz(z), perform the normal score transform of z data into y data with a standard normal CDF;
3. Check for bivariate normality of the normal score *y* data. If the multivariate Gaussian model cannot be retained, then consider alternative models such as mixture of Gaussian populations or an indicator-based algorithm for the stochastic simulation.
4. If a multivariate Gaussian RF model can be adopted for the *y* variable, proceed with program **sgsim.exe** and sequential simulation, i.e.,
   - Define a random path that visits each node of the grid once. At each node **u,** retain a specified number of neighboring conditioning data including both original y data and previously simulated grid node *y* values;
   - Use SK with the normal score variogram model to determine the parameters (mean and variance) of the CDF of the RF $Y(\mathbf{u})$ at location **u**.
   - Draw a simulated value $y^{(1)}(\mathbf{u})$ from that CDF
   - Add the simulated value $y^{(1)}(\mathbf{u})$ to the data set.
   - Proceed to the next node, and loop until all nodes are simulated.
5. Backtransform the simulated normal values $\{y^{(1)}(\mathbf{u}), \mathbf{u} \in A\}$ into simulated values for the original variable.

Classification of Mineral Resources at the Lamego Deposit

The classification of mineral resources at the Lamego deposit uses the definitions from JORC (*Australasian Joint Ore Reserves Committee*), which classifies the mineral resources into measured, indicated, or inferred categories, depending on the confidence level of the estimate. A schematic classification and the extension to reserves are illustrated in Figure 27.

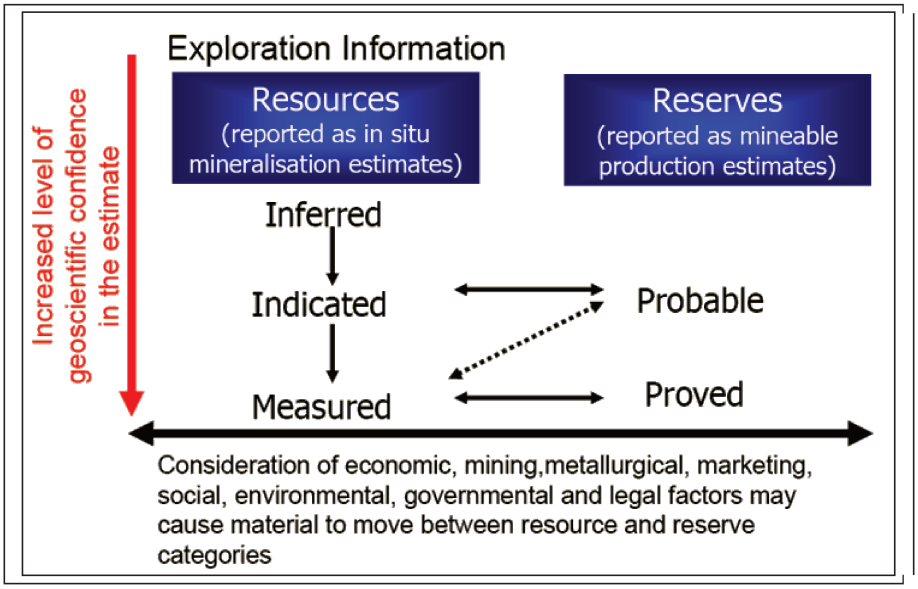

Figure 27 – Classification of Mineral Resources and Ore Reserves according to the JORC (2004).

The criteria for defining categories at the Lamego deposit were based on economic aspects associated with the uncertainty of a geological unit for a given, pre-defined production scale. The 15% uncertainty was used, where:

- **Measured resources:** mineral resources shall have a uncertainty no greater than 15% with 90% confidence for a volumetric panel equivalent to a three-month production;
- **Indicated resources:** mineral resources shall have a uncertainty no greater than 15% with 90% confidence for a volumetric panel equivalent to a twelve-month production;
- **Inferred resources:** obtained by geological knowledge and common sense, with an uncertainty greater than 15% and with 90% confidence.

For calculations of uncertainty in panels relating to quarterly or annual periods, the methodology commonly used is the Sequential Gaussian Simulation, which generates a

distribution of 100 possibilities or realizations of grades and thicknesses for each estimated SMU (Selective Mining Unit). SGSIM is used for accessing the uncertainties of the process related to the evaluation of the deposit, as well as for generating probabilistic estimates of the parameters that shall confirm the variability of the sampled populations. The spatial distribution resulting from the calculated values makes it possible to access the uncertainty.

In this study, the statistical uncertainty was calculated for the gold content (in ounces) of each SMU by multiplying the tonnage uncertainty parameter (accessed by the thickness variance) by the grade variance, thereby obtaining the overall uncertainty expressed in gold ounces. Table 5 shows how the final uncertainty used in the classification of the resources at the Lamego deposit was determined.

Table 5 – Evolution of uncertainty calculated for quarterly periods considering 11 panels.

UNCERTAINTY - Au (grade g/t)

3 Months	Tonnes	R1 (Au g/t)	R2 (Au g/t)	R3 (Au g/t)	...	R99 (Au g/t)	R100 (Au g/t)	Average (Au g/t)	P5	P95	Uncertainty*
Painel 1	71 229	7.58	7.29	7.62		7.86	7.97	7.73	7.05	8.43	**0.09**
Painel 2	72 908	7.08	7.71	7.43		7.59	7.68	7.72	7.12	8.42	**0.08**
Painel 3	68 573	8.17	7.26	7.66		7.85	7.29	7.63	6.90	8.40	**0.10**
Painel 4	71 413	8.07	7.19	8.83		8.71	7.20	7.75	6.99	8.71	**0.11**
Painel 5	73 850	7.99	7.40	7.51		8.28	7.12	7.63	6.80	8.42	**0.11**
Painel 6	75 056	7.00	8.11	7.72		7.93	8.46	7.71	6.91	8.69	**0.12**
Painel 7	73 102	7.30	7.79	7.02		6.87	7.93	7.65	6.66	8.91	**0.15**
Painel 8	72 067	7.86	8.30	8.09		6.53	7.97	7.87	7.03	8.84	**0.11**
Painel 9	73 549	6.90	6.67	8.90		7.70	7.56	7.91	7.02	8.69	**0.11**
Painel 10	69 170	7.88	8.28	7.55		6.34	7.93	7.82	6.79	8.79	**0.13**
Painel 11	67 314	7.63	7.31	8.20		7.33	7.97	7.63	6.87	8.41	**0.10**

***Uncertainty(Grade)=(((Average-P5)/Average)+((P95-Average)/average))/ 2.3**

UNCERTAINTY - Thickness (m)

3 Months	Tonnes	R1 (m)	R2 (m)	R3 (m)	...	R99 (m)	R100 (m)	Average (m)	P5	P95	Uncertainty*
Painel 1	71 229	1.70	1.76	1.73		1.88	1.69	2.06	1.58	2.90	**0.32**
Painel 2	72 908	2.30	1.82	1.67		2.16	1.94	2.06	1.65	2.72	**0.26**
Painel 3	68 573	2.16	1.59	1.73		1.39	3.40	2.11	1.59	2.74	**0.27**
Painel 4	71 413	2.20	1.67	3.09		1.65	2.13	2.34	1.56	3.26	**0.36**
Painel 5	73 850	2.10	1.94	3.18		2.44	3.05	2.65	1.94	3.51	**0.30**
Painel 6	75 056	2.78	2.17	2.23		4.39	2.60	2.91	2.23	3.75	**0.26**
Painel 7	73 102	2.61	2.65	3.15		3.23	3.85	3.28	2.61	4.01	**0.21**
Painel 8	72 067	3.48	3.29	4.28		3.14	4.62	3.72	3.09	4.31	**0.16**
Painel 9	73 549	2.22	2.22	2.57		2.17	2.32	2.18	1.96	2.49	**0.12**
Painel 10	69 170	2.32	2.40	2.51		2.38	2.21	2.24	2.00	2.51	**0.11**
Painel 11	67 314	2.06	2.03	2.50		1.94	2.70	2.38	1.92	3.03	**0.23**

*** Uncertainty(thickness)=(((Average-P5)/Average)+((P95-Average)/average))/2.3**

UNCERTAINTY - TONAGE

3 Months	Tonnes	R1 (Tonnes)**	R2 (Tonnes)	R3 (Tonnes)	...	R99 (Tonnes)	R100 (Tonnes)	Average (Tons)	P5	P95	Uncertainty*
Painel 1	71 229	58 834	60 807	59 943		65 112	58 656	71 229	54 820	100 368	**0.32**
Painel 2	72 908	81 140	64 469	58 891		76 276	68 630	72 908	58 375	95 993	**0.26**
Painel 3	68 573	70 218	51 725	56 107		45 175	110 309	68 573	51 543	89 019	**0.27**
Painel 4	71 413	67 223	50 886	94 305		50 502	65 177	71 413	47 525	99 644	**0.36**
Painel 5	73 850	58 448	54 034	88 470		67 976	84 984	73 850	54 032	97 633	**0.30**
Painel 6	75 056	71 717	56 135	57 462		113 270	67 055	75 056	57 462	96 809	**0.26**
Painel 7	73 102	58 067	58 927	70 228		72 022	85 706	73 102	58 047	89 289	**0.21**
Painel 8	72 067	67 333	63 744	82 817		60 738	89 532	72 067	59 882	83 465	**0.16**
Painel 9	73 549	75 052	75 169	86 974		73 458	78 218	73 549	66 118	84 073	**0.12**
Painel 10	69 170	71 455	74 035	77 429		73 483	68 111	69 170	61 782	77 429	**0.11**
Painel 11	67 314	58 266	57 503	70 579		54 850	76 395	67 314	54 358	85 754	**0.23**

***Uncertainty(Tonage)=(((Average-P5)/Average)+((P95-Average)/Average))/ 2.3**
**** R1(Tonnes) = (R1(Thickness)/R1Average(Thickness))*Tonnes (Painel1)**

UNCERTAINTY - Ounces

3 Months	Tonnes	R1 (Oz) ***	R2 (Oz)	R3 (Oz)	...	R99 (Oz)	R100 (Oz)	Average (Oz)	P5	P95	Uncertainty*
Painel 1	71 229	14 336	14 256	14 678		16 446	15 034	17 397	13 145	25 308	**0.35**
Painel 2	72 908	18 478	15 974	14 059		18 613	16 939	17 809	13 674	24 712	**0.31**
Painel 3	68 573	18 437	12 076	13 810		11 403	25 845	16 576	12 104	22 284	**0.31**
Painel 4	71 413	17 449	11 764	26 776		14 138	15 077	17 459	10 961	25 347	**0.41**
Painel 5	73 850	15 014	12 857	21 348		18 091	19 455	17 824	12 798	24 027	**0.31**
Painel 6	75 056	16 139	14 630	14 260		28 886	18 230	18 365	13 935	23 963	**0.27**
Painel 7	73 102	13 637	14 751	15 845		15 905	21 857	17 745	13 639	22 411	**0.25**
Painel 8	72 067	17 017	17 011	21 548		12 745	22 948	17 899	14 053	22 949	**0.25**
Painel 9	73 549	16 639	16 111	24 900		18 185	19 002	18 323	15 677	22 073	**0.17**
Painel 10	69 170	18 097	19 707	18 785		14 971	17 359	16 969	14 853	20 503	**0.17**
Painel 11	67 314	14 292	13 515	18 610		12 927	19 571	16 249	12 566	21 336	**0.27**

*** Uncertainty(Ounces)=(((Average(Oz)-P5)/Average(Oz))+((P95-Average(Oz))/Average(Oz)))/ 2.3**
***** R1(Oz) = (R1(Au g/t)*R1(Tonnes))/31.1035**

The steps for the classification of the Lamego deposit resources are the following: (a) selection the most significant orebody in terms of grades and tonnage (metal content), which shall be subjected to SGSIM; (b) rotation of the selected orebody to minimize the processing time (Figure 28); (c) data transformation to the Gaussian space (NSCORE); (d) simulation (SGSIM) of

the Au grade and thickness; (e) data back-transformation to the real space; (f) validation of the SGSIM; (g) measurement of the uncertainty per production unit; (h) assignment of the uncertainty and the category to the adjacent minor orebodies that show similar variability conditions and levels of information (Figure 29); (i) reproduction of the calculated uncertainty back to the 3D model; (j) establishment of a knowledge-driven procedure to adjust the categorized panels.

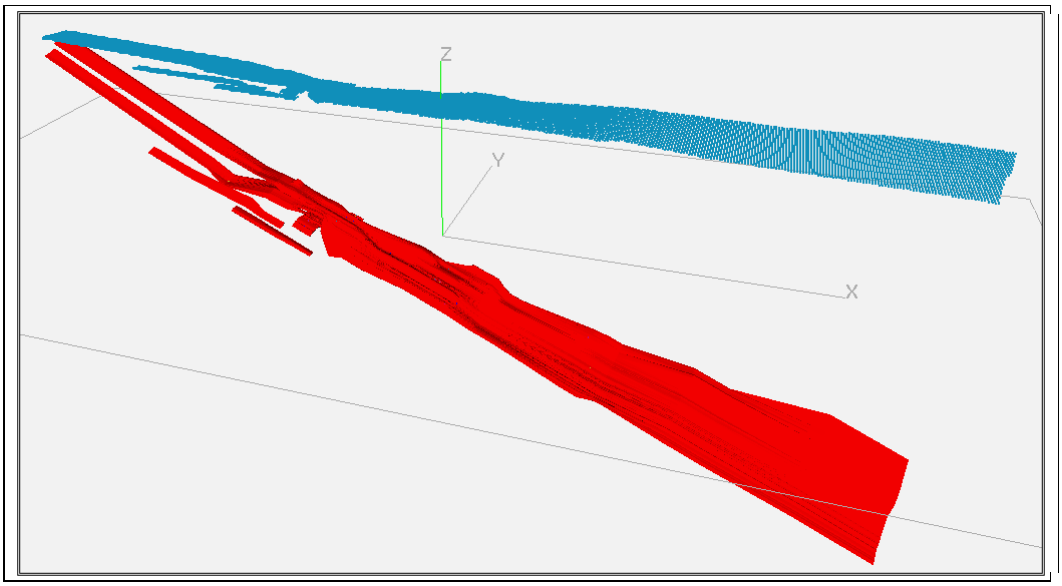

Figure 28 – 3D-view comparing the two coordinate systems: before and after projection

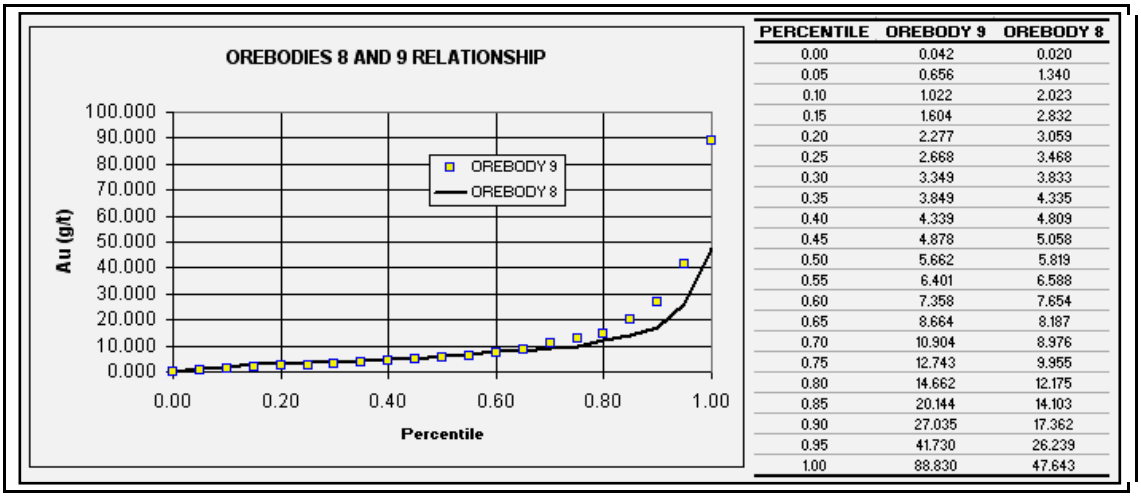

PERCENTILE	OREBODY 9	OREBODY 8
0.00	0.042	0.020
0.05	0.656	1.340
0.10	1.022	2.023
0.15	1.604	2.832
0.20	2.277	3.059
0.25	2.668	3.468
0.30	3.349	3.833
0.35	3.849	4.335
0.40	4.339	4.809
0.45	4.878	5.058
0.50	5.662	5.819
0.55	6.401	6.588
0.60	7.358	7.654
0.65	8.664	8.187
0.70	10.904	8.976
0.75	12.743	9.955
0.80	14.662	12.175
0.85	20.144	14.103
0.90	27.035	17.362
0.95	41.730	26.239
1.00	88.830	47.643

Figure 29 – Percentiles of orebodies 9 and 8 showing similar variability conditions.

Prior to accepting the result of the simulation as a tool to assist in the quantification of uncertainties, a comparative appraisal must be performed. This considers the results of the original samples mean and the mean of the values obtained by ordinary kriging estimation, together with the mean of the results from 100 realizations, yielded through the sequential

simulation (Figures 30 and 31). It is also necessary to compare the variogram models produced on the basis of the original database with the variograms produced from the simulated results.

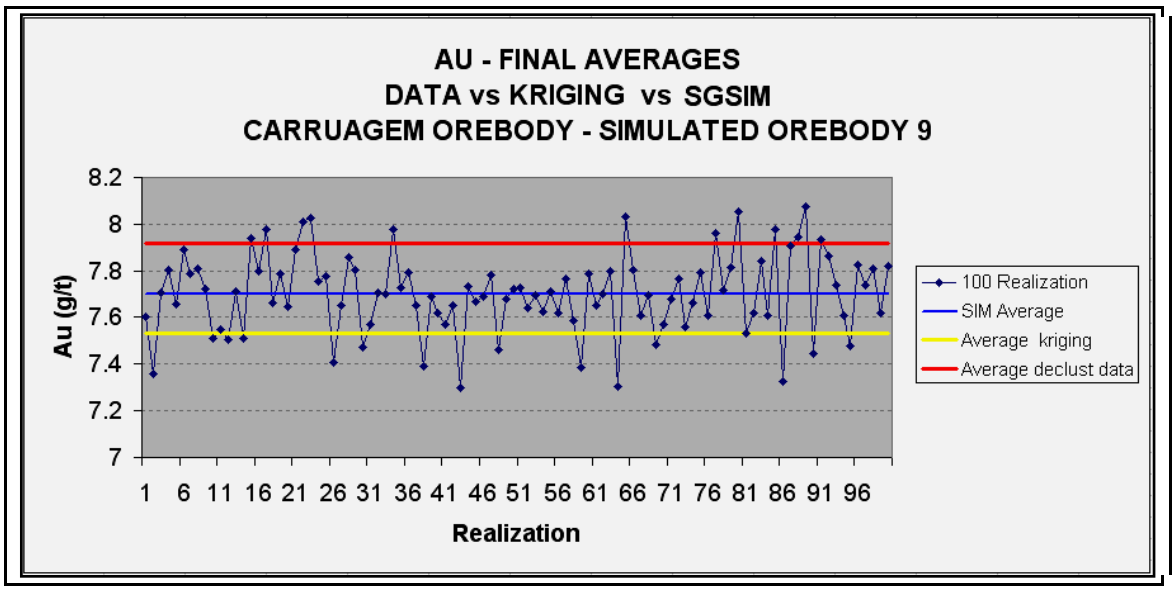

Figure 30 – Au averages data *vs* kriging *vs* sequential simulation. Carruagem orebody.

Figure 30 shows the average value for Au obtained from 100 realizations was slightly higher than the mean value of the ordinary kriging estimate and slightly lower than the mean value of the samples that correspond to the declustered original database. Conversely, the average thickness resulting from the sequential simulation showed slightly higher values when compared with the mean value of the actual thicknesses displayed by the 3D geological modelling (Figure 31).

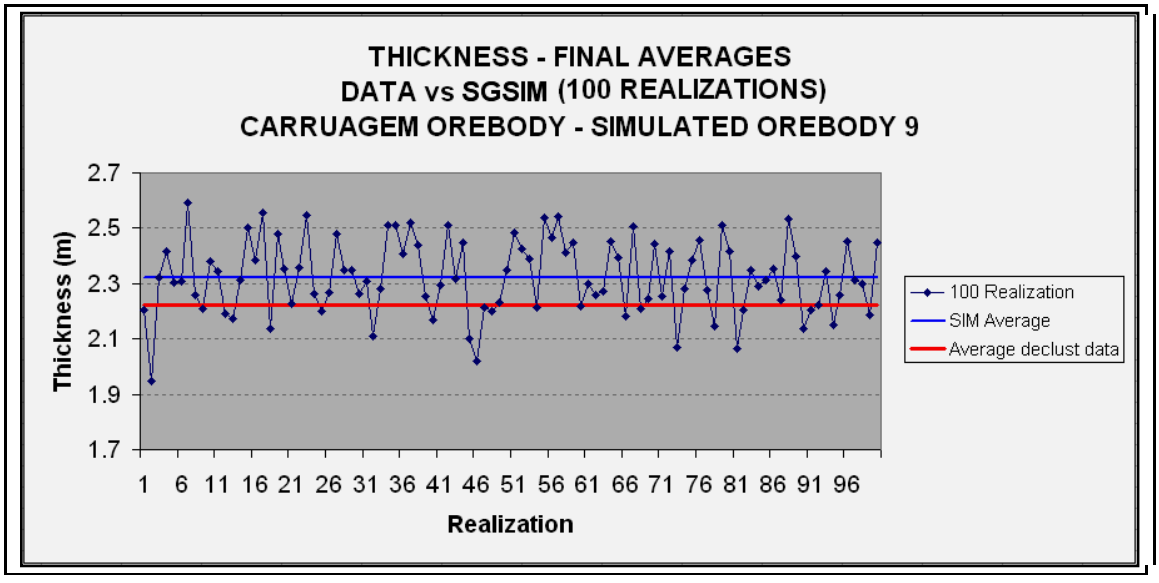

Figure 31 – Average thickness data *vs* sequential simulation. Carruagem orebody.

Figures 32 and 33 show the variogram validation considering the simulations of gold grades and thickness values of the Carruagem orebody. In this validation, the models for the two main directions of the ellipsoid are compared with the clouds yielded from the simulated realizations (lines shown in gray).

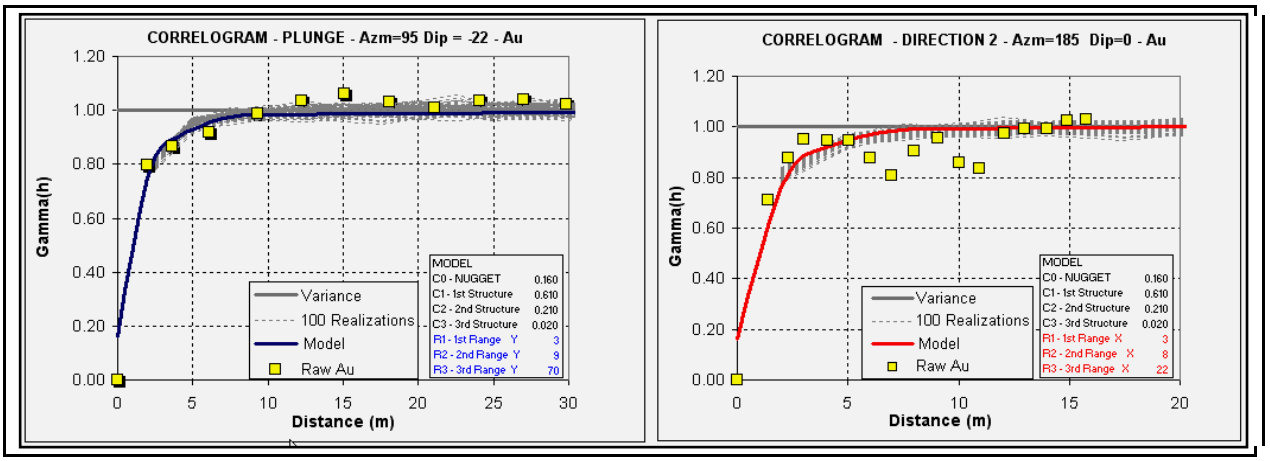

Figure 32 – Au simulation validation - simulated variograms (100 realizations) *vs* original variograms.

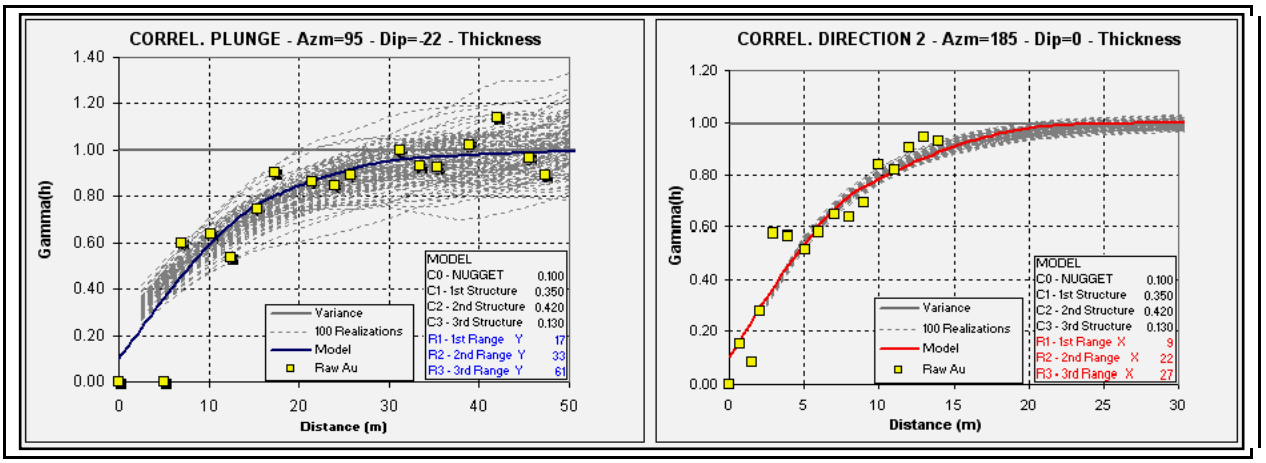

Figure 33 – Validation of simulated thickness-simulated variograms (100 realizations) *vs* original variograms (blue and red).

The clouds of the simulated variograms reproduced well the variographic information and were significantly coherent with the original database - in the same manner that the average plots indicated a qualitatively acceptable validation. However, the uncertainty obtained with the simulation of gold grades, conjugated with the variability of the thickness, show that there is no measured resource for the Carruagem orebody, considering such methodology. Although the uncertainty in the gold grade variability persisted under 15% in a group of production panels, thickness variability was quite significant, contributing for a total uncertainty greater than 15% in all panels related to a 3-month production, for a confidence interval of 90% (Figure 34A). The

uncertainty obtained for annual production intervals (Figure 34B) considering the upper panel, which contains information from level 1 (practically fully developed), did not exceed 13%. In the intermediate panel, which contains part of level 2 (under development), the variability remained at about 15%. Therefore, these two panels can be characterized as indicated resource.

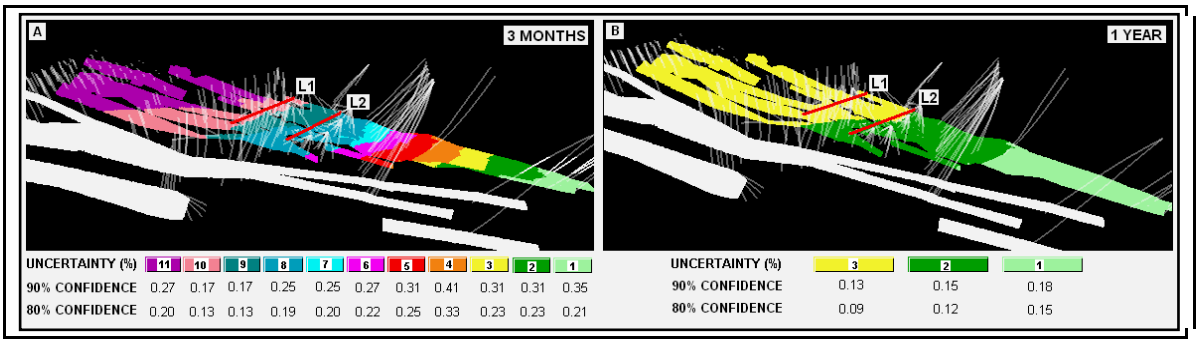

Figure 34 – Uncertainties resulting from the simulation process for 3-months (A) and annual (B) production panels. Carruagem orebody.

The summarized resource classification for the Carrruagem orebody is shown in Figure 35. In Figure 35A, the classification takes into account a confidence interval of 90% (according to the 15% uncertainty). Note that there are only indicated and inferred resources, as the minimum uncertainty was of about 17%. The lower limits of the indicated resources was defined by the panel related to the annual production, with uncertainty equal to and lower than 15%.

Allowing for a less stringent confidence interval of 80% (Figure 35B), two panels of measured resources are positioned between levels 1 and 2, and a significant part above level 1.

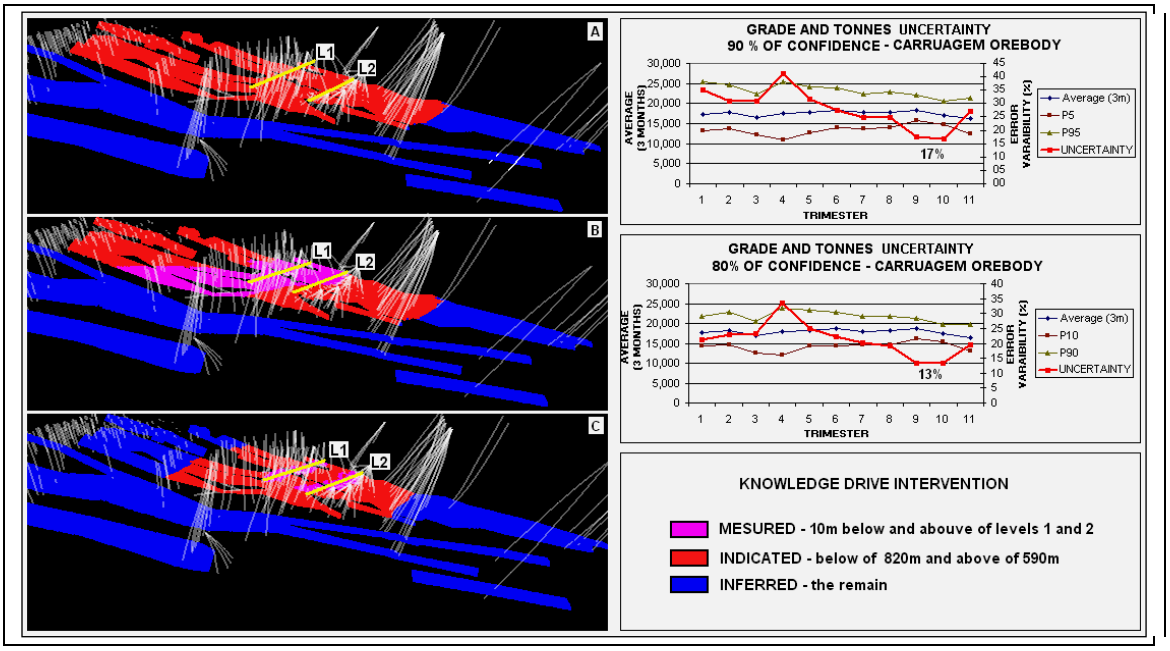

Figure 35 – Classification of the Carruagem orebody and uncertainties yielded through the simulation process. A – 90% confidence; B – 80% confidence; C – knowledge-driven inference.

The conditional simulation process – which considers the uncertainties obtained in the realizations for the variables gold and thickness (tonnage) – was insufficient to characterize measured resources at the Carruagem orebody. However, two 20m panels, each of which 10m above and below levels 1 and 2, respectively (Figure 35C), were considered to be measured resources, based on underground geological knowledge. Also, the following constraints were defined for indicated resources: i) above 820m, where the geotechnical characteristics indicate uncertainties concerning geomechanical instabilities, due to the proximity of the oxidation surface; and ii) below 590m, where only two drill holes support a panel of more than 200m along the strike. The orebodies to the south are at a distance sufficiently large to warrant a more accurate financial evaluation to ascertain the economics, and thus are considered as part of the inferred resources.

Another important aspect to consider is that the spacing of drill holes made from the underground drilling district (i.e, that spans a panel of more than 70m below level 2 and was performed with a spacing of approximately 25m along the plunge and 25m along the strike), was insufficient to classify the resource in this panel as measured resource. Therefore, further drilling campaigns should consider a closer spaced grid – for example, 10m along the strike and 20m along the plunge.

This same resource classification method was used for the other orebodies of the Lamego deposit. Figure 36 shows, in an integrated manner, the resource classification for the other orebodies – Arco da Velha, Cabeça de Pedra, Queimada, and Alvo NE – as well as for the Carruagem orebody detailed above.

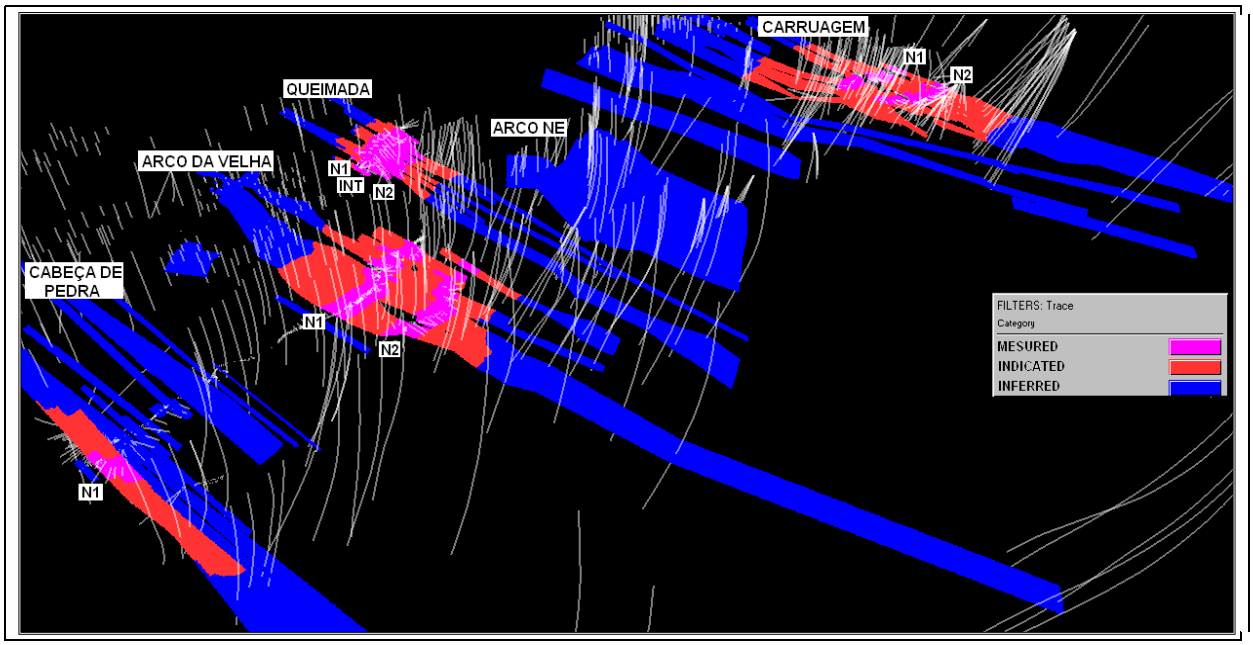

Figure 36 – Lamego orebodies – 3D classification of geological resources.

Figure 37 shows the classification of resources at the Lamego deposit from December/2004 to June/2008. Note that a change in the classification methodology, particularly in 2008, had a significant impact on the categorization. Nevertheless, the complex geometry of the orebodies was in fact the main cause of reduction among measured and indicated resources over time. Such complexity was only revealed lately, after the opening of the levels and densification of the grid spacing between drill holes.

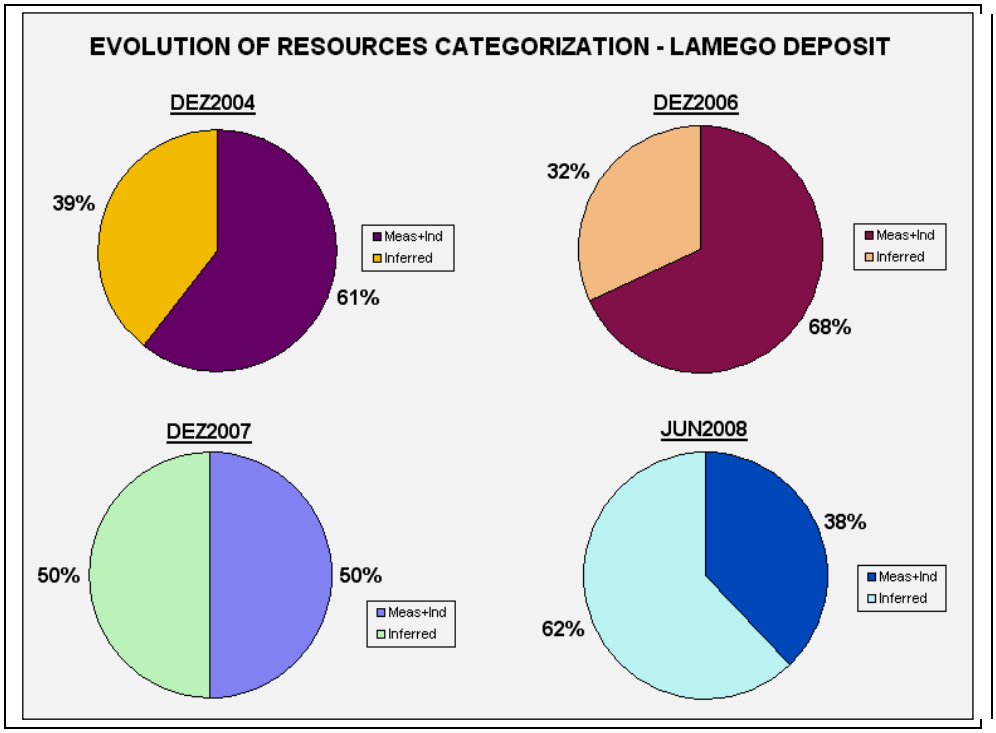

Figure 37 – Classification of resources at the Lamego deposit between 2004-2008.

Figure 38 shows an illustration of the annual progressive conversion of geological resources into mineable resources planned for the Lamego deposit. The increasing evolution of measured and indicated resources is proportional to the underground development and the periodical drilling campaign, including surface and underground drill holes. In each panel of 50m thick is input the amount of geological and mineable resources. Only the measured plus indicated geological resources are considered during the conversion into mineable resources; in addition, vertical sustentation pillars and shallow safety crown pillars with residual gold ore must be subtracted of the mineable resources, getting thus the final number of reserves. Exceptionally in Arco da Velha orebody, only the mineralized material above the level 3 was considered in life of mine at this moment.

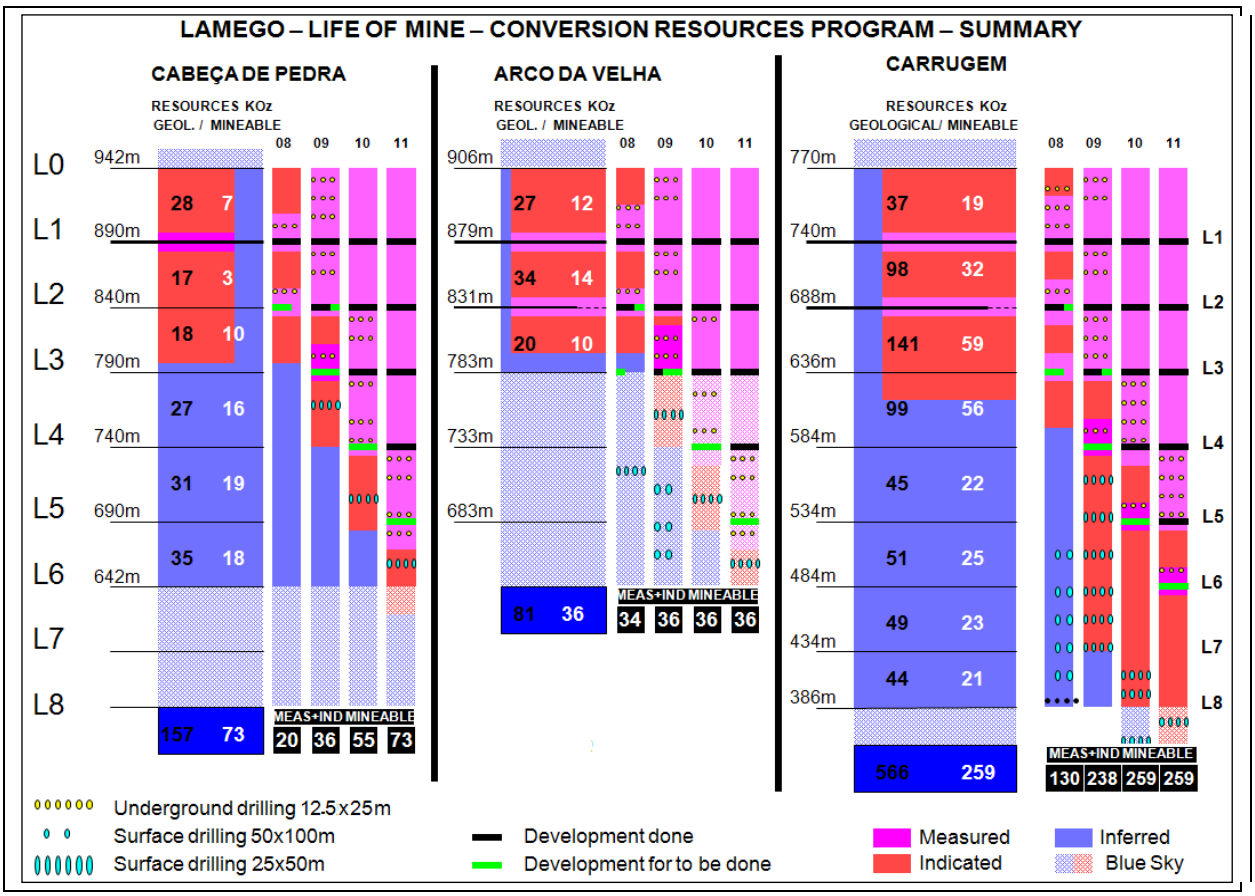

Figure 38 – Simplified conversion resources program planned for the Lamego deposit.

3 – CONCLUSIONS

All geostatistical procedures applied on this work were very useful to support the estimation of the metallic content of the Lamego gold deposit. Also, they supported the categorization of the mineral resources and in the improvement of the geological knowledge of the orebodies.

The study of average gold values, which preceded the ordinary kriging estimation, proved important as to reinforce the care needed during the execution of each evaluation phase of a mineral deposit. For this purpose, the analysis of the frequency histograms of the regional variables was also relevant in assisting the quantification and identification of the unexpected variations.

An eventual inadequate tree dimensional geological modelling of the orebodies can result in serious inaccuracy during the evaluation of any mineral deposit, because the geometry is strongly related to tonnage. Therefore, genetic issues, such as structural and stratigraphic criteria, must be considered during 3D modelling. Mainly in gold deposits, attention to dilution should be intensified. The lack of accuracy in sample location inside or outside the modeled orebody can lead to underestimated or overestimated results. Also, field demarcation of the mining areas must be rigorous in terms of topographic precision and follow the modeling of 3D limits for this type of gold deposits that have narrow and sufficiently varied thickness.

Among other studies, the bi-variant study of Au and S (scatter plots) was probably the most significant to define the guide reefs of the Lamego deposit. The correlation factors vary for different orebodies. For example, this factor is much lower for the Carruagem orebody (0.22) if compared with the others, implying that there is a population with high gold and low sulfur grades. At these sites, gold is frequently associated to micro-fractures and occurs as free gold. This type of occurrence can also be recognized in the directional correlograms typified by their high nugget effect. The Carruagem and Arco da Velha orebodies particularly show a high free gold content mainly in the gray quartz veins host rock, which makes difficult the visual control during underground development galleries since they are usually guided by high sulfide contents. The Queimada is the orebody with the highest Au and S correlation index (above 50%). This feature matches the visually observed high sulfide content at this orebody, which can reach over 30% of sulfides. The Cabeça de Pedra orebody exhibits an Au and S correlation index close to 0.5, but contains exceptionally lower gold grades. The latter are examples that sulfide content can

be considered as a guide during the underground development operations, although there are exceptions, as is the case verified at the Carruagem orebody.

The validation results of ordinary kriging estimation performed on Lamego orebodies confirmed that the correlograms and search ellipsoids parameters were coherently adjusted to each other, proving this to be a trustworthy evaluation method. Kriging validation procedures also allowed a few conclusions that, although yet preliminary, can assist in developing a strategy to enhance the time span of the Lamego mine. For instance, the mean gold distribution of the horizontal volumetric panels indicates that gold grades are lower with increasing depth both in the Carruagem and Arco da Velha orebodies. Considering the few samples taken in deeper levels, this interpretation cannot be conclusive, but the data indicates such tendency. Conversely, the mean gold distribution of the vertical volumetric panels indicates that gold grades slightly increase following the North direction. This feature can be associated to deformation episodes (that are coincident to the mineralizing hydrothermal fluid accumulation at those sites) and/or to structural traps in the northern sectors of the aforementioned orebodies.

Sequential Gaussian Simulation process was performed through 100 realizations of the variables. The results were useful to quantify the variability and so, to predict the uncertainty of production in panels related to quarters or annual periods. SGSIM results took in account the uncertainty for both the gold and thickness (tonnage) variables. The high uncertainty result has shown that measured resources in the Carruagem orebody could not be classified as such, considering a 90% trustworthy interval. However, considering the geological knowledge gathered from underground mapping and drilling core logs in the analysis, two panels of 20 meters (10 meters above and below levels 1 and 2) could be conclusively classified as measured resources.

CAPÍTULO 3

CONCLUSÕES FINAIS E PRINCIPAIS CONTRIBUIÇÕES

Acredita-se que os resultados do desenvolvimento desta pesquisa forneceram um razoável incremento no conhecimento geológico do deposito Lamego e dos alvos satélites estudados. As abordagens geológicas, geofísicas, geoestatísticas e metodológicas desenvolvidas nesta tese demonstram a importância da integração de dados multi-fonte, quando se procura compreender e desvendar as complexidades inerentes à geologia de depósitos auríferos. A busca incessante pela localização de novos corpos mineralizados em pesquisas exploratórias para diversas substâncias minerais, vem gerando uma tendência ascendente no avanço das tecnologias aplicadas às ciências da terra, que devem ser cada vez mais exploradas e plicadas em estudos geológicos.

A complexidade da mineralização aurífera no depósito Lamego, atribuída principalmente aos controles estruturais, variações expressivas na geometria e espessura dos corpos estudados, ausência de guia estratigráfico bem definido dos horizontes mineralizados e principalmente a baixa correlação dos teores de ouro com os índices de sulfetação, dificultam consideravelmente o desenvolvimento e abertura das galerias subterrâneas. Essa complexidade foi comprovada após a abertura e mapeamento geológico do segundo nível. As direções e mergulhos dos bolsões mineralizados apresentaram boa correlação com as medidas de lineações minerais; por outro lado os níveis mineralizados raramente se associam a um horizonte estratigráfico específico, principalmente nos locais onde as massas de quartzo possuem espessura de mais de 10m. Nesses casos, conforme ilustrado nos mapas geológicos dos níveis 1 e 2, os corpos de minério ora posicionam-se próximos à capa ora próximos a lapa e freqüentemente encontram-se inseridos no interior dos bolsões de quartzo. Já o estudo bi-variante simplificado mostrou, através dos diagramas de dispersão, índices de correlação relativamente baixos entre ouro e enxofre. Por fim, os resultados obtidos na simulação condicional gaussiana fortalecem e comprovam o alto nível de variabilidade não só dos teores de ouro, mas principalmente da espessura.

Os resultados do processamento dos dados dos levantamentos geofísicos, juntamente com a aplicação dos métodos de inversão para a região do depósito Lamego e dos alvos satélites, apresentaram um elevado índice de correlação com os corpos sulfetados e anomalias de solo, tanto em superfície quanto em profundidade. As anomalias de EM e IP (principalmente a IP1), após a inversão geofísica, mostraram uma aderência geométrica e posicional proeminente em

praticamente todos os cinco corpos sulfetados do depósito Lamego. Além disso, as seções de IP contribuíram para mostrar a continuidade SW do Corpo Carruagem, comprovada pelos resultados positivos da sondagem adicional de superfície. A anomalia de cargabilidade localizada no prolongamento NE do corpo Carruagem foi modelada e testada. Os resultados obtidos pela sondagem comprovaram a anomalia pela presença de intensa sulfetação em xisto carbonoso com pequenas venulações de quartzo, porém sem resultados expressivos de ouro.

As anomalias de IP nos alvos São José, Biquinha, Sobradinho e Bom Caminho apresentaram boas correlações com as informações geológicas e geoquímicas de superfície e foram comprovadas pelos resultados obtidos nas sondagens exploratórias.

Uma tabela síntese, com as proporções específicas de sulfetos dos corpos do depósito Lamego e alvos satélites, em conjunto com as respectivas intensidades de sinais de cargabilidade, resistividade e EM, foi produzida, permitindo caracterizar comparativamente as assinaturas geoquímicas e geofísicas dos diversos corpos estudados. Essa síntese tem um aspecto pioneiro e pode ser usada para auxiliar em pesquisas exploratórias auríferas em outros *greenstone belts.*

Os resultados obtidos pelos métodos das múltiplas seções horizontais submetidas aos operadores de lógica *fuzzy* apresentaram uma razoável correlação geométrica com o produto do processo de inversão geofísica dos dados de EM no depósito de Morro da Glória, embora com resoluções e escalas diferenciadas.

Os procedimentos geoestatísticos aplicados e desenvolvidos no segundo capítulo auxiliaram no esclarecimento de um conjunto de questões metalogenéticas associadas ao depósito Lamego. O estudo bi-variante mostrou o baixo fator de correlação Au x S principalmente nos corpos Arco da Velha e Carruagem, corroborando com a dificuldade de se considerar a sulfetação como guia prospectivo nessas áreas. Já nos corpos Queimada e Cabeça de Pedra, o índice de correlação entre essas duas variáveis são um pouco superiores. No entanto, sugere-se cautela para uso dos teores de enxofre como guia prospectivo nesses dois corpos.

Os resultados apresentados nos painéis volumétricos horizontais apontam um empobrecimento relativo dos teores de Au em profundidade nos corpos Carruagem e Arco da Velha. Como o número de informações em níveis mais profundos é muito menor, tal conclusão pode ser ainda questionável, embora os números apontem tal tendência. Já os resultados obtidos nos painéis volumétricos verticais indicam enriquecimento dos teores à medida que se avança para Norte. Tais fenômenos podem estar associados a pulsos de deformação, onde o acúmulo de fluidos hidrotermais mineralizantes é concentrado nesses locais e/ou associados à *traps*

estruturais que ajudam a acumular os fluidos nas porções setentrionais e mais rasas desses corpos. Além disso, a macro estrutura do Lamego poderia ter sido formada originalmente ao longo de um eixo com a mesma direção do acamamento, porém com mergulho acentuado p\ NE. O Corpo Carruagem estaria em um nível crustal mais profundo, enquanto o corpo Cabeça de Pedra estaria associado a níveis crustais mais rasos. Esta questão poderia ser então relacionada a esse relativo enriquecimento dos teores de ouro à medida que se aproxima do extremo NE do Depósito.

Os resultados obtidos através das 100 realizações na simulação condicional gaussiana apontam um elevado índice de incerteza associado principalmente à geometria dos corpos mineralizados e a variabilidade dos teores de ouro, o que interfere no cuidado ao se declarar recursos medidos no depósito estudado.

Principais Contribuições

O acervo de informações e conhecimentos produzidos e desenvolvidos nesta pesquisa contribuiu para avanços científicos a respeito da caracterização geológica, geofísica e geoquímica do depósito Lamego a adjacências, bem como permitiu um incremento do conhecimento metalogenético deste depósito.

Como parte dos resultados, foi gerada uma tabulação inédita da associação entre intensidades de sinais geofísicos com diferentes proporções de sulfetos em rochas específicas do Grupo Nova Lima no Quadrilátero Ferrífero, hospedeiras de mineralizações auríferas em ambientes mesotermais. Essa síntese tem desdobramentos em ciência básica (na medida em que proporciona um avanço no conhecimento da relação entre variáveis físicas e químicas em rochas com mais alto conteúdo metalífero); e tecnológicos, visto que permite uma sintonização de ferramentas exploratórias baseadas em instrumentos geofísicos.

A metodologia de programação das seções de IP (longitudinal à direção do *strike*) e a investigação da projeção das evidências de superfície são também mecanismos apresentados que podem ajudar em programas de exploração mineral.

A intensidade da sulfetação definitivamente não deve ser considerada como guia no avanço e desenvolvimento dos níveis dos corpos do Lamego, principalmente Carruagem e Arco da Velha, visto sua baixa correlação espacial com teores mais altos de ouro.

Um modelo de configuração de um programa de adição e conversão de recursos foi proposto como parte da pesquisa e pode também se usado como referência em outros depósitos com características semelhantes.

O detalhamento geológico dos corpos no nível 2 do depósito Lamego, com base nos dados de sondagem e canaletas, juntamente com modelagem 3D dos corpos de minério, possibilitou avanços no conhecimento geológico e distribuição das mineralizações e teores em estruturas complexas, poli-deformadas.

REFERENCES

Alkmim, F. F., Marshak S., 1998. T*ransamazonian orogeny in the southern São Francisco Craton region, Minas Gerais, Brazil: evidence for Paleoproterozoic collision and collapse in the Quadrilátero Ferrífero*. Precambrian Research, 90, issues 1-2, 2229-58.

An, P., Moon, W.M. & Rencz, A., 1991. Application of Fuzzy set theory to integrated mineral exploration. Canadian Journal of Exploration Geophysics, Vol.27, No.1, December 1991, p.1-11.

Baltazar O. F. & Zucchetti, M., 2006. Lithofacies associations and structural evolution os the Archean Rio das Velhas greenstone belt, Quadrilátero Ferrífero, Brazil: A review of the settings of gold deposits. *Ore Geology Reviews*. Artigo aceito para publicação

Bonham-Carter, G.F., Agterberg, F.P. & Wright, D.F., 1988. Integration of geological datasets for gold exploration in Nova Scotia. Photogrammetric Engineering and Remote Sensing, Vol.54, No.11, November 1988, pp.1585-1592.

Bonham-Carter, G. F. 1994. *Geographic Information Systems for geoscientists – Modeling with GIS*. Pergamon, 400p.

Bonham-Carter, G.F., 1997. GIS methods for integrating exploration data sets. In: Proceedings of Exploration 97: Fourth Decennial International Conference on Mineral Exploration, ed. A.G. Gubins, 1997, p.59-64

Braghin, M.A., 1998. Utilização das Lógicas Booleana e Fuzzy para Análise Metalogenética na Folha Pilar do Sul (SP) via Sistema de Informações Geográficas. Dissertação de Mestrado. Universidade Estadual de Campinas. 144p.

Chinn, G.T. & Ascough, G.L., 1997. Mineral potential mapping using an expert system and GIS. In: Proceedings of Exploration 97: Fourth Decennial International Conference on Mineral Exploration, ed. A.G. Gubins, 1997, p.105-114

CPRM, UFMG 2005. Projeto Geologia do Quadrilátero Ferrífero - Integração e Correção Cartográfica em SIG com Nota Explicativa.

Dorr II, J.V.N., 1969, *Physiographic, stratigraphic and structural development of the Quadrilátero Ferrífero, Minas Gerais, Brazil*. Washington. *U.S. Geol. Sur.*

Dentith, M.C. (ed), 2003, Geophysical Signatures of South Australian Mineral Deposits. UWA, Centre for Global Metallogeny Pubn. 31, ASEG Sepcial Pubn. 12, 289p.

Deutsch, C. & A. Journel C., 1998, Geostatistical Software Library and User's Guide.Oxford University Press, New York, 2nd edition, 1998.

Dorr II, J.V.N .1969. *Physiographic, stratigraphic and structural development of the Quadrilátero Ferrífero, Minas Gerais, Brazil*. Washington. *U.S. Geol. Surv.*

Duchini Jr., J. 1992. Internal Report – AgloGold Ashanti.

Fullagar, P.K., 2004, VPmg User documentation: Fullagar Geophysics Pty Ltd Technical Memorandum FGR01F-4

G. Matheron, 1962, Traité de Géostatistique Appliquée. Vol. 1 (1962), Vol. 2 (1963), ed. Technip, Paris, 1962.

Groves, D. I.; Condie, K.C.; Goldfarb, R.J.; Hronsky, J. M.A.; Vielreicher, R.M. 2005 - *100th Anniversary Special Paper: Secular Changes in Global Tectonic Processes and heir Influence on the Temporal Distribution of Gold-Bearing Mineral Deposits.* Economic Geology, v. 100, pp. 203–224

Guimarães, F.R., Souza Filho, C.R, Da Costa, M.A. 2006. *Crustal "Tomography": 3D Fuzzy Logic Spatial Analysis and Geophysical Inversion Applied to Underground Prospectivity Mapping of Gold Ores in the Quadrilátero Ferrífero, Brazil.* SIMEXMIN - Simpósio Brasileiro de Exploração Mineral – Ouro Preto, 2006.

Guimarães, F.R., Souza Filho, C.R, Penha, U.C., Cordeiro, E.Z., Vicencio, T.R. 2008. *Inversão Geofísica de Dados Eletromagnéticos aéreos, de Resistividade e Polarização Induzida como Ferramenta Exploratória e de Caracterização do Depósito de Ouro Lamego e Imediações, Quadrilátero Ferrífero, MG.* SIMEXMIN - Simpósio Brasileiro de Exploração Mineral – Ouro Preto, 2008.

Guidelines for the Reporting of Exploration Results, Mineral Resources and Ore Reserves for 2007. AngloGold Ashanti Internal Paper.

Hewett, T., 1986, Fractals distributions of reservoir heterogeneity and their influence on fluid transport. SPE paper # 15386, 1986.

JORC *Australasian Joint Ore Reserves Committee*

Journel, A., 1993, Modeling Uncertainty: Some Conceptual Thoughts. In R. Dimitrakopoulos, editor, *Geostatistics for the Next Century*, pages 30-43. Kluwer, Dordrecht, Holland, 1993.

Journel, A., 1994, Resampling from stochastic simulations. *Environmental and Ecological Statistics*, 1:63-84,1994.

Journel, A.G., 1996, The abuse of principles in model building and the quest for objectivity: Opening keynote address. In *Fifth International Geostatistics Congress*, Wollongong, September 1996.

Journel A., and F. Alabert, 1990, New method for reservoir mapping. *J. of Pet. Technology*, pages 212-18, Frebruary 1990.

Klinkert, P.S., Leggatt, P.B., and Hage, T.B. 1997. The Spectrem Airborne Electromagnetic System - Latest Developments and Field Examples. In: "Proceedings of Exploration 97: Fourth Decennial International Conference on Mineral Exploration" edited by A.G. Gubins, 1997, p. 557–564

Li, Y. and Oldenburg, D.W., 2003, Fast inversion of large-scale magnetic data using wavelet transforms and logarithmic barrier method: Geophys. J. Int, 152, 251–265.

Lobato, L.M. Vieira, F.W 1998. *Styles of Hydrohermal Alteration and Gold Mineralizations Associated with the Nova Lima Group of the Quadrilátero Ferrífero: Part I, Description of Selected Gold deposits*. RBG 28(3):339-354, setembro de 1998.

Lobato, L.M. & Vieira, F.W 1998. *Styles of Hydrohermal Alteration and Gold Mineralizations Associated with the Nova Lima Group of the Quadrilátero Ferrífero: Part II, the Archean Mesothermal Gold-Bearing Hydrothermal System.* RBG 28(3):355-366, setembro de 1998.

Lobato, L.M, Ribeiro-Rodrigues, L.; Zucchetti,M.; Noce, C.M.; Baltazar,O.; Silva, L.; Pinto, C. 2001 - *Brazil's premier gold province. Part I: The tectonic, magmatic, and structural setting of the Archean Rio das Velhas greenstone belt, Quadrilátero Ferrífero.* Mineralium Deposita. Volume 36, Numbers 3-4, 228-248, DOI: 10.1007/s001260100179

Nóbrega, R. P. 2001. *Análise espacial "knowledge-driven" e "data-driven" uso das lógicas booleana, fuzzy e redes neurais para geração de mapas de favorabilidade mineral na região centro-leste da Bahia*. Dissertação de Mestrado, UNICAMP, Instituto de Geociências, Campinas, SP.

Nykanen, V. 2008. Spatial data analysis as a tool for mineral prospectivity mapping. Academic Dissertation. Espoo 2008, Finland.

Mutton, A. J., 1997. The application of geophysics during evaluation of the Century zinc deposit: 4th Decennial Internat. Conf. Min. Expl., Proceedings, 599–614.

Oldenburg, D. W. and Pratt, D. A. 2007. *Geophysical Inversion for Mineral Exploration: a Decade of Progress in Theory and Practice.* In "Proceedings of Exploration 07: Fifth

Decennial International Conference on Mineral Exploration" Toronto, edited by B. Milkereit, 2007, p. 61-95.

Oldenburg, D.W. and Li, Y. 2005. Inversion for applied geophysics: a tutorial. Near -surface geophysics, SEG investigations in geophysics series No 13, editor Dwain Butler, pp 89–150.

Phillips, N., Oldenburg, D.W. Chen, J. Li, L. and Routh, P., 2001, Cost effectiveness of geophysical inversion in mineral exploration: applications at San Nicolas.: The Leading Edge, 20, pp1351– 1350.

Pratt, D.A., McKenzie, K.B., White, A.S., Foss, C.A., Shamin, A. and Shi, Z., 2001 A user guided expert system approach to 3D interpretation of magnetic anomalies. Extended Abstracts, ASEG 15th Geophysical Conference and Exhibition, Brisbane.

Pratt,D.A., Foss, C.A. and Roberts, S., 2006 User Guided Inversion & Visualisation of Interpretation Confidence. Extended Abstract AESC Conference, Melbourne.

Pratt, D.A., Foss, C.A., Shi, Z, White,A.S., McKenzie, K.B, Gidley, P.R. and Mann,S., 2007, Encom ModelVision Pro, Encom AutoMag - the 3D workbench for magnetic and gravity interpretation, Reference Manual. Encom Technology, 504 p.

Ribeiro-Rodrigues, L.C. 1998. Gold in Archean Badend Iron-Formation of the Quadrilátero Ferrífero, Minas Gerais, Brazil - The Cuiabá Mine. Aachen University of Technology, Aachen, Germany, Aachener Geowissenschaftliche Beitrage, Band 27, Ph. D. Thesis, 264 p.

Santos Salles, M.A. – *The Geological Setting of the Lamego Banded Iron Formation hosted gold Deposits, Quadrilatero Ferrifero District, Minas Gerais state, Brazil.* MsC Thesis –Queen's University, 1998.

Santos Sales & Holcombe, 2004. Internal Report – AgloGold Ashanti.

Silva, J. B. C.; Medeiros, W. E.; Barbosa, V. C. F. 2001. Potential-field inversion: Choosing the appropriate techniqueto solve a geologic problem. GEOPHYSICS, VOL. 66, NO. 2 (MARCH-APRIL 2001); P. 511–520.

SRTM, 2006. Shuttle Radar Topography Mission, Nasa.

Spectrem Aerial Survey Lamego-Cuiaba Area. 2002 - Internal Report – AngloGold Ashanti Brasil Mineração Ltda.

Telford, W.M., Geldart L. P., Sheriff R. E. 1990. Applied Geophysics. 2nd ed. Cambridge University Press.

Toledo, C.L.B. 1997. Controle Estrutural da Mineralização Aurífera na Mina de Cuiabá, Setor Noroeste do Greenstone Belt Rio das Velhas, Quadrilátero Ferrífero. Inst. De Geociências, Universidade Estadual de Campinas, Campinas. M. Sc. Thesis, 166 p.

Vial, D.S.; DeWitt, E.; Lobato, L.M.; Thorman,C.H. 2007. The geology of the Morro Velho gold deposit in the Archean Rio das Velhas greenstone belt, Quadrilátero Ferrífero, Brazil. Ore Geology Reviews, V (32), Issues 3-4; P. 511-542.

Vieira, F. W. R., Oliveira G. A. 1988. *Geologia do Distrito Aurífero de Nova Lima, Minas Gerais*. In: Schobbenhaus, C. & Coelho C. E. S. (coord). Principais depósitos minerais do Brasil. Brasília, DNPM/CVRV, V (3): 377-391.

Vieira, F. W. R. 1991. Textures and process of hydrothermal alteration and mineralization in the Nova Lima Group, Minas Gerais, Brazil. In: Ladeira, E.A. ed. Brazil Gold ´91. The Economics, Geology, Geochemistry and Genesis of Gold Deposits. Belo Horizonte, 1991.

Vogel, C. R., 2001, Computational methods for inverse problems: Society of Industrial and Applied Mathematics, Frontiers in Applied Mathematics.

Zucchetti, M., Baltazar O. F., Raposo F. O. 1996. *Estratigrafia. Projeto Rio das Velhas, Mapa Geológico Integrado*. *Escala 1:100.000. Texto Explicativo*. Programa de Estudos Mineiros. Convênio DNPM/CPRM. Belo Horizonte, 1996

Zucchetti, M., Baltazar O. F. 2007. Lithofacies associations and structural evolution of the Archean Rio das Velhas greenstone belt, Quadrilátero Ferrífero, Brazil: A review of the settings of gold deposits. *Ore Geology Reviews*, 32:471–499.